Mitochondrial dysfunction as a driver of cellular senescence

Hanna Malgorzata Salmonowicz

A thesis submitted for the degree of Doctor of Philosophy

Biosciences Institute

Newcastle University

Campus for Ageing and Vitality

Newcastle upon Tyne

January 2021

Published material & conference attendance

Manuscripts published during PhD studies:

Cellular senescence mediates fibrotic pulmonary disease
Schafer MJ, White TA, Iijima K, Haak AJ, Ligresti G, Atkinson EJ, Oberg AL, Birch J, Salmonowicz H, Zhu Y, Mazula DL, Brooks RW, Fuhrmann-Stroissnigg H, Pirtskhalava T, Prakash YS, Tchkonia T, Robbins PD, Aubry MC, Passos JF, Kirkland JL, Tschumperlin DJ, Kita H, LeBrasseur NK.
Nat Commun. 2017 Feb 23;8:14532.

Detecting senescence: a new method for an old pigment
Salmonowicz H, Passos JF.
Aging Cell. 2017 Jun;16(3):432-434. doi: 10.1111/acel.12580.

Mitochondria and cellular senescence: Implications for musculoskeletal ageing
Habiballa L, Salmonowicz H, Passos JF.
Free Radic Biol Med. 2018 Oct 15, doi: 10.1016/j.freeradbiomed.2018.10.417

Integrating cellular senescence with the concept of damage accumulation in aging: Relevance for clearance of senescent cells
Ogrodnik M, Salmonowicz H, Gladyshev VN.
Aging Cell. 2019 Feb;18(1), doi: 10.1111/acel.12841.

Length-independent telomere damage drives post-mitotic cardiomyocyte senescence
Anderson R, Lagnado A, Maggiorani D, Walaszczyk A, Dookun E, Chapman J, Birch J, Salmonowicz H, Ogrodnik M, Jurk D, Proctor C, Correia-Melo C, Victorelli S, Fielder E, Berlinguer-Palmini R, Owens A, Greaves LC, Kolsky KL, Parini A, Douin-Echinard V, LeBrasseur NK, Arthur HM, Tual-Chalot S, Schafer MJ, Roos CM, Miller JD, Robertson N, Mann J, Adams PD, Tchkonia T, Kirkland JL, Mialet-Perez J, Richardson GD, Passos JF.
EMBO J. 2019 Mar 1;38(5), doi: 10.15252/embj.2018100492.

Expansion and Cell-Cycle Arrest: Common Denominators of Cellular Senescence
Ogrodnik M, Salmonowicz H, Jurk D, Passos JF.
Trends Biochem Sci. 2019 Jul 22, doi: 10.1016/j.tibs.2019.06.011.

Whole-body senescent cell clearance alleviates age-related brain inflammation and cognitive impairment in mice
Ogrodnik M, Evans SA, Fielder E, Victorelli S, KrugerP, Salmonowicz H, Weigand MB, Patel AD, Pirtskhalava T, Inman CL, Johnson KO, Dickinson SL, Rocha A, Schafer MJ, Zhu Y, Allison DB, von Zglinicki T, LeBrasseur NK, Tchkonia T, Neretti N, Passos JF, Kirkland JL, Jurk D.
Aging Cell. 2021 Jan 20, DOI: 10.1111/acel.13296

A complete list of published work can be found in MyBibliography:
https://www.ncbi.nlm.nih.gov/myncbi/18GV9xYfOwrApM/bibliography/public/

Conferences and courses attended during PhD studies:

2016: "7th Aliance for Healthy Ageing Conference" (Newcastle upon Tyne, UK)

2019: "Light Microscopy Workshop" organised by the BioImaging Unit, Newcastle University (Newcastle upon Tyne, UK)

2019: "Genome editing with the use of CRISPR/Cas system", a course organised at the European Molecular Biology Laboratory, Heidelberg, Germany, presentation of a poster: "Mitochondrial DNA leakage as a driver of cellular senescence"

2019: Senescence Symposium 2019 (Edinburgh, UK), presentation of a poster: "Mitochondrial DNA leakage as a driver of cellular senescence"

2020: American Aging Association (AGE) meeting "AGE goes virtual"

2020: 7th Aging Research & Drug Discovery Meeting

Thesis abstract

Cellular senescence is a stress response implicated in ageing and age-related diseases (Baker *et al.*, 2016; von Zglinicki, 2002). Senescent cells are characterised by mitochondrial dysfunction (Dalle Pezze *et al.*, 2014; Korolchuk *et al.*, 2017; Passos *et al.*, 2007). Importantly, mitochondria were shown to regulate the senescence-associated secretory phenotype (SASP) (Correia-Melo *et al.*, 2016). However, the exact mechanisms via which mitochondria contribute to the SASP as well as its conservation between the main studied models of senescence, remains to be elucidated.

In this thesis, I discovered that senescent cells are characterized by a sub-lethal mitochondrial apoptotic stress, consisting of the activation of pro-apoptotic factor, BAX and the release of cytochrome *c* and mtDNA into the cytosol. BAK and BAX are required for the SASP in damage-induced senescence (DIS), however, their genetic depletion in oncogene-induced senescence (OIS), increases it. A pharmacological inhibition of BAX after the establishment of cell cycle arrest, ameliorates SASP in OIS. Cells in DIS secrete higher levels of mtDNA than proliferating cells. However, the level of circulating mtDNA is not a strong biomarker of senescence burden in mice and humans.

Next, I demonstrate OIS and DIS are characterised by a different degree of mitochondrial apoptotic stress as well as oxidative phosphorylation (OXPHOS) dysfunction. Mitochondrial network was confirmed to be hyperfused in DIS (Dalle Pezze *et al*., 2014), however, it was found to be fragmented in OIS. Interfering with mitochondrial dynamics by inducing mitochondrial fusion exacerbates the SASP in both models of senescence. In contrast, a shift to mitochondrial fragmentation reduces the SASP in the model of DIS and exacerbates it in OIS.

Finally, I found myxovirus resistance protein B (MxB) plays an important function in maintaining the integrity of mitochondrial network and mitochondrial bioenergetics, as MxB depletion induces mitochondrial apoptotic stress and activates mitochondrial biogenesis. In DIS, MxB is highly up-regulated and translocates from mitochondria to the nucleus. MxB was found to be a key factor required for the SASP development.

Acknowledgements

First, I would like to express my gratitude to my supervisors, Dr Joao Passos, Dr Viktor Korolchuk and Dr Nathan LeBrasseur for their guidance and support throughout my PhD studies. I thank Dr Joao Passos for introducing me to the field of cellular senescence and thought-provoking discussions. I thank Dr Viktor Korolchuk for his ability to make me feel heard, as well as lots of interesting advice (*i.e.* Chekhov's gun). I thank Dr Nathan LeBrasseur for the access to various study materials that extended the scope of my studies. I am also very grateful to Dr Alberto Sanz and Dr Laura Greaves for their support as my thesis assessors.

Special thanks are to my collaborators for an opportunity to learn beyond the expertise of the laboratories I worked at. Many thanks to Dr Hong Cao for the collaboration on MxB project, to Dr Haiming Dai for our collaboration on FPLC/BAX oligomerisation, to Dr Padraig Flannery for our collaboration on MxB project/Seahorse experiments. I am thankful to Dr Glyn Nelson and Dr Duane Deal for their help with the microscopes. Special thanks to Dr Jodie Birch, Dr Clara Correia-Melo, Dr James Chapman, Dr Stella Victorelli and Dr Anthony Lagnado from Dr Passos lab, for the collaboration on various projects. I also thank Dr Lucia Sedlackova and George Kelly from Dr Korolchuk lab for their help with experiments during the most challenging times. Many thanks to Becca Reeds from Dr Sanz lab for the collaboration on the "Oroboros" experiment. Many thanks to Dr Tom White, Dr Marissa Schafer, Ashley Brown, Daniel Mazula and Kurt Johnson from Dr LeBrassuer lab, for their guidance and help and well as sharing the study materials. I would also like to thank Dr Mikolaj Ogrodnik for working together on various projects, *i.e.* the two recent review/opinion articles that were both a great lesson and fun.

Immense thanks is for my parents, Dr Barbara Salmonowicz and Marek Salmonowicz, for their immense help and support throughout my PhD. My appreciation also goes to my brother, Wojciech Salmonowicz, for his passion and example.

I also thank my friends: Stefania Wachowiak, Matylda Niewinska, Joanna Zielinska, Aleksandra Cupial, Dr Tarja Hoffmeyer, Dr Olena Kucheryavenko, Edwige Picazo, Valeria Pintar, Moritz Weigl, Dr Anthi Faka, Dr Larissa Langhi Prata, Nino Giorgaze, Dr Zaira Aversa, Klaudia Stano, Raffaella Blaylock-Smith, Vera Pils and Melanie Weigand for their support and companionship during the turbulent five years of my PhD studies and beyond.

Finally, I would like to thank Medical Research Council and Mayo Clinic for the funding of my PhD project. I would like to point out my special thanks to Medical Research Council for the financial support during my parental leave of 9 months.

Table of contents

List of figures

List of tables

List of abbreviations

3MA	3-methyladenine
AIF	Apoptosis inducing factor
AIM1	Absent in melanoma 1 protein
AKT	Protein kinase B
AMP	Adenosine monophosphate
AMPK	5' Adenosine monophosphate-activated protein kinase
A-SAAs	acute-phase serum amyloids
ATF	Activating transcription factor
ATFS-1	Stress activated transcription factor
ATM	Ataxia-telangiectasia mutated
ATP	Adenosine triphosphate
ATR	Ataxia telangiectasia and RAD3-related
BAD	BCL-2-associated agonist of cell death
BAK	BCL-2 homologous antagonist killer
BAX	BCL-2-associated X protein
BCB	BAX channel blocker
BCL-2	B-Cell lymphoma 2
BMI	Body mass index
BNIP3	BCL-2 interacting protein 3
BRAF	B-RAF proto-oncogene
BSA	Bovine serum albumin
BSE	Bundle signalling elements
bZIP	Basic region: leucine zipper
C/EBPβ	CCAAT-enhancer-binding protein β
CAD	Caspase activated DNAse
CAMKII	Ca^{2+}/calmodulin-dependent protein kinase II
CCF	Cytosolic chromatin fragment
CDKN2A	Cyclin-dependent kinase inhibitor 2A
cDNA	Complementary DNA
cGAMP	Cyclic GMP-AMP
cGAS	Cyclic GMP-AMP Synthase
CHAPS	3-((3-cholamidopropyl) dimethylammonio)-1-propanesulfonate
CHK1	Checkpoint-1
CHK2	Checkpoint-2
CHOP	C/EBP homologous protein
CHS	Cardiovascular health study
CL	Cardiolipin
CLR	C-type lectin receptors
CLR	C-type lectin receptors
CLSM	Confocal laser scanning microscopy
COX IV	Mitochondrial cytochrome *c* oxidase subunit IV
CPT	carnitine palmitoyltransferase-1

CREB	cAMP response element-binding protein
CRISPR	Clustered regularly interspaced short palindromic repeats
CXCL1	Chemokine (C-X-C motif) ligand 1
DAMPs	Damage associated molecular patterns
DAPI	4’,6-diamidino-2-phenylindole
DDR	DNA damage response
DFO	Deferoxamine
DIS	Damage-induced senescence
DNA	deoxyribonucleic acid
dNTPs	deoxyribonucleotide triphosphates
DRP1	Dynamin related protein 1
DSB	Double stranded break
DTT	Dithiothreitol
ECL	Enhanced chemiluminescence
EDTA	Ethylenediaminetetraacetic acid
EFN	Ephrin ligands
EGFP	Enhanced green fluorescent protein
EGTA	ethylene glycol-bis(β-aminoethyl ether)-N,N,N′,N′-tetraacetic acid
ELISA	Enzyme linked immunosorbent assay
ER	Endoplasmic reticulum
ERK	Extracellular signal-regulated protein kinase
ETC	Electron transport chain
FADH2	Flavin adenine dinucleotide
FBS	Foetal bovine serum
FCCP	Carbonyl cyanide-4-(trifluoromethoxy)phenylhydrazone
FIS1	Mitochondrial fission protein 1
FKBP12	FK506-binding protein
FOXO4	Forkhead box protein 4
FPLC	Fast protein liquid chromatography
GAPDH	Glyceraldehyde-3-phosphate dehydrogenase
GCV	Ganciclovir
GFP	Green fluorescent protein
GLB1	Galactosidase beta 1
GM-CSF	Granulocyte-macrophage colony-stimulating factor
GP78	Glycoprotein 78
GPS2	G-protein pathway suppressor 2
GTP	Guanosine-5'-triphosphate
H3K9me3	Tri-methylation of histone 3 lysine 9
HEK	Human embryonic keratinocytes
HEPES	N-2-hydroxyethylpiperazine-N-ethanesulfonic acid
HF-LPLI	High-fluence low-power laser irradiation
HHR	High-resolution respirometry
HIV-1	Human immunodeficiency virus 1
HMG	High mobility group
HRP	Horseradish peroxidase

HRPE	Human retinal pigment epithelial
HSP	Heat shock protein
HSP	H-strand promoter
HSV-TK	Herpes simplex virus 1 thymidine kinase
HUVEC	Human umbilical vein endothelial cell
IFI16	Interferon γ-inducible protein
IFN	Interferon
IGF	Insulin-Like growth factor
IKK	Inhibitor of nuclear factor kappa-B kinase
IKK	IκB kinase
IL	Interleukin
IMM	Inner mitochondrial membrane
INK-ATTAC	INK-linked apoptosis through targeted activation of caspase
IP-10	IFNγ inducible protein-10
IPF	Idiopathic pulmonary fibrosis
IRAK	Interleukin 1 receptor-associated kinase 1
IRF3	Interferon Regulatory Factor 3
ISC	Iron-sulphur clusters
JNK	c-Jun N-terminal kinases
LDs	Lipid droplets
LINE-1	Long interspersed element-1
LIR	LC3-interacting region
LSEC	Liver sinusoidal endothelial cell
LSP	L-strand promoter
MAF	Mouse adult fibroblasts
MAM	Mitochondria-associated membranes
MAP1LC3/LC3	Microtubule associated protein 1 light-chain 3
MAPK	Mitogen-activated protein kinase
MAVS	Mitochondrial anti-viral signalling
MCP-1	Monocyte chemoattractant protein 1
MDH1	Malate dehydrogenase
MDVs	Mitochondria-derived vesicles
MFF	Mitochondrial fission factor
MiDAS	Mitochondrial dysfunction-associated senescence
miMOMP	Minority mitochondrial outer membrane permeabilisation
MiNA	Mitochondrial network analysis
MMP	Mitochondrial membrane potential
MNRR1	Mitochondria nuclear retrograde regulator 1
MOMP	Mitochondrial outer membrane permeabilisation
MOTS	Mitochondrial open reading frame of the twelve S rRNA type-c
MPT	Mitochondrial permeability transition
MPTP	Mitochondrial permeability transition pore
mRNA	Messenger ribonucleic acid
MSK	Mitogen- and stress-activated protein kinase
mtDNA	Mitochondrial DNA

MFN1	Mitofusin 1
MFN2	Mitofusin 2
mTOR	Mechanistic target of rapamycin
MUL1	Mitochondrial E3 ubiquitin protein ligase 1
MVA	Modified vaccinia virus Ankara
MxA	Myxovirus resistance factor A
MxB	Myxovirus resistance factor B
NAD	Nicotinamide adenine dinucleotide (oxidised)
NADH	Nicotinamide adenine dinucleotide (reduced)
NAFLD	Non-alcoholic fatty liver disease
NAMPT	Nicotinamide phosphoribosyl transferase
NAO	Nonyl acridine orange
ND2	NADH dehydrogenase 2
NDP52	Nuclear domain 10 protein 52
NEMO	NF-κB essential modulator
NF-κB	Nuclear factor kappa-light-chain-enhancer of activated B cells
NLRP3	NLR family pyrin domain containing 3
NLRP3	Nucleotide Binding Domain and Leucine-Rich Repeat Pyrin Domain Containing 3
NLRs	NOD-like receptors
NLS	Nuclear localisation signal
NOD	Nucleotide binding and oligomerisation domain
NOTCH	Neurogenic locus notch homolog protein 1
NTR	Nitroreductase
OCR	Oxygen Consumption Rate
OIS	Oncogene-induced senescence
OMM	Outer mitochondrial membrane
OPA1	Optic atrophy 1
OXPHOS	Oxidative phosphorylation
MAPK p38	Mitogen-activated protein kinases p38
PAI2	Plasminogen-activated inhibitor-2
PBS	Phosphate-buffered saline
PD	Population doubling
PDGF-AA	Platelet-derived growth factor AA
PDK1	3-phosphatidylinositol-dependent kinase 1
PGC-1α	Peroxisome proliferator-activated receptor gamma coactivator 1-alpha
PGC1β	Peroxisome proliferator-activated receptor gamma coactivator 1-beta
PI	Phosphatidylinositol
PI3KCD	Phosphatidylinositol-4,5-bisphosphate 3-kinase delta catalytic subunit
PINK	PTEN-induced kinase 1
PINK1	PTEN Induced Kinase 1
PIP2	Phosphatidylinositol-biphosphate
PKC	Protein kinase C
PMSF	Phenylmethylsulphonyl fluoride
PNP	Polynucleotide phosphorylase

PNP	Polynucleotide phosphorylase
PRR	Pattern recognition receptor
PTEN	Phosphatase and tensin homolog
qPCR	Quantitative polymerase chain reaction
RANTES	Regulated on activation, normal T cell expressed and secreted
RB	Retinoblastoma protein
RFP	Red fluorescent protein
RIG-1	Retinoic acid-inducible gene-I
RLR	RIG-I-like receptors
RNA	Ribonucleic acid
RNR	Ribonucleotide reductase
ROS	Reactive oxygen species
RRM2	Ribonucleotide reductase M2
SAGA	Senescence-associated growth arrest
SAHF	Senescence associated heterochromatin foci
SASP	Senescence associated secretory phenotype
SA-ß-Gal	Senescence associated ß-galactosidase
SCAP	Senescent cell anti-apoptotic pathways
SDHA	Succinate dehydrogenase complex, subunit A
SIM	Structured illumination microscopy
SIRT3	Sirtuin 3
SLP2	SPFH family scaffold protein stomatin-like protein 2
SMAC	Second mitochondria-derived activator of caspases
SMS	Senescence-messaging secretome
SQSTM1/p62	Sequestosome 1
SSB	Single-strand DNA-binding protein
STING	Stimulator of interferon genes
TANK	TRAF family member-associated NF-kappa-B activator
TBK	TANK-binding kinase 1
TBK1	TANK Binding Kinase 1
TC	Tissue culture
TCA	Tricarboxylic acid cycle
TCA	Trichloroacetic acid
TEMED	Tetramethyl ethylenediamine
TFAM	Transcription factor A, mitochondrial
TGF-ß	Transforming growth factor-ß
TLRs	Toll-like receptors
TMRE	Tetramethyl rhodamine
TNF	Tumour necrosis factor
TOM20	Outer membrane translocase domain 20
TREX	Three prime repair exonuclease 1
TRF1	Telomeric repeat binding factor 1
TRF2	Telomeric repeat binding factor 2
UK	United Kingdom
UPR	Unfolded protein response

UQCRC2	Ubiquinol-cytochrome *c* reductase core protein 2
USA	United States of America
UV	Ultraviolet
VEGFA	Vascular endothelial growth factor A
VHL	Von Hippel-Lindau tumour suppressor
γH2Ax	Phosphorylated histone H2Ax

Chapter 1. Introduction

1.1 Cellular senescence

1.1.1 Preface – ageing and cellular senescence

Ageing is defined as an inevitable, time-dependent decline of organ and system functions leading to increased vulnerability to death (Lopez-Otin *et al.*, 2013; Zhang *et al.*, 2020). From the clinical standpoint, ageing is also the primary risk factor for the major chronic pathologies, known as age-related diseases, such as cancer, cardiovascular disorders including hypertension, stroke and heart failure; neurodegenerative diseases such as Alzheimer's disease, Parkinson's disease or frontotemporal dementia; osteoarthritis, diabetes mellitus and osteoporosis (Jaul *et al.*, 2017). At the cellular and molecular level, various processes are considered to drive these common ageing trajectories. The most fundamental of them being the accumulation of various deleterious changes to all biological molecules comprising the cell and the organism, commonly referred to as molecular damage. The manifestations of these uncountable nano-failures at the cellular scale were classified into the so-called hallmarks of ageing: genomic instability, telomere attrition, epigenetic alterations, loss of proteostasis, deregulated nutrient sensing, mitochondrial dysfunction, **cellular senescence**, stem cell exhaustion, and altered intercellular communication (Lopez-Otin *et al.*, 2013). Cellular senescence may be seen as a consequence of the most basic process of ageing – a consequence of endogenous stress, however also exogenous insults that multiple with age. From another perspective, senescence may be seen as a driver of ageing if the latter is defined as increased susceptibility to death. I will leave this semantic dilemma as an open question, however in accordance to a large number of recent publications, cellular senescence may be hailed as a cause and a common denominator of various age-related diseases. Importantly, cellular senescence is a clinically targetable phenomenon. Since the milestone discoveries demonstrating the feasibility to target cells in the state of senescence, similarly to cancer cells being targeted during anti-cancer therapies, the field of cellular senescence has become one of the most rapidly developing branches of the biology of ageing (Baker *et al.*, 2016; Baker *et al.*, 2011; Xu *et al.*, 2018; Zhu *et al.*, 2015). The efforts to manipulate cellular senescence for therapeutic purposes are motivated by the potential to delay not one but various age-related conditions, improving healthspan and potentially prolonging the lifespan. This is in line with the "geroscience hypothesis", which posits that developing therapies targeting the fundamental ageing process has a potential to be more

successful at treating age-related conditions than treating each individually (Robbins *et al.*, 2020). Strategies aimed at eliminating senescent cells are known as **senotherapies** and are currently being tested in clinical trials (Ellison-Hughes, 2020; Kirkland, Tchkonia, *et al.*, 2017; Zhu *et al.*, 2017). With high probability, interventions targeting cellular senescence will become one of the future tools in medicine (Gorgoulis *et al.*, 2019; Myrianthopoulos *et al.*, 2019). Meanwhile, uncharted territories of yet unexplored nuances in the mechanisms constituting the complex phenomenon of cellular senescence remain open for cell biologists, such as myself.

1.1.2 Cellular senescence - definition

Cellular senescence was initially described as an irreversible cycle arrest observed in human fibroblasts (Hayflick, 1965; Hayflick *et al.*, 1961). Since then, the understanding of this phenomenon has developed significantly, and now, cellular senescence is seen more broadly as a stress-response program or "cell fate" entered upon exposure to various endogenous or exogenous stressors which are not forceful enough to induce apoptosis (Childs *et al.*, 2014; Gorgoulis *et al.*, 2019; Kuilman *et al.*, 2010). Upon entering senescence, cells undergo profound phenotypic changes. Some of these constitute the senescence program – preventing cells from resuming cycling or allowing for communication with the microenvironment via Senescence-Associated Secretory Phenotype (SASP) (Coppe *et al.*, 2008; Kuilman *et al.*, 2008). From an evolutionary perspective, cellular senescence probably appeared as mechanism mediating physiological processes that require tissue remodelling, such as organ patterning during embryonic development and would healing – due to the inseparable secretory status (Demaria *et al.*, 2014; Munoz-Espin *et al.*, 2013). Numerous findings point out cellular senescence is the first barrier against tumorigenesis, again proposing an evolutionary origin and indicating its beneficial role for the organism (Courtois-Cox *et al.*, 2008; Serrano *et al.*, 1997; Sharpless *et al.*, 2001). However, the unresolved pro-inflammatory status, apoptotic resistance and metabolic alterations constitute the dark sides of cellular senescence, exerting detrimental effects on the tissue and organ function where senescent cells' abundance crosses a certain threshold (Coppe *et al.*, 2010). Especially in the context of their prolonged survival during ageing, when the clearance mediated by immune cells is compromised, senescent cells repeatedly prove to be responsible for organ dysfunction and age-related pathologies (Baker *et al.*, 2016; Gorgoulis *et al.*, 2019).

1.1.3 Models of cellular senescence *in vitro*

In cell culture, cellular senescence may be triggered by a variety of different stimuli. The first context where the term "senescence" appeared was the discovery by Hayflick and Moorhead in 1961, who described that the primary cells have a finite lifespan when cultured *in vitro* (Hayflick, 1965; Hayflick *et al.*, 1961). Replicative senescence defined as a limited proliferative potential of primary cells in culture has been later mechanistically linked to the replication-dependent telomere attrition (Bodnar *et al.*, 1998; Harley *et al.*, 1990; von Zglinicki, 2002). Eukaryotic cells possess linear chromosomes capped by the so-called telomeres, repetitive DNA sequences of TTAGGG (Meyne *et al.*, 1989). Telomeres are thought to form a lariat-like structure called telomere-loop (t-loop) which is stabilised by several telomere binding proteins collectively known as the "shelterin" complex, composed of several proteins, such as telomeric repeat factor 1 (TRF1) and 2 (TRF2) and others (Longhese *et al.*, 2012). Their role is to prevent chromosome end fusion. Each cell division, however, results in shortening of the telomeres due to the inability of DNA polymerases to replicate the telomere C-rich lagging-strand. During the process of lagging-strand synthesis, RNA primers allow DNA polymerases to initiate DNA replication, however, upon removal of the last primer from the 3′ end, the newly synthesised strand will inevitably become shorter (d'Adda di Fagagna *et al.*, 2003; de Lange, 2002; Griffith *et al.*, 1999; McClintock, 1941; Watson, 1972). Exposure of the telomere end is able to activate DNA damage response (DDR) that further signals to mediators of cell cycle arrest. *The DDR-mediated cell cycle arrest in described in detail in section 1.4.1.* Ectopic expression of telomerase was shown to allow for the bypass of senescence-induced cell cycle arrest (Bodnar *et al.*, 1998). Therefore, telomere shortening was established as the mechanism explaining the phenomenon of replicative senescence. Due to telomere-independent functions of telomerase, however, it is possible that other mechanisms, such as improved mitochondrial function, could mediate the longer replicative lifespan of cells upon telomerase overexpression, challenging the view that replicative senescence is solely telomere-driven (Ahmed *et al.*, 2008; Martens *et al.*, 2019).

In contrast to replicative senescence, other types of cellular senescence are more rapid and referred to as premature senescence. Until this date, dozens of premature cellular senescence phenotypes have been reported (Petrova *et al.*, 2016). The first group of senescence types, broadly referred to as stress- or damage-induced senescence, can be caused by broad-range damage to cellular components, for example, via ionizing or UV irradiation and oxidative stress (Gorgoulis *et al.*, 2019; Pascal *et al.*, 2005; Roper *et al.*, 2004; Toussaint *et al.*, 2000;

Toussaint *et al.*, 2002; von Zglinicki, 2002). It has been shown, however, that damage to specific cellular sub-compartments is sufficient to induce cellular senescence. Genotoxic compounds affect nuclear genome stability through several mechanisms, including DNA replication stress, inhibition of DNA topoisomerase, as well as cross-linking of DNA strands (Aird *et al.*, 2015; Di Leonardo *et al.*, 1994; Di Micco *et al.*, 2006; Petrova *et al.*, 2016; Santarosa *et al.*, 2009; te Poele *et al.*, 2002). This type of senescence is referred to as DNA-damage induced senescence (Di Leonardo *et al.*, 1994). Increasing proteotoxic stress by interfering with proteasome function, ER stress, unresolved unfolded protein response (UPR) as well as autophagy also lead to the induction of cellular senescence (Cormenier *et al.*, 2018; Kang *et al.*, 2011; Pluquet *et al.*, 2015; Torres *et al.*, 2006).

Activation of oncogenes or inactivation of tumour suppressors constitute another group of cellular stressors that trigger, the so-called, oncogene-induced senescence (OIS) (Serrano *et al.*, 1997). The landmark study by Serrano and colleagues (1997) demonstrated that activation of oncogenic signalling does not necessarily lead to unlimited proliferation, but an intrinsic anti-tumour mechanism in the form of senescence is able to prevent it. Oncogenes whose overexpression or activation initiates cellular hyperproliferation that ceases due to engagement of senescence mechanisms, include: *RAS* (Braig, Lee, Loddenkemper, Rudolph, Peters, Schlegelberger, Stein, Dorken, *et al.*, 2005; Collado *et al.*, 2005; Mason *et al.*, 2004), *CCNE1* encoding cyclin E (Bartkova *et al.*, 2006), *MYC* (Vafa *et al.*, 2002), *BRAF(V600E)* (Dankort *et al.*, 2007; Dhomen *et al.*, 2009), *MOS*, *CDC6* and *E2F1* (Braig *et al.*, 2006; Gorgoulis *et al.*, 2010; Maya-Mendoza *et al.*, 2015). Among these, OIS driven by protein RASV12 activation (thereafter, referred to as "driven by RAS" for simplicity) is one of the most commonly studied models. There are in fact 3 *RAS* genes in humans: *K*-, *H*- and *N*-*RAS*. *RAS* genes encode low molecular weight G proteins that play a role in mediating the communication between cell surface receptors and intracellular effects regulating cellular growth, survival and metabolism (Fiorucci *et al.*, 1988). Their activity is orchestrated by binding of guanine nucleotides (GTP). Following activation and GTP binding, RAS activates several downstream effectors including mitogen-activated protein kinase (MAPK) cascade and phosphoinositide 3-kinases (PI3K) - protein kinase B (AKT) pathways (Maruta *et al.*, 1994). Mutations in RAS genes that are frequent in human cancers concern the GTP binding site, locking RAS in a constitutively active state (Maya-Mendoza *et al.*, 2015; Primo *et al.*, 2019). V12 in protein name indicates the protein's activated state (Primo *et al.*, 2020). OIS is thought to be triggered by the initial aberrant proliferation causing DNA replication stress and chromosome instability (Di Micco *et*

al., 2006; Suram *et al.*, 2012). Even though the event of hyperproliferation during the course of OIS development does not characterise other types of senescence such as damage-induced senescence, the fact that it leads to DDR activation, suggests a mechanistic overlap (Kuilman *et al.*, 2010). Additional mechanisms act to ensure sufficient nuclear DNA damage and cell cycle arrest. For example, OIS was found to be associated with down-regulation of ribonucleotide reductase M2 (RRM2) – a regulatory component of the ribonucleotide reductase (RNR), a complex that executes the rate-liming step in *de novo* pathway of deoxyribonucleotide triphosphates (dNTPs) generation. dNTPs are the building blocks during DNA synthesis for nuclear and mitochondrial DNA replication as well as repair processes. Down-regulation of RRM2 leads to a significant reduction in dNTPs levels (Aird *et al.*, 2013; Mannava *et al.*, 2013). Manipulating the levels of dNTPs via ectopic expression of RRM2 or supplementation of exogenous nucleosides prevents the initial aberrant replication and further cell cycle arrest (Aird *et al.*, 2013). This finding highlights the importance of DDR for the establishment of cell cycle arrest in OIS. Within OIS group, there are also other mechanisms that are independent from aberrant proliferation and replication stress - DDR-independent, such as metabolic imbalance, that play a role in mediating senescence. Inactivation of tumour suppressor genes – *PTEN*, *VHL*, *RB* and *NF1* - serve as examples of this senescence variant (Jung *et al.*, 2019; Larribere *et al.*, 2015; Young *et al.*, 2008).

Cellular senescence may also be induced as a consequence of metabolic imbalance independent on oncogene-activation (Wiley & Campisi, 2016). Especially in conditions indicating insufficient energy supply, cellular senescence comes into play. Several important energy sensors – when signalling inadequate energy levels, were shown to mediate cellular senescence. AMP-activated protein kinase (AMPK) is an evolutionarily conserved fuel-sensing enzyme. It is activated in response to the increased cellular concentration of adenosine monophosphate (AMP) relative to adenosine triphosphate (ATP) – the key energy carrier within the cell (Garcia *et al.*, 2017). Constitutively active AMPK or its pharmacological activation induces cellular senescence (Wang *et al.*, 2003). Another energy sensing hub concerns the process of transporting the reduced form of nicotinamide adenine dinucleotide (NAD^+) – NADH, between mitochondrial intermembrane space and mitochondrial matrix. NADH, next to ATP, is another critical energy carrier, generated via glycolysis. Mitochondrial inner membrane is impermeable to NADH, while it is needed inside the mitochondria to enter tricarboxylic acid cycle (TCA). The shuttle consists of enzymes that oxidise it again – by reducing oxaloacetate to malate, which is able to cross the membrane. Inhibiting oxidation of

NADH through depletion of cytosolic malate dehydrogenase (MDH1), a component of the malate-aspartate shuttle was shown to be another metabolic imbalance-associated senescence inducer (Lee *et al.*, 2012). Similarly, an impairment of the NAD^+ salvage pathway, a recycling process for cellular NAD^+ pools, can cause cellular senescence (van der Veer *et al.*, 2007). Various interventions that interfere with mitochondrial function have also been shown to induce senescence, including inhibition of electron transport chain complexes (Moiseeva *et al.*, 2009; Stockl *et al.*, 2007; Yoon *et al.*, 2006), proton gradient uncoupling (Stockl *et al.*, 2007), mtDNA depletion (Wiley, Velarde, *et al.*, 2016), as well as interfering with fission/fusion machineries (Lee 2007, Park 2010). Mitochondrial stresses are considered to induce the sub-type of cellular senescence, referred to as Mitochondrial Dysfunction-Associated Senescence (MiDAS) (Wiley, Velarde, *et al.*, 2016).

Considering that such a wide variety of stressors drives cells into senescence, the phenomenon of cellular senescence appears as a universal stress-response programme (Serrano *et al.*, 1997; te Poele *et al.*, 2002; Wiley, Velarde, *et al.*, 2016). A very diverse range of alterations to normal cellular function may lead to a variant of cellular senescence. In the following section, I would like to describe the mechanisms that govern cellular senescence and where sufficient knowledge is available, I aim to highlight the differences between the studied models of senescence.

1.1.4 Mechanisms of cellular senescence

There are several hallmarks that unify different variants of cellular senescence. The core ones that invariably define senescence are the stable proliferative arrest and the altered secretome known as SASP. The cell cycle arrest combined with activated growth pathways enforces cells to undergo morphological alterations, such as an increase in the soma size (Ogrodnik, Salmonowicz, Jurk, *et al.*, 2019; Soto-Gamez *et al.*, 2019). Senescent cells activate pro-survival pathways – another conserved feature of senescence – that allow them to survive despite sublethal stresses (Soto-Gamez *et al.*, 2019). Moreover, senescent cells enhance the lysosomal hydrolase activity, a characteristics termed senescence-associated β-galactosidase (SA-β-gal) as a result of overexpression and accumulation of the lysosomal β-galactosidase (Dimri *et al.*, 1995). Another canonical feature includes the down-regulation of lamin-B1, a protein constituting the nuclear lamina, bedding the nuclear envelope from the inside (Freund *et al.*, 2012; Ivanov *et al.*, 2013; Shimi *et al.*, 2011). Ultimately, senescence cells undergo remodelling of chromatin that, among other functions, enhances SASP through activated gene expression (Shah *et al.*, 2013). Senescent cells are also characterised by an ongoing loss of the nuclear

DNA via formation of cytosolic chromatin foci (CCFs) (Ivanov *et al.*, 2013). Arguably, most of the other senescence characteristics are less specific. For example, chromatin remodelling process that leads to the formation of heterochromatin domains, known as senescence-associated heterochromatin foci (SAHF), responsible for the maintenance of the stable cell cycle arrest as well as apoptosis resistance, is not present in all types of senescence (Kosar *et al.*, 2011). Even though several common denominators of senescence may be defined, they still differ in terms of the mechanistic regulation and the final form, for example, the exact composition of the secretory phenotype. In the following sections, I would like to discuss in detail the mechanisms governing cellular senescence that are of the highest importance in the light of this thesis, namely establishment of cell cycle arrest, regulation of SASP, mitochondrial biology and pro-survival pathways.

1.1.4.1 Establishment of irreversible cell cycle arrest

Cells are equipped with the ability to enter a transient cycle arrest in response to relatively mild stresses with the purpose of repairing damage before allowing the cell to resume proliferation (Branzei *et al.*, 2008). Cellular senescence is characterised by an irreversible cell-cycle arrest, also referred to as senescence-associated growth arrest (SAGA). Entry into cellular senescence is regulated by two major signalling pathways: DNA damage response (DDR) pathway that is mediated by p53 and a p16INK4a/RB-dependent (p16-RB) pathway (Herbig *et al.*, 2006). Typically, both p53-p21 axis and p16-RB are engaged in the establishment of the cell cycle arrest in cellular senescence, and p53-p21 upregulation constitutes the first line of action, as observed for replicative, RAS-driven oncogene- and γ-irradiation-induced senescence in human fibroblasts (De Cecco *et al.*, 2019; Stein *et al.*, 1999). Even though these two mechanisms are canonical and serve as senescence markers, their engagement may differ between different senescence variants and cell types (Campisi *et al.*, 2007).

The first of these pathways involves a signal amplification cascade - DNA damage response as the mediator of cell cycle arrest (Campisi *et al.*, 2007). Telomere shortening, DNA damage due to exogenous stress as well as replication stress resulting in DNA lesions activate the DNA damage sensor – ataxia telangiectasia mutated (ATM), which is recruited to the sites of DNA double-stand breaks. Ataxia telangiectasia and Rad3-related protein (ATR) is recruited to the sites of DNA single stand breaks. These are the seeds for subsequent recruitment of repair machinery, involving DNA damage checkpoint protein-1 and 53BP-1, which play the boosters role in the positive feedback loop to further recruit ATM complexes, and activate checkpoint-

1 and 3 (CHK1 and CHK2) (d'Adda di Fagagna, 2008; Jackson *et al.*, 2009). CHK1 and 2 are then able to diffuse in the nucleus and relay the signal to sites distant to DNA damage in the nucleus. This recruits the major cellular stress sensor, p53. Depending on the stress load, activation of p53 may result in different cell fates (Campisi *et al.*, 2007). In the context of senescence, p53 induces expression of multiple target genes which control the cell cycle progression (Childs *et al.*, 2014; Rufini *et al.*, 2013). The main and widely studied is the cyclin-dependent kinase inhibitor 1, or p21 (known also as p21Cip1, or p21Waf1). p21 inactivates cyclin complexes, such as E/CDK2 which function is to phosphorylate the tumour suppressor retinoblastoma protein (RB). These phosphorylation events lead RB-mediated transcription of genes required for DNA replication and cell cycle progression. The downstream section of the pathway of cyclin complexes inhibition is shared with the second critical pathway maintaining the cell cycle arrest - p16-RB axis. Another stress-induced cyclin-dependent kinase inhibitor p16INK4A but also other INK4 family proteins, including p15INK4b, p18INK4c, and p19INK4d, are in place to prevent phosphorylation of RB (Campisi *et al.*, 2007; Rufini *et al.*, 2013).

ATM-p53-p21 axis is engaged in models induced by DNA-damaging agents, but also in oncogene-induced senescence. DNA damage and DDR in OIS driven by RAS are primarily caused by aberrant proliferation and replication stress, which occur during the initial hyperproliferation phase (Di Micco *et al.*, 2006). Replicative and damage-induced senescence are known to further activate a positive feedback loop, where DDR is maintained by p21 mediated changes to mitochondria, resulting in an increased mitochondrial ROS production (Passos *et al.*, 2010). Mitochondrial ROS cause - in a direct or indirect manner – the formation of new DNA damage foci (Passos *et al.*, 2010). DDR in OIS driven by RAS was also linked to mitochondrial dysfunction with increased ROS generation (Moiseeva *et al.*, 2009). Collectively, DDR activation is a common mechanism between the major studied models of senescence, such as damage-induced and oncogene-induced senescence driven by RAS.

DDR activation is not characteristic to all senescence models, even such that still rely on p53-p21 axis. This mechanism is termed DDR-independent cell cycle arrest (van Deursen, 2014). When OIS is considered, the hyperproliferation phase does not occur in all types classified as oncogene-induced, for example: *BRAF(V600E)* expression, loss of *PTEN*; ectopic expression of p19Arf - an alternate reading frame protein product of the *CDKN2A* locus, programmed developmental senescence (Alimonti *et al.*, 2010; Freund *et al.*, 2011; Kaplon *et al.*, 2013; Munoz-Espin *et al.*, 2013; Storer *et al.*, 2013). It is worth highlighting that the

epithelial model of RAS activation engages a distinct mechanism mediating cell cycle arrest than the commonly used fibroblast model, and is also DDR-independent (Cipriano *et al.*, 2011). A mechanism that drives p53 activation independently of DDR has been deciphered for *PTEN* loss-induced senescence. PTEN is the major negative regulator of the PI3K/AKT pathway. A recent study found that mechanistic target of rapamycin (mTOR) kinase, the component of mTOR complex 1 (mTORC1) and mTOR complex 2 (mTORC2), a critical relay molecule downstream of PI3K/AKT, is able to directly bind and phosphorylate p53 at serine 15 (Jung *et al.*, 2019). Another model of senescence suggested to occur independently from DDR is the MiDAS (Wiley, Velarde, *et al.*, 2016). In the fibroblast model overexpressing RAS, where DDR was confirmed, another layer of DDR-independent p53 activation was characterised. Namely, p53 is additionally activated via a downstream kinase in the MAPK signalling cascade, called p38-regulated/activated protein kinase, PRAK. PRAK may be considered a tumour suppressor gene and is able to directly phosphorylate p53 (Sun *et al.*, 2007). Finally, developmental senescence occurring during tissue remodelling and embryonic development, was found to be p21-dependent however p53-independent (Munoz-Espin *et al.*, 2013; Storer *et al.*, 2013). These studies would point out that p21-dependent cell cycle arrest is therefore a universal mechanism in various types of senescence. Yet, there are also types of senescence, where the two pathways: p53-p21 and p16-RB, are not activated at all. For example, another model of OIS driven by oncogenic RAF, lying directly downstream from RAS in MAPK signalling pathway, serves as an example. In fibroblast and epithelial models, senescence is established independently of p53 function (Olsen *et al.*, 2002). In the fibroblast model, senescence still relies on increased expression of p16. In epithelial cells, however, both p21 and p16 are dispensable (Olsen *et al.*, 2002). Overall, these findings are of significant importance, as they indicate senescence is possible without the canonical senescence effectors.

1.1.4.2 Senescence-Associated Secretory Phenotype

An altered secretome, a common feature of senescent cells, is known as SASP or senescence-messaging secretome (SMS) (Kuilman *et al.*, 2009). An interesting view on cellular senescence and SASP was proposed in a recent review article by Lopes-Paciencia and colleagues (2019). Namely, senescence is seen as a gene reprogramming process that "turns any cell type into a secretory cell" (Lopes-Paciencia *et al.*, 2019). SASP is composed of growth factors, extracellular matrix (ECM) degrading proteins, angiogenic factors, pro-inflammatory cytokines and chemokines, lipids, such as bradykines, ceramides, and prostanoids, microRNAs,

extracellular vesicles and probably other, yet unidentified types of bioactive molecules (Robbins *et al.*, 2020). In the still early days of cellular senescence research, when only some of the senescence markers were known, increased levels of plasminogen activator inhibitor-1 (PAI-1), serine protease inhibitor, was found to be secreted by cells in OIS (Serrano *et al.*, 1997). SASP, as a complex phenotype, was described only later by Coppe *et al.* (2008). The composition of SASP across different senescence variants, indicating the degree of up-regulation of specific components, has been summarised in the review by Freund *et al.* (2010) as well as recently, taking into account the newly discovered classes of biomolecules, by Robbins *et al.* (2020). SASP composition depends on the tissue of origin (Coppe *et al.*, 2008), senescence inducer (Childs *et al.*, 2015; Hernandez-Segura *et al.*, 2017) as well as the role of cells that enter senescence. For example, SASP of senescent cells associated with tissue repair include matrix metalloproteinases (MMPs) and growth factors, such as platelet-derived growth factor subunit A (PDGF-A) and vascular endothelial growth factor (VEGF). The major pro-inflammatory factors known for DIS and OIS, are not secreted in this context (Storer *et al.*, 2013). In contrast, age-associated or therapy-induced senescent cells mainly increase the inflammatory factors, including the major interleukin 6 (IL6) and interleukin 8 (IL8) (Coppe *et al.*, 2010; Freund *et al.*, 2010). Interestingly, IL6 and IL8, are absent in MiDAS (Wiley, Velarde, *et al.*, 2016). Apart from the qualitative SASP composition, also quantitative differences in terms of transcription and translation of SASP factors are observed (Coppe *et al.*, 2010; Coppe *et al.*, 2008). For example, the SASP of oncogene-induced senescence, even though lacks certain components such as growth factors and proteases (Coppe *et al.*, 2010), is significantly more powerful in terms of the levels of the pro-inflammatory cytokines, including IL6 and IL8, at both transcriptional and secretory levels (Coppe *et al.*, 2008; Takahashi *et al.*, 2018).

The function of SASP is thought to primarily allow for the communication with immune system. Senescent cells possess intrinsically enhanced survival mechanisms that prevent them from dying via apoptotic pathway. SASP factors recruit immune cells, such as macrophages, natural killer (NK) cells or T cells into tissues, whereby mediate immunological clearance of senescent cells (Biran *et al.*, 2015; Irvine *et al.*, 2014; Krizhanovsky *et al.*, 2008). Various SASP factors may play additional roles, influencing tissue microenvironment. For example, transforming growth factor beta 1 (TGF-β) that is considered an early SASP component, promotes proliferative arrest of neighbouring cells. However, the majority of cytokines are thought to either promote tumorigenesis or drive senescence of neighbouring cells. Secreted

metalloproteinases may support tissue repair but on the flip side, also allow for tumour progression (Liu *et al.*, 2007). Especially, prolonged SASP – not resolved within a specific frame of time - has a detrimental impact on the tissue function and contributes to age-related low-grade inflammation (Lopes-Paciencia *et al.*, 2019; Salminen *et al.*, 2012). Another remarkable consequence of the long-term persistence of senescent cells in the tissue is the exhaustion of stem cell function, impairing regeneration (Robbins et al. 2020). Importantly, several studies thus far demonstrated that the two key features of senescence – cell cycle arrest and SASP - can be molecularly uncoupled (Correia-Melo *et al.*, 2016; Dou *et al.*, 2017; Laberge *et al.*, 2015; Lau *et al.*, 2019). It is generally assumed that supressing SASP without bypassing the proliferative arrest is therapeutically desired, therefore much attention is devoted to the mechanisms that govern the pro-inflammatory phenotype of senescent cells. In the following paragraphs, I would like to discuss the most upstream mechanisms inducing SASP, including the well-established nuclear DNA damage (Rodier *et al.*, 2009) and the relatively recent findings of innate immunity machineries involved in the orchestration of SASP (Dou *et al.*, 2017; Gluck *et al.*, 2017; Takahashi *et al.*, 2018)); transcriptional regulation of SASP as well as SASP enhancement processes such as the prominent intracrine/autocrine interleukin loops and metabolic control (Freund *et al.*, 2010; Lopes-Paciencia *et al.*, 2019; Salminen *et al.*, 2012; Salotti *et al.*, 2019).

At the transcriptional level, the control of SASP relies on several key transcription factors that are generally associated with the regulation of cellular stress and inflammatory signals, among others - the nuclear factor kappa-light-chain-enhancer of activated B cells (NF-κB) and CCAAT-enhancer-binding protein β (C/EBPβ) (Huggins *et al.*, 2013; Lopes-Paciencia *et al.*, 2019; Salotti *et al.*, 2019). These two signals act in cooperation, where C/EBPβ may stimulate NF-κB. There is also a significant overlap of the target genes between the two transcription factors.

NF-κB signalling is known as an important immune regulator orchestrating innate and adaptive immunity systems (Solt *et al.*, 2008). In general, NF-κB transcription factors consist of complexes of NF-κB components and the Rel-like domain-containing proteins. One subunit of each family together form a dimer where p50/p65 (known as RelA) heterodimer is reported as the most abundant form. However, the combinations of dimers that may be formed, determine the heterogeneous regulation of NF-κB target genes (Solt *et al.*, 2008). The complexes are presented in inactive forms in the cytoplasm. Their inhibition depends on the binding to IκB inhibitory proteins, such as the nuclear factor of kappa light polypeptide gene

enhancer in B-cells inhibitor, alpha (IκBα). A multi-subunit IκB kinase (IKK) complex that consists of two kinases - IKKα and IKKβ, and a regulatory subunit known as NF-κB essential modulator (NEMO), phosphorylates the inhibitory factors, which in turn undergo the ubiquitin-dependent proteasomal degradation. The release of the inactive complexes by inhibitory factors – turning them into active complexes, and their translocation to the nucleus constitute the basis of NF-κB signalling. Other mechanisms may facilitate the activation of NF-κB signalling. For example, NF-κB was found to be regulated by C/EBPβ. C/EBPβ may down-regulate the transcription of one of the inhibitory factors, IκB-α (Cappello *et al.*, 2009). Another important mechanism includes p38 mitogen-activated protein kinase (p38MAPK) – a key cellular stress sensor – that is activated in response to various stimuli, such as oxidative stress, metabolic imbalance, DNA damage, heat shock or mechanical stress (Freund *et al.*, 2011; Salminen *et al.*, 2012). It is established that p38MAPK activates mitogen- and stress-activated protein kinases, MSK1 and MSK2, which can potentiate NF-κB signalling by phosphorylating the transactivating p65 subunit of the NF-κB complex (Salminen *et al.*, 2012). A study that demonstrated the degree of involvement of NF-κB in the context of cellular senescence, identified the p65 subunit of NF-κB as one of the most significantly enriched factors bound to the chromatin in senescent cells. NF-κB signalling is thought to be driven by an essential component of DDR, ATM kinase and mediate the expression of IL6 and IL8 (Rashi-Elkeles *et al.*, 2006; Rodier *et al.*, 2009). Later, Chien and colleagues (2011) demonstrated that NF-κB is a master regulator of the SASP beyond IL6 and IL8, as well as it performs a tumour suppressive, anti-proliferative function in cellular senescence (Chien *et al.*, 2011). The target genes activated by NF-κB concern SASP factors, such as cytokines (IL6, IL8, tumour necrosis factor α (TNFα)), chemokines (monocyte chemoattractant protein 1 (MCP1), regulated on activation, normal T cell expressed and secreted (RANTES), chemokine (C-X-C motif) ligand 1 (CXCL1)) but also the cell cycle regulatory and anti-apoptotic factors (B-cell lymphoma 2 (BCL2), BCL2-related protein A1 (BFL1), BCL2-like protein 2 known also as BCL-W) (Chen, Edelstein, *et al.*, 2000; Pahl, 1999).

Although the study by Chien *et al.* (2011) did not focus on C/EBPβ, it confirmed C/EBPβ as the second transcription factor the most strikingly enriched in the chromatin of senescent cells, whose role was first demonstrated by Sebastian and colleagues (2005) for RAS-driven senescence and Kuilman and colleagues (2008) for the BRAF(V600E) model (Kuilman *et al.*, 2008; Sebastian *et al.*, 2005). C/EBPβ is known to participate in transcriptional regulation of inflammatory responses as well as cell cycle regulation. It belongs to the transcription factors

family of CCAAT/enhancer binding proteins containing the basic region: leucine zipper (bZIP), binding to DNA as a dimer - either as a homo- or as a heterodimer. Interestingly, the heterodimer consisting of C/EBPβ and another member of the family, C/EBPγ, inhibits senescence, while C/EBPβ homodimer drives the phenotypes of senescence (Huggins *et al.*, 2013). This includes the expression of IL1β, IL6 and IL8. An interesting finding described the kinetics of C/EBPβ action in relation to neurogenic locus notch homolog protein 1 (NOTCH1) in the model of OIS (Hoare *et al.*, 2016). Authors of the study identified an early phase of SASP, aka "first wave", occurring around 2-4 days post senescence induction that depends on NOTCH1 signalling, and comprises of TGF-1β. NOTCH1-mediated signalling is then replaced by a second wave of SASP mediated via C/EBPβ. The second wave comprises of the SASP factors that are commonly associated with this type of senescence, such as IL6 and IL8 (Hoare *et al.*, 2016). It must be highlighted that these cornerstone studies utilised mainly the models of OIS, including only limited data on other senescence models. With regards to the activation of NOTCH1, it has independently been reported for primary human endothelial cells entering replicative senescence (Venkatesh *et al.*, 2011). When the initial triggers of C/EBPβ are considered, it is a downstream component of MAPK cascade - extracellular signal-regulated protein kinase (ERK1/2) that executes the activating phosphorylation of C/EBPβ. This pathway is directly activated by RAS and its downstream targets, therefore in various modes of OIS, C/EBPβ is inevitably activated. Apart from OIS, in cellular senescence induced by topoisomerase inhibition by camptothecin, the levels of phosphorylated ERK were also found to be elevated (Takauji *et al.*, 2016). In contrast, replicative senescence is associated with a downregulation of ERK signalling while the restoration of nuclear ERK activity leads to the senescence bypass and extends cells' replicative lifespan (Lorenzini *et al.*, 2002; Tresini *et al.*, 2007).

Recently, several articles demonstrated the role of cytosolic DNA and its sensing by cyclic GMP-AMP synthase (cGAS), as key process for SASP development. It is generally established that senescent cells are characterised by the transcriptional down-regulation of Lamin B1 (Shimi *et al.*, 2011) and its autophagy-mediated degradation (Ivanov *et al.*, 2013) – processes that allow for nuclear DNA release in the form of cytosolic chromatin foci (CCF). DNA damage is of key importance in this context as it allows for disassociation of chromatin buds that are defined by the markers of DNA damage. The recent studies on the involvement of cGAS pathway in cellular senescence utilised the widest range of senescence models, in contrast to the previous articles focusing on mainly one and usually OIS or replicative

senescence models. Collectively, Dou *et al*. (2017), Gluck *et al.* (2017), and Takahashi *et al.* (2018) demonstrated the role of cGAS pathway as well as the formation of cytosolic chromatin fragments in: mouse embryonic fibroblasts induced to senescence via oxidative stress, γ-irradiation and palbociclib, a pharmacological compound that inhibits cyclin-dependent kinase 4 (CDK4) as well as human senescence models: DIS induced by γ-irradiation, OIS driven by HRasV12, genotoxic stress induced using etoposide and replicative exhaustion. Moreover, one of these studies that reported a down-regulation of cytosolic DNAses – a process that allows for accumulation of cytosolic DNA in the cytoplasm of senescent cells, apart from utilizing replicative and oncogene-induced senescence in human diploid fibroblasts, additionally, tested primary human retinal pigment epithelial (HRPE) and primary human embryonic keratinocyte (HEK) cells (Takahashi *et al.*, 2018). Therefore, the phenomenon of cGAS pathway involvement in SASP regulation is a universal aspect of various models of senescence. In brief, cGAS signalling pathway begins by cGAS binding to the cytosolic DNA and the production of a secondary messenger, cyclic GMP–AMP (cGMP) which in turn activates the adaptor protein known as stimulator of interferon genes (STING). Next, STING traffics through the ER to the Golgi apparatus. There, it phosphorylates TANK-binding kinase 1 (TBK1), which in turn phosphorylates the interferon regulatory factor 3 (IRF3) upon its docking at STING. Phosphorylation signal activates IRF3 that dimerises and translocates into the nucleus to induce the transcription of type I interferons (IFN-1). However, STING relays the signal also in another major direction, namely NF-κB. Specifically, it was found to interact with IKK kinase that mediates the activation of NF-κB (Balka *et al.*, 2020). Dou *et al.* (2019) demonstrated that IRF3 arm of cGAS signalling pathway is inhibited in senescence (at least, the early stage of senescence investigated in their article) by p38MAPK (Dou *et al.*, 2017). Importantly, STING may become activated via a non-canonical pathway triggered by DNA damage that is independent from cGAS (Dunphy *et al.*, 2018). The study that reported this alternative pathway pointed out the key role of ATM in this process. Interestingly, cGAS independent pathway preferentially activates NF-κB over IRF3, which might be of importance in senescence that is characterised by high level of DNA damage, a strong reliance on NF-κB and initial absence of IRF3 signalling (Dou *et al.*, 2017; Dunphy *et al.*, 2018). When IRF3 comes into play in the context of cellular senescence, however, was reported recently by De Cecco *et al.* (2019) who identified a late phase of SASP consisting of IFN-1. It is driven by de-repression of long interspersed element-1 (LINE-1) retrotransposable elements – an event that does occur during early senescence, however is inhibited by other mechanisms, such as a high expression of RB

and cytosolic DNAse three prime repair exonuclease 1 (TREX1). Failure of the host surveillance systems for these elements 16 weeks post senescence induction allows for the levels of LINE-1 cDNA to rise and be detected by cGAS, driving IFN genes expression. This phenomenon was observed for damage-, oncogene- induced and replicative senescence (De Cecco *et al.*, 2019).

Another group of cytosolic DNA sensors constitute the pattern-recognition receptors (PRRs) that trigger inflammatory responses. Among these, enzymatically active complexes known as the inflammasomes were identified to play a role in cellular senescence. Inflammasome complexes are composed of multiple subunits, where the members of the nucleotide binding and oligomerisation domain (NOD)-like receptors (NLRs) are critical for activation by nucleic acids and other DAMPs (Platnich *et al.*, 2019). Upon activation, inflammasomes recruit and induce proteolytic activity of the cysteine-aspartic protease caspase-1 that mediates maturation of cytokines such as IL1α, IL1β or IL18. NLR family pyrin domain containing 3 (NLRP3) inflammasome were shown to regulate SASP, allowing for maturation of IL1α – a key cytokine that reinforces SASP (*described below*) (Acosta *et al.*, 2013). Other inflammasome adaptors that were identified to function in cellular senescence are absent in melanoma 2 (AIM2) and gamma-interferon-inducible protein IFI16 (IFI16) (Chen *et al.*, 2018; Choubey *et al.*, 2016). According to my knowledge, however, even though inflammasomes are known to be activated by DAMPs that were shown to be present in senescent cells, no study thus far demonstrated what kind of DAMPs activate this pathway specifically in senescent cells.

Another PRRs shown to be of key importance in the regulatory network of SASP are the toll-like receptor 2 (TLR2) and its partner TLR10. A recent study added another layer to the complex picture of SASP regulation where these two factors are engaged (Hari *et al.*, 2019). The study demonstrated TLRs' engagement in both cell cycle inhibitory process and the SASP. Remarkably a novel class od DAMPs in the context of cellular senescence and SASP had been identified – acute-phase serum amyloids (A-SAAs), A1 and A2. The expression of A-SAAs is coordinated with the expression of TLR2 in the model of OIS (at day 5 post senescence induction), and TLR2 silencing supresses their expression, while its activation or overexpression induces it (Hari *et al.*, 2019). Moreover, A-SAAs are secreted outside of the cells and interact with TLR2 that further signals to p38MAPK and NF-κB, indicating the multiplicity of directions from which the activating signals arrive at these key SASP nodes. The whole set of experiments was performed in OIS, however authors mention that the mechanism is likely to act in other acute stresses such as oncogene activation (such as BRAFV600E) or

DNA damage, but not in replicative senescence, based on the TLR2, SAA1, and SAA2 expression in these models (Hari *et al.*, 2019).

High mobility group (HMG) family of proteins, the non-histone chromatin-binding proteins, relay a danger signal when present outside of its regular location, also in cellular senescence. In contrast to HMGA proteins that play roles in senescence by accumulating in the chromatin of senescent cells, structurally supporting SAHFs and to HMGB2 that stays in the nucleus and reinforces SASP by preventing the incorporation of SASP genes into SAHFs, HMGB1 is exported from the nucleus and further secreted outside of the cell in an oxidised form. Extracellular HMGB activates toll-like receptor 4 (TLR4) that signals down to NF-kB to induce SASP (Davalos *et al.*, 2013; Nacarelli *et al.*, 2017). Davalos *et al.* (2013) highlight that HMGB1 induces rather than reintroduces SASP, as the loss of HMGB1 is observed very early in the course of senescence development, before the SASP develops. This process was described for several models of senescence, such as OIS.

Positive feedback loops between transcriptional factors and cytokines constitute critical regulators of SASP (Acosta *et al.*, 2008; Gonzalez-Meljem *et al.*, 2018; Orjalo *et al.*, 2009). Several of such feedback loops have been described and include autocrine signalling of a secreted cytokine binding to a membrane receptor to further amplify the signal, as well as intracrine loops. For example, IL1α and its cell surface receptor (IL1R) are critical mediators of SASP (Orjalo *et al.*, 2009). Even though IL1α is secreted at relatively low levels comparing to other cytokines, its intracellular level increase in senescence. Its cell surface bound version was shown to mediate secretion of IL6 and IL8 via NF-κB, as well as reinforce the senescence growth arrest. IL1β was also shown to be able to bind to IL1R and act in a similar manner (Gonzalez-Meljem *et al.*, 2018). This mechanism was confirmed in replicative, DNA damage-induced via bleomycin, oncogene-induced and epigenetic stress-induced senescence via sodium butyrate (NaB) - a histone deacetylase inhibitor (Orjalo *et al.*, 2009). Among the cytokines, IL6 was found to be the main driver OIS, as its depletion at the mRNA level causes a collapse of the inflammatory network and prevents senescence entry and maintenance. This study pointed out an intracrine function of this cytokines as the neutralizing antibody against IL6 did not replicate the senescence bypass achieved by silencing of IL6 expression (Kuilman *et al.*, 2008). Importantly, also negative feedback loops are known to regulate SASP. For example, Bhaumik and colleagues (2009) observed that IL1α signalling induces a delayed expression of miRNA known as miR-146a/b. It serves as an inhibitor of interleukin 1 receptor-associated kinase 1

(IRAK1) mRNA, leading to decreased secretion of IL6 and IL8 (Bhaumik *et al.*, 2009). An attempt to depict the complex regulatory network of SASP is presented in Figure 1.1.

Beyond the scope of Figure 1.1, there is yet another layer of SASP regulation, namely the metabolic control over SASP. Mechanistic target of rapamycin (mTOR) is considered a metabolic master-node – also in the context of SASP. mTOR is a serine/threonine kinase and a major component of the protein complexes, mTOR complex 1 (mTORC1) and mTOR complex 2 (mTORC2). mTORC1 regulates protein translation, nucleotide and lipid biogenesis as well as it inhibits the catabolic process of autophagy in response to changing cellular conditions such as availability of growth factors, nutrients, stress, and other stimuli (Liu *et al.*, 2020). The status of mTOR activation during senescence is a matter of debate. Some studies demonstrate its activation immediately upon senescence-inducing insult. For example, Correia-Melo *et al.* (2016) found a progressive activation of mTOR in irradiation-induced senescence between 6 and 72 hours post senescence induction (Correia-Melo *et al.*, 2016). In a model of etoposide-induced senescence, the time-course of mTOR activation indicated a transient activation of mTOR 9h after the treatment with etoposide (Young *et al*., 2009). When the time-point of established senescence, in the case of DIS, is reached, there are some conflicting results. One study found decreased levels of phosphorylated ribosomal protein S6 kinase beta-1 (S6K1) - a downstream substrate of mTOR kinase in irradiation-induced senescence (Young *et al*., 2009). Another study found no difference in respect to mTOR activation between control and senescent cells (Carroll *et al*., 2017). However, the authors showed a defect in amino acid and growth factor sensing in senescent cells induced to DIS and OIS, namely mTOR was constitutively active even upon withdrawal of nutrients (Carroll *et al.*, 2017). With regards to OIS, Young and colleagues (2009) also reported the kinetics of mTOR activation in RAS-driven senescence, where it is was strongly up-regulated between 8-48 hours upon induction of RAS activation, and down-regulated afterwards.

Regardless of the basal mTOR status, there is compelling evidence on the effects of mTOR inhibition for the SASP. mTOR, as its name indicates, can be inhibited by a pharmacological compound - rapamycin. Rapamycin binds to FK506-binding protein (FKBP12), which is an inhibitor of the mTORC1 (Laplante *et al.*, 2009). Consistently for various senescence models, including replicative senescence, oncogene-induced senescence, oxidative stress-induced senescence and genotoxic stress-induced senescence, rapamycin supresses SASP (Herranz *et al.*, 2015; Laberge *et al.*, 2015; Xu *et al.*, 2014). Interestingly, the specific mechanism by which SASP is suppressed upon mTOR inhibition between the two

major settings of senescence: DIS and OIS, were found to differ. Namely, in DIS, mTOR modulates the translation of the MAP kinase-activated protein kinase 2 (MAPKAPK2) through eukaryotic translation initiation factor 4E-binding protein 1 (4EBP1), which leads to the inhibitory phosphorylation of an RNA-binding protein ZFP36L1, whose role is to degrade the transcripts of SASP components. Rapamycin activates ZFP36L1 to induce SASP component degradation in this model of senescence (Herranz *et al.*, 2015). In OIS, mTOR activates translation of IL1α, which role in driving the positive feedback loop with NF-κB was described previously. Therefore, SASP regulation in OIS is thought to occur at the translational level (Laberge *et al.*, 2015). mTOR was also found to impact on mitochondrial biogenesis through transcriptional activation of peroxisome proliferator-activated receptor gamma coactivator 1-beta (PGC1-β), a mitochondrial biogenesis regulator. Expansion of dysfunctional mitochondria in turn drives the production of reactive oxygen species (ROS) which reinforces DDR and SASP (Correia-Melo *et al.*, 2016; Passos *et al.*, 2010). Mitochondria, in fact, were shown to be critical mediators of SASP in damage-induced senescence (Correia-Melo *et al.*, 2016). This study demonstrated that mitochondrial depletion by activation of wide-spread mitophagy, resulted in a reduction of senescence markers, including reduced SASP and ROS generation, not affecting the cell cycle arrest. The state mitochondria acquire during senescence is the subject of the following section.

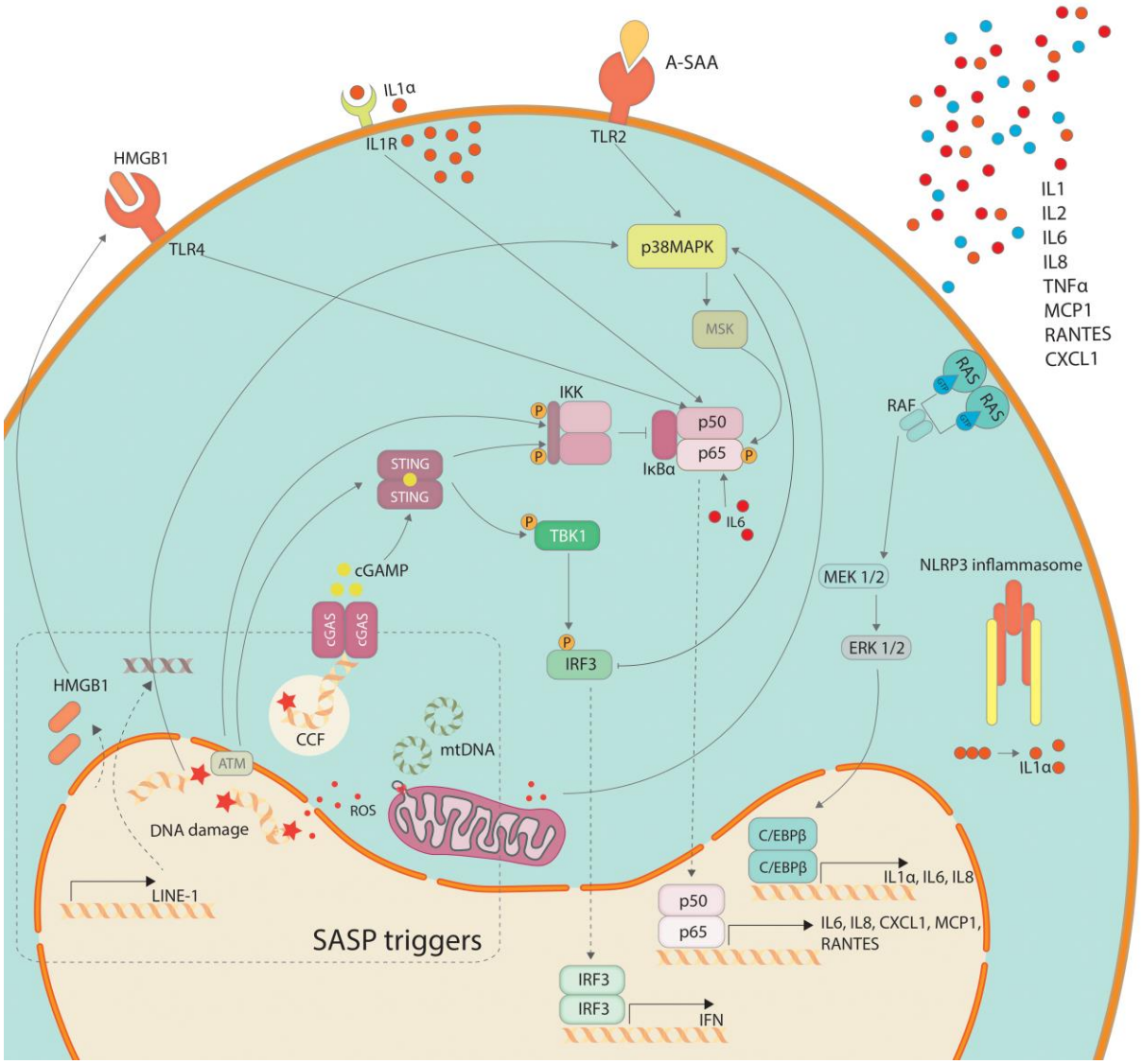

Figure 1.1: Regulation of SASP

SASP trigger mechanisms include: DNA damage response (DDR), the release of HMGB1, the formation of cytosolic chromatin foci (CCFs) from nuclear DNA, the expression of LINE-1. As a prelude to my findings presented in Chapter 3, the leakage of mtDNA is depicted within SASP triggers, serving as another pro-inflammatory damage-associated molecular pattern (DAMP), in might to activate cytosolic DNA sensing pathways. Activation of RAS-RAF-MEK1/2-ERK1/2 pathway is another SASP mediator of key importance for the model of oncogene-induced senescence. The key effectors of SASP are NF-κB and C/EBPβ. Cytokine feedback loops serve as mechanisms reinforcing SASP.

1.1.4.3 Mitochondria in cellular senescence

A profound alteration that occurs during the development of senescence is an increase in mitochondrial mass. This is consistent across various models of senescence, including replicative, damage-induced and oncogene-induced senescence (Correia-Melo *et al.*, 2016). Kinetic analysis of damage-induced senescence indicates that the increase in mitochondrial mass takes place within the early stages of senescence development, *i.e.* 2–3 days after the damage induction, but before establishment of SASP (Passos *et al.*, 2010). These data are complemented by kinetics of PGC1- β, which is also temporarily upregulated during the early DNA damage response, and further suppressed in established senescence. PGC-1β up-regulation is mediated by p53, where p53 induces degradation of hypoxia inducible factor 1 α (HIF-1α) by murine double minute 2 (MDM2), leading to the release of PGC-1β inhibition by HIF-1α in the model of irradiation-induced senescence (Bartoletti-Stella *et al.*, 2013).

Despite mitochondrial expansion in senescence, mitochondria are considered to harbour several features of dysfunction: decreased efficiency of oxidative phosphorylation, lowered mitochondrial membrane potential, increased proton leak, and elevated generation of ROS that contribute to senescence development as well as its maintenance (Passos *et al.*, 2010; Passos *et al.*, 2007). As mentioned previously, mitochondrial ROS were shown to contribute to DNA damage amplification loop, required for the establishment of cell cycle arrest, partially explaining the role of mitochondria in senescence development for replicative, damage- and oncogene-induced senescence that rely on DDR (Moiseeva *et al.*, 2009; Passos *et al.*, 2010). A recent study demonstrated another mechanism via which mitochondria and mitochondrial ROS contribute to senescence phenotypes, specifically the SASP. Namely, ROS activate the stress-activated c-Jun N-terminal kinases (JNK) kinase. In senescence conditions, this induces an interaction of JNK with 53-binding protein 1 (53BP1), which restrains the inhibitory function of 53BP1 against CCF formation (Vizioli *et al.*, 2020). The same study also added a new characterisation of mitochondrial dysfunction during senescence. Namely, the authors observed a significant down-regulation of nuclear-encoded mitochondrial genes in senescent cells induced to DIS at the time-point senescence is considered as established (10 days post-senescence induction). This means that despite the network expansion that occurs during early senescence, ultimately, the concentration of the functional OXPHOS machinery in these models of senescence is decreased (Correia-Melo *et al.*, 2016; Vizioli *et al.*, 2020).

It is important to mention that mitochondria in cellular senescence, despite all the above-mentioned alterations, do conduct oxidative phosphorylation, however, its efficiency and

preferred substrates differ when compared to proliferating cells. As mitochondrial mass increases in cellular senescence in various models, the absolute oxygen consumption rate is detected as higher for senescent cells. This does not equal efficient oxidative phosphorylation. In fact, in damage-induced senescent fibroblasts, mitochondria were found to have a lower respiratory control ratio, which indicates the capacity to generate ATP by coupled respiration. Increased contribution of ATP generated via glycolysis was also demonstrated for this model (James *et al.*, 2015; Korolchuk *et al.*, 2017; Wiley & Campisi, 2016; Zwerschke *et al.*, 2003). In OIS, an increase of glucose consumption (Moiseeva *et al.* 2009) and glycolysis, assessed by the levels of pyruvate (Kaplon *et al.*, 2013; Mazurek *et al.*, 2001) were observed, however, also enhanced TCA cycling, as in case of oncogene-induced senescence by expression of mutated oncogene BRAFV600E (Kaplon *et al.*, 2013). From the perspective of mitochondrial function, the ratio between NAD^+/NADH is an important indicator of whether a cell shifts towards glycolysis or relies on mitochondrial oxidative phosphorylation. OIS is characterised by an increased NAD^+/NADH ratio, which informs of efficient NADH utilisation for TCA. In contrast, MiDAS, is characterised by a decrease in NAD^+/NADH ratio (Wiley & Campisi, 2016). Juxtaposing the data on mitochondrial OXPHOS function with NAD^+ metabolism, one can conclude that in OIS both glycolysis and mitochondrial respiration are up-regulated and the reliance on mitochondrial function stronger than in other models.

In line with this notion stands another intriguing study demonstrating that cells in OIS primarily utilise fatty acid oxidation for energy generation. Inhibition of fatty acid oxidation using a compound etomoxir, an irreversible inhibitor of carnitine palmitoyltransferase-1 (CPT-1) - an outer mitochondrial membrane protein that catalyses the rate-limiting step in fatty acid oxidation, or its knock-down, leads to significant reduction in oxygen consumption. The same is not true in the case of proliferating cells. Interestingly, this phenomenon occurs despite a general decrease in fatty acid synthesis in OIS (Quijano *et al.*, 2012). Authors of this paper compare the observations in OIS to replicative senescence, where they report no adequate changes. A similar approach was taken to study DIS of murine hepatocytes and fibroblasts (Ogrodnik *et al.*, 2017). In contrast to the findings on OIS, upon inhibition of fatty acid oxidation by etomoxir, oxygen consumption was only mildly affected in senescent cells and reduced in proliferating cells, while the stimulation of fatty acid oxidation by palmitate results in a stronger activation of fatty acid oxidation in proliferating control cells than senescent. Authors conclude that damage-induced senescence is characterised by a defect in fatty acid oxidation (Ogrodnik *et al.* 2017). Considering the study by Quijano *et al.* (2012) and Ogrodnik

et al. (2017) together, the contrasting results indicate a difference in mitochondrial functionality between the studied models, which may contribute to differential outcomes of fatty acid inhibition in two models. Another key difference between these two articles lies in the utilisation of human fibroblasts, and murine cells, respectively. This might potentially explain the contrasting effects of etoxomir on proliferating cells. However, replicative senescence obtained in human fibroblasts seem to be similarly regulated as damage-induced senescence in murine cells, which points the two senescence types might be more similar in this respect than cells induced to OIS.

Mitochondrial morphology and network structure are critical indicators of their and the whole cell's health status. In damage-induced senescence mitochondrial network is reported to acquire an elongated phenotype, referred to also as "hyperfusion" or "giant mitochondria" (Dalle Pezze *et al.*, 2014; Mai *et al.*, 2010; Yoon *et al.*, 2006; Ziegler *et al.*, 2015). The study by Mai *et al.* (2010) demonstrated that in a model of DIS of epithelial cells, mitochondrial elongation is initiated 24h after x-ray irradiation, with the initial response in the form of network fragmentation occurring within 2-8h. Moreover, the elongated network in DIS, was also found to be more rigid, characterised by lower fusion and fission rates (Dalle Pezze *et al*., 2014). Based on these findings, irradiation-induced senescence on fibroblasts and epithelial background leads to mitochondrial elongation. A similar phenotype was also observed in cells exposed to oxidative stress (Yoon *et al*., 2006), a known senescence inducer, and in response to a plethora of other stresses, such as inhibition of cellular transcription and translation, and iron-chelating agents, however with limited reports on other senescence markers in the latter cases (Yoon *et al*., 2006, Tondera *et al*., 2009). This indicates that mitochondrial elongation serves as a stress response to various non-apoptotic stimuli, and constitutes an element of the senescence programme, at least in some senescence models. Interestingly, the treatment with ethidium bromide which was shown to induce features of senescence, classified as MiDAS (Wiley, Velarde, *et al.*, 2016), does not lead to mitochondrial elongation (Yoon *et al*., 2006). That study investigated mitochondrial network changes up to four days after the treatment, therefore their findings may, in fact, be relevant only the early stages of senescence. In conclusion, even though the majority of studies on the regulation of SASP or cell cycle arrest focus primarily on OIS, our knowledge on mitochondrial function in senescence derives predominantly from damage-induced models. Moreover, many publications, including review articles, describe senescence-associated mitochondrial dysfunction pooling all the mitochondrial characteristics in often one sentence, even if the primary data was obtained on

models as distinct as BRAFV600E and replicative senescence - referring broadly to cellular senescence. The mitochondrial aspect of the biology of cellular senescence requires a deeper approach, considering that mitochondria are often referred to as one of the main controllers of the SASP.

1.1.4.4 Anti-apoptotic pathways

The ability to resist apoptosis is another prominent feature of senescent cells. Various mechanisms that senescent cells employ in this respect are collectively referred to as senescent cell anti-apoptotic pathways (SCAPs) – currently being investigated as targets of senolytic strategies. Increased apoptotic resistance of senescent cells manifests itself in conditions of various noxious stresses, such as in response to serum withdrawal, UV irradiation, oxidative stress or treatment with extrinsic apoptosis inducers or cytotoxic compounds (Ryu *et al.*, 2007; Soto-Gamez *et al.*, 2019). Paradoxically, senescent cells that basally carry a higher load of damage (Ogrodnik, Salmonowicz, & Gladyshev, 2019) are better equipped to survive such detrimental conditions than non-senescent, healthy counterparts (Wang, 1995). Studies investigating the survival pathways engaged in cellular senescence accelerated upon the seminal studies demonstrating the beneficial effects of senescent cells clearance in the organismal context (Baker *et al.*, 2016; Baker *et al.*, 2011), exposing the potential of these mechanisms as therapeutically exploitable targets. However, several articles covering the topic of SCAPs appeared already in the 2000' or earlier.

The first study by Wang (1995) pointed out to the one of the most prominent pro-survival pathway senescent cells depend on, namely the upregulation of the anti-apoptotic members of B-cell lymphoma 2 (BCL-2) family of proteins in the context of serum withdrawal, specifically the archetypal BCL-2 (Wang, 1995). BCL-2 family of proteins include multiple anti- and pro-apoptotic members. BCL-2 belongs to the subfamily of multi-domain anti-apoptotic members including BCL-XL, BCL-W, MCL-1, BFL1/A1. Interactions of the anti-apoptotic with pro-apoptotic BCL-2 proteins at the outer mitochondrial membrane determine whether a cell is going to survive a stressor or undergo apoptosis through the intrinsic pathway involving mitochondrial outer membrane permeabilisation (MOMP). The initial study by Wang (1995), for the first time, showed increased levels of BCL-2 using an immuno-fluorescence approach as well as western blotting. Upon serum withdrawal, proliferating as well as density arrested – quiescent human fibroblasts, down-regulated BCL-2 and eventually underwent apoptotic cell death, while replicatively senescent cells did not. A similar phenomenon occurs in response to various other stressful stimuli, such as apoptosis-inducing compound,

staurosporine, thapsigargin that induces ER stress by depleting Ca^{2+} store in the ER, DNA damage-inducing agent – etoposide, a bioactive lipid - ceramide or oxidative stress induced with hydrogen peroxide. Consistently, senescent fibroblasts survive deferring to down-regulate BCL-2 (Ryu *et al.*, 2007). The effect was abrogated upon BCL-2 silencing (Ryu *et al*., 2007). A mechanism explaining the failure to down-regulate BCL-2 was proposed – expression of BCL-2 depends on a transcription factor known as cAMP response element-binding protein (CREB). In contrast to senescent cells, in young cells, activity of protein phosphatase 2A (PP2A) that regulates CREB increases with stressors such as staurosporine, thapsigargin and hydrogen peroxide, whereby it reduces the expression of BCL-2 (Ryu *et al*., 2007). Moreover, activation of NF-κB in senescent cells may be one of the intermediate mechanism ensuring high expression of BCL-2 family members, as its target genes include BCL2, BFL1, BCL-XL (Soto-Gamez *et al.*, 2019).

The dependence of senescent cells on BCL-2 proteins was later confirmed in a study aimed at deciphering targets for senolytic strategies – interventions that would target senescent cells in an organism in order to heal senescence associated dysfunctions. Senolytic strategies rely on senescent cells' Achilles heels (more than just one). When these are targeted, senescent cells appear as more sensitive to cell death and can be eliminated while the proliferating counterparts are spared. Small molecule compounds targeting anti-apoptotic BCL-2 proteins induced death of senescent cells with higher efficiency than in proliferating counterparts. This finding was consistent between OIS and DIS, as well as across several human and murine cell types, such as fibroblasts, pre-adipocytes and epithelial cells (Yosef *et al.*, 2016; Zhu *et al.*, 2015). The observations suggest senescent cells may be "primed to death" similarly to cancer cells, which more easily undergo mitochondrial apoptosis than normal cells (Lopez *et al.*, 2015). Strikingly then, despite being more resistant to unspecific stressors, specific targeting of the mechanisms they are addicted to in order to survive, leaves them more vulnerable. In order to confirm death priming of senescent cells, however, more research is needed. A potential experimental approach would include BH3 profiling allowing to better understand anti- and pro-apoptotic regulation in senescent cells (Certo *et al.*, 2006).

The specific engagement of the different anti-apoptotic members of BCL-2 family differs between the models of senescence. Yosef *et al.* (2016) found BCL-W and BCL-XL to be upregulated at the protein level in three models of human fibroblasts senescence – DIS, OIS and replicative senescence, and two models of mouse embryonic fibroblasts senescence, DIS and OIS. BCL-2 was upregulated in DIS and replicative senescence in human and mouse model,

but not in OIS. At the transcriptional level, BCL-W gene was expressed at higher level in all three human senescence models, while BCL-XL was only upregulated in OIS. Interestingly, even though the small molecule inhibitor, ABT-737, that simultaneously blocks BCL-W, BCL-XL and BCL-2, efficiently eliminated cells that underwent senescence via the three modes, specific inhibition of BCL-2 only did not result in increased cell death of DIS and replicative senescence, while it significantly reduced the survival of cells in oncogene-induced senescence. These data suggest that the protein level is not the main determinant of the protein's role in apoptotic resistance (Yosef *et al.*, 2016).

Interestingly, p21 has also been shown to enhance survival of senescent cells (Yosef *et al.*, 2017). Silencing of p21 in DIS cells enhanced DDR via resumption of DNA synthesis and via ATM, NF-κB and TNF-α signalling activated JNK kinase that led to increased cell death. Only a combined inhibition of JNK and caspase-3 signalling rescued this effect. This suggests that alternative death pathways additional to apoptosis may also be prevented via these mechanisms. Interestingly, this pathway was found to operate only in DIS and not in OIS, however was conserved across human and murine fibroblasts in DIS (Yosef *et al*., 2017). This data stand in line with the previous study by Zhu and colleagues (2015) who also identified p21 as a senolytic target.

Two other mechanisms that are involved in the survival of senescent cells are related to the most studied senolytics used both in pre-clinical studies as well as human clinical trials, namely, dasatinib and quercetin (Grosse *et al.*, 2020; Robbins *et al.*, 2020; Zhu *et al.*, 2015). Their mechanism of action was found via an unbiased approach of RNA sequencing of senescent human umbilical vein cells (HUVECs) – epithelial cells and human preadipocytes, followed by RNA interference screen (Zhu *et al*., 2015). Using this approach, the authors identified phosphatidylinositol-4,5-bisphosphate 3-kinase delta catalytic subunit (PI3KCD), a member of phosphatidylinositol-3 kinase (PI3K) family. In brief, PI3K signalling is activated upon insulin-like growth factor 1 (IGF-1) binding to tyrosine kinase receptor for IGF-1 (IGF1R). This leads to the recruitment of PI3K to the cell membrane, and phosphorylation of phosphatidylinositol-biphosphate (PIP2) into phosphatidylinositol-triphosphate (PIP3). Increased concentration of PIP3 phospholipids at the cell membrane signals to 3-phosphatidylinositol-dependent kinase 1 (PDK1), which in the next step phosphorylates Akt at position T308 that serves as an activation signal (Fruman *et al.*, 2017). This pathway is especially important in the context of mTORC1 activation and increased mitochondrial biogenesis in senescent cells, as it was shown to mediate the senescence-associated changes to

mitochondria (Correia-Melo *et al*., 2016). However, PI3K or Akt pathway is also known as a key mediator of cellular survival pathways, also in the context of senescence (Soto-Gamez *et al.*, 2019). One of the mechanisms by which PI3K may promote survival is via mTORC2 that upon activation by PI3K phosphorylates Akt in a different position - S473. Activated Akt was shown to block the pro-apoptotic BCL-2 family protein BAD whose role is to promote the BAK/BAX-mediated mitochondrial apoptotic cascade (Datta *et al.*, 1997). Dasatinib, a compound that was used in clinics to treat cancer, was then identified also as a senolytic candidate due to its PI3K inhibitory function and shown as efficient at clearing senescent HUVEC cells (Zhu *et al.*, 2015).

Another pro-survival mechanism identified in the same study (Zhu *et al*., 2015) concerned the upregulation of ephrin dependence signalling in senescent cells via the ephrin ligands (EFN) B1, and EFNB3. Receptors for these pathways belong to the so-called dependence receptors, meaning they activate signalling pathways ensuring cell survival in the presence of the ligand, while eliciting apoptosis in the absence of a ligand. Quercetin is a natural flavonoid, an antioxidant as well as an ephrin ligand that interferes with EFNB-dependent suppression of cell death (Zhu *et al*., 2015, Soto-Gamez *et al*., 2019).

Another mechanism assuring enhanced survival ability of senescent cells was identified by Baar *et al.* (2017). These authors found increased levels of a transcription factor forkhead box protein O4 (FOXO4) at mRNA and protein levels in damage-induced senescence. FOXO4 belongs to a forkhead box protein family of transcription factors that includes FOXO1 and 3 that are known from the studies on ageing, among others as downstream components of insulin/IGF signalling pathway. In the context of senescence, FOXO4 was found to interact with the key senescence mediator p53 and ensure its nuclear translocation. This mechanism as a key pro-survival process was identified by interfering with it using a FOXO4 peptide which prevents the interaction with p53 and leads to p53 nuclear exclusion (and potentially mitochondrial localisation). In conclusion, the role of p53 is necessary for cells to enter senescence and not apoptosis, while disrupting this senescence-specific process - not found in proliferating cells - may be therapeutically targeted as a senolytic strategy (Baar *et al.*, 2017).

1.1.5 Senescent cells *in vivo* and their targeting as a therapeutic strategy

Cellular senescence is defined as a stress-induced proliferative arrest accompanied by the failure to re-enter the cell division cycle in response to mitogenic and oncogenic stimuli (Sharpless *et al.*, 2015). Meeting criteria for this definition is easier to test *in vitro* than *in vivo*.

Moreover, when working with cells in culture, an experimenter is presented with a homogenous population of senescent cells induced using the same method. Nevertheless, despite being more elusive and existing in heterogenous populations of cells of various types, functions, chronological age *etc*., cells bearing known characteristics of senescence have been identified also *in vivo* (Robbins *et al*., 2020). Their detection in such conditions may still pose a challenge. Multiplicity of the senescence markers tends to be individually nonspecific and some features were found in cells that are not senescent. For example, high SA-β-Gal activity, p16 and p21 expression were detected in activated macrophages or post-mitotic tissues (Hall *et al.*, 2016; Ogrodnik, Salmonowicz, Jurk, *et al.*, 2019; Robbins *et al.*, 2020). Currently, several markers are therefore required to be assessed collectively in order to conclude on a cellular senescence burden in a tissue (Sharpless & Sherr, 2015, Gorgoulis *et al*., 2019).

Age-related accumulation of senescent cells as well as their increased abundance in organs affected by specific age-related diseases have been reported in humans and other mammals (Baker *et al.*, 2016; Burd *et al.*, 2013; Dimri *et al.*, 1995; Grosse *et al.*, 2020; Omori *et al.*, 2020; Yamakoshi *et al.*, 2009). The physiological relevance as well as the causality of cellular senescence for ageing has been shown through the genetic clearance of cells marked as senescence by high expression of p16INK4a - also known as senescence-ablator mice. Inducible elimination of p16INK4a-positive cells through targeted activation of caspases was achieved by utilizing a modified version of a genetic construct known as fat apoptosis through targeted activation of caspase (FAT-ATTAC) (Pajvani *et al.*, 2005). Subsequently, the promoter specific to adipose tissue within FAT-ATTAC cassette was replaced with a fragment of p16INK4a promoter, creating INK-ATTAC cassette. INK-ATTAC mice express an inactive human caspase 8. During the transition to cellular senescence, p16INK4a promoter becomes activated. Administration of a chemical compound, AP20187, activates caspase 8 and induces apoptosis in cells expressing p16INK4a. Clearance of p16INK4a-positive cells using this method was shown to significantly delay age-associated pathologies in various models of ageing and age-related diseases (Baker *et al.*, 2016; Baker *et al.*, 2011). Notably, also alternative models are available to target senescent cells, such as p16-inducible three modality reporter (p16-3MR) mice. This system uses a suicide gene - a truncated herpes simplex virus 1 thymidine kinase (HSV-TK). Apoptosis is induced in p16-expressing cells upon administration of ganciclovir (GCV) (Demaria *et al.*, 2014). p16-NTR is a system based on the expression of nitroreductase which turns a nontoxic drug metrodinazole into a cytotoxic metabolite by NTR (Childs *et al.*, 2016). Novel strategies to eliminate p16-expressing cells were published last year

(2020), and rely on a knock-in strategy for inserting the genetic constructs (*i.e.* after the native p16 promoters) allowing for tracking and elimination of senescent cells, known as $p16^{High}$ (Grosse *et al*., 2020, Omori *et al*., 2020). These new-generation models also contain improved reporter systems that allow for more efficient visualisation of endogenously labelled p16-expressing cells, such as using the fluorescent protein tdTomato (Liu *et al.*, 2019; Omori *et al.*, 2020).

Another approach worth mentioning as a strategy to investigate the role of senescent cells *in vivo* is known as the transplantation of senescent cells, where a small number of senescent cells generated *in vitro* is injected into tissues. For example, this intervention targeting a knee joint was sufficient to cause osteoarthritis, while a transplantation of senescent cells into adipose tissue reduced the murine lifespan (Xu *et al.*, 2018).

Finally, based on the pioneering results from pharmaco-genetic models of senescent cells removal that paved the way to study the role of senescence *in vivo*, a branch investigating the use of chemical compounds, broadly referred to as senotherapeutics, have experienced a rapid development. Senotherapeutics may either target detrimental features of senescent cells, such as SASP in order to ameliorate it; or aim at complete removal of senescent cells (senolytics). Senolytics are based on senescent cells' Achilles' heel. The results of the pre-clinical trials using senolytics match the data from proof-of-principle studies using pharmaco-genetic approaches the majority of the time. Currently studied senolytics, being an extremely timely topic, have been revied by many authors, among others: Robbins *et al.* (2020), Borghesan *et al.* (2020) and Kirkland *et al.* (2020). In the following sections, I would like to summarise chosen findings demonstrating the role of cellular senescence in age-related conditions. I would also like to mention some of the possible side-effects of the removal of senescent cells, indicating where senescent cells may play beneficial roles.

The very first study that reported on the role of senescent cells in age-related pathologies used a progeroid model that results from insufficiency of spindle assembly checkpoint protein, known as mitotic checkpoint serine/threonine-protein kinase BuBR1. BuBR1 ensures proper separation of duplicated chromosomes during mitosis (Baker *et al.*, 2004). BuBR1 hypomorphic mutant mice, due to increased levels of genomic instabilities, were characterised by an increased burden of senescent cells across several tissues such as adipose tissues, eye and skeletal muscle. Clearance of senescent cells in this model delayed the onset of kyphosis and cataracts (Baker *et al.*, 2011). Later, Baker and colleagues (2016) demonstrated that the same strategy employed in wild type mice is also efficient at killing senescent cells, preventing age-

related kidney dysfunction, fat loss, as well as delaying tumorigenesis and prolonging the mean lifespan by 23 percent (Baker *et al.*, 2016). Recently, articles investigating the involvement of cellular senescence in specific, age-associated pathologies have multiplied rapidly. Oftentimes, they employ both pharmaco-genetic approaches to clear senescent cells as described before and purely pharmacological approaches using senolytics. The examples mentioned hereafter may refer to both or either strategies.

Idiopathic pulmonary fibrosis (IPF), a progressive and fatal disease characterised by interstitial remodelling that leads to severely compromised lung structure and function, was shown to associate with increased abundance of senescent cell markers (Schafer *et al.*, 2017). The authors of this paper (that I co-author) demonstrated that SASP may be the key fibrogenic factor in the course of disease development. Elimination of cells expressing p16INK4a by a pharmaco-genetic strategy or using senolytics, dasatinib and quercetin, in a mouse model of IPF, improved pulmonary function, body composition, and physical performance (Schafer *et al.*, 2017).

Senescent cells were also implicated in atherosclerosis (Childs *et al.*, 2016). The authors showed that accumulation of the foamy macrophages, characterised by the abundance of triacylglycerol-rich lipid bodies, with senescence markers in the subendothelial space occurred during atherosclerosis. Senescent macrophages were further responsible for expression of key atherogenic and pro-inflammatory cytokines and chemokines. Moreover, senescent cells were found to promote the features of plaque instability by elastic fibre degradation, as metalloproteases are the components of the SASP. The authors proved beneficial effects of the senolytic approach (Childs *et al*., 2016).

Another group of age-related pathologies where a senotherapy has been tested concerns the adipose tissue inflammation and dysfunction as consequences of obesity (Palmer *et al.*, 2019). These authors found that senescent cells have a direct pathogenic role in the development of insulin resistance and diabetes in the context of diet-induced obesity. Removal of senescent cells was achieved using pharmaco-genetic systems – both p16-3MR and INK-ATTAC as well as a senolytic approach with dasatinib and quercetin. The interventions improved glucose tolerance as measured in an intraperitoneal glucose tolerance test (GTT) that assesses the levels of glucose upon its injections. Generally, the lower levels of glucose indicate its higher uptake by body organs and indicate a health status. The treatments also improved insulin sensitivity as assessed in an insulin tolerance test (ITT). Insulin injection leads to a higher degree reduction in glucose levels in animals that are insulin sensitive, and persistence of a higher glucose levels

in animals that are insulin resistant. Another way to look at insulin sensitivity is through the assessment of glucose infusion rate during hyperinsulinemic clamping – this measure was also improved in mice treated with senolytics. Moreover, senolytic interventions reduced the levels of haemoglobin A1c (HbA1c) – a glycated version of haemoglobin that serves as a marker of a long-term blood glucose concentration. Several markers of metabolic health and inflammatory status were assessed in plasma and adipose tissue of the animals, and the senolytic approaches generally improved these parameters, for example decreased levels of plasma IFN-γ, IL-1β and activin A or increased plasma adiponectin. With regards to adipose tissue, adipogenic transcription factors and their targets were increased upon the treatments indicating improved adipogenic potential (Palmer *et al*., 2019).

Another metabolic condition which prevalence rises with age is hepatic steatosis. It was found that this condition is associated with increased senescent cells' markers in the liver. Clearance of senescent cells in an ageing model as well as diet-induced obesity, decreased the levels of liver fat, indicating that at least in the murine model, senescent cells are accumulating fat, being responsible for the condition (Ogrodnik *et al*., 2017). Interestingly, this study was recently reproduced using a different model for the removal of p16-expressing cells (a new-generation model) based on diphtheria toxin receptor (DTR) expression (Omori *et al*., 2020).

Among age-related conditions, the role of senescent cells was also studied in the case of osteoarthritis (Jeon *et al.*, 2017). Senescent cells were ablated from a model of osteoarthritis induced with anterior cruciate ligament transection, which causes a mechanical trauma in the knee joint. The effect of the treatment included decreased articular cartilage erosion, reduced levels of inflammatory markers and increased expression of proteins constituting extracellular matrix, creating a "pro-chondrogenic environment" (Jeon *et al*., 2017).

With regards to the study I mentioned before, identifying a novel senolytic molecule - FOXO4 peptide, the authors found it had a potential to mitigate the toxic effects of doxorubicin therapy, *i.e.* loss of body weight and liver toxicity (Baar *et al.*, 2017). Next, the same strategy was used to clear senescent cells from a progeroid mouse model known as $Xpd^{TTD/TTD}$, a model corresponding to the human premature aging syndrome resulting from defects in DNA repair – trichothiodystrophy. Senotherapy using FOXO4 peptide restored fitness, fur density and kidney function in the progeroid model as well as in naturally ageing mice (Baar *et al*., 2017).

At least two research articles demonstrated the potential side-effects of senescent cells clearance, highlighting the physiological roles senescent cells play and explain the reasons why this stress-response programme evolved. The first of the studies set out to investigate the effect

of senotherapy in the context where senescent cells were shown to appear transiently, namely upon skin wounding (Demaria *et al*., 2014). The authors described that endothelial and mesenchymal cells underwent senescence, its markers peaked around 6 days after injury and resolved between 9 and 12 days (in the case of females). This process was significantly delayed upon senescent cells clearance using 3MR model as well as in p16/p21 double knock-out mice. Further, the authors identified platelet-derived growth factor AA (PDGF-AA) as a key SASP factor secreted by senescent cells in this context. It has a mitogenic function for cells of mesenchymal origin expressing PDGF-Rα receptor and facilitates myofibroblasts differentiation from the wound site fibroblasts that is required for the proper wound healing, *i.e.* via wound contraction. Interestingly, the treatment with a recombinant PDGF-AA rescued the delayed wound closure as well as the insufficient myofibroblast differentiation, indicating serotherapies may be supplemented with additional treatments to reduce the side effects of the primary interventions.

Another study that demonstrated negative consequences of senescent cells clearance was published recently (2020) and used three novel genetic models (Grosse *et al.*, 2020). One allowed for tracking of p16-positive cells based on the expression of a fluorescent protein (enhanced green fluorescent protein, EGFP) under the native promoter, while two others allowed for ablation of p16-expressing cells either in a continuous or acute fashion. Precisely, the cells expressing high levels of p16 were engineered to undergo cell death using a diphtheria toxin-based system (Grosse *et al*., 2020). The authors showed that the highest levels of p16-positive cells appear in the liver with age, where the majority of them constituted the vascular endothelial cells, specifically liver sinusoidal endothelial cells (LSECs). Continuous removal of senescent cells led to unexpected detrimental effects such as skin ulceration and increased morbidity measures requiring euthanasia. The authors found that in their model, LSECs are not effectively replaced upon the clearance – this means that the key detoxifying cells decrease in numbers and in their place, only the fibrotic scars appear (collagen depositions). In fact, it was true not only for the liver sinusoids which are lined with LSECs, but also other organs such as lung, heart and kidney that upon the treatment, had reduced levels of a specific type of epithelial cells marked by cluster of differentiation 31, CD31. The authors found the same was true when senescent cells were removed acutely at a later age (1.5 years old). Moreover, they showed that the intervention led to the disruption of blood-tissue barrier as well as to thrombocytopenia, that results from insufficient production of thrombopoietin by the liver. Finally, having access to the efficient reporter model, the authors turned to identify whether the same type of cells is

removed by dasatinib and quercetin cocktail, which was repeatedly shown to bring positive outcomes. They found these senolytics target macrophages rather than epithelial cells in the liver, hence the contrasting effects (Grosse *et al.*, 2020). Collectively, these data indicate that continuous removal of senescent cells might not be an ideal senolytic regime, and only acute, single dose approaches might bear promise for clinical use – as usually discussed among senescence researchers. In this specific context, the ablator models, also the one allowing for acute clearance, might have been too efficient, leading to detrimental consequences. Senolytic approaches must be fine-tuned eliminating "just enough" of senescent cells. Finally, tracking which cells are targeted by specific interventions is crucial for the analysis of the performance of various senotherapies, especially if side-effects are observed.

1.2 Mitochondria

1.2.1 An overview of mitochondrial functions

Mitochondria are cellular organelles of an endosymbiotic origin. Incorporating the α-proteobacteria as proto-mitochondria benefited the eukaryotic or pre-eukaryotic cells, by providing the ability to utilise chemical energy of oxygen – the process termed oxidative phosphorylation (OXPHOS) (Timmis *et al.*, 2004). This event during the evolution of eukaryotes constituted a significant metabolic upgrade from reliance on ancient glycolytic pathways only (Castresana *et al.*, 1995).

In consequence of endosymbiotic engulfment of proto-mitochondria, modern mitochondria are formed of two membranes – the inner and the outer mitochondrial membrane (IMM and OMM, respectively), and two aqueous compartments – the intermembrane space and mitochondrial matrix. The outer membrane resembles the cell membrane in regard to protein-to-phospholipid ratio and is a home for various protein channels allowing for mitochondrial import and export (Zeth, 2010). The inner membrane is characterised by a very high protein-to-phospholipid ratio, harbouring OXPHOS machinery. The inner membrane is invaginated forming the so-called cristae, making the inner mitochondrial membrane several-fold larger than the outer membrane (Pfanner *et al.*, 2019).

OXPHOS is performed by five electron transport chain (ETC) complexes anchored within the mitochondrial inner membrane. However, for it to occur, the tricarboxylic acid cycle (TCA, Krebs) is required. In brief, TCA cycle, a sequence of biochemical reactions occurring in the mitochondrial matrix, provides reduced nicotinamide adenine dinucleotide (NADH) and flavin adenine dinucleotide ($FADH_2$), by harnessing energy contained in the acetyl coenzyme

A, a product of glycolysis or fatty acid oxidation. NADH and $FADH_2$, in turn, feed electrons to complex I and II of the ETC, respectively. Complexes I-III and two additional mobile electron carriers, ubiquinone and cytochrome *c*, are then involved in passing the electrons up to complex IV. Complex IV transfers the electrons back into the matrix where they react with oxygen and hydrogen ions, forming water molecules. The electron flow drives the so-called proton pumping by complex I, III and IV – transfer of hydrogen ions - to generate an electrochemical gradient between mitochondrial matrix and the intermembrane space, referred to as mitochondrial membrane potential (MMP) ($\Delta\Psi m$). Accumulated protons within the intermembrane space contain kinetic energy that is utilised by the complex V or ATP synthase, "the power generator", which allows the protons to flow through its F0 subunit, "the turbine", generating rotational energy that is transferred into the chemical energy of phosphate bonds in ATP molecules at the F1 subunit (Huttemann *et al.*, 2007; Watt *et al.*, 2010).

The bioenergetics processes occurring within mitochondria are considered their primary function. To visualise the engagement of mitochondria into generation of ATP and other processes, it is useful to consider that among about 1500 proteins localizing to mitochondria in humans, only around 15% are involved in energy metabolism, including the enzymes that comprise catabolic pathways and structural subunits of ETC. However, when mitochondrial protein mass is considered, these 15% of mitochondrial proteome make more than half of the total protein content (Pfanner *et al.*, 2019). These data indicate that mitochondrial role as "cellular powerhouses" is indeed central, however also points to various other cellular duties. In fact, 2 billion years of coevolution of mitochondria and eukaryotic cells led to an intricate relationship of mitochondria with the rest of the cell (Lang *et al.*, 1999). Mitochondria became entrusted to regulate other aspects of metabolism by producing metabolic precursors for biosynthetic processes of lipids, proteins, DNA and RNA (Spinelli and Haigis 2018); synthesizing and storing multifunctional co-factor molecules, known as iron-sulphur clusters (ISC) (Braymer *et al.*, 2017); regulating innate immunity by reinforcing anti-viral/anti-bacterial signalling, coordinating stem cell function, as well as executing cellular adaptations to various stresses and finally, by constituting a platform for the critical - apoptotic cascade – during the process of cell death, therefore orchestrating the decision between survival and death (McBride *et al.*, 2006; Riley *et al.*, 2020; Spinelli *et al.*, 2018; Sun *et al.*, 2016).

Importantly, mitochondria do not exist as separate entities but stay in constant interaction with other components of the cells. They maintain a strong communication axis with the nucleus, which allows for the regulation of their biogenesis in response to changing cellular

conditions. Mitochondria also stay in constant touch - via vesicle transport or direct membrane contact sites - with the most of the cellular organelles (Gordaliza-Alaguero *et al.*, 2019; Jain *et al.*, 2017; Xia *et al.*, 2019). Through the contact with the endoplasmic reticulum (ER) at the so-called mitochondria-associated membranes (MAMs), they perform yet another critical function of regulating calcium signalling (Rizzuto *et al.*, 2012). For metabolite transfer and proper metabolite compartmentalisation, mitochondria interact with lysosomes (Todkar *et al.*, 2017). Mitochondria also house lipid metabolism pathways (Rutter *et al.*, 2015), and in order to execute oxidation of fatty acids as well as lipid synthesis mitochondria must interact with lipid droplets (LDs) and peroxisomes (Benador *et al.*, 2018; Lackner, 2019; Sugiura *et al.*, 2014; Wanders *et al.*, 2015). Studies of mitochondria and LDs interaction in particular, point to yet another layer of understanding in mitochondrial cell biology – namely, mitochondria in one cell may be vastly different from each other forming subcellular "specialised" sub-populations. Depending on whether mitochondria maintain an interaction with an organelle – in this case a LD – their proteome, metabolic capability and IMM ultrastructure may differ from unbound counterparts, a process that is assured by specific modifications in their fission/fusion machineries (Benador *et al.*, 2018). In conclusion – mitochondria are extremely complex systems in yet more complex systems of cellular environment, and it is useful to consider them as true parts of it rather than as separate organelles of distinct functions.

1.2.2 Mitochondrial DNA

Mitochondria are unique among organelles as they contain their own DNA, or, in fact, the whole genetic system. It is the mitochondrial genome, but also the factors that regulate its replication and transcription, as well as a distinct from cytosolic, translation system of mitochondrial ribosomes (Enriquez *et al.*, 1998). Human mtDNA is a double-stranded, circular molecule that counts 16 569bp in length. Mitochondrial nucleoids are packaged into nucleoprotein complexes and reside in the mitochondrial matrix (Yasukawa *et al.*, 2018). Individual cells contain between a thousand to ten thousands of copies of mtDNA (Hance *et al.*, 2005), while a single nucleoid typically contains one mtDNA molecule (Kukat *et al.*, 2011). Moreover, an average size of a mitochondrial nucleoid was determined as around 100 nm in diameter (Brown *et al.*, 2011).

The major protein component of the mtDNA nucleoid is the mitochondrial transcription factor A (mtTFA or TFAM), a factor regulating mtDNA packaging, transcription and replication. TFAM belongs to the high mobility group (HMG) box domain family, and binds to DNA without sequence specificity (Gaspari *et al.*, 2004; Kanki *et al.*, 2004). It contains two

DNA binding sites, and its role in the nucleoid's architecture is compacting the DNA, creating cross-stand bonds and facilitating loop formation (Falkenberg, 2018).

mtDNA encodes 37 genes, comprised of 13 mRNAs that encode subunits of the oxidative phosphorylation chain, as well as 2 ribosomal RNAs and 22 tRNAs. Genes within human mtDNA are organised in a compact fashion, where they lack introns within protein-coding sequence. Proteins that are encoded by mtDNA are the hydrophobic subunits of the OXPHOS complexes in the mitochondrial inner membrane (Pfanner *et al.,* 2019). The remaining OXPHOS components and all other mitochondrial proteins are encoded in the nuclear genome, translated in the cytoplasm and imported into mitochondria. These characteristics generally concern animal mtDNA, and mtDNA in fungi, plants and protists may vastly differ with respect to all described characteristics (Ladoukakis *et al.,* 2017).

The double-stranded mtDNA is composed of the so-called heavy (H)- and light (L)-strands, which owe their names to the nucleotide composition: a different proportion of heavier (adenine and guanine) and lighter (cytosine and thymine) nucleotides. mtDNA contains little of non-coding regions. Within its single longer non-coding region, there are three promoters for transcription initiation: L-strand promoter (LSP) and two H-strand promoters (HSP1 and HSP2). Notably, mitochondrial transcripts are polycistronic and only further processed to individual transcripts, unlike the majority of transcripts originating from the nuclear DNA (Yasukawa *et al.,* 2018). The origin of replication for the heavy strand (O_H) is also located within the noncoding region, while the second origin of replication - for the light strand (O_L), is located approximately 11kb downstream of O_H. The noncoding region also contains the so-called displacement loop (D-loop) where a third DNA strand is found, specifically a prematurely terminated product of H-strand synthesis of a length of approximately 0.65kb, called 7S DNA (Falkenberg, 2018). The presence of this additional fragment of DNA suggests that mitochondrial DNA replication is strongly regulated at the level of termination, and the specific termination site called termination-associated sequence (TAS) allows for termination of unwanted mtDNA replication. From the perspective of this thesis, the D-loop fragment is of importance, as the existence of the third strand makes the D-loop sequence more abundant than all other mitochondrial DNA regions within the cell (Nicholls *et al.,* 2014).

Replication of mtDNA is a critical process constantly occurring in both proliferating and post-mitotic cells, including neuronal and cardiac cells (Yasukawa *et al.,* 2018). Interestingly, nucleoids that undergo replication have been found to localise to sites that contact ER. This is also where mitochondrial fission takes place. Therefore, this process is considered

to assure even distribution of newly synthesised nucleoids within the mitochondrial network (Falkenberg, 2018). mtDNA transcription and replication are uniquely coupled, as RNA transcripts serve as replication primers, in contrast to the nuclear DNA synthesis which requires specific primases for synthesising separate RNA primers (Falkenberg, 2018). The enzyme responsible for the replication of mtDNA is known as DNA polymerase γ (PolG). It is the only of the fifteen DNA polymerases (in mammals) to be localised to mitochondria (Kaguni, 2004). Its action is facilitated by various auxiliary proteins, such as mitochondrial single-stranded DNA binding protein (mtSSB), mtDNA helicase (Twinkle), and a number of others. Human polymerase γ consists of a catalytic subunit: a 140kDa protein with DNA polymerase activity as well as 3′–5′ exonuclease and 5′ dRP lyase activities; and a homodimer formed of two accessory subunits, 55kDa each, that is required for DNA binding (Chan *et al.*, 2009). There is still no final consensus, by what exact mechanism mtDNA is replicated, and the "replication modes" are probably related to cellular conditions (Holt *et al.*, 2012). In brief, mtDNA replication begins at the O_H, where the helicase Twinkle unwinds the double stranded DNA. While the heavy stand is being synthesised along the light strand, the heavy strand is being covered by the mtSBB. After the progression of about two thirds of the nascent heavy strand replication, the O_L is exposed to start the replication of the light strand along the heavy strand and mtSBB disassociates. Another model of mtDNA replication, termed RITOLS (RNA Incorporated Throughout Lagging Strand), also posits that the leading strand (H-strand along the L-strand) is synthesised first, while RNA is laid down along the lagging strand before being converted to DNA. While the studies on the details of this process continue, mitochondrial DNA replication can be considered to occur in an asymmetric and asynchronous fashion (McKinney *et al.*, 2013). Importantly, due to polymerase γ 3′ → 5′ proofreading exonuclease activity, it is responsible for repairing its own errors. Moreover, polymerase γ was shown to remove linear fragments of DNA formed upon the induction of the double-stand breaks formed within mtDNA (Nissanka *et al.*, 2018). Without this function of polymerase γ, mtDNA accumulates mutations as well as larger mtDNA deletions.

1.2.3 Mitochondrial biogenesis

Mitochondria cannot be synthesised *de novo*, but replicate through the recruitment of new proteins and phospholipids, which are added to the pre-existing organelles. Interestingly, it has been estimated that the half-life of mitochondrial pool in murine hepatocytes *in vivo* is around 40h (Miwa *et al.*, 2008). An active biogenesis system must operate constantly, replenishing the

pool of healthy mitochondria. Mitochondrial biogenesis entails the replication of mtDNA described above, but also the transcription, and translation of mtDNA-encoded genes, coordinated transcription and translation of nuclear encoded mitochondrial genes, finally the import and assembly of phospholipids and nuclear-encoded proteins within specific mitochondrial compartments (Ploumi *et al.*, 2017). Translation within mitochondria is coupled to cytosolic translation which gives rise to around 80 proteins constituting the mitochondrial ribosomes and their import into the mitochondria (Battersby *et al.*, 2013; Jones *et al.*, 2012). Importantly, a synchronous transcription and translation of nuclear and mitochondrial genes encoding OXPHOS complexes is critical for the generation of new mitochondria, as an imbalance between the two can induce mitochondrial degradation (Matsuda *et al.*, 2010).

Central to the regulation of mitochondrial biogenesis are the nuclear transcription factors that include the nuclear respiratory factors, NRF1, NRF2, and others, such as the cAMP response element binding protein, CREB (Gopalakrishnan *et al.*, 1994) or initiator element binding factor, YY1 (Basu *et al.*, 1997). All these transcription factors orchestrate broader cellular response programmes beside mitochondrial biogenesis. For example, NRF1 and NRF2 regulate expression of antioxidant and xenobiotic-metabolizing enzyme genes (Ohtsuji *et al.*, 2008) as well as many others. In the context of mitochondria, NRFs have been identified initially as responsible for the induction of expression of cytochrome *c* and cytochrome oxidase subunit genes (Scarpulla, 2006, 2008). Importantly, NRFs also induce the expression of mitochondrial transcription factors A, B1 and B2 - TFAM, TFB1M and TFB2M, which are responsible for the mtDNA arm of mitochondrial genes expression during mitochondrial biogenesis, therefore NRFs also control mtDNA gene expression indirectly (Piantadosi *et al.*, 2006).

Another group of master regulators of mitochondrial biogenesis consists of co-activators of transcription factors - peroxisome proliferator-activated receptor gamma coactivator family, PGC-1α, PGC-1β, PGC-1α related coactivator, PRC, and a truncated alternatively spliced isoform, NT-PGC-1α (Martínez-Redondo *et al.*, 2015). Co-activators are found within multiprotein complexes, where their role is the modulation of the transcriptional potency and chromatin remodelling. For example, by binding to NRF-1, they are able to promote the expression of nuclear respiratory genes and mitochondrial mass expansion (Scarpulla, 2008). PGC-1α was first discovered as a critical factor regulating mitochondrial biogenesis during adaptive thermogenesis in brown adipose tissue (Puigserver *et al.*, 1998). Other signals that activate PGC-1α are the low cellular energy status indicated by ATP/AMP

and NADH/NAD^+ ratios, phosphorylation of AMPK, mTOR inhibition, and, in organismal context, exercise and cold exposure (Liu *et al.*, 2011).

Thermogenesis or adaptation to low nutrient conditions can be considered as anterograde signalling in the regulation of mitochondrial biogenesis, meaning the regulation of mitochondrial processes from the nucleus in response to external and internal stimuli, excluding specifically mitochondrial signals. An alternative is the retrograde signalling, which concerns mitochondria-initiated communication (Butow *et al.*, 2004). Retrograde signalling is considered a sensor of mitochondrial dysfunction. Various factors may relay the signal and induce transcriptional changes or even chromatin remodelling allowing for the restoration of mitochondrial homeostasis. These signals include the reduced cellular or mitochondrial ATP levels or NADH/NAD^+ ratio, oxidative stress and deregulation of cellular Ca^{2+} homeostasis. It is interesting to consider this concept may be understood more broadly, encompassing non-canonical "signals", such as mitochondrial molecules released into the cytosol, such as cytochrome *c* and mtDNA, during cell death or autophagy defects, initiating immune responses (Nakahira *et al.*, 2011; Shimada *et al.*, 2012). Mitochondrial signals communicating their health status with the rest of the cell may also take the form of mitochondrial-derived peptides (MDPs), such as humanin; mitochondrial open reading frame of the twelve S rRNA type-c, MOTS-c, and others, encoded within mtDNA rRNA genes. Humanin has been shown to play various roles, among others a protective role in cellular survival by binding and inhibiting the pro-apoptotic BAX (Guo *et al.*, 2003). In the context of mitochondrial biogenesis, humanin stimulates expression of NRF1 and PGC-1α (Morris *et al.*, 2019; Qin *et al.*, 2018). MOTS-c is able to bind to nuclear DNA and regulate the transcription of NRF2 (Yong *et al.*, 2018).

1.2.4 Mitochondrial quality control

1.2.4.1 Mitochondrial responses to stress

Mechanisms ensuring mitochondrial quality protect from, or facilitate recovery from, various mitochondrial dysfunctions. Mitochondrial proteostatic quality mechanisms include ATP-dependent and independent proteases that cleave misfolded and oxidised proteins within mitochondrial matrix and the intermembrane space (Käser *et al.*, 2000) as well as the cytosolic ubiquitin-proteasome system, UPS, that degrade proteins localised to the outer mitochondrial membrane (Karbowski *et al.*, 2011). Mitochondrial unfolded protein response (UPRmt) is a variant of the mitochondrial retrograde signalling that induces broader cellular adaptations in response to proteotoxic stress. Unfolded protein response (UPR) has been first described for

proteotoxic stress in the lumen of ER (Pahl, 1999). Later, it was demonstrated that mitochondria activate UPRmt in response to misfolded proteins, but also defects in protein import, inhibition of mitochondrial translation, OXPHOS impairment by toxins or genetic interventions, and mtDNA depletion (Shpilka *et al.*, 2018). All these perturbations may induce an imbalance of mitochondrial to nuclear proteins. Importantly, the accumulation of unassembled OXPHOS components in mitochondria or mistargeting of mitochondrial proteins in the cytoplasm was shown to be toxic (Wang *et al.*, 2015; Wrobel *et al.*, 2015).

In response to proteotoxic stresses, cells undergo various adaptations, orchestrated by several critical transcription factors, such as C/EBP homologous protein (CHOP), or activating transcription factors, for example ATF4 and ATF5 (Melber *et al.*, 2018). In some specific conditions, *i.e.* accumulation of misfolded proteins in mitochondrial intermembrane space, oestrogen receptor (ERα) is mediating the transcriptional response (Papa *et al.*, 2011). In *C. elegans*, there is a mechanism allowing for assessment of mitochondrial protein import efficiency utilizing a transcription factor, stress activated transcription factor-1 (ATFS-1). Defect in its import into mitochondria, where it would usually become degraded by a mitochondrial matrix protease Lon, leads to its translocation to the nucleus and activation of UPRmt (Nargund *et al.*, 2012).

Cellular adaptations in response to UPRmt start from expression of mitochondrial chaperones, proteases and proteasomes (Shpilka *et al.*, 2018; Wrobel *et al.*, 2015). Increased expression of superoxide dismutase, glutathione and ubiquinone synthesis machineries protect from ROS toxicity. A reduction in global protein synthesis due to phosphorylation of the eukaryotic translation initiation factor 2 subunit 1 (eIF2α) reduces the import of newly synthesised proteins into mitochondria, which spares the proteostatic machinery from overload. Metabolic remodelling that includes expression of glycolysis components, also contributes to a reduced protein folding burden and allows for cell survival. Finally, mitochondrial biogenesis is activated, including mitochondrial protein import machineries (Melber *et al.*, 2018). One of the specific mechanisms constituting UPRmt in response to proteotoxic aggregates in mitochondria, is the translocation of a nuclear transcription factor, ROX1, belonging to the family of HMG (high mobility group) box containing proteins – similarly to TFAM, into the mitochondria. ROX1 then binds to mtDNA and maintains the transcription of genes encoded within mtDNA (Poveda-Huertes *et al.*, 2020).

1.2.4.2 Mitochondrial degradation

Autophagy is a process that allows for selective or non-selective degradation of cellular components, including organelles such as mitochondria (Mizushima *et al.*, 2008). In brief, autophagy begins with the sequestration of the cytosolic cargo by a double-membraned phagophore which expands to form an autophagic vesicle. Through the action of multiple proteins, autophagosome fuses with a lysosome, another organelle of vesicular shape containing hydrolytic enzymes that digest proteins, lipid, carbohydrates and nucleic acids. Subsequently, the products of lysosomal degradation such as amino acids, monosaccharides and free fatty acids are released from the autolysosome into the cytoplasm for reuse. Therefore, autophagy is considered a cellular recycling mechanism (Dikic *et al.*, 2018). In the context of mitochondria, two variants of autophagy are utilised, the nonselective autophagic degradation, concerning the bulk and random portions of the cytosolic content, or mitochondrial-specific autophagy – mitophagy (May *et al.*, 2012).

It is important to note here, before describing the mitochondrial dynamics in detail (*section 1.2.5*), that mitochondrial fragmentation is a process facilitating mitophagic degradation. It was shown that dynamin-related protein 1 (DRP1)-dependent fission allows for the engulfment of mitochondria by autophagosomes (Burman *et al.*, 2017; Gomes *et al.*, 2011; Tanaka, 2010). However, there is also contrasting evidence that DRP1 is not essential, and a phagophore may engulf a fragment of a larger mitochondrion. This variant of mitophagy has been observed in conditions such as hypoxia or upon exposure to deferiprone (DFP), an iron-chelating drug (Song *et al.*, 2015; Yamashita *et al.*, 2016).

Several pathways may direct mitochondria for mitophagy that ultimately merge at the common event of stabilisation of the so-called LC3 interaction region (LIR) at OMM, allowing the mitophagy machinery to interact with the targeted mitochondrion and proceed with autophagosomal engulfment and lysosomal degradation. The canonical axis mediating mitophagy includes the PTEN-induced putative kinase 1 (PINK1) (Jin *et al.*, 2010). In non-stress conditions, PINK1 is transported into mitochondria, where it is processed and targeted for degradation. Under various kinds of mitochondrial stresses that lead to mitochondrial membrane depolarisation, PINK1 does not enter mitochondria but instead, localises and accumulates on the outer mitochondrial membrane. PINK1 phosphorylates and activates the E3 ubiquitin ligase, Parkin. Parkin, in consequence, ubiquitinates specific mitochondria, where ubiquitin chain serves as one of the major signals for mitophagy receptors containing the critical LIR domains, such as optineurin and nuclear domain 10 protein 52 (NDP52) (Shpilka *et al.*,

2018). The alternative mitophagy pathways still involve ubiquitination of proteins at the OMM, however by other than Parkin E3 ubiquitin ligases. Interestingly, some of the ligases, glycoprotein 78 (GP78) and mitochondrial E3 ubiquitin protein ligase 1 (MUL1) were shown to ubiquitinate mitofusin 1 (MFN1) and mitofusin 2 (MFN2), major mediators of mitochondrial elongation and by targeting them for proteasomal degradation, additionally facilitate mitochondrial fragmentation (Fu *et al.*, 2013). Alternative variants of mitophagy pathways involve other than ubiquitin signals for mitophagy receptors, for example, BCL-2 interacting irotein 3 (BNIP3) and NIX, the pro-apoptotic members belonging to the BCL-2-family that reside in the OMM, as well as a non-protein molecule – cardiolipin, when externalised from the inner to the outer mitochondrial membrane (Chu *et al.*, 2013).

Not only mitochondria but also mitochondria-derived vesicles (MDVs) can be targeted for lysosomal degradation. MDVs are small vesicular carriers formed of mitochondrial membranes - either only the OMM, or including the IMM and matrix content. Their disassociation from the network occurs through fission-independent mechanisms. MVDs were found to mediate transport between mitochondria and peroxisomes but also, to carry damaged mitochondrial cargo to the lysosomes (Andrade-Navarro *et al.*, 2009; Soubannier *et al.*, 2012; Sugiura *et al.*, 2014).

1.2.5 Mitochondrial dynamics

1.2.5.1 Mitochondrial dynamics machinery

Mitochondria form complex, interconnected and dynamic networks. Mitochondrial dynamics comprises the processes of fusion (elongation) and fission (fragmentation) events determining the structure of mitochondrial network, as well as the movement of mitochondria along the filaments of the cytoskeleton. Fission and fusion within mitochondrial network require membrane remodelling events orchestrated by conserved large dynamin-like GTPase proteins, indicating their dependence on GTP hydrolysis. The main players are DRP1 – mentioned in the context of mitophagy, responsible for fission; mitofusins 1 and 2 (MFN1 and MFN2) that mediate OMM fusion, and optic atrophy gene 1, OPA1, that executes the IMM fusion (Escobar-Henriques *et al.*, 2014). All of them are targets for various post-translational modifications that lead to activation or repression, pushing the network state either towards fragmentation or elongation.

MFN1 and MFN2 reside at OMM and, during fusion, form homo-oligomers or hetero-oligomers at two adjacent mitochondria, tethering them together. The conformation of

mitofusins – permissive or constraint, may dictate whether fusion will occur. Interestingly, depletion of MFN1 and MFN2 leads to somewhat distinct phenotypes of mitochondrial fragmentation, where MFN1 deficiency causes "hyper-fragmentation", while MFN2 deficiency - aggregation of fragmented mitochondrial clusters (Chen *et al.*, 2003). In the organismal context, their homozygous knock-out is embryonically lethal (Chen *et al.*, 2003).

OPA1 resides in mitochondrial intermembrane space, anchored at the IMM and is present at isoforms of different length. The long L-OPA1 is required for the fusion of IMM. Both L-OPA1 and the short S-OPA1 isoforms are however present at equimolar concentrations at basal conditions, while stresses that lead to mitochondrial fragmentation, including execution of apoptosis, lead to L-OPA1 proteolytic cleavage and predominance of the S-OPA1 isoform – that is soluble in the intermembrane space. However, there are more than two length variants of OPA1, which is a result of alternative gene splicing (Del Dotto *et al.*, 2018). The various isoforms are linked to alternative OPA1 functions, such as stabilisation of mtDNA and maintenance of mitochondrial cristae, including mediating the assembly of ECT complexes (Alavi *et al.*, 2013). OPA1 deficiency leads univocally to mitochondrial fragmentation (MacVicar *et al.*, 2016).

The mechanism of mitochondrial fission, orchestrated via DRP1, has been thoroughly described. Prior to DRP1 recruitment, the sites of mitochondrial fission are first engulfed and constricted by ER. This process has been shown to assure mtDNA synthesis before mitochondrial division (Sprenger *et al.*, 2019). Subsequently, a ring-like structure from DRP1 self-oligomers forms around the constriction sites of dividing mitochondria. The final scission requires GTP binding and hydrolysis. DRP1 is supported by several proteins bound to OMM, including mitochondrial fission factor (MFF), a mitochondrial outer-membrane receptor for DRP1 and fission protein 1 (FIS1) (Sebastián *et al.*, 2017). Their function is to recruit DRP1 to OMM (Wai *et al.*, 2016). Various post-translational modifications impact of DRP1 performance, including activating and inhibitory phosphorylation, ubiquitination and SUMOylation. Mitochondria in cells deficient in DRP1 adapt a hyper-fused network (Wai *et al.*, 2016).

1.2.5.2 Mitochondrial network's adaptations to stress

Mitochondrial morphology is linked to its functions. Dynamic remodelling of mitochondrial network via fission and fusion is an important element during normal cellular life-cycle – mitochondria elongate in G1/S phase and fragment during G2/M phase (Babbar *et al.*, 2013). It

is also a part of various stress responses or metabolic shifts. Mitochondria can rapidly transition into states of fragmentation, hyper-fragmentation, elongated tubules or hyper-fusion, depending on the conditions (Wai *et al.*, 2016).

Mixing of mitochondria via fusion is considered to facilitate dilution of "local mitochondrial defects", maintenance of functional mtDNA pool, increased OXPHOS and generation of ATP (Wai *et al*., 2016). It is associated with non-lethal stresses such as UV irradiation (UV-C), inhibition of nuclear transcription via actinomycin D or inhibition of translation using cycloheximide (Tondera *et al.*, 2009). This phenotype has been named as Stress-induced Mitochondrial Hyper-fusion (SiMH) (Tondera *et al*., 2009). Also during nutrient depletion, including growth factor depletion or amino-acid deprivation, mitochondria adopt an elongated state (Tondera *et al*., 2009). The function of mitochondrial elongation during starvation has been shown to be related to mitophagy – elongated mitochondria are spared from degradation and allow for cell survival (Gomes *et al.*, 2011; Rambold *et al.*, 2011). Mechanistically, several important protein players as well as post-translational modifications have been involved in mediating the hyper-fusion phenotypes. Tondera and colleagues (2009) identified SPFH family scaffold protein Stomatin-like protein 2 (SLP2), a protein that otherwise is known to be up-regulated during mitochondrial stresses and stabilise mitochondrial proteins, such as OXPHOS complexes (Da Cruz *et al.*, 2008), as critical for the phenotype. In the case of glucose deprivation, deacetylation of MFN1, a post-translational modification that promotes its stability, was shown to regulate mitochondrial fusion (Lee *et al.*, 2014). Nutrient deprivation also activates the fission inhibitory signal, phosphorylation of serine-637 of DRP1 by protein kinase A (PKA), which as a cAMP-dependent enzyme, can sense nutrient status (Rambold *et al*., 2011). Interestingly, the findings of elongated mitochondrial morphology during starvation are relevant for *in vivo* conditions, where caloric restriction and other fasting-mimicking interventions, such as inhibition of mTOR, suppression of insulin/IGF1 signalling or AMPK overexpression is also known to promote mitochondrial elongation in non-mammalian and mammalian model organisms (Faitg *et al.*, 2019; Sebastián *et al.*, 2017; Sharma *et al.*, 2019).

On the other hand, fission is associated with mitophagic elimination of damaged organelles, or with apoptotic cascade. Mitochondrial fragmentation may be considered an acute stress response to a stressor which is powerful to induce apoptosis or sub-lethal when the cell's survival depends on the repair capacity. Mitochondrial fragmentation has been reported in response to various stresses, to name a few: oxidative stress induced by high-fluence low-power laser irradiation (HF-LPLI) (Wu *et al.*, 2011), cigarette smoke (Aravamudan *et al.*, 2014), or

inhibitors of ETC (Toyama *et al.*, 2016). Mechanistically, fragmentation of mitochondria is mediated by several mechanisms. In the study by Wu *et al*. (2011), fragmentation induced by HF-LPLI caused overexpression of DRP1 and its translocation to mitochondria. In the case of ETC complexes inhibition, AMPK that senses cellular energetic status was responsible for the phosphorylation of MFF (Toyama *et al*., 2016). Interestingly, also a focal laser injury to plasma membrane induced a rapid mitochondrial fission with DRP1 accumulation at the site of injury (Horn & Jaiswal, 2020; Horn, Raavicharla, *et al.*, 2020). In this case, mitochondrial fragmentation is needed to generate local redox signal required for plasma membrane repair, including localised assembly of F-actin. During apoptosis induced by genotoxic stress, ubiquitination and proteasomal degradation of MFN2 was shown to mediate mitochondrial fragmentation (Leboucher *et al.*, 2012) Also, phosphorylation of DRP1 at serine-616 by Ca^{2+}/calmodulin-dependent protein kinase II (CAMKII) and protein kinase C (PKC) has also been found during cell death (Sprenger *et al.*, 2019). Importantly, serine-616 phosphorylation of DRP1 is also performed by cyclin-dependent kinase 1 (CDK1)/cyclin B kinase, and is seen during normal cell division.

From the metabolic standpoint, mitochondrial fragmentation occurs during nutrient excess (Sprenger *et al*., 2019). For example, high glucose concentration induces mitochondrial fragmentation which is mediated by calcium influx into the cell and activation of the mitogen-activated protein kinase extracellular signal-regulated kinase 1/2 (ERK1/2) (Yu *et al.*, 2011) which phosphorylates DRP1 (Kashatus *et al.*, 2015). Importantly, certain stressful stimuli, such as x-ray irradiation (utilised to induce cellular senescence) were shown to result in an immediate mitochondrial fragmentation followed by hyper-fusion. Mai *et al*. (2010) demonstrated that mitochondrial fragmentation occurs within 2-8h after x-ray irradiation, and after 24h, cells shift towards elongated networks in human endothelial cells (Mai *et al*., 2010). This response is mediated by down-regulation of DRP1 and FIS1 expression. Consistently with these findings, Yoon *et al.* (2006) showed that the formation of "elongated giant mitochondria" in deferoxamine (DFO)-induced senescent is also mediated by down-regulation of FIS1 expression (Yoon *et al*., 2006). These reports suggest that mitochondrial network readily adapts to changing cellular conditions even during one type of stress, and therefore, experiments aimed at studying mitochondrial dynamics during cellular stress responses require kinetic analyses for final conclusions.

1.2.6 Mitochondria in innate immunity

1.2.6.1 Mitochondrial outer membrane permeabilisation

One of the prominent functions of mitochondria is their engagement in the regulation of cell death. In particular, a type of caspase-dependent regulated cell death – apoptosis. In fact, mitochondria participate not only in apoptosis but also mitochondrial permeability transition (MPT)-driven necrosis and parthanatos (Sedlackova *et al.*, 2019). During apoptosis, mitochondria undergo mitochondrial outer membrane permeabilisation (MOMP) which is an essential step occurring between mitochondria and cytoplasm. MOMP is controlled by pro-apoptotic and anti-apoptotic members BCL-2 protein family, with BAK and BAX as the main executioners. In normal conditions, BAX resides in the cytoplasm, while BAK at the OMM (Cosentino *et al.*, 2017). Apoptotic stimuli lead to activation of BAK and BAX via BCL-2 family members known as activators, such as BID, PUMA or BIM, as well as the loss of interaction with anti-apoptotic members of BCL-2 proteins, such as BCL-2, BCL-XL, BCL-W and others. The activator proteins contain BH3 domain that binds to a hydrophobic groove within BAK and BAX (Westphal *et al.*, 2011). Activation consists of an extensive conformational change, as well as BAX translocation to mitochondria (Westphal *et al.*, 2011). Interestingly, exposure of BH3 domain of BAK and BAX can lead to reciprocal activation, and propagation of the signal. Further, active BAK and BAX oligomers induce and stabilise the, so-called, lipidic pores in the mitochondrial outer membrane (Schafer *et al.*, 2009; Tait *et al.*, 2013; Zhang *et al.*, 2017). Lipidic pores occur when inner and outer leaflets of phospholipid membranes fuse together. BAK and BAX pores are considered to be "macropores" as they can grow above 100 nm in diameter, even up to 300 nm (Gillies *et al.*, 2014). MOMP has been imaged at high resolution and at high-speed, demonstrating that it is initiated at a specific sub-fraction of mitochondria, and propagate in a wave-like fashion across all the mitochondria (Bhola *et al.*, 2009; Lartigue *et al.*, 2008; Rehm *et al.*, 2009). During MOMP, BAK and BAX macropores allow the release of the intermembrane space components: cytochrome *c*, second mitochondria-derived activator of caspases (SMAC or DIABLO), and mitochondrial serine protease HtrA2/Omi (Martinou *et al.*, 2000; van Loo *et al.*, 2002). Subsequently, mitochondrial network undergoes hyper-fragmentation. Finally, blebs of the inner mitochondrial membrane herniate through the pores, where some of them lose integrity and mitochondrial matrix components, including mtDNA and TFAM, are released into the cytoplasm (McArthur *et al.*, 2018; Riley *et al.*, 2018; Tait *et al.*, 2013; Vringer *et al.*, 2019).

Herniation and breakage of inner mitochondrial membranes through BAK and BAX pores and mis-localisation of mitochondrial constituents is a hardly reparable damage. Further activation of caspases, a class of cysteine-dependent aspartate-specific proteases, was described as "orchestrating a global program of cellular demolition" (Taylor *et al.*, 2008; White *et al.*, 2014), as over 1,000 protein substrates are targeted for cleavage (Crawford *et al.*, 2011). Therefore, typically, it is considered as a point of no return. Yet, it was shown that in some conditions provided they include caspase inhibition, cells are able to survive MOMP. For example, postmitotic sympathetic neurons deprived of neurotrophic factor survive MOMP if the neurotrophic factor is reconstituted (Deshmukh *et al.*, 2000). Survival beyond MOMP has also been shown in proliferating cells upon lethal dose of staurosporin when caspases were inhibited and the expression of glyceraldehyde-3-phosphate dehydrogenase (GAPDH) reinforced genetically (Colell *et al.*, 2007). Finally, the only example when caspase activity was maintained, and cells survived MOMP is anastasis upon exposure to ethanol and its subsequent removal (Tang *et al.*, 2018). Mitochondria were able to recover and cells resumed proliferation.

Metabolic reprogramming of a cell to glycolysis during such a critical mitochondrial dysfunction was found necessary to survive MOMP (Tait *et al.*, 2013). Moreover, survival beyond MOMP requires that a fraction of mitochondria evades MOMP, probably due to increased levels of anti-apoptotic BCL-2 family proteins on their outer membrane, and repopulates the cell, while autophagy degrades the dysfunctional counterparts. Interestingly, GAPDH, beyond its metabolic role, was also shown to stimulate autophagy in these conditions (Tait *et al.*, 2010). These examples illustrate that cells have a "regenerative" potential to overcome a catastrophic event of MOMP owning to the mitochondrial degradation and biogenesis capacity.

In contrast to this widespread event, a more subtle MOMP on a limited population of mitochondria has also been observed and named minority MOMP (miMOMP). miMOMP has been observed upon inhibition of anti-apoptotic proteins using BH3-mimetic drugs (Ichim *et al.*, 2015). Physiologically, miMOMP is detectable under invasion of various pathogens, both viruses and intracellular bacteria (Brokatzky *et al.*, 2019). Interestingly, activation of miMOMP induces expression of pro-inflammatory cytokines, showing that MOMP can be pro-inflammatory is some conditions as opposed to typically immunologically silent apoptosis (Martin *et al.*, 2012) (*mechanisms discussed in section 1.2.7.3*). Moreover, caspase activation during miMOMP causes nuclear DNA damage, indicating its pro-tumorigenic role (Brokatzky *et al.*, 2019; Ichim *et al.*, 2015).

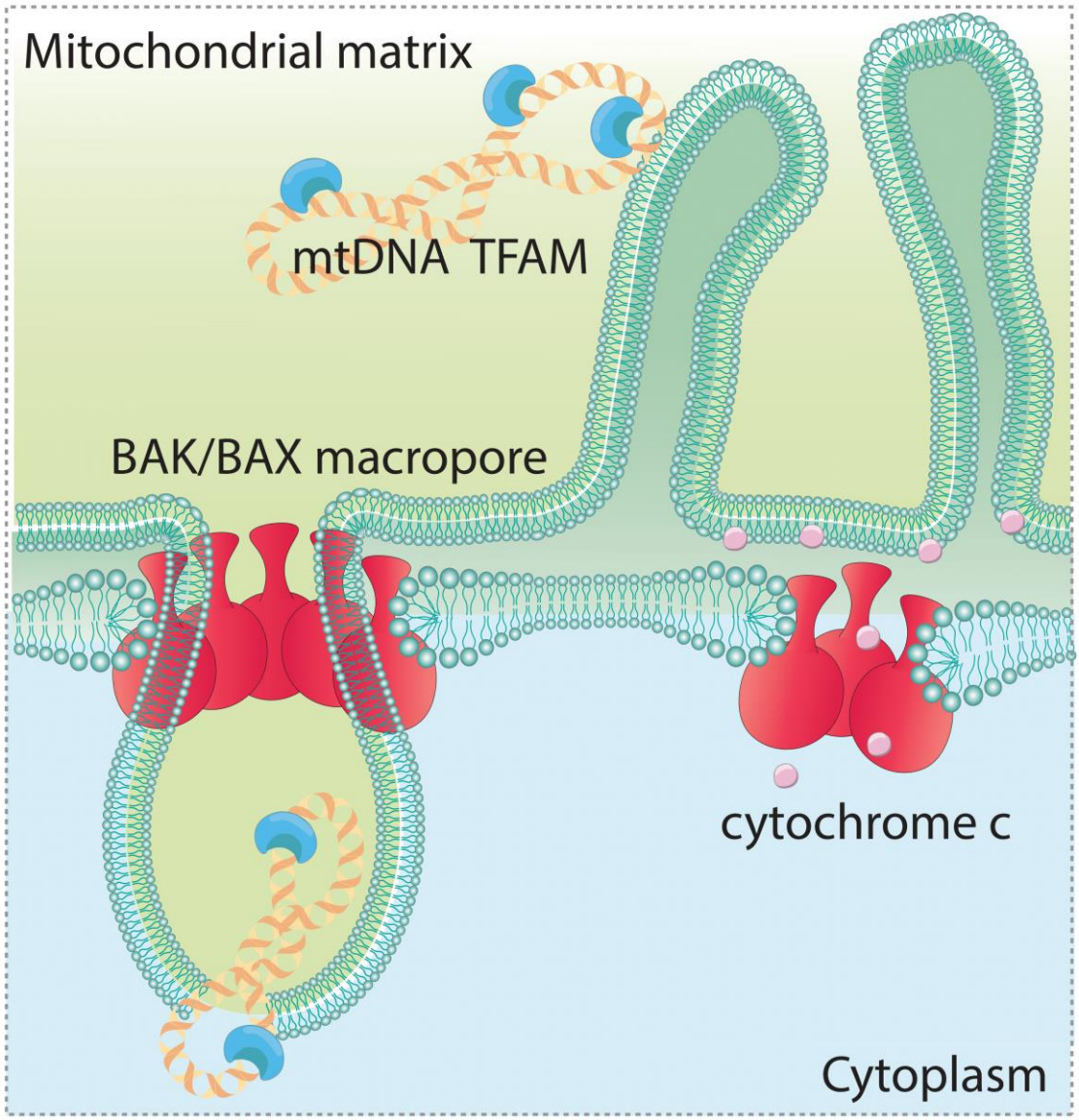

Figure 1.2: Mechanism of mtDNA leakage

Formation of BAK/BAX pores at the outer mitochondrial membrane allows for cytochrome *c* release and mitochondrial inner membrane herniation through the pore, releasing mitochondrial matrix constituents, such as mtDNA and TFAM, into the cytoplasm.

1.2.6.2 Mitochondria-derived DAMPs

Innate immunity comprises systems that protect the cells from pathogen invasion as well as intracellular stress or damage. There are two broad groups of molecules that activate innate immune responses: pathogen-associated molecular patterns (PAMPs) which comprise molecules frequently found in pathogens, and damage-associated molecular patterns (DAMPs) which are molecules released by damaged cells or organelles. Such molecules are detected by receptors, known as pattern-recognition receptors (PRRs). PRRs include NOD-like receptors (NLRs), Toll-like receptors (TLRs), retinoic acid-inducible gene-I (RIG-I)-like receptors (RLRs) and C-type lectin receptors (CLRs) (Banoth *et al.*, 2018; Riley *et al.*, 2020).

Mitochondria contain several types of molecules that have an immunostimulatory potential. Mitochondrial DNA, cardiolipin or N-formyl peptides are the most widely studied mitochondrial DAMPs (Grazioli *et al.*, 2018). mtDNA harbours several features that make it pro-inflammatory. mtDNA is a small, circular, double-stranded molecule that contains remnants of bacterial sequences but also carries a specific pattern of methylation that makes it distinct from nuclear DNA (Grazioli *et al*., 2018). Moreover, even though novel mtDNA repair pathways are being discovered (Kazak 2012), mtDNA is still more prone to oxidative damage considering its localisation within mitochondria. Studies, in fact, point out to oxidation as a necessary step for mtDNA becoming a proinflammatory molecule (Pazmandi *et al.*, 2014; Shimada *et al.*, 2012).

It has been shown that not only mtDNA but also its transcripts, RNA:DNA hybrids and long stretches of single stranded DNA forming during transcription, are immunostimulatory (Dhanwani *et al.*, 2018; Rigby *et al.*, 2014). A recent study described also an atypical mitochondrial double-stranded RNA species (dsRNA) that are hybrids of the transcripts arising from the heavy and lights strands of mtDNA. The lifespan of dsRNAs is usually very short and regulated by mitochondrial helicase SUV3 and polynucleotide phosphorylase (PNPase). Upon their depletion, dsRNA accumulates in the cytoplasm and triggers anti-viral signalling in the form of type I interferon response (Dhir *et al.*, 2018). Finally, TFAM itself may become a proinflammatory molecule (Chaung *et al.*, 2012; Little *et al.*, 2014; Schindler *et al.*, 2018).

1.2.6.3 Cytosolic sensing of mtDNA

mtDNA was shown to activate several of the PRRs, including cGAS, TLR9 and inflammasomes (Riley *et al.*, 2020; West *et al.*, 2017). The first of them – cGAS – is a cyclic GMP-AMP synthase able to bind to double-stranded DNA. cGAS is able to recognise fewer than 20 base pairs, but it is not sufficient to activate cGAS. In fact, fragments above 45 base pairs are required

for cGAS activation (Andreeva *et al.*, 2017). In cells, cGAS forms dimers that bind to a bent DNA molecule. Protein crystallography revealed the presence of the so-called DNA protein ladders, where two cGAS dimers can bind to two DNA molecules (Andreeva *et al*., 2017). DNA binding to cGAS leads to a conformational transition that allows for conversion of ATP and GTP into cyclic 2′3′-cyclic-GMP–AMP (cGAMP), acting as a second messenger. cGAMP binds to the stimulator of interferon genes – STING, residing in endoplasmic reticulum. This leads to phosphorylation of TANK-binding kinase 1 - TBK1, and interferon regulatory factor 3 (IRF3), which acts as a transcription factor allowing transcription of interferon stimulated genes. Recognition of mtDNA by cGAS has been shown in several studies, including the context of apoptosis (Shimada 2012) as well as viral and bacterial infections (West 2015). Interestingly, binding of cytosolic mtDNA to TFAM, can strongly stimulate DNA sensing by cGAS. The mechanism involves the induction of the U-turns and bends in DNA when it is bound to TFAM, but also to other proteins (*e.g.* HMGB), in the case of nuclear DNA (Andreeva *et al*., 2017).

It is important to point out that apoptosis, despite the release of mitochondrial content into cytoplasm and activation of cGAS-STING pathway, is a mode of cell death that is immunologically silent. This is due to the apoptotic caspases' ability to dampen the pro-inflammatory response resulting from mtDNA in the cytoplasm (Rongvaux *et al.*, 2014; White *et al.*, 2014). A recent study revealed a mechanism via which this occurs. Namely, caspase-3 in humans and caspase-7 in mice, cleave cGAS, IRF3 as well as mitochondrial anti-viral signalling protein (MAVS) (Ning *et al.*, 2019). Alternatively, caspase-dependent nucleases could also degrade mtDNA (Nagata, 2005; Rongvaux *et al.*, 2014).

Another mechanism that is involved in the detection of cytosolic mtDNA includes multi-subunit complexes, the inflammasomes. Inflammasomes consist of receptor proteins, such as the nucleotide-binding domain, leucine-rich repeat containing proteins (known as NOD-like receptors, NLRs) and absent in melanoma 2 (AIM2). Activation of inflammasome receptors lead to their oligomerisation and binding to adaptor molecules, finally forming a scaffold for activation of caspase-1. Activated caspase-1 cleaves the pro-inflammatory IL-1 family of cytokines into their mature versions ready for secretion, namely IL-1β and IL-18 (Guo *et al.*, 2015). mtDNA has been shown to trigger inflammasome activation in a model of autophagy deficiency (Nakahira *et al.*, 2011). This report demonstrated that deletion of genes involved in autophagy (LC3B and BECLIN-1) results in an accumulation of dysfunctional mitochondria generating elevated levels of ROS. As the study focused on macrophages, authors

stimulated the cells with lipopolysaccharide (LPS) or ATP, which caused mtDNA to be released into the cytoplasm. The inflammatory response relied on the presence of specific inflammasome receptor, NLRP3, in this context (Nakahira *et al*., 2011).

1.2.6.4 Circulating mtDNA

Upon entering the cytoplasm, mtDNA may eventually reach circulation, potentially exerting an effect on the whole organism. The first report on extracellular, organismal effect of mtDNA was published by Collins *et al.* (2004) who demonstrated its immunostimulatory properties when injected into the joints of mice, causing arthritis (Collins *et al.*, 2004). Subsequently, several reports showed the presence of mtDNA in plasma of patients suffering from mechanical trauma and non-infectious inflammation, indicating mtDNA role as a DAMP (Hu *et al.*, 2017; Simmons *et al.*, 2013). mtDNA appears also in the context of inflammaging, which is "the chronic, low-grade inflammation that develops with age and predicts susceptibility to age-related pathologies (Franceschi *et al.*, 2000). It comprises both innate and adaptive immunity, or at least certain of their functions, that is overstimulated in the elderly people. The traditional view on where the pro-inflammatory stimuli come from pointed to long-lasting exposure to viral infections as the main trigger. Nowadays, many studies show evidence favouring "cellular debris", misplaced and/or misfolded self-molecules" (Franceschi *et al.*, 2017). Such molecules include hundreds of different species, to name a few: lipofuscin, advanced-glycation products (AGEs), misfolded proteins, but also normal cell components that start to pose the risk when present outside their regular location, such as mtDNA, N-formyl peptides, cardiolipin and TFAM (Little *et al.*, 2014) outside mitochondria; nuclear DNA, HMGB1 and histones outside the nucleus, even triphosphate nucleotides, such as ATP and UTP, outside the cell, and many others (Grazioli *et al.*, 2018).

1.3 Aims and objectives

Ageing is a major risk factor for chronic diseases. Cellular senescence, a cellular stress response programme, translates into higher-order pathology of organs and systems, has been identified as a driver of multiple age-related conditions. Therefore, a deep understanding of senescence mechanisms is of critical importance. Mitochondria are considered to be the key players in the complex phenotype of cellular senescence – considered dysfunctional yet mechanistically implicated in mediating the senescence phenotypes, such as the SASP. The overall goal of my thesis research was to investigate novel mechanisms linking mitochondria to the pro-inflammatory phenotype of senescent cells.

Aims for Chapter 3 - Mitochondrial apoptotic stress and its role in the regulation of SASP in cellular senescence

Mitochondria have been found to regulate the pro-inflammatory status of senescent cells, as their depletion leads to the amelioration of this phenotype (Correia-Melo *et al*., 2016). However, the exact mechanisms of mitochondrial involvement have not been elucidated. Cytosolic DNA of nuclear origin has been found critical for the SASP development (Dou *et al*., 2017; Gluck *et al*., 2017; Yang *et al*., 2017). Whether mitochondria may also constitute a source of cytosolic DNA remains to be elucidated.

The objectives of this chapter are to:

- describe the potentially pro-inflammatory processes occurring at the mitochondria during cellular senescence, in particular, the sub-lethal engagement of mitochondrial apoptosis signalling at the minority of mitochondria (referred to throughout this thesis as mitochondrial apoptotic stress) that could constitute a source of cytosolic mtDNA,
- target mitochondrial apoptotic stress to modulate SASP,
- study whether mtDNA is a biomarker of cellular senescence burden at the organismal level.

Aims for Chapter 4 - Comparative analysis of oncogene- and damage-induced senescence with the focus on mitochondria and the role of mitochondrial network structure in SASP regulation

Two widely studied model systems of senescence – oncogene- and damage-induced senescence, possess common and distinct features. However, mitochondrial function has not been thoroughly characterised in a comparative manner across these two modes. Specifically, an elongated mitochondrial network (also referred to as mitochondrial hyper-fusion) has been observed in some models of cellular senescence, including damage-induced senescence (Dalle Pezze *et al.*, 2014; Mai *et al.,* 2010; Yoon *et al.,* 2006). Whether mitochondrial hyper-fusion is a universal feature of all senescence types, including oncogene-induced senescence, remains to be established. This thesis aims to expand the understanding of mitochondrial function and morphology in two commonly studied models of senescence, and investigate the link between mitochondrial morphology and the pro-inflammatory status of senescence cells.

The specific aims of this study are to:

-characterise a range of established senescence markers in oncogene- and damage-induced senescence,

-compare mitochondrial function in two models of cellular senescence, with a focus on mitochondrial morphology,

-modulate mitochondrial morphology and assess its effects on the pro-inflammatory status in the two studied models of cellular senescence.

Aims for Chapter 5 – The role of MxB in regulating mitochondrial function and SASP in damage-induced senescence

Myxovirus resistance proteins, MxA and MxB, are innate immunity factors involved in cellular defence against viral infections. Recently, MxB was shown to localise to mitochondria and play a house-keeping function (Cao *et al.,* 2020). Moreover, its depletion resulted in elevated markers of mitochondrial apoptotic stress (Cao *et al.,* 2020). The aim of this study is to investigate whether MxB may be involved in other cellular stress responses than viral infections, such as cellular senescence.

The specific aims of this study are to:

-measure the expression levels and sub-cellular localisation of MxB in the studied models of senescence,

-assess the impact of MxB depletion on mitochondrial functions in cellular senescence,

-investigate the role of MxB in mediating the pro-inflammatory phenotype of senescent cells.

Chapter 2. Materials and methods

2.1 Cell culture

2.1.1 Cell culture conditions and media

Human embryonic lung MRC5 fibroblasts (ECACC, Salisbury, UK) and IMR90 (a kind gift from Dr Peter Adams) were cultured in Dulbecco's Modiefied Eagle's Medium (DMEM) (Sigma, D5796), supplemented with 10% heat-inactivated foetal bovine serum (FBS). FBS was purchased from Sigma (12133C) when working at Newcastle University (Newcastle upon Tyne, UK) and Gibco (15450584) when working at Mayo Clinic (Rochester, USA). Media was further supplemented with 100μg/ml streptomycin and 100units/ml penicillin solution (Sigma, P4333) and 2mM L-glutamine (Sigma, G3126). Cells were incubated at 37°C, 5% CO2 in a humidified incubator HeraCell 150i CO_2 (Thermo Fisher Scientific) at Newcastle University (Newcastle upon Tyne, UK) or HeraCell Vios 160i Co_2 (Thermo Fisher Scientific). Human fibroblasts MRC5 were cultured in a chamber with atmospheric oxygen conditions. Human fibroblasts IMR90 were cultured in a chamber with low oxygen (3%) conditions. Cell culture media were pre-warmed before use at 37.0°C Isotemp GDP10 "water bath" (Fisher Scientific). Cell handling was performed under Biological Safety Cabinet (1300 Series Class II, Type A2 (Thermo Fisher Scientific, 1323TS). For cell splitting, cells were washed in autoclaved phosphate-buffered saline (PBS) at pH 7.4 prepared from powder (Sigma, P3813) using distilled water. To detach cells from cell culture dishes for splitting, cells were trypsinised using Trypsin-EDTA solution (Sigma, T4049).

The two types of human embryonic fibroblasts that constituted my main study models differ in size, therefore the seeding conditions were optimised: MRC5 cells were seeded at the density of 60 000/well in a 6-well plate and 30 000/well in a 12-well plate for the majority of assays. IMR90 cells were seeded at the density of 100 000/well in a 6 -well plate and 60 000/well in a 12-well plate for the majority of assays. This resulted in the cell density reaching approximately 70% two days after, optimal for the majority of assays. For specific assays, for example siRNA transfection, seeding density was optimised, (in this case, 110 000/well in a 12-well plate). Models and manufacturers of cell culture consumables are provided in a table below.

Mouse adult fibroblasts (MAF) were maintained in Dulbecco's Modiefied Eagle's Medium (DMEM/F12) (Thermo Fisher Scientific, 12634010), supplemented with 10% heat-inactivated foetal bovine serum (FBS) (Biowest, S1520), 100μg/ml streptomycin and

100units/ml penicillin (Sigma, P4333) and 2mM L-glutamine (Sigma, G3126), and incubated at 37°C in low oxygen conditions (3% oxygen), 5% CO_2 in HeraCell Vios 160i Co_2 (Thermo Fisher Scientific).

HEK293T cells used for lentiviral transduction and were maintained in DMEM (Sigma, D5796) supplemented with 10% heat-inactivated foetal bovine serum (FBS) (Sigma, 12133C), 100µg/ml streptomycin, 100units/ml penicillin (Sigma) and 2mM L-glutamine (Sigma, G3126) with further supplementation using 1% non-essential amino acids (Sigma, M7145), Geneticin (10µl/ml) (Sigma, A1720) and sodium pyruvate (5ml of 100mM stock solution) (Sigma, S8636). HEK293T were a kind gift from Dr Viktor Korolchuk.

Table 2.1: Cell culture consumables

Consumable	Manufacturer/Vendor	Catalogue number
75cm² U-Shaped Canted Neck Cell Culture Flask with Vent Cap	Corning	430641U
150cm² U-Shaped Canted Neck Cell Culture Flask with Vent Cap	Corning	430825
12-well Clear TC-treated Multiple Well Plates	Costar	3513
6-well Clear TC-treated Multiple Well Plates	Costar	3516
100 mm TC-treated Culture Dish	Corning	430167
30mm low 60 µ-Dish	Ibidi	80136
Serological pipettes 10 ml	Sarstedt	86.1253.001
Serological pipettes 25 ml	Sarstedt	86.1254.001
Serological pipettes 50 ml	Sarstedt	86.1685.001
Glass Pasteur pipettes	VWR	14673-043
Eppendorf Safe-Lock Tubes, 1.5 ml	Eppendorf	0030120086
Eppendorf Safe-Lock Tubes, 2.0 mL	Eppendorf	0030120094
15 ml Conical Tube	Falcon	352097
50 ml Conical Tube	Falcon	352098

2.1.2 Isolation of primary mouse fibroblasts

In order to isolate primary mouse fibroblasts (referred to also as mouse adult fibroblasts, MAF), 2 ear punches were used (round pieces of ear tissue, ~0.5cm diameter). They were next submerged in DMEM/F12 (Thermo Fisher Scientific, 12634010) culture media without FBS and transferred into a 12-well plate. The samples were washed with 800µl of DMEM/F12 without FBS. 1mg/ml DPBS of Collagenase II (Gibco, 10738473) was prepared from powder and 300µl of Collagenase II solution was added to each well. The ear samples were cut into small pieces using surgical scissors. Then, the samples were incubated for 2 hours at 37°C, in the cell culture incubator with low oxygen concentration. After the incubation, 700µl of warm, DMEM/F12 with FBS (R&D Systems, S11150) was added, and the sample was thoroughly mixed using the pipette P1000. Subsequently, the sample was pressed through a syringe with 23G needle (Thermo Fisher Scientific, 15344467) and transferred into 1.5ml microfuge tube, and centrifuged for 10min at 1000rpm, at room temperature. Pellet was resuspended in DMEM/F12 with FBS and cells were seeded in a new 12-well plate. Cells were monitored for contamination in the subsequent days, and the successful isolations were continued in culture.

2.1.3 Population doubling calculations

Human fibroblast culture was initiated from cell aliquots (1M cells) frozen at PD = x + 16.0 – 22.0 Population Doubling defined as "the total number of times the cells in the population have doubled since their primary culture" (Hayflick *et al*., 1961). At each cell splitting, medium-suspended cells were transferred to a haemocytometer (VWR International UK) and the number of cells within 8 squares was determined under a microscope (DMIL Leica), subsequently multiplied by $1x10^4$ to obtain cell concentration per millilitre, and by the total volume of suspension to obtain the total number of cells.

To calculate the Population Doubling (PD) the following formula was used:

$PD = X + (\ln(Nt/Ns)/\ln(2))$, X – initial PD, Nt – total number of cells, Ns – number of seeded cells

Young, control cells were utilised at maximum PD = x + 25.

2.1.4 Induction of cellular senescence

Replicative senescence model was obtained by passaging MRC5 fibroblasts until reaching replication limit at PD> x+38. Cells were then maintained for additional 4 weeks to confirm ceased population doubling.

Stress-induced senescence model was obtained by exposing proliferating fibroblasts at early passage to x-ray irradiation at 10Gy (in case of MAFs) and 20Gy in case of human fibroblasts, using an X-Ray Irradiator (PXI X-Rad 225, RPS Services Ltd). Media was refreshed immediately after irradiation. Cells were maintained in culture for 10 days after irradiation for the full development of senescence phenotype.

Oncogene-induced senescence model in IMR90 human primary fibroblast is driven by expression of inducible construct ER:RAS (Innes Gil 2019). Transduced cells were a kind gift from Dr Peter Adams. Cells were treated with 4-hydroxy-tamoxifen (4-OHT) over the course of 10 days at the final concentration of 100nM (1:10 000 from 1mM stock). Media was changed every second day containing a new dose of 4-OHT maintain the expression of the transgene. 4-OHT was resuspended in filtered 100% ethanol.

2.1.5 Cryogenic storage

For long-term storage, human and mouse fibroblasts were trypsinised and centrifuged at 800xg. $1x10^6$ cells were suspended in of 5% DMSO (Sigma, D2650) in FBS (Biosera, Gibco or Biowest, depending on the cell type and location) and aliquoted into a cryogenic vial (such as Thermo Fisher Scientific, 377267, various used throughout the studies). Prior to storage in liquid nitrogen, cryogenic vials were placed in a Mr. Frosty™ Freezing Container (ThermoFisher, 5100-0001) container for 24 hours at -80°C. To defrost the cells, the cryo-vials were placed shortly in a "water bath" at 37°C and seeded into a 75 cm^2 flask. Fresh media was replaced no later than after 24h in order to remove residual DMSO.

2.2 Genetic engineering and RNA interference

2.2.1 Lentiviral transduction for gene deletion via CRISPR/Cas9

In order to generate stable BAK and BAX depleted cell lines, lentiviral transduction was performed following class II safety procedures. The viruses were packaged in HEK293T. HEK293FT cells were cultured in complete DMEM media (Sigma, D5796) with addition of 1mM sodium pyruvate (Sigma, S8636), 0.1mM non-essential amino acids (Sigma, M7145) and

antibiotic Geneticin (Sigma, A1720). On the first day of the procedure, HEK293T cells were seeded at the density of $6x10^6$ per 10cm dish (Corning, 430167) in complete DMEM media without penicillin and streptomycin solution. The following day (afternoon), cells were transfected using LipofectamineTM 3000 reagent (Invitrogen, L3000015) with 3 plasmids: two 2nd generation lentiviral packaging plasmids: psPAX and pCMV-VSV-G, and the plasmid encoding Cas9 with guide RNA (gRNA) against the genes of interest LentiCRISPR v2 hBAK and LentiCRISPR v2 hBAX – plasmid maps are provided below. Both plasmids were a kind gift from Dr Stephen Tait. In the case of double knock-out, the mixture of two plasmids encoding sgRNA against two genes of interest was used. On the third day of the procedure, media was replaced with the target cells media, complete DMEM media without antibiotics solution. On the fourth day of the procedure and 48h after transfection, virus-containing media was collected from HEK293FT culture and filtered through 0.45µm PVDF filters (Starlab, P7166-6800). Virus-containing media was subsequently mixed with hexadimethrine bromide (known as polybrene) (Sigma, H9268) at the concentration of 10ug/ml. Virus-containing media was then added to the target cells that were seeded to reach about 70% of confluency at the fourth day of the procedure. Cells were kept in virus-containing media for 24h (instead of 48h as typically for immortalised cell lines). On day 5, media was replaced with complete media containing antibiotics (100µg/ml streptomycin and 100units/ml penicillin solution). Between days 6-8 of the procedure, cells were kept under selection using Puromycin (Santa Cruz, sc-108071A) at the concentration of 50ng/ml. Puromycin selection was optimised as the initial concentration (1µg/ml) was too toxic for primary cells. The effect of gene deletion was confirmed by immunoblotting.

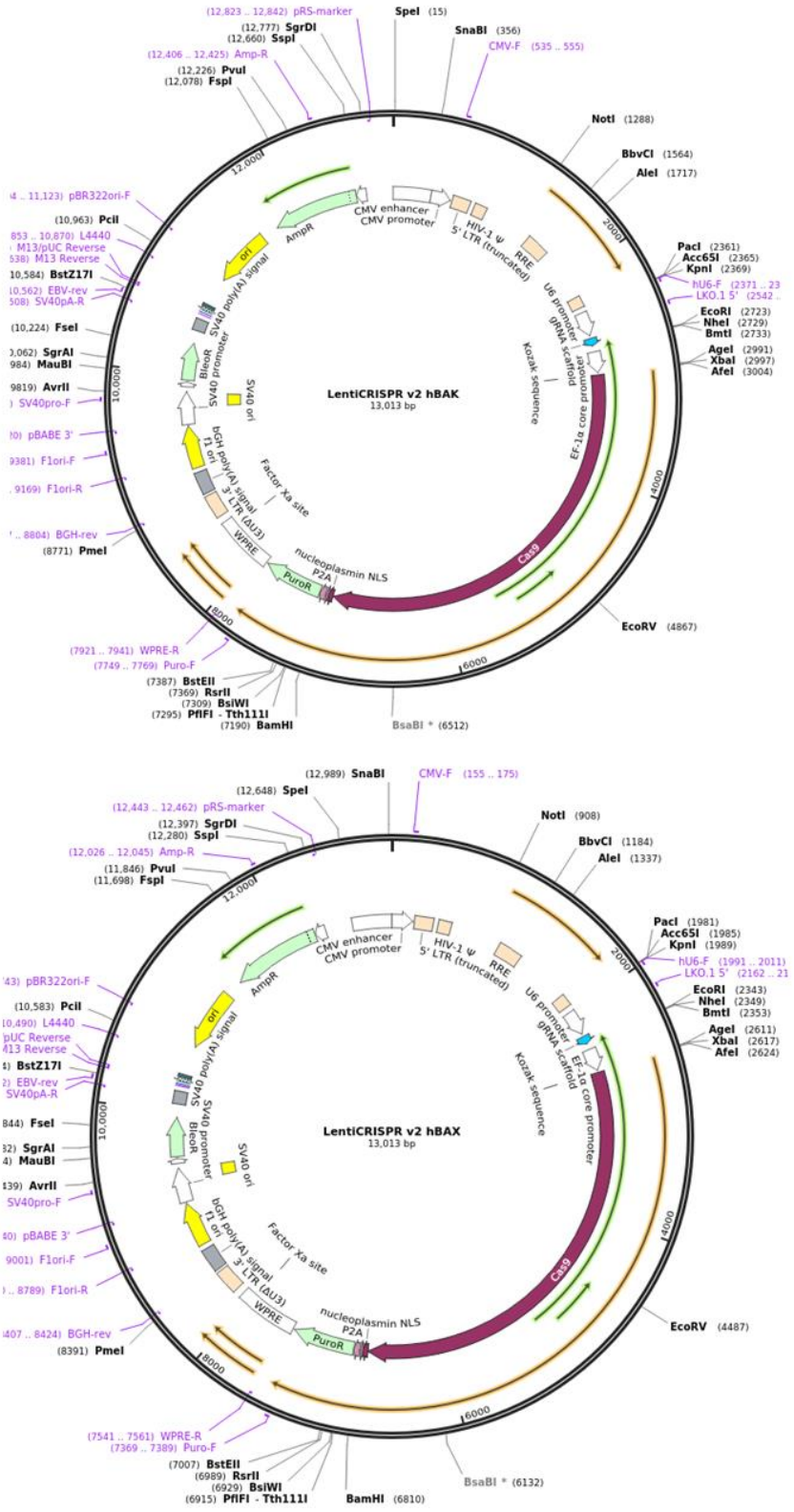

Figure 2.1: Maps of plasmids

2.2.2 RNA interference

For siRNA transfection, Lipofectamine RNAiMAX (Thermo Fisher Scientific, 13778075) was used according to manufacturer's protocol. Cells were grown in 6- or 12-well plate to the confluency of approximately 80%. Opti-MEM™ I Reduced Serum Medium (Gibco, 31985-070) was used for siRNA suspension.

The following reagents were combined and incubated for 10 minutes at room temperature. A mix: For 6 wells in a 6-well plate transfected with the same siRNA: 1080ul Opti-MEM (90µl for 1 well in a 12 well plate or 180µl for 1 well in a 6 well plate) + 60µl siRNA (for 6 wells). B mix: For all 6 wells in a 6 well plate, 72µl of Opti-MEM (6µl for 1 well in a 12 well plate or 12µl for 1 well in a 6 well plate) + 36ul Lipofectamine (3µl per 1 well in a 12 well plate or 6µl per 1 well in a 6 well plate, RNAiMAX from Invitrogen). A and B solutions were subsequently combined (AB mix) and incubated for 20 minutes at room temperature. In the meantime, cells were washed 2 times with HBSS (Corning, 21-021-CV) and 2 times with Opti-MEM to remove residual FBS. 800µl of fresh Opti-MEM and 200ul of AB mix to total of 1ml per 1 well in a 12 well plate (400µl of Opti-MEM and 100 µl of AB mix to total of 500 µl per 1 well in a 12 well plate). 20% FBS DMEM (using typical reagents for human fibroblasts culture) after 5-6h post transfection to make 2ml in a well of a 6-well plate or 1ml in a well of a 12-well plate. The final siRNA concentration in the well was 5pM. Knockdown efficiency was evaluated by qPCR and/or immunoblotting.

A general scheme of an experiment including senescence induction following siRNA transfection:

Day 1 siRNA transfection + 20%FBS DMEM addition

Day 3 Cells split and seeded into final dishes (for example 12-well plate with coverslips or 6-well plate) except for OIS that require further splitting

Day 4 Senescence induced by irradiation (DIS) or addition of 4-OHT (OIS)

Day 5 Proliferating cells collected

Day 7 OIS cells seeded in final dishes

Day 11-13 Senescent (both DIS and OIS) cells collected

Experiment performed in collaboration with Dr Hong Cao (the first round of transfection was performed and demonstrated by Dr Hong Cao, subsequently adapted to perform in our laboratory).

Utilised siRNA were purchased from Dhamacon as ON-TARGETplus siRNA – SMARTpool, a mix of 4 siRNA, 5nmol. siRNA was resuspended in Nuclease-Free Water (Qiagen, 129114) to the stock concentration of 50nM.

Table 2.2: siRNA

siRNA	Vendor	Catalogue number
siDRP1	Dharmacon	L-012092-00-0005
siMFN2	Dharmacon	L-012796-00-0005
siMxB	Dharmacon	L-011736-00-0005
Non-targeting pool (siNT)	Dhamacon	D-001810-10-05

2.3 Treatment with pharmacological compounds

Each utilised pharmacological compound was re-suspended in an appropriate solution, according to manufacturer's protocol. Utilised pharmacological compounds were diluted in cell culture media before the addition to the cells. The list of all compounds and concentrations used is presented in the table below.

Table 2.3: Pharmacological compounds

Pharmacological compound	Concentration	Vendor	Catalogue number
BAX channel blocker	2.5μM	Adooq Biosciences	A15335
Rotenone	1μM, 10μM	Sigma	R8875
ABT-737	10μM, 20μM	Abcam	ab141336
Bleomycin	50μg/ml, 100μg/ml	Sigma	B8416
QVD	1μM	Abcam	ab141421
4-Hydroxytamoxifen	100nM	Sigma	H6278

For the screen of conditions inducing MxB expression, glucose free cell DMEM (Gibco, A14430-01) was used supplemented with D-galactose (Sigma, G0750) at the final concentration of 10mM. The medium also contained 10% FBS (Sigma, 12133C), 100 U/ml penicillin/streptomycin (Sigma, P4333), 4mM L-glutamine (Sigma, G3126) and 10mM HEPES (Sigma, H3375).

For the screen of conditions inducing MxB expression, "hyperlipid medium" was based on standard complete DMEM/F12 (Thermo Fisher Scientific, 12634010) containing 100 U/ml penicillin/streptomycin (Sigma, P4333), 4mM L-glutamine (Sigma, G3126), supplemented with 20 mM sodium L-lactate (Sigma, 71718), 2 mM sodium pyruvate (Sigma, S8636) and 4 mM octanoic acid (Sigma, C2875).

2.4 Microscopy techniques

2.4.1 Immunofluorescence

Cells were grown on coverslips (18mm, VWR VistaVision, 16004-300) in 12-well plates, PBS washed 2X, fixed in 4% paraformaldehyde (VWR, 9713.9010) with addition of 0.2% glutaraldehyde (Sigma, G5882) for 5 minutes, PBS (Sigma, P3813, at pH 7.4 prepared from powder using distilled water, non-autoclaved) washed 2x and permeabilised in 0.1% Triton-X (Sigma, X100) in PBS for 5 minutes, blocked in 5% normal goat serum (NGS) (Vector lab, PK-6101) for 1 hour. Overnight incubation at 4˚C with primary antibodies at concentration indicated in the table below, was followed by 3x PBS washes, and secondary antibody incubation for 1h at room temperature at a rocking device. Secondary antibodies were diluted in blocking solution. Secondary antibodies used are listed in a table below. Coverslips were mounted using ProLong® Gold antifade reagent with DAPI (Molecular Probes, P36935) on microscope slides (Diamond White Gladd, Globe Scientidic Inc., 1384-50W).

Table 2.4: Primary antibodies for immunofluorescence

Primary antibody	Concentration	Vendor	Catalogue number
BAX6A7	1:100	Santa Cruz	Sc-23959
TOMM20	1:200	Sigma	HPA011562
cytochrome *c*	1:1000	Biolegend	612301
DNA	1:100	MerckMillipore	CBL186
p-DRP1	1:100	Cell Signaling	3455S
Ki67	1:1000	Abcam	ab15580
TFAM	1:100	Cell Signaling	8076S
COX IV	1:100	Abcam	ab33985
H3K27me3	1:100	Cell Signaling	9733S
γH2Ax	1:1000	Cell Signaling	9718S

Table 2.5: Secondary antibodies for immunofluorescence

Secondary antibody	Concentration	Vendor	Catalogue number
Goat anti-Rabbit IgG (H+L), Superclonal™ Recombinant Secondary Antibody, Alexa Fluor 647	1:1000	Thermo Fisher Scientific	A27040
Goat anti-Rabbit IgG (H+L) Cross-Adsorbed Secondary Antibody, Alexa Fluor 488	1:1000	Thermo Fisher Scientific	A-11008
Goat anti-Rabbit IgG (H+L) Cross-Adsorbed Secondary Antibody, Alexa Fluor 594	1:1000	Thermo Fisher Scientific	A-11012
Goat anti-Mouse IgG (H+L) Highly Cross-Adsorbed Secondary Antibody, Alexa Fluor 594	1:1000	Thermo Fisher Scientific	A-11032
Goat anti-Mouse IgG (H+L) Cross-Adsorbed Secondary Antibody, Alexa Fluor 647	1:1000	Thermo Fisher Scientific	A-21235
Goat anti-Mouse IgG (H+L), Superclonal™ Recombinant Secondary Antibody, Alexa Fluor 488	1:1000	Thermo Fisher Scientific	A28175

2.4.2 Measurement of mitochondrial membrane potential

For mitochondrial membrane potential measurement, cells were seeded into glass-bottom dishes designated for live-cell imaging (Ibidi, 35mm low µ-Dish, 80136). DIS was induced in the µ-Dish. Cells were induced to OIS in 75cm^2 flasks and seeded into µ-Dish at day 4-5 upon senescence induction. Cells were stained with tetramethylrhodamine (TMRE) (Thermo Fisher Scientific, T669) at 15nM concentration and nonyl acridine orange (NAO) (Biotum, 70012) at 100nM concentration. Following a 30 minutes incubation in the dark at 37°C, the media was changes to dye-free media. Cells were imaged at 37°C, 3% O_2 and 5% CO_2 using LSM780 Zeiss CLSM.

2.4.3 Mitochondria-labelling in live cells

For time-laps CLSM microscopy of mitochondrial dynamics analysis as well as in combination with immunofluorescence, CellLight™ Mitochondria-RFP, BacMam 2.0 was used to label mitochondria (Invitrogen, C10505). The product contains a ready-to-use construct encoding RFP fused to the leader sequence of E1 alpha pyruvate dehydrogenase. 18µl of CellLight™ was added into one well of a 12-well plate or 1 µ-Dish. Cells were imaged or fixed 2 days after transfection.

2.4.3 Senescence-associated β-galactosidase staining

For senescence-associated β-galactosidase staining, cells were grown in 6-well plates, fixed in 2% paraformaldehyde and 0.2% glutaraldehyde for 10 minutes. After 3x PBS washes, cells were incubated in SA-β-Gal staining solution (1.5ml of 1M NaCl, 20µl of 1M Mg Cl_2, 800µl of 0.5M citric acid, 1.2ml of 0.1M sodium phosphate, 5ml distilled water, pH adjusted to 6.0, volume made to 10ml; 8.8ml of the solution was mixed with 1ml potassium ferro-cyanide and 200µ X-gal at 20mg/ml in dimethylformamide), at 37°C for 24h. Cells were subsequently washed 3x in PBS.

2.4.4 Cryo-thin section and immunogold electron microscopy

Cells were first fixed with 0.1% glutaraldehyde and 4% paraformaldehyde in 0.1 mol/l phosphate buffer for 2h, harvested and centrifuged at 900xg for 5 minutes. The cell pellets were then cryoprotected by immersion in 2.3 mol/l sucrose in 0.1 mol/l phosphate-buffer overnight and frozen in liquid nitrogen. Thin cryosections (60 nm) were cut with Leica cryo-microtome (Leica Microsystem Inc., Bannockburn, IL). Samples were incubated overnight at 4°C with primary antibody in 10% fetal calf serum/phosphate-buffered saline solution diluted 1:20. Sections were then incubated with a 10nm anti-mouse IgG gold secondary antibody (Sigma, G7652) for 2 hours at room temperature. After washing, sections were further fixed in 1% glutaraldehyde embedded in 2% methyl cellulose solution containing 0.3% uranyl acetate. The specimens were then observed using a Jeol 1200 electron microscope (Jeol USA Inc., Peabody, MA) operating at 60 to 80 kV. Samples were prepared by Dr Bing Huang from Mayo Core Microscopy Facility.

2.4.5 Microscopes

Microscopy was performed at BioImaging Unit at Newcastle University (Newcastle upon Tyne, UK) and Microscopy and Cell Analysis Core at Mayo Clinic (Rochester, US).

Table 2.6: Microscopes

Type of microscopy	Model and manufacturer	Location
widefield fluorescence microscopy	DMi8 Leica	Newcastle University
widefield fluorescence microscopy	DM6 Leica	Newcastle University
fluorescence stereo microscopy	Leica M205FA	Newcastle University
widefield fluorescence microscopy	Leica DM5500	Mayo Clinic
confocal microscopy	SP8 Leica	Newcastle University
confocal microscopy	LSM780 Zeiss	Mayo Clinic
confocal microscopy with AiryScan type detector	LSM800 Zeiss AiryScan	Newcastle University
Structured Illumination Microscopy (SIM)	Zeiss Elyra PS.1 Super Resolution	Mayo Clinic
Transmission electron microscopy	Joel 1200	Mayo Clinic

2.4.6 Analysis of microscopic data

For the analysis of cytosolic cytochrome *c*, CLSM images were subjected to deconvolution using AutoQuant X3 Deconvolution Software available through Microscopy and Cell Analysis Core at Mayo Clinic (Rochester, US). Pearson's R value was subsequently determined for each cell using Coloc2 ImageJ plugin.

For the 3D visualisation of fragmented mitochondria positive for BAX6A7 marker, Imaris 9.6 Image Visualisation and Analysis Software was used.

The analysis of mitochondrial membrane potential was performed using ImageJ. Upon marking the region of interest, a ratio of TMRE to NAO was determined using raw integrated density values.

To analyse mitochondrial network structure, a manual scoring system was employed. A score on the scale from 1-3 that best represented a cell's mitochondrial phenotype was assigned to each analysed cell. Below, examples of mitochondrial networks representative of each possible score are provided. The percentage of cells with elongated, fragmented, and mixed types of mitochondria was calculated and plotted.

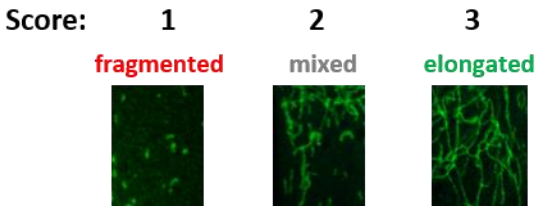

Figure 2.2: Guide to manual assessment of mitochondrial network

Alternatively, MiNA analysis, an ImageJ macro-tool for analyzing mitochondrial network morphology, was employed to assess the effect of BAK and BAX deletion on mitochondrial network structure in cells induced to OIS. The analysis was performed according to the instructions described in Valente *et al.* (2017). In short, CLSM microscopic images were processed using several ImageJ filters, *i.e.* Unsharp mask, Enhance Local Contrast and Median. Subsequently, the image was converted into binary (Make Binary) and skeletonised (Skeletonised). The obtained 2D skeleton of mitochondrial network was analysed with regards to the following parameters: mean branch length, mean summed branch length and mean number of branches/network. "The network" here is understood as one entity separated from other elements of the network within one cell. Below, I provide a guide explaining the meaning of the analysed parameters.

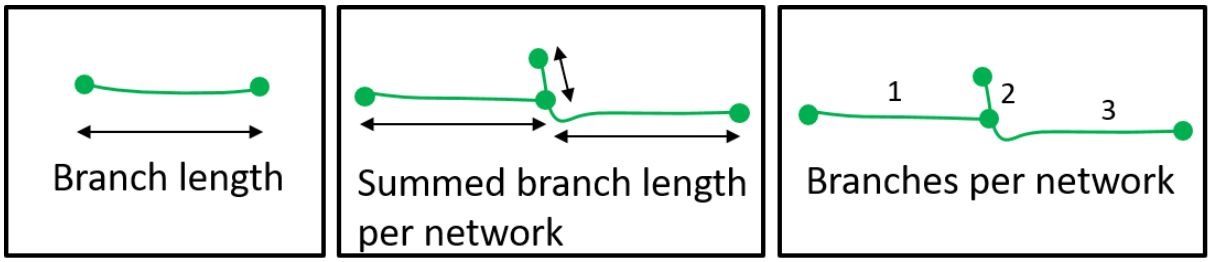

Figure 2.3: Guide to MiNA analysis

Table 2.7: MiNA analysis parameters

Parameter	Description
branch length mean	The mean length of all the lines used to represent the mitochondrial structures.
summed branch lengths mean	The mean of the sum of the lengths of branches for each independent structure (as represented by the morphological/topological skeleton). This is the sum of all branch lengths divided by the number of independent skeletons.
network branches mean	The mean number of attached lines used to represent each structure.

2.5 Fractionation and purification techniques

2.5.1 Cell fractionation (focus of cytosolic fraction)

Cells were grown in 150cm^2 flasks, tripsinised and counted. 7x10^6 cells were collected in 15ml falcons and centrifuged at 900xg for 5 minutes, supernatant was discarded ad cells were re-suspended in 3ml of PBS. Cell suspension was transferred into 2 1.5ml eppendorf tubes. Cells were centrifuged at 600xg for 5 minutes. The pellet from one tube was frozen and considered as "whole cell fraction". The second pellet was re-suspended in 500µl Buffer1 (150 mM NaCl, 50mM HEPES pH 7.4, 25ug/ml digitonin (Sigma, D141)) and incubated for 10 minutes at room temperature. Cells were subsequently centrifuged at 150xg at 4°C – the pellet was considered as "western blot fraction" and the supernatant considered as "cytosolic fraction" was further centrifuged 2x at 150xf at 4°, and 1x at 17000xg for 10 minutes. Collected samples were stored at -80°C. DNA from the "whole cell fraction" was isolated using a kit DNeasy Blood & Tissue Kit (Qiagen, 69504) according to manufacturer's protocol and the DNA concentration was measured using NanoDrop® ND-1000 Spectrophotometer. "Cytoplasmic fraction" was subjected to a clean-up procedure using Qiaquick Nucleotide Removal Kit (Qiagen, 28115) according to manufacturer's protocol and DNA concentration was measured using NanoDrop® ND-1000 Spectrophotometer.

2.5.2 Cell fractionation (focus on mitochondria-enriched fraction)

Cells were grown in 75cm^2 dishes. Before sample collection, cells were rinsed in ice-cold 1xPBS. 5ml of ice-cold 1xPBS was added and cells were scraped from the well and collected into a 50ml falcon tube. Samples were centrifuged at 800xg for 5 minutes at 4°C and re-suspended in Mitochondrial Isolation Solution (20mM HEPES-KOH pH 7m 220mM mannitol,

70mM sucrose, 1mM EDTA, 0.5 mM PMSF, 2mM DTT). Cells were broken open using 60 strokes using a glass homogeniser. The homogenate was centrifuged for 5 minutes at 800xg, 4°C. The supernatant containing mitochondria was subsequently centrifuged again for 5 minutes at 800xg, 4°C. An aliquot of the supernatant was collected as "whole cell extract". The remaining sample was centrifuged for 10 minutes at 16100xg, 4°C. The supernatant was collected as "cytosolic fraction". 1ml of Mitochondrial Isolation Solution was added to the pellet containing mitochondria and centrifuged for 10 minutes at 16100xg, 4°C. This step was repeated. The pellet was finally re-suspended in 100µl of Mitochondrial Isolation Solution. All fractions stored at -80°C.

2.5.3 Purification of extracellular vesicles

10ml of conditional media from cell culture was centrifuged for 10 min at 300xg, 4. After transferring the supernatant into a new tube, the sample was centrifuged for 30 min at 3000xg. 1 ml of supernatant was collected as a control, and the remaining 9ml were filtered using a 0.2µm filter (Sigma, 16534K). 1ml of filtered media was collected as a control and the remaining was subjected to ultracentrifugation for 1.5 h at 100000xg, 4°C. Pellets were resuspended in sterile (autoclaved) PBS (at pH 7.4 prepared from powder from Sigma, P3813) and the centrifugation step was repeated either in a micro-ultracentrifuge or ultracentrifuge at the same conditions. Pellet was resuspended in 100µl of sterile (autoclaved) PBS and further used for DNA isolation by Qiagen DNeasy Blood & Tissue Kit (Qiagen, 69504 or 69506) and exosome analysis using Nanosight nanoparticle analyser (NanoSight NS300).

2.6 Quantitative PCR

2.6.1 RNA extraction

Cells were grown in 6-well plates and cells from one well were used. Cells were trypsinised and centrifuged at 150xg for 5 minutes at 4°C, washed with PBS and centrifuged again at 150xg for 5 minutes at 4°C. RNA extraction from cell pellets was carried out using the RNeasy Mini Kit (QIAGEN, 74106), according to the manufacturer's instructions. RNA pellets were resuspended in Nuclease-Free Water (Qiagen, 129114). RNA quality and yield were assessed using NanoDrop One (Thermo Scientific, ND-ONE-W).

2.6.2 cDNA synthesis

0.3-0.5μg (depending on the experiment, equal within an experiment) of RNA was used per reverse transcription reaction. HighCapacity cDNA Reverse Transcription Kit (ThermoFisher Scientific, 4368814) was used, according to the manufacturer's instructions using MiniAmp Plus Thermo Cycler (Applied Biosystems, A38076) using the following conditions: 25°C for 10 minutes, 37°C for 120 minutes, 85°C for 5 minutes and 4°C hold.

2.6.3 DNA extraction for mtDNA copy number analysis in cells

Cells were trypsinised and centrifuged at 150xg for 5 minutes at 4°C, washed with PBS and centrifuged again at 150xg for 5 minutes at 4°C. DNA extraction from cell pellets was performed using DNeasy Blood & Tissue Kit (Qiagen, 69504), according to manufacturer's protocol and the concentration was measured using NanoDrop® NanoDrop One (Thermo Scientific, ND-ONE-W).

2.6.4 Quantitative PCR reaction

Quantitative real-time PCR was conducted using two different systems, at a) Newcastle University (Newcastle upon Tyne, UK) and b) Mayo Clinic (Rochester, USA)

a) Each qPCR well contained 10μl of reaction mix, which consisted of 4μl of cDNA/DNA, 5μl Power Syber® Green PCR Master Mix (Invitrogen, 4367659), 0.2μl of 10μM reverse and forward primers, and 0.8μl deionised H_2O. Reactions were performed in a C1000TM Thermal Cycler (Bio-Rad). The thermocycler conditions at C1000TM Thermal Cycler (Bio-Rad) were 95°C for 10 seconds, 95°C for 15 seconds, 60°C for 1 minute for 45 cycles; 65°C for 5 seconds.

b) Each qPCR well contained 20μl of reaction mix, which consisted of 5μl of cDNA/DNA, 10μl ToughMix Perfecta (PerfeCTa qPCR ToughMix, QuantaBio, 95112-250), 1μl of qPCR Primer Assay, and 4μl deionised H2O. Reactions were performed using CFX96TM Real-Time System (Bio-Rad). The thermocycler conditions at CFX96TM Real-Time System (Bio-Rad) were 95°C for 30 seconds, 95°C for 1 seconds, 60°C for 20 seconds for 40 cycles.

2.6.5 Quantitative PCR primers

The following primers/ TaqMan™ Gene Expression Assay were used for the detection of mtDNA, D-loop region, ND2, in cytosolic and whole cell fractions, as well as for mtDNA copy

number analysis in human fibroblasts a) at Newcastle University (Newcastle upon Tyne) and b) at Mayo Clinic (Rochester, USA):

a) human MT-Dloop

5'-CATCTGGTTCCTACTTCAGGG-3'

5'-CCGTGAGTGGTTAATAGGGTG-3'

b) human MT-7S: Hs02596861-s1 (ThermoFisher)
human MT-ND2: Hs02596874-g1 (ThermoFisher)
mouse MT-Dloop: 5'-AATCTACCATCCTCCGTGAAACC-3'
5'-TCAGTTTAGCTACCCCCAAGTTTAA-3'

Primers for gene expression analysis were purchased from Integrated DNA Technologies (IDT) as PrimeTime qPCR Primer Assays chosen from pre-designed sequences (products' details provided below). Lyophilised primers were resuspended in TE Buffer (10mM Tris, 0.1mM EDTA, pH 8.0) or ready-made 1X TE Solution pH 8.0, 0.2µm filtered (IDT, 11-05-01-09).

Table 2.8: qPCR Primer Assays

qPCR Primer Assay	Vendor	Product number
IL6	IDT	Hs.PT.58.40226675
IL8	IDT	Hs.PT.58.39926886.g
RSP16	IDT	Hs.PT.58.366374
p21	IDT	Hs.PT.58.38492863.g
MMP2	IDT	Hs.PT.58.39114006
IL10	IDT	Hs.PT.58.2807216
TNFα	IDT	Hs.PT.58.45380900
MxB	IDT	Hs.PT.58.5524200
GLB1	IDT	Hs.PT.58.1143964
PGC1α	IDT	Hs.PT.58.14965839
PGC1β	IDT	Hs.PT.58.38577994

In order to quantify cytosolic mtDNA content, the mean Ct value obtained through a qPCR analysis for "cytosolic fraction" was normalised by subtraction of the mean Ct value for "whole cell fraction". Fold change of mtDNA content in "cytosolic fraction" was quantified between two conditions (e.g. young control cells and irradiated cells).

In order to quantify mRNA expression levels, obtained Ct values were normalised to the levels of a house-keeping control transcript (RSP16). mRNA expression was calculated using the ΔΔC(t) method.

2.7 Immunoblotting

2.7.1 Sample collection

Cells were grown in 6-well plates, PBS washed and treated with 80µl of RIPA buffer (150mM NaCl, 1% TritonTM X-100, 0.5% sodium deoxycholate, 0.1% SDS and 50mM Tris pH 8.0) supplemented with and 2x protease and phosphatase inhibitors (Thermo Scientific, 78442). Cells from at least 2 wells were pooled together or cells from a 10cm dish were used. Cells were scraped using plastic cell scrapers (Corning, CLS3010). Cell lysates were transferred into 1.5ml Eppendorf tubes. Lysates were centrifuged at 16 000xg for 10 minutes at 4°C. Protein concentration was determined using BioRad Protein Assay (BioRad, Reagent A, 500-0113; Reagent B, 500-0114; Reagent C, 500-0115). Absorbance was measured using FLUOstar Omega microplate reader (BMG Labtech). Lysates were mixed with loading buffer (4X Laemmli buffer, BioRad 161-0737) to normalise protein concentration. At least 15µg of protein was loaded per lane.

2.7.2 Immunoblotting

Extracted protein was subjected to electrophoresis using acrylamide Tris-glycine gels of appropriate percentage depending on the protein sise (gel recipes provided in a table below). Electrophoresis was powered by PowerEase™ 90W Power Supply (230 VAC) (Life technologies, 15240394).

Table 2.9: Running and stacking gels

Solution	Polyacrylamide %				
	4%	10%	12%	15%	20%
Distilled H_2O	5.1 ml	3.9 ml	3.5 ml	2.9 ml	1.9 ml
SureCast Resolving buffer (Thermo Fisher Scientific, 15530445)	2.0 ml	2.0 ml	2.0 ml	2.0 ml	2.0 ml
20% SDS (Thermo Fisher Scientific, 10607443)	50 µl	50 µl	50 µl	50 µl	50 µl
SureCast Acrylamide 40% (Thermo Fisher Scientific, HC2040)	0.8 ml	2.0 ml	2.4 ml	3.0 ml	4.0 ml
10% APS (Sigma, A3678)	80 µl	80 µl	80 µl	80 µl	80 µl
TEMED (Sigma, T9281)	8 µl	8 µl	8 µl	8 µl	8 µl

Solution	4%
Distilled H2O	1.92 ml
SureCast Stacking buffer (Thermo Fisher Scientific, 15558055)	0.75 ml
20% SDS (Thermo Fisher Scientific, 10607443)	7.5 µl
SureCast Acrylamide 40% (Thermo Fisher Scientific, HC2040)	0.3 ml
10% APS (Sigma, A3678)	30 µl
TEMED (Sigma, T9281)	3 µl

Upon electrophoresis, protein was transferred to PVDF membrane (Millipore, IPVH00010) or BioTrace NT nitrocellulose (Pall Corporation, 66485) using a Trans-Blot® SD Semi-Dry Transfer Cell (Biorad) (the same model was used at both Newcastle University and Mayo Clinic locations). Transfer efficiency was evaluated using Ponceau S solution (Sigma, P7170) incubated with the membrane for approximately 5 minutes, subsequently rinsed with water. Blocking was performed using PBST milk (0.1% Tween® 20, 5% milk powder). Subsequently, the membrane was incubated with primary antibody diluted in PBST milk or 5% Bovine Serum Albumin (BSA, Sigma, A2153) (overnight at 4°C). Secondary antibody was diluted in 5% milk and added to the membrane for 1 hour, incubated at room temperature and rocked. The lists of primary and secondary antibodies used are provided below. Enhanced chemi-luminescence (ECL) reaction was performed using ClarityTM ECL Western Blot Substrate (Bio-Rad, 170-5060) at Newcastle University (Newcastle upon Tyne, UK) and KwikQuant Western blot detection kit (Kindle Bioscience, R1100) at Mayo Clinic (Rochester, USA), according to manufacturer's protocol. Imaging was performed using the LAS4000 (Fujifilm) at Newcastle University (Newcastle upon Tyne, UK) and KwikQuant Imager (Kindle Bioscience, D1001) at Mayo Clinic (Rochester, USA). Bands intensity was quantified using ImageJ software.

Table 2.10: Primary antibodies for immunoblotting

Primary antibody	Concentration	Vendor	Catalogue number
Bax (D2E11)	1:1000	Cell Signaling	5023
BAK (D4E4)	1:1000	Cell Signaling	12105
SDHA	1:1000	Cell Signaling	5839
GAPDH (D16H11)	1:5000	Cell Signaling	D16H11
cleaved caspase-3	1:500	Cell Signaling	9664S
IL8	1:500	Abcam	ab18672
α-tubulin	1:1000	Cell Signaling	2144S
p-IRF3(Ser396) (D6O1M)	1:500	Cell Signaling	4947
IRF-3 (D83B9)	1:1000	Cell Signaling	4302
Lamin B1	1:1000	Abcam	ab16048
p21	1:1000	Cell Signaling	2947
p16	1:500	BD Pharmingen	550834
BCL-W (31H4)	1:1000	Cell Signaling	2724
A1/BFL1 (D1A1C)	1:1000	Cell Signaling	14093
PGC1β	1:1000	Abcam	ab61249
UQCRC2	1:1000	Abcam	Ab103616
p-MAPK(Erk1/2) (Thr202/Tyr204)	1:1000	Cell Signaling	9101
MAPK (Erk1/2)	1:1000	Cell Signaling	9102
p-DRP1 (Ser616)	1:1000	Cell Signaling	3455
DRP1	1:500	In-house made, a kind gift from Dr Mark McNiven	
MFN2	1:500	Abcam	ab262915
FIS1	1:500	Millipore-Sigma	ABC67
OPA1	1:500	BD Biosciences	612606
actin	1:1000	Sigma	A2060
MxB		Novus Biologicals	NBP1-81018
MT-CO1/COX1	1:250	Abcam	ab14705

Table 2.11: Secondary antibodies for immunoblotting

Secondary antibody	Concentration	Vendor	Catalogue number
Goat AntiRabbit HRP Conjugated	1:5000	Abcam	A0545
Goat AntiMouse HRP Conjugated	1:5000	Abcam	A2554

2.7.3 FPLC

For FPLC, cells were grow in 150cm^2 flasks. 3 150cm^2 flasks were combined in order to extract sufficient study material. Cells were tripsinised, washed with PBS and centrifuges at 900xg for 5 minutes. Subsequently, cell pellets were lysed using CHAPS lysis buffer (1% [w/v] CHAPS, 20 mM HEPES at pH 7.4, 150 mM NaCl, 1% [v/v] glycerol, 1 mM PMSF, 10 µg/mL leupeptin, 10 µg/mL pepstatin, 100 mM NaF, 10 mM sodium pyrophosphate, 1 mM sodium vanadate, 20 nM microcystin) for 30 minutes at 4°C. 200µl of samples diluted to contain 10 mg/ml of protein were injected onto a Superdex S200 size exclusion column. 20 500µl fractions were collected. 4% of each fraction (20µl of each 500µl obtained for each fraction) was first subjected to immunoblotting, however, this amount of sample did not allow to detect any BAX or BAK signal even upon over-night chemiluminescent signal exposure toa photographic film. Subsequently, protein was precipitated using trichloroacetic acid (TCA) precipitation. 1/10th sample volume of 10% Triton-x100 was added to the samples, followed by addition of 1/5th sample volume of 100% ice cold TCA. Samples were incubated on ice for 20 minutes. Samples were centrifuges for 5 minutes at 800xg at 4ºC. Supernatant was removed and pellet washed 1x with 1ml ice-cold 10% TCA and 2x with 1ml acetone at -20ºC. Samples were left to air dry at room temperature. Dried pellets were solubilised in sample buffer (4x Laemmli Sample Buffer (Biorad, 1610747) with 1% 2-mercaptoethanol (Biorad, 1610710), 40µl per sample was added to suffice for two gels. Protein was separated using 4-20% gradient acrylamide Tris-Glycine gel, generated using Gradient Former (Biorad, Model 230, 165-2700). Protein was transferred to BioTrace NT nitrocellulose (Pall Corporation, 66485) and immunoblotted according to the protocol described in the previous section. Primary and secondary antibodies used for this assay are listed in the table above. Experiment performed in collaboration with Dr Haiming Dai.

2.8 ELISA

For ELISA analysis, cells were grown in 6-well plates and incubated in serum free DMEM for 24h. The medium was collected for the analysis. Concentrations of cytokines IL-6 and IL-8 in cell culture media were determined using sandwich ELISA (R&D Systems; DY206/DY208). 96-well plates were coated with the Capture Antibody diluted at the concentration of 240µg/ml by an overnight incubation. Plates were washed using a Wash Buffer (0.05% PBS-Tween20). Plates were blocked using Reagent Diluent (1% BSA in PBS) for 1.5h at room temperature and washed. 25µl of samples and standards were added to each well. For highly concentrated media samples, as in OIS experiments, media was diluted 1:100 in order to obtain absorbance values in the range of the standards. Plates were covered with an adhesive strip and incubated for 2h at room temperature and washed. 25µl of Detection Antibody was added to each well and incubated for 2h at room temperature, washed. 25µl of Streptavidin-horseradish peroxidase (HRP) dilution was added to each well and plated were incubated for 20 minutes at room temperature, washed. 25µl of Substrate Solution (1:1 mixture of Colour Reagent A (H_2O_2) and Colour Reagent B (Tetramethylbenzidine) was added to each well, plates were incubated for 20 minutes at room temperature. 25µl of Stop Solution (2N H_2SO_4) was added to each well. Using a microplate reader, optical density at 450nm was determined. Readings were corrected by subtracting the readings at 540nm.

2.9 Mitochondrial bioenergetics assessment

2.9.1 High resolution respirometry

For high resolution respirometry, cells were cultured in 75cm^2 flasks in order to obtain 1 million cells. Prior to the assay, cells were tripsinised, counted and centrifuges at 900xg for 5 minutes. Supernatant was removed and the cell pellet was resuspended in 100ul Mitochondrial Respiration Medium (110mM saccharose, 60mM lactobionic acid, 0.5mM EGTA, 3mM $MgCl_2 \cdot 6H_2O$, 20mM taurine, 10mM KH_2PO_4, 20mM HEPES, adjusted to pH 7.1 with KOH at 37C, 1g/l BSA, fatty acid free) and added into the chamber of the OROBOROS Oxygraph-2k system. Cellular respiration was set to stabilise for approximately 10 minutes. Endogenous basal respiration termed Routine was measured without addition of any substrates. Subsequently, 10µl of 1µg/ml oligomycin was added and Leak state respiration was measures. Next, 1µM titration of FCCP was performed and electron transport chain (ETS) maximum capacity was measured, termed Maximum. Finally, cells were inhibited using 1µl of 0.5uM rotenone and 1ul of 2.5uM antimycin A in order to take the measurement of residual respiration.

The Oxygraph-2k chambers were left to equilibrate after the addition of each pharmacological compound. All measurements were carried out in 2ml volume at 37°C.

Experiment performed in collaboration with Becca Reeds from Dr Alberto Sanz laboratory.

2.9.2 Seahorse

For Seahorse analysis, cells were seeded into Seahorse XF96 cell culture microplates (Agilent, 101085-004). Cells density was optimised to 15000 cells (IMR90) per well on the day of seeding in the case of proliferating conditions, and 3000 per well on the day of seeding in the case of cells that were induced to DIS (irradiated within the Seahorse microplate). One day prior to Seahorse assay, Agilent Seahorse XFe96 Sensor Cartridge was hydrated in Seahorse XF Calibrant at 37°C incubator (Boekel) overnight. The procedure was repeated 1 hour before the assay, upon 1x wash with water. Cellular oxygen consumption rates (OCR) was measured using Agilent Seahorse XFe96 Analyser, according to manufacturer's instructions. Cell media was changed to unbuffered basic medium, 45 mg/l dextrose, 110mg/l sodium pyruvate (Sigma, S8636), 4mM L-glutamine (Sigma, G3126). During the experiment, the following pharmacological compounds were added: 0.5µM oligomycin, 2.5µM FCCP, 0.5µM rotenone with 2.5µM antimycin A. The generated OCR values were normalised to cell numbers quantified after the assay using Automated Cell Counter. Graphs representing OCR throughout the Seahorse XF assay were generated using Wave 2.4 software and further edited in GraphPad Prism. Experiment performed in collaboration with Dr Padraig Flannery from Dr Trushina laboratory.

2.10 Experiments based on mouse and human plasma

2.10.1 Mouse plasma collection

200µl of mouse blood was collected from facial vein. Alternatively, total blood was collected from inferior vena cava in anesthetised mice. Blood samples in EDTA tubes were centrifuged at 1300xg for 15 minutes, at 4°C. DNA isolation was performed using Qiagen DNeasy Blood & Tissue Kit (Qiagen, 69504), according to manufacturer's protocol. After DNA extraction, sample was eluted in 50µl of eluent.

For comparison of the circulating levels of mtDNA between young and old mice, wild type mice of C57BL/6 × BALB/c background were used. Ages are indicated in the graphs.

For comparison between lean and obese mice, $Lepr^{db}$ transgenic mice were used. $Lepr^{db}$ (referred to as db/db) mice contain mutation in leptin receptor gene and constitute a type II

diabetes model. Homozygous mice (db/db) exhibiting obese phenotype were compared to heterozygous littermates (db/+). Plasma samples were obtained thanks to curtesy of Dr Kirkland's laboratory.

For the comparison between healthy mice and mice suffering from pulmonary fibrosis, wild type as well as INK-ATTAC transgenic mice of C57BL/6 × BALB/c background of aged 2.5–8 months old who received PBS or 2 U kg^{-1} bleomycin (Bleomycin for injection, USP, APP Pharmaceutical, LCC Schaumburg, IL) through aerosolised intratracheal delivery (as described in Schafer *et al.*, 2017) were used. Bleomycin treated mice were subjected to the treatment with AP20187 (10 mg kg−1, six treatments) delivered by intraperitoneal injection, dasatinib (5 mg kg−1) plus quercetin (50 mg kg−1) delivered by oral gavage or vehicle. The treatment started 5 days post-intratracheal instillation and the mice were sacrifised 3 weeks post-intratracheal instillation. The blood was collected from facial vein at autopsy. Bleomycin plasma samples were obtained thanks to curtesy of Dr Marissa Schafer.

For the MT-D-LOOP oligonucleotide total 90bp from IDT (20nmole Ultramer Duplex):

5'-AATCTACCATC CTCCGTGAAA CCAACAACCC GCCCACCAAT GCCCCTCTTC TCGCTCCGGG CCCATTAAAC TTGGGGGTAG CTAAACTGAA-3'

2.10.2 Human plasma collection

Human blood in EDTA tubes was centrifuged at 2000xg for 10min. 400µl or 200µl of plasma was transferred into a new 1.5ml microfuge tube and further subjected to DNA isolation using Qiagen DNeasy Blood & Tissue Kit (Qiagen, 69504) according to manufacturer's protocol.

Blood samples for method optimisation were obtained thanks to curtesy of Dr Amir Sadighi Akha from Laboratory for Medicine and Pathology, Mayo Clinic. 400µl of plasma was used for DNA extraction. After DNA extraction, DNA sample was eluted in 80µl of eluant.

Blood samples in the frailty study were collected in EDTA at the time of the surgical procedure, from 93 patients. After plasma isolation, samples were frozen in -80°C. 200µl of plasma was used for DNA extraction. Human plasma samples from the "frailty study" were obtained thanks to curtesy of Dr Marissa Schafer.

PCR Primer Assays used for mtDNA detection are listed in section 2.6.5.

The following sequences of oligonucleotide standards were used for determination of mtDNA concentration in plasma.

For the MT-D-LOOP oligonucleotide total 110 bp from IDT (20nmole Ultramer Duplex)

5’-
AACCCCCCCTCCCCCGCTTCTGGCCACAGCACTTAAACACATCTCTGCCAAACCC
CAAAAACAAAGAACCCTAACACCAGCCTAACCAGATTTCAAATTTTATCTTTTGG-
3’

Quantification of mtDNA copy number in plasma or cell culture media was performed based on a standard curve generated using an oligonucleotide (sequence provided above) matching the sequence of the amplicon amplified during the qPCR reaction using the corresponding primers. The oligonucleotide was diluted 500µl in Nuclease-Free Water (Qiagen, 129114) to the concentration of 40nM. Next, a serial dilution was performed with diluting factor 10x. The mass of DNA in the standard’s samples was calculated using an online calculator: https://www.wolframalpha.com/widgets/view.jsp?id=b9648e4dc6a5ad47bea0c9023e810dfd Next, an online calculator for determining the number of double-stranded DNA copies was used, such as the one available under the link: http://cels.uri.edu/gsc/cndna.html, in order to determine DNA copy number in each utilised standard sample. Finally, an exponential plot was generated using obtained Ct values and DNA copy number in standard samples. From the plot equation, DNA copy number was calculated in the study samples.

Clinical frailty index was based on the Cardiovascular Health Study (CHS) criteria (Friend et al. 2001). These concern five core components of the frailty: unintentional weight loss (greater than or equal to 10 pounds in the prior year), low grip strength (less than 17–21 kg for women and 29–32 kg for men, normalised to BMI), exhaustion (self-report, on the Center for Epidemiological Studies Depression Scale), low gait speed (less than 0.83 m per second), and low physical activity by the Physical Activity Scale for the Elderly (men, less than 383 kcal expended per week; women, less than 270 kcal expended per week) (Schafer *et al*., 2016).

The list of SASP factors correlated to the levels of circulating mtDNA: ADAMTS13, CCL3, CCL4, CCL5, CCL17, CCL22, FAS, GDF15, GDNF, ICAM1, IL-15, IL-6, IL-7, IL-8, MMP2, MMP9, OPN, PAI1, SOST, TNFR1, TNF-α, VEGFA, ACTIVIN A, PAI2. All but ACTIVIN A and PAI2 were quantified from EDTA plasma using commercially available multiplex magnetic bead immunoassays (R&D Systems) based on Luminex xMAP multianalyte profiling platform and analysed on a MAGPIX System (Merck Millipore). ACTIVIN A concentration was analysed by a Quantikine ELISA Kit (R&D Systems), according to the manufacturer’s instructions. PAI2 levels were quantified by an ELISA Kit (Cloud-Clone Corp.) (Schafer *et al.*, 2016; Schafer *et al.*, 2020).

Correlations between mtDNA copy number, frailty score, BMI and concentration of plasma cytokines were assessed using Pearson's (for datasets of normal distribution) or Spearman's (for datasets of non-normal distribution) rank correlation test.

2.11 Statistical analysis

GraphPad Prism 9 software was used for the generation of graphs and statistical analyses. All data were assessed for normality Shapiro-Wilk normality test. Further statistical tests used and obtained p-values are indicated in figure description. P-values are also indicated by the number of asterisks above the graphs, where ns means $p>0.05$, the symbol "*" means $p\leq0.05$, "**" means $p\leq0.01$, "***" means $p\leq0.001$. Error bars represent SEM when the experiment has been repeated 3 or more times. For graphs representing intercellular variation (variation within cell population), error bars representing SD were used.

Chapter 3 Results - Mitochondrial apoptotic stress and its role in the regulation of SASP in Cellular Senescence

3.1 Introduction

Mitochondrial dysfunction constitutes a hallmark of cellular senescence and includes increased mitochondrial biogenesis and mass, disrupted energetic processes, elevated levels of reactive oxygen species (ROS) production and morphological alterations (Chapman *et al.*, 2019; Korolchuk *et al.*, 2017; Zwerschke *et al.*, 2003). These complex changes are not a mere "feature" but a driving force of other phenotypes of cellular senescence. Mitochondrial ROS were shown to reinforce the cell cycle arrest by inflicting DNA damage in the nucleus and telomere shortening (Passos *et al.*, 2010; Passos *et al.*, 2007). Later, mitochondria were found as critical regulators of SASP, as their depletion by wide-spread mitophagy prevented the development of a pro-inflammatory phenotype (Correia-Melo *et al.*, 2016). The exact mechanism of how mitochondria drive the SASP remains to be elucidated. Independently, recent studies demonstrated the reliance of SASP on cytosolic DNA sensing pathway, cGAS-STING (Dou *et al.*, 2017; Gluck *et al.*, 2017; Yang *et al.*, 2017). These studies pointed to nuclear DNA in the form of cytosolic DNA fragments (CCFs) as the source of cytosolic DNA. The role of mtDNA in senescence remains unexplored, despite its known role in innate immune responses (Fang *et al.*, 2016).

Senescent cells are known to be highly resistant to apoptosis. Among several mechanisms, they maintain high expression of anti-apoptotic members of BLC-2 family that allow for the maintenance of mitochondrial integrity (Yosef *et al.*, 2016). Specifically, this class of proteins inhibit the initiation stage of the apoptotic cascade - the activation of pro-apoptotic members of BCL-2 family, BAK and BAX. Activation of BAK and BAX results in a process called mitochondrial outer membrane permeabilisation (MOMP) and the release of mitochondrial constituents into the cytoplasm. MOMP has originally been considered a binary, all-or-nothing event that inevitably leads to cell death (Martinou *et al.*, 2000). However, it has been observed that in certain conditions MOMP occurs at a minority of mitochondria – termed minority MOMP (miMOMP), in the absence of cell death (Ichim *et al.*, 2015). Initially, miMOMP was described in conditions when the anti-apoptotic BCL-2 family proteins were inhibited with the use of BH3 mimetics (Ichim *et al.*, 2015). Later, it was found to play a role in physiological processes orchestrating inflammation caused by pathogen invasion (Brokatzky *et al.*, 2019). Considering the fact that mitochondrial network in senescent cells undergoes a

vast expansion, while senescent cells generally experience a high molecular damage burden and various mitochondrial dysfunctions (Korolchuk *et al.*, 2017; Ogrodnik, Salmonowicz, & Gladyshev, 2019), I considered a hypothesis that the protection against MOMP mediated by overexpression BCL-2 family of proteins might not be perfectly efficient, allowing for MOMP to occur. In this chapter, I set out to investigate whether miMOMP - also referred to throughout this thesis as mitochondrial apoptotic stress, occurs during cellular senescence and contributes to the development of SASP.

3.2 Activated BAX is found in senescent cells

In healthy cells, BAK resides in the outer mitochondrial membrane (OMM) whereas BAX in the cytosol with a small fraction in the OMM (Cosentino *et al.*, 2017). Mitochondrial BAX is constantly retrotranslocated from mitochondria to the cytosol in order to prevent apoptosis (Edlich *et al.*, 2011). BAK and BAX form tight globular structures consisting of nine α-helices. In an instance of apoptotic stress, signalling must proceed rapidly, therefore these two key effector proteins, rather than being regulated at the level of gene expression, undergo a process referred to as activation (Cosentino *et al*., 2017). This process depends on the interaction of the so-called triad of the BCL-2-type proteins: pro-apoptotic BAK and BAX, pro-apoptotic BH3-only proteins such as BIM, BID or Puma; and pro-survival multi-domain BCL-2 members, such as BCL-2 or BCL-W. BH3-only proteins directly activate BAK and BAX via BH3:groove interaction or promote their activation indirectly, by displacing BAK and BAX from the pro-survival BCL-2 proteins, such as BCL-2 or BCL-W, utilizing the same binding site. Activation consists of a conformational change that consists of displacement of unstructured loop between α-helices 1 and 2, mobilisation of the C-terminal α-9 in case of BAX (Westphal *et al.*, 2011), exposure of BH3 domains, as well as exposure of N-terminal end of the protein, known as 6A7 epitope (Gavathiotis *et al.*, 2010). BAX activation is followed by its translocation to the OMM that occurs due to the newly exposed α-9 that inserts as a transmembrane domain. The "structural metamorphosis" further leads to homo-dimerisation due to exposure of BH3 domain that allows for the interaction with a hydrophobic groove of another BAK or BAX molecule – this autoactivation propagates the "death" signal (Gavathiotis *et al.*, 2010). Symmetric homodimers are considered as basic units for higher order oligomerisation (Uren *et al.*, 2017) – a process that eventually leads to the formation of pores that pierce mitochondrial outer membrane.

To study the activation of BAX, I utilised a mouse monoclonal antibody that binds to the epitope formed by the 12 to 24 N-terminal amino-acids, referred to as anti-BAX6A7. The

antibody allows for the detection of active BAX only in native conditions. Even a treatment with non-ionic detergents that are generally used for membrane-bound proteins extraction to preserve their structure, leads to epitope exposure and "false positive" detection of, in-fact, monomeric, inactive BAX (Hsu *et al.*, 1997). Considering this, I decided to take an immuno-fluorescence approach using paraformaldehyde solution as fixative that does not denature proteins. I utilised an established model of senescence using human embryonic fibroblasts, MRC5, triggered to enter the senescence programme by 20Gy γ-irradiation. Cells 10 days post irradiation are considered to enter a state of damage-induced senescence (DIS).

Proliferating and senescent cells were immuno-stained against BAX6A7 and an outer membrane protein, TOMM20. For cell imaging, I utilised both confocal laser scanning microscopy (CLSM) and super-resolution microscopy, precisely the Structured Illumination Microscopy (SIM). CLSM proved the most handy for quantification purposes. Rapid scanning combined with eliminating the out-of-focus signal allowed to evaluate the cell on the whole, critical when working with senescent cells that are approximately 8 times larger than proliferating controls, and with the phenomena that are subtle and sometimes "hard to spot". SIM was employed for capturing the most representative examples at the highest available resolution.

I found that senescent cells were characterised by the presence of infrequent but pronounced foci of BAX6A7, a fraction of which co-localised with TOMM20 signal (Figure 3.1 A). I observed that BAX6A7-positive mitochondria are often disassociated from the main mitochondrial network that in damage-induced senescence displays a hyper-fused morphology. The fragmented mitochondria positive for BAX6A7 were either globular as in Figure 3.1 A and B - or tubular (an example of such mitochondrion is further provided in Figure 3.12 A). The measurement of BAX6A7 foci diameter revealed the size of BAX pores on mitochondria may reach 500 nm in diameter (Figure 3.1 C). Quantification of the frequency of cells positive for BAX6A7 co-localising with mitochondria, revealed that this initial stage of apoptotic signalling occurs in nearly 60% of cells during DIS and only approximately 5% in proliferating cells (Figure 3.1 D).

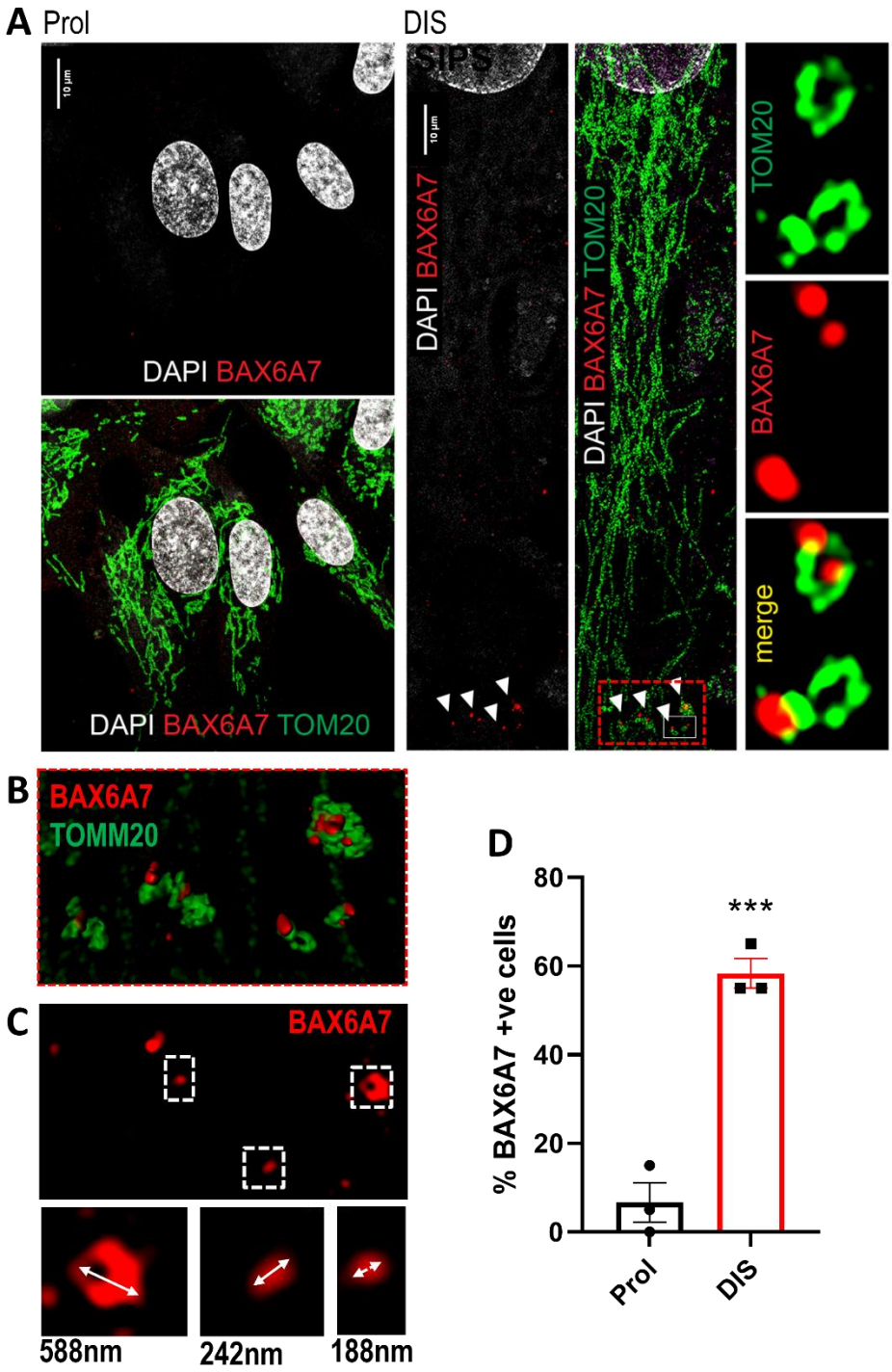

Figure 3.1: Activation of BAX in human embryonic fibroblasts MRC5 in damage-induced senescence

(A) Representative super-resolution SIM microscopy images of activated BAX stained with anti-BAX6A7 antibody and mitochondria stained with anti-TOMM20 antibody. Scale bar represents 10µm. (B) Representative 3D image generated using Imaris software, depicting the region of circular mitochondria positive for activated BAX - based on the same image as in A (C) Example image displaying the BAX6A7 foci diameter- based on the same image as in A (D) Quantification of the percentage of cells positive for BAX6A7 co-localising with mitochondrial signal TOMM20 using CLSM. N=3 independent replicates/coverslips, 20 cells/replicate. Analysed using Student's t-test: Prol vs DIS p=0.0007. Error bars represent SEM.

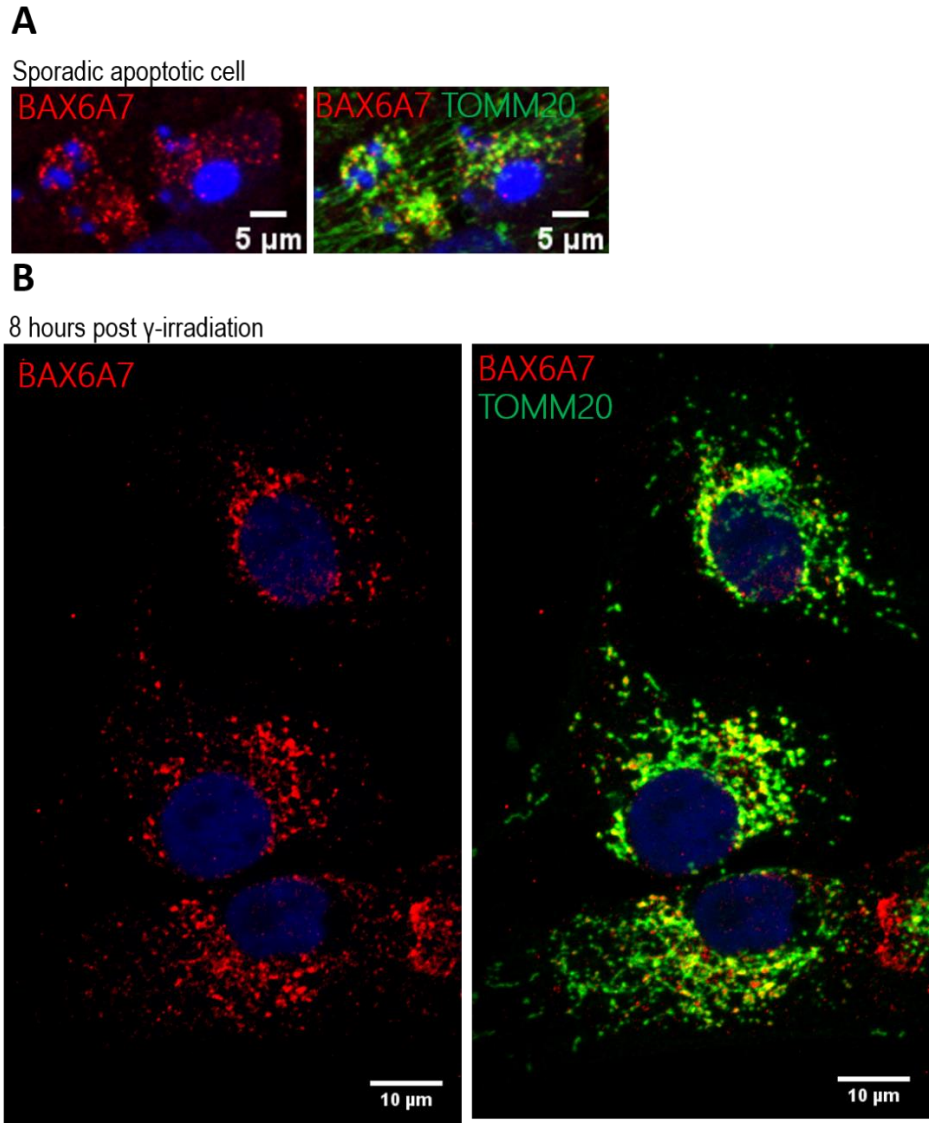

Figure 3.2: BAX activation during apoptosis or acute stress

(A) Representative CLSM images of activated BAX stained with anti-BAX6A7 antibody and mitochondria stained with anti-TOMM20 antibody in a sporadic apoptotic cell defined by its shrunken size and fragmentation of its nucleus. Provided as a positive control. Scale bar represents 5µm. **(B)** Representative CLSM images of activated BAX stained with anti-BAX6A7 antibody and mitochondria stained with anti-TOMM20 antibody in IMR90 cells 8 hours upon 20Gy γ-irradiation. Provided as a positive control. Scale bar represents 10µm.

In order to prove the reliability of this method to stain mitochondria that undergo apoptotic stress, I present an example of an apoptotic cell, defined by its shrunken shape, fragmented nucleus and mitochondria. The cell displayed a strong BAX6A7 signal covering the majority of its mitochondria (Figure 3.2 A). Furthermore, in cells fixed 8 hours post γ-irradiation, I found a fraction of cells with a pronounced BAX6A7 staining that also co-localised with the majority of mitochondria (Figure 3.2B).

To corroborate the finding of BAX activation during senescence, I performed size exclusion fast protein liquid chromatography (FPLC) that allows for separation of protein samples from cell lysate depending on molecular size and detection of BAX self-oligomers (Yethon *et al.*, 2003). BAK behaves in a similar manner with regards to self-oligomer formation during apoptosis, therefore its activation may also be detected using FPLC approach. Lysing the cells in CHAPS buffer protects the native state of self-oligomers (Brustovetsky *et al.*, 2010). By subjecting cell lysate to FPLC, I obtained 20 fractions ranging from 600kDa (B15 fraction) to 10kDa (C4 fraction), subsequently immunoblotted for BAX and BAX. Analysis of the concentrated samples for BAX and BAK by western blotting revealed the formation of self-oligomers in senescent cells but not proliferating cells: BAX - Figure 3.3 A and BAK – Figure 3.3 B.

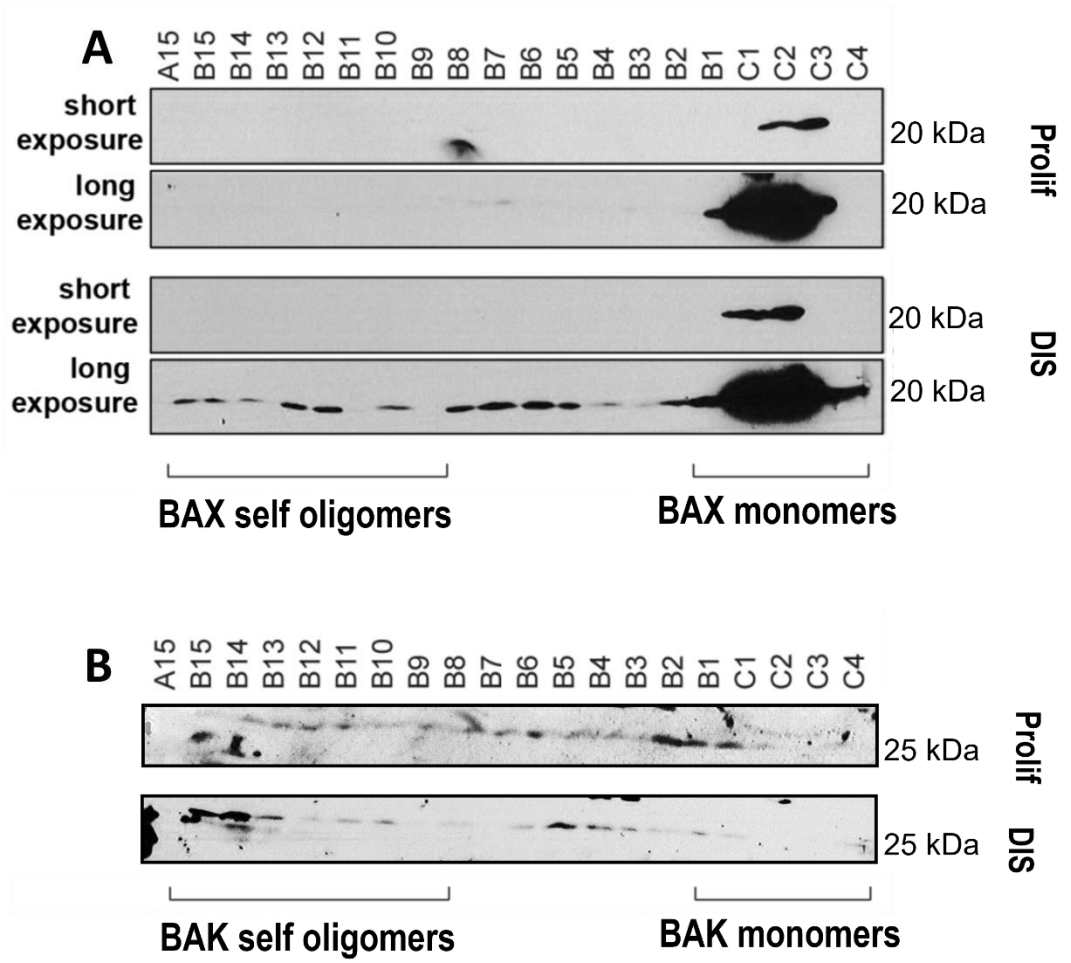

Figure 3.3: Presence of self-oligomers of BAX and BAK in human embryonic fibroblasts MRC5 in damage-induced senescence

(A) Western blots of BAX upon FPLC fractionation and protein precipitation. Fractions of decreasing protein molecular weight are shown from the left to the right. Short exposure represents films exposed for approximately 2 minutes while long exposure represents films exposed overnight, n=1, **(B)** Western blots of BAK upon FPLC fractionation and protein precipitation. Fractions of decreasing protein molecular weight are shown from the left to the right, n=1. Performed in collaboration with Dr Haiming Dai from Prof Scott Kaufmann laboratory, at the Division of Oncology Research, Department of Oncology, Mayo Clinic (Rochester, Minnesota, USA).

3.3 Cytochrome *c* is released into the cytoplasm of senescent cells

Having observed the activation of BAX and BAK during damage-induced senescence, the following step was to assess whether mitochondrial apoptotic stress proceeds further leading to the release of the cytochrome *c*. Cytochrome *c*, when present in the cytoplasm, is a principal apoptogenic factor due to its role in the formation of the apoptosome complex that directly regulates the activation of apoptotic effector caspases. Cytochrome *c*, an IMM protein, is present as loosely and tightly bound - attached to the IMM by its association with anionic phospholipids, primarily cardiolipin (Ott *et al.*, 2002). Solubilisation of cytochrome *c* is required for its release via outer membrane permeabilisation. Recent studies revealed cytochrome *c* release is an immediate process upon MOMP initiation and precedes the release of the matrix components such as TFAM and mtDNA by approximately 5 minutes – based on kinetic quantitation of live-cell imaging using Lattice Light-Sheet Microscopy (LLSM), the state of the art technology to study dynamics processes (McArthur *et al.*, 2018).

In order to assess the release of cytochrome *c* into the cytoplasm during cellular senescence, I employed SIM microscopy imaging of cells immune-stained for cytochrome *c* and TOMM20. Generally, the two signals displayed strongly overlapping patterns representative of mitochondrial networks (Figure 3.4 A). However, cells in DIS when compared to proliferating counterparts, were distinctively characterised by the presence of cytosolic cytochrome *c* in the form of large puncta (Figure 3.4 A) as depicted by the example in the upper part of the image representing the senescent cell, or larger clusters in proximity to circular mitochondria, separated from the main network, as depicted in the lower part of the image representing the senescent cell (Figure 3.4 A). This observation has been independently made and quantified by my lab colleague, Dr James Chapman (Figure 4.3 B), who evaluated co-localisation using Huygens software (Figure 4.3 B). The Pearson's Correlation Coefficient – a statistical measure of linear correlation between two variables, here the signal representing cytochrome *c* and TOMM20, was lower in senescent cells (both DIS and replicative senescence) than in proliferating cells (Figure 4.3 B).

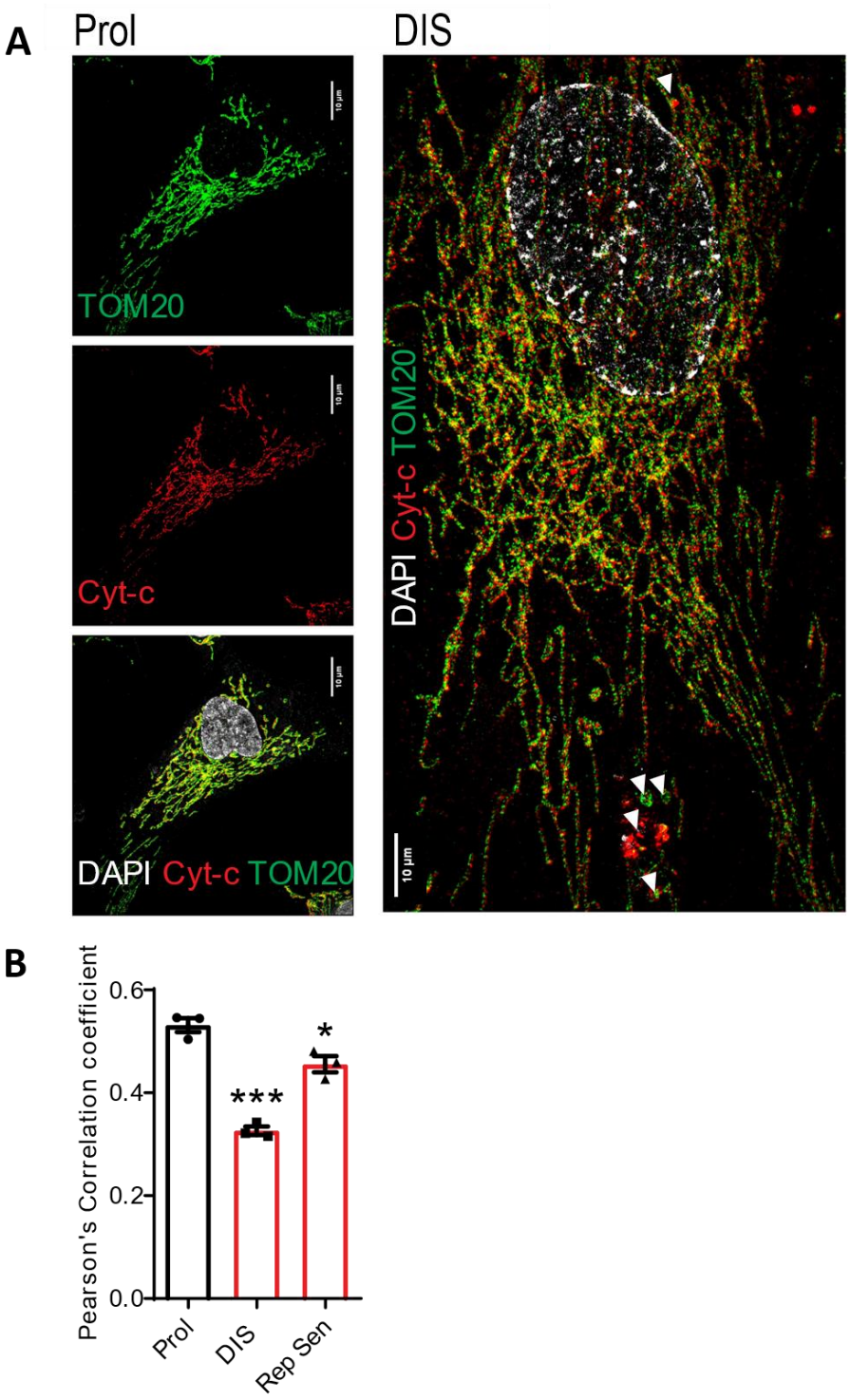

Figure 3.4: Release of cytochrome *c* in human embryonic fibroblasts MRC5 in damage-induced senescence and replicative senescence

(A) Representative super-resolution SIM microscopy images of cytochrome *c* and TOMM20. Scale bar represents 10µm. **(B)** Quantification of the co-localisation of cytochrome *c* and TOMM20 expressed as Pearson's correlation coefficient, n=3 independent replicates/coverslips, minimum 158 cells total/condition. This analysis was performed by James Chapman based on a similar staining and confocal microscopy images. Analysed using Student's t-test: Prol vs DIS p=0.0002, Prol vs Rep Sen p=0.0216. Error bars represent SEM.

3.4 Senescent cells are characterised by mtDNA leakage

The presence of distinct foci of activated BAX detected by super-resolution SIM microscopy that may reach the size of 200-500 nm suggested that BAX, and presumably BAK, pores become large enough to allow for mtDNA leakage, therefore mediate the full apoptotic cascade in senescent cells. To test whether senescent cells are indeed characterised by increased cytosolic content of mtDNA, I used several complimentary approaches.

First, I performed an immuno-fluorescence staining against DNA using a monoclonal anti-DNA antibody that does not have mtDNA specificity and a mitochondrial marker, TOMM20. The majority of the DNA signal was visible as distinct foci following the network of mitochondria, suggesting that the antibody allowed for identification of mtDNA (Figure 3.5 A). The same tool was utilised by other studies to detect mtDNA (Kukat *et al.*, 2011; West *et al.*, 2015). Quantification of the number of DNA foci that did not co-localise with mitochondria, neither with the nucleus or other large blebs of DNA marked with DAPI that might be considered CCFs, pointed out that cells in DIS contain significantly more cytosolic DNA (Figure 3.5 A). In Figure 3.5 B and C, I show separately the number of cytosolic DNA foci that are visible per single z-plane (Figure 3.5 B) or for the whole cell, based on a confocal microscopy image containing data from several z-planes covering the whole cell in z-axis (Figure 3.5 C). I also quantified the number of cytosolic mitochondrial transcription factor A (TFAM) foci, which indicated that at least a portion of the cytosolic DNA is of mitochondrial origin (Figure 3.5 D).

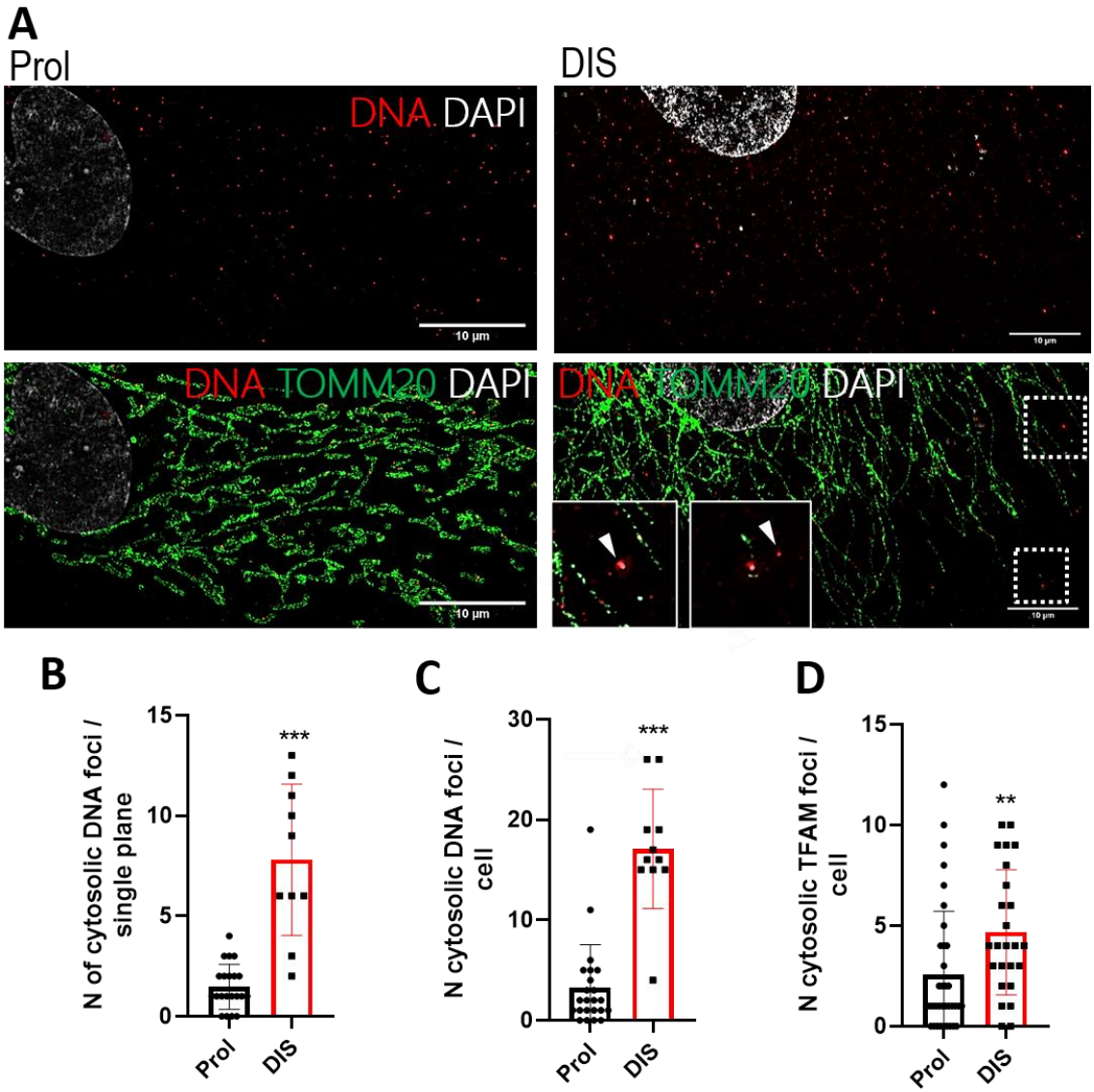

Figure 3.5: Leakage of mtDNA in human embryonic fibroblasts MRC5 in damage-induced senescence – microscopy approach

(A) Representative SIM microscopy images of DNA and TOMM20. Scale bar represents 10µm. **(B)** Quantification of the number of cytosolic DNA foci based on DNA and TOMM20 staining using CLSM – per single z-plane, n=minimum 10 cells/condition, Student's t-test: Prol vs DIS $p<0.0001$ **(C)** Quantification of the number of cytosolic DNA foci based on DNA and TOMM20 staining using CLSM – per cell, n=minimum 11 cells/condition, Mann-Whitney test: Prol vs DIS $p<0.0001$ **(D)** Quantification of the number of cytosolic TFAM foci based on TFAM and TOMM20 using CLSM– quantified per cell, n=minimum 24 cells/condition, Mann-Whitney test: Prol vs DIS $p=0.0028$. Error bars represent SD.

To directly test whether cytosolic DNA foci represent mtDNA, I optimised a staining using both anti-DNA and anti-TFAM antibody with mitochondria visualised using CellLight™ Mitochondria-RFP system, a construct encoding RFP fused to the leader sequence of E1 alpha pyruvate dehydrogenase (PDH) – a mitochondrial enzyme, packaged in the insect virus baculovirus, known as BacMam 2.0. The triple-labelling imaged using super-resolution AiryScan microscopy confirms that some of the cytosolic DNA co-localised with TFAM, therefore represents mtDNA nucleoids or its fragments (Figure 3.6 A).

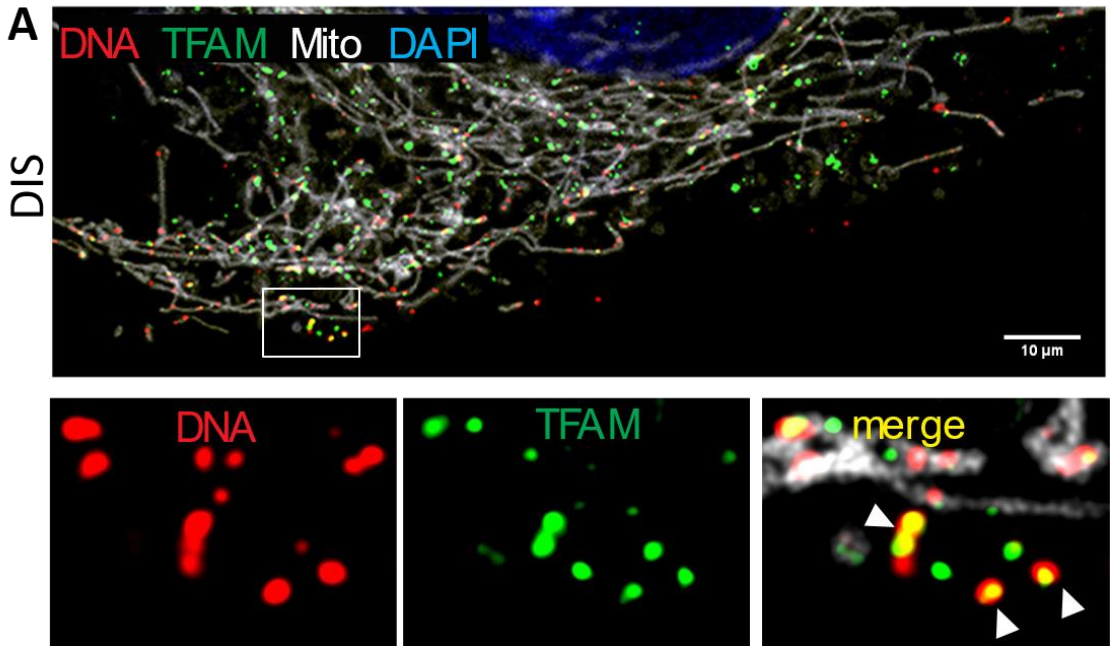

Figure 3.6: Co-localisation of cytosolic DNA and TFAM in human embryonic fibroblasts IMR90 in damage-induced senescence

(A) Representative image of mtDNA leakage obtained using super-resolution AiryScan microscopy, DNA was stained using anti-DNA and anti-TFAM antibodies, and mitochondria using an anti-TOMM20 antibody - an example of DIS. Scale bar represents 10µm.

Independently from microscopy approaches, I utilised an unbiased, qPCR-based method that allows for the detection of mtDNA levels in fractionated cytosol. Using digitonin as a mild detergent for a short duration of time, mitochondria stay intact while cell membrane breaks down releasing the cytosolic content. Cytosolic fraction is purified by subsequent centrifugation steps. To demonstrate the absence of mitochondrial proteins in the cytosolic fraction, I performed a western blot for succinate dehydrogenase complex, subunit A (SDHA). This analysis informed about the lack of mitochondrial contamination (Figure 3.7 A). qPCR analysis of nuclear gene - haemoglobin (HGB) on extracted DNA samples from the cytosolic fraction and whole cell lysates revealed that no nuclear DNA was detected in the cytosolic fraction, indicating the purity of cytosolic fraction (data not shown). The cytosolic content of mtDNA was normalised to the whole cell content, and expressed as fold change between proliferating and senescent cells. The levels of D-loop region of mtDNA in the cytosol was increased by two- to fifteen-fold in DIS, and four- to ten-fold in replicative senescence (Figure 3.7 B).

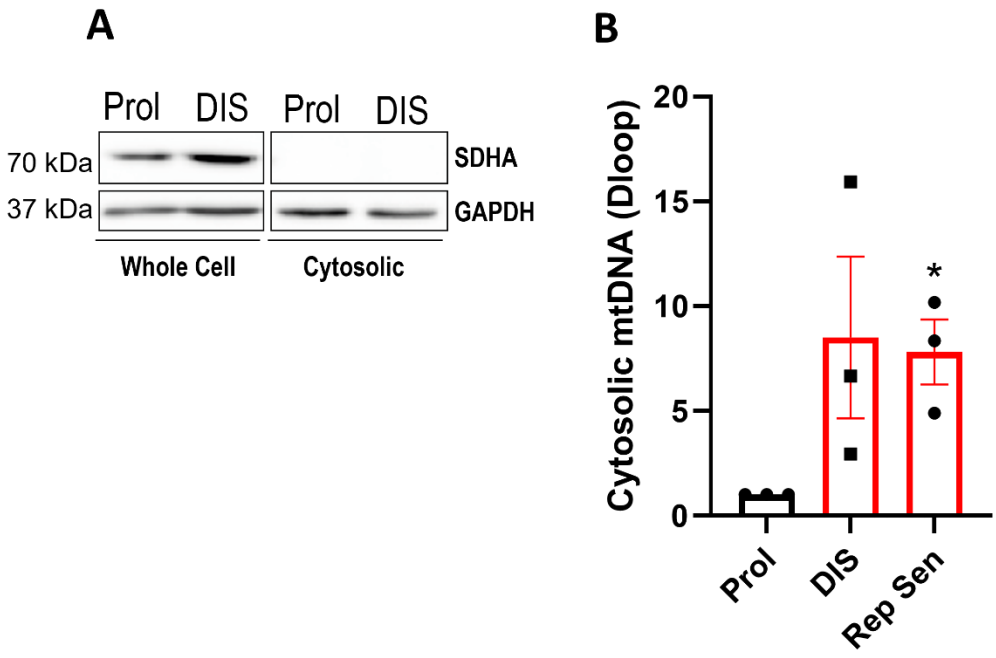

Figure 3.7: Leakage of mtDNA in human embryonic fibroblasts MRC5 in damage-induced senescence and replicative senescence - cellular fractionation/qPCR approach

(A) Representative western blot of SDHA and GAPDH demonstrating the purity of the cytosolic fraction obtained using sub-cellular fractionation **(B)** Levels of cytosolic mtDNA (D-loop region) upon sub-cellular fractionation and qPCR, normalised to the levels of total cellular mtDNA and to Prol control. n=3 independent replicates/sub-cellular fractionations. Analysed with Student's t-test: Prol vs DIS p =0.1238, Prol vs Rep Sen p=0.0117. Error bars represent SEM.

3.5 A small sub-population of circular mitochondria among otherwise hyper-fused network is marked by fission signal in senescent cells

Mitochondrial fission has been widely described to accompany apoptosis. In contrast, senescent cells have been shown to be characterised by a hyper-fused mitochondrial network (Dalle Pezze *et al.*, 2014; Yoon *et al.*, 2006). A more careful analysis of mitochondrial morphology in the model of DIS, pointed my attention to a small sub-population of mitochondria that is disassociated from the main mitochondrial network, in the form of globular or short-tubular entities. Examples of such mitochondria are visible in the Figures 3.1 A-B, 3.4 A, 3.5 A, 3.6 A. Here, I set out to characterise them further and performed an immuno-fluorescent staining for phosphorylated DRP-1 (p-DRP1) at Serine-616, which is one, among several fission signals, promoting mitochondrial fragmentation (Kashatus *et al.*, 2015; Roe *et al.*, 2018). A double staining of p-DRP1 and cytochrome *c* oxidase I (COX1) as a mitochondrial marker, revealed the fission signal was indeed present at some of the globular mitochondria in DIS (Figure 3.8 A).

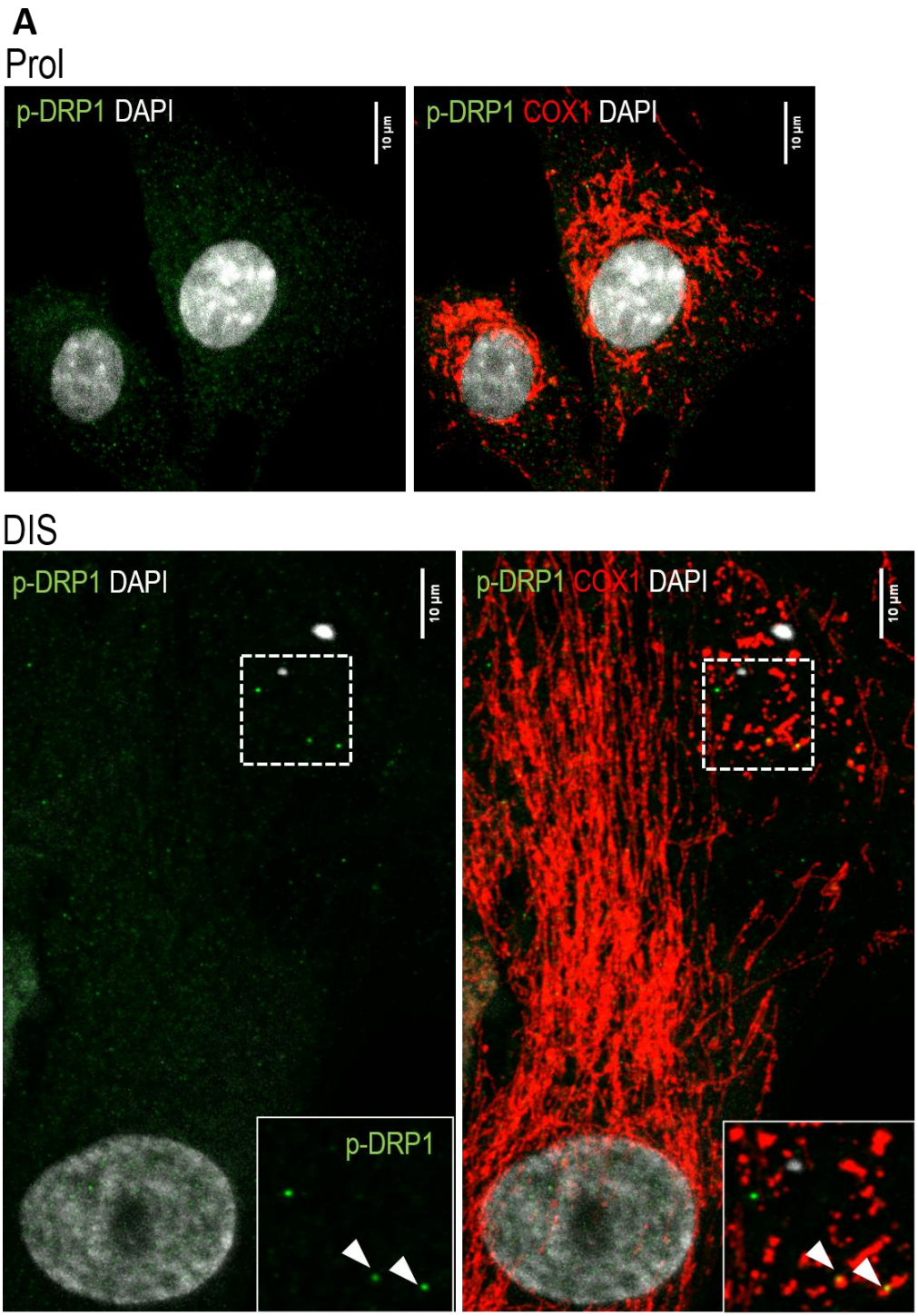

Figure 3.8: Association of p-DRP1(Ser-616) with circular mitochondria in human embryonic fibroblasts IMR90 in damage-induced senescence

(A) Representative CLSM image of p-DRP1 and mitochondria stained using anti-COX1 antibody. Scale bars represent 10µm.

3.6 Elevated levels of cleaved caspase-3 are detected in senescent cells

Mitochondrial apoptotic cascade leads to the activation of cytosolic caspases, proteolytic enzymes and executioners of apoptosis (Riedl *et al.*, 2004). For it to happen, cytochrome *c* in the cytoplasm must bind to apoptotic protease activating factor 1 (APAF-1) that together, form a higher-order structure, multimeric apoptosome. Apoptosome recruits and activates caspase-9, an initiator caspase, that further targets effector caspases. Caspase-3 is considered one of the most deleterious of the effector caspases, as it is able to cleave hundreds of other proteins (Riedl *et al.*, 2004).

Having observed all the pre-requisites for the potential caspase activation *i.e.* BAX activation, release of cytochrome *c* and leakage of mtDNA, I decided to evaluate this final step of apoptotic cascade. A western blot assay for caspase-3 cleavage that detects two bands representing caspase-3 cleaved versions, revealed that in DIS both bands were more pronounced than in proliferating counterparts (Figure 3.9 A), indicating caspase-3 activation.

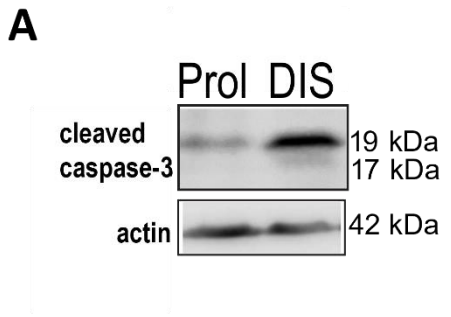

Figure 3.9: Detection of cleaved caspase-3 in human embryonic fibroblasts MRC5 in damage-induced senescence

(A) Representative western blot of cleaved caspase-3. A representative image of n=3. Data by James Chapman.

3.7 Damage-induced senescence in mouse fibroblasts is characterised by mtDNA leakage

As mice, *Mus musculus,* serve as a common animal model for studying the mechanisms of human disease, particularly the role senescent cells play in age-related pathologies, I performed some of the developed assays using primary mouse fibroblasts (mouse adult fibroblasts, MAFs). My aim was to establish whether the observed phenomena are conserved across different mammalian species. MAFs were freshly isolated from ear punches that contain both skin and cartilage tissue. Studied cells are therefore a combination of skin and cartilage fibroblasts. Damage-induced senescence in MAFs has previously been shown to be triggered by a γ-irradiationat the dose of 10Gy (Jurk *et al.*, 2014). I found MAFs induced to DIS, were characterised by increased amount of cytosolic mtDNA, as quantified based on CLSM images of DNA and SDHA that served as a mitochondrial marker (Figure 3.10 A) and using sub-cellular fractionation/qPCR approach (Figure 3.10 B). At this stage of the project, I decided to extend the analysis and added yet another methodology, namely Immuno-Transmission Electron Microscopy (Immuno-TEM) (Figure 3.10 C). By utilizing this method, I aimed to observe not only the cytosolic DNA but "snap-shots" of the process of its release, *i.e.* signs of disrupted mitochondrial membrane or IMM herniation. Cells were stained using the same generic anti-DNA antibody as in immuno-fluorescence assays. Due to technical limitations related to the processing of cells for immune-gold labelling that generally decreases the quality of cellular components ultrastructure (in contrast to TEM, performed without any staining) this experiment only allowed to confirm the observation that cells upon senescence induction have higher content of cytosolic DNA. In young cells most of the black dots, which correspond to gold-labelled DNA molecules, are located inside mitochondrial matrix, while in senescent cells a considerable amount of signal was present in the cytosol. By using this method, I did not observe any signs of severely damaged mitochondria or IMM herniation.

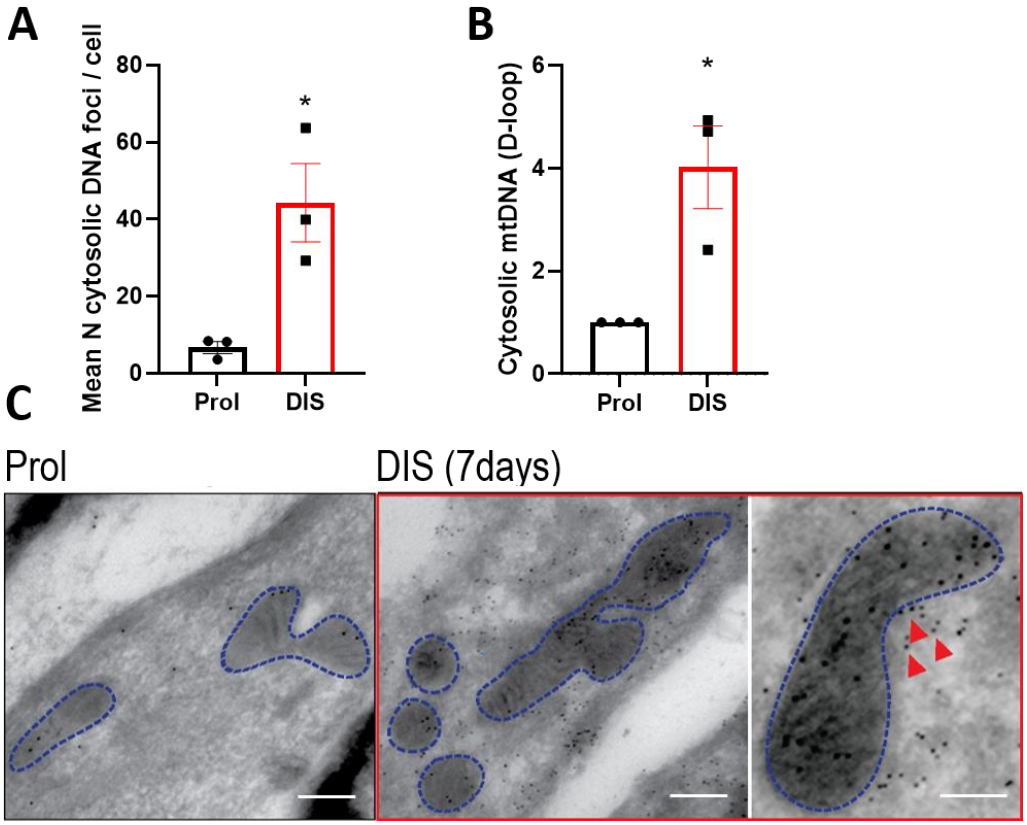

Figure 3.10: Leakage of mtDNA into the cytoplasm in mouse adult ear fibroblasts in damage-induced senescence

(A) Quantification of the mean number of cytosolic DNA foci based on CLSM images where DNA was stained using anti-DNA antibody and mitochondria using anti-SDHA antibody, n=3 independent replicates/coverslips, minimum 10 cells/replicate. Analysed using Student's t-test: Prol vs DIS p=0.0218 **(B)** Levels of cytosolic mtDNA (D-loop region) upon sub-cellular fractionation and qPCR, normalised to the levels of total cellular mtDNA and to Prol control. N=3 independent replicates, in this case, cells derived from 3 different animals and subjected to separate sub-cellular fractionations. Analysed using Student's t-test: Prol vs DIS p=0.02. **(C)** Representative electron microscopy images of immuno-gold labelling using an anti-DNA antibody. Representative examples of n=2 independent experiments. Scale bars represent 200nm. Error bars represent SEM.

3.8 Oncogene-induced senescence in characterised by mtDNA leakage

So far, my data concerned damage-induced senescence model or replicative senescence. Here, I set out to study whether another established and commonly-used model of senescence - oncogene-induced senescence (OIS), is also characterised by features of mitochondrial apoptotic stress. OIS was obtained using ER:RAS inducible system, where the oncogene, H-RASG12V, is fused to a 4-hydroxytamoxifen (4-OHT)-responsive Estrogen Receptor ligand binding domain and incorporated into the genome via retroviral transduction. It is constitutively expressed, and upon the treatment with 4-OHT, the fusion protein becomes activated, *i.e.* the levels of the active GTP-bound RAS increase. In this study, I utilised human embryonic fibroblasts, IMR90, termed IMR90 ER:RAS or IMR90RAS (Innes *et al.*, 2019; Tarutani *et al.*, 2003). CLSM for quantification purposes and super-resolution, particularly AiryScan, microscopy for obtaining the highest quality visualisations, allowed to conclude that an increased number of cytosolic DNA foci (Figure 3.11 A, B, C) and cytosolic TFAM foci (Figure 3.11D) are a feature of OIS, similarly to other models of senescence.

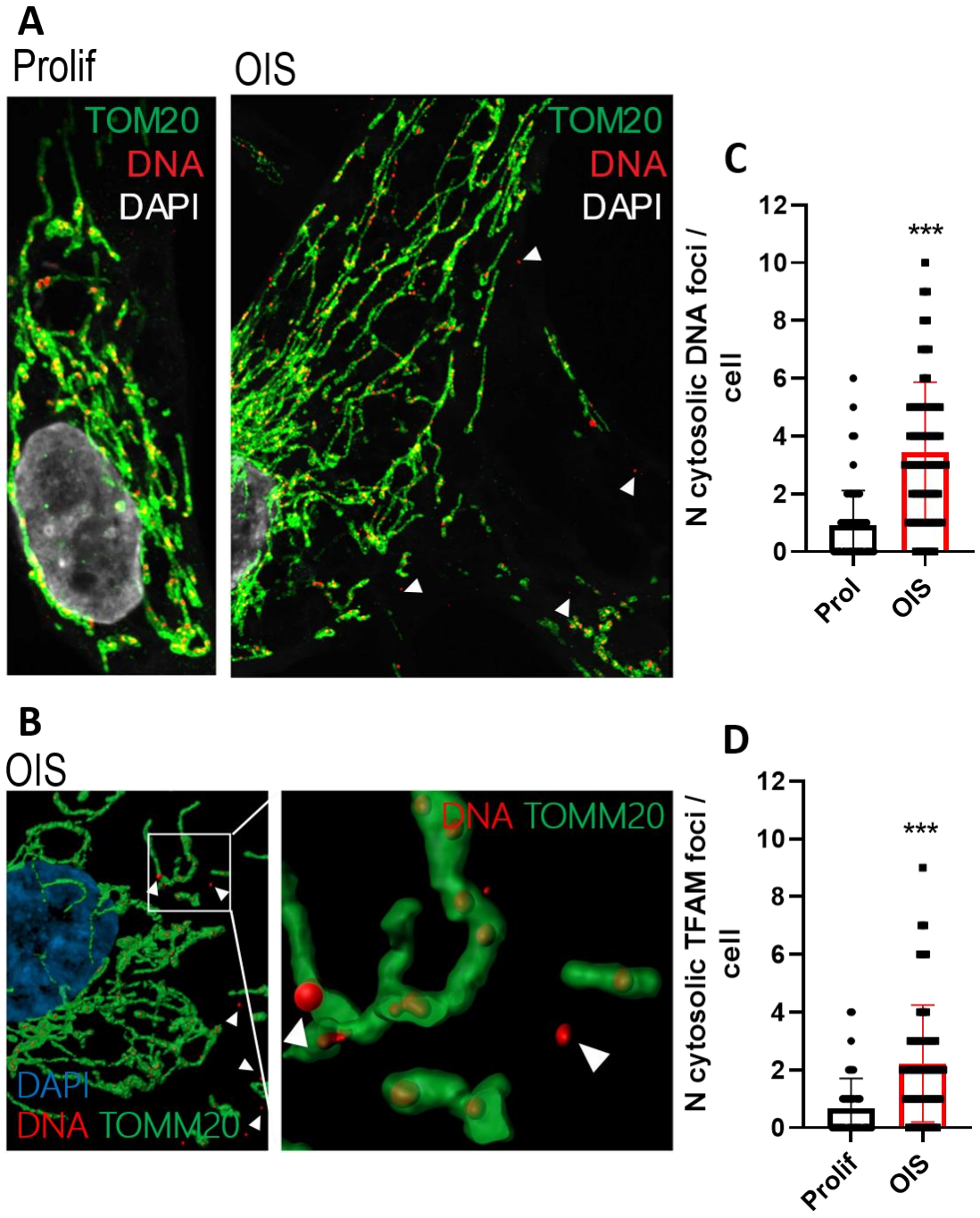

Figure Figure 3.11: Leakage of mtDNA into the cytoplasm in human embryonic fibroblasts IMR90 in oncogene-induced senescence

(A) Representative super-resolution AiryScan microscopy images of cells stained with anti-DNA and anti-TOMM20 antibodies. Scale bar represents 5µm. **(B)** 3D representation of mitochondrial network and mtDNA where the most is contained within mitochondria and some in the cytoplasm, generated using Imaris software **(C)** Quantification of the number of cytosolic DNA foci per cell, n=minimum 63 cells/condition. Analysed using Mann-Whitney test: Prol vs OIS $p<0.0001$ **(D)** Quantification of the number of TFAM foci per cell, n=45 cells/condition. Analysed using Mann-Whitney test: Prol vs OIS: $p<0.0001$. Error bars represent SD.

3.9 The degree of mitochondrial apoptotic stress is higher in damage- than in oncogene-induced senescence

Insight gained while working with different models of senescence pointed my attention to the differences in the degree mitochondrial apoptotic stress might characterise the damage-induced and oncogene-induced types of cellular senescence. For example, the number of cytosolic DNA foci for DIS on MRC5 background was above 15 (Figure 3.5 C), while for OIS using IMR90ER:RAS, less than 4 (Figure 3.11 C). I decided to perform a comparative analysis of mitochondrial apoptotic stress in these two models. I utilised IMR90ER:RAS cells and induced them to OIS and DIS alongside, and collected at the exactly same time-points post senescence induction. This stricter approach allowed to exclude the possibility the observed differences were related to the type of studied fibroblasts or a technical artifact linked to specificities of a particular experiment.

The analysis of all the subsequent steps of the apoptotic cascade, revealed that DIS is indeed characterised by a more pronounced mitochondrial apoptotic stress than OIS. I found a significantly higher percentage of cells containing activated BAX foci co-localising with mitochondria among cells in DIS than OIS (Figure 3.12 A and 3.13 A). Co-localisation of TOMM20 and cytochrome *c* was significantly lower for DIS than OIS cells (Figure 3.13 B). Moreover, an analysis of the levels of cytosolic mtDNA using sub-cellular fractionation/qPCR approach (Figure 3.13 C) and CLSM microscopy approach (Figure 3.13 D) indicated that DIS possesses more cytosolic mtDNA. Finally, a western blot analysis of cleaved caspase-3 confirmed higher caspase-3 activation in DIS than OIS, indicating a higher sub-lethal apoptotic stress (Figure 3.13 E).

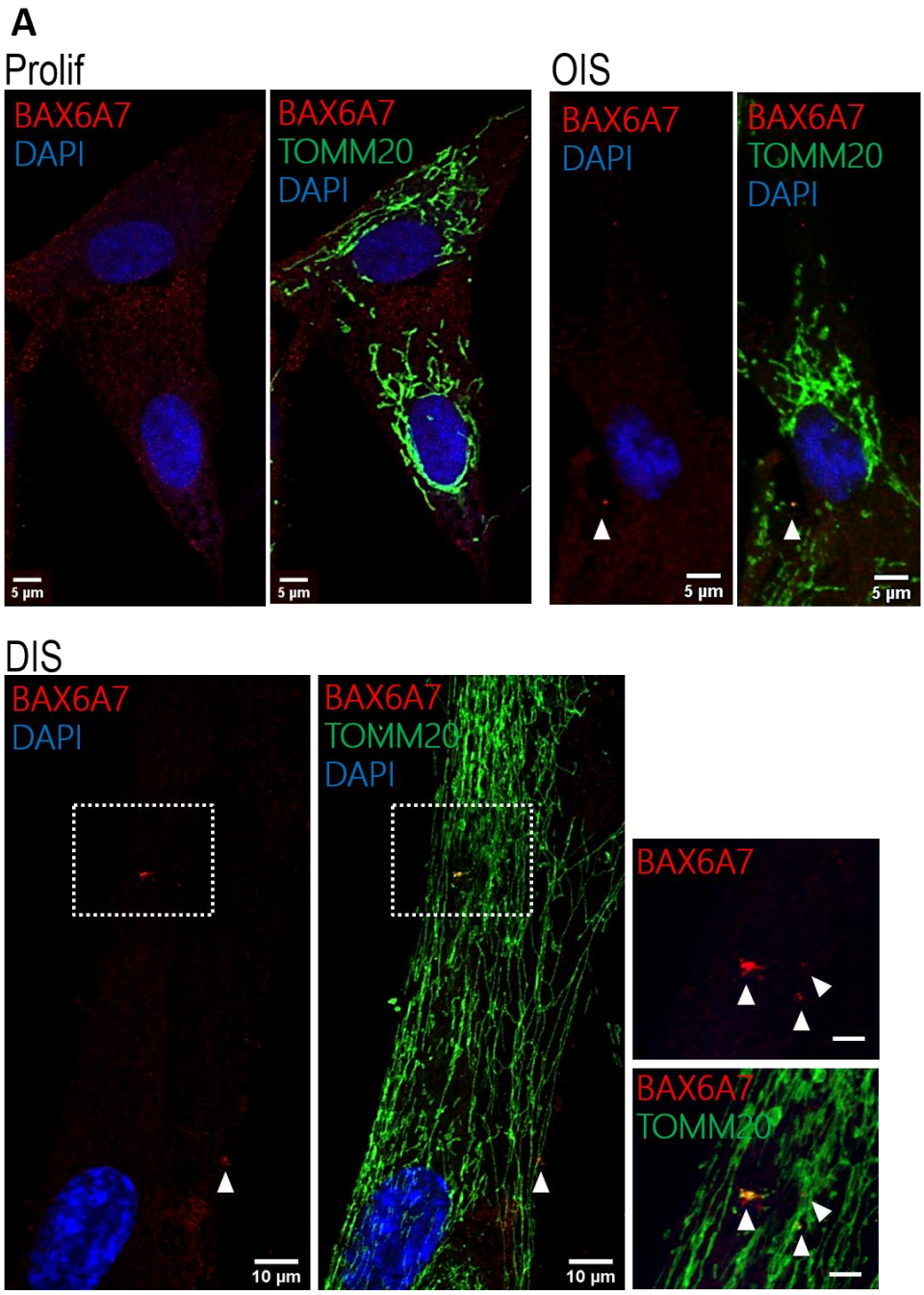

Figure 3.12: BAX activation in human embryonic fibroblasts IMR90 in oncogene- and damage-induced senescence

(A) Representative CLSM images of activated BAX stained with anti-BAX6A7 antibody and mitochondria stained with anti-TOMM20 antibody 10 days after γ-irradiation. Scale bar represents 5µm for Prolif, OIS and magnified fragment of DIS images, or 10µm for DIS.

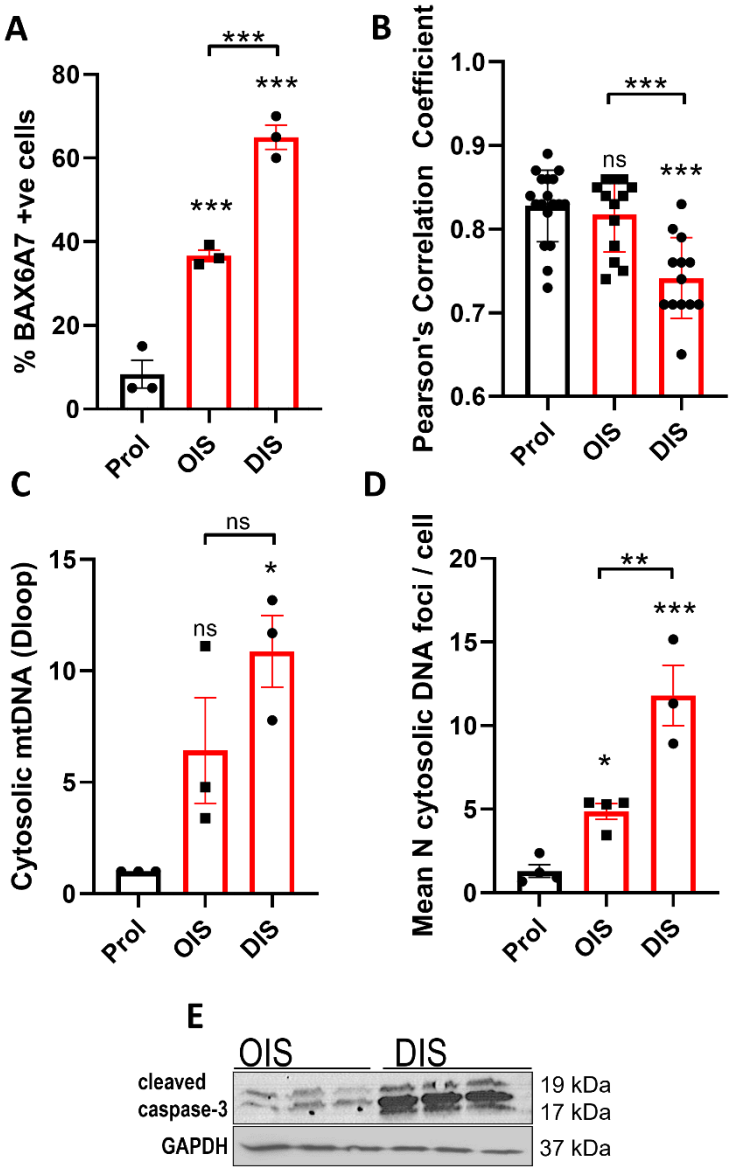

Figure 3.13: Comparative analysis of mitochondrial apoptotic stress in human embryonic fibroblasts IMR90 in OIS and DIS

(A) Quantification of the percentage of cells positive for BAX6A7 co-localising with mitochondrial signal TOMM20, n=3 independent replicates/coverslips, minimum 20 cells/replicate. Analysed with 1-way ANOVA Tukey's multiple comparison test: Prol vs OIS p=0.0007, Prol vs DIS p=<0.0001, OIS vs DIS p=0.0007 **(B)** Analysis of co-localisation between cytochrome *c* and TOMM20 expressed as Pearson's correlation coefficient, n=minimum 12 cells/condition. Analysed with 1-way ANOVA Tukey's multiple comparison test: Prol vs OIS p=0.8125, Prol vs DIS p=<0.0001, OIS vs DIS p=0.0003 **(C)** Levels of cytosolic mtDNA (D-loop region) upon sub-cellular fractionation and qPCR, normalised to the levels of total cellular mtDNA and Prol control. n=3 independent replicates/sub-cellular fractionations. Analysed with 1-way ANOVA Tukey's multiple comparison test: Prol vs OIS p=0.1288, Prol vs DIS p=0.0131, OIS vs DIS p=0.2181 **(D)** Quantification of the number of cytosolic DNA foci stained using an anti-DNA antibody, mitochondria stained with anti-TOMM20 antibody, n=3-4 independent replicates/coverslips. Analysed with 1-way ANOVA Tukey's multiple comparison test: Prol vs OIS p=0.0461, Prol vs DIS p=0.0001, OIS vs DIS p=0.0020 **(E)** Western blot of cleaved caspase-3, n=3 independent replicates/wells. Error bars represent SEM for A, C and D, error bars represent SD for B.

3.10 Depletion of BAK and BAX in damaged-induced senescent cells ameliorates the SASP

Thus far, I characterised mitochondrial apoptotic stress consisting of BAX (and BAK) activation, release of cytochrome *c*, leakage of mtDNA to the cytoplasm and caspase-3 activation across several models of cellular senescence. In order to 1) understand whether the downstream processes, such as mtDNA leakage depend on BAK and BAX protein in the context of cellular senescence, as well as 2) understand whether mitochondrial apoptotic stress regulates the pro-inflammatory phenotype of senescent cells, I sought out to determine the effects of BAK and BAX knock-out on mtDNA leakage and SASP during cellular senescence.

For that, BAK and BAX were depleted in human embryonic MRC5 fibroblasts using CRISPR/Cas9 technology delivered to the cells on lentiviral vectors via second generation lentiviral transduction. Upon selection, BAK/BAX^{CRISPR} cells were induced to DIS, and BAX and BAK protein levels were assessed by western blotting (Figure 3.14 A). Next, an analysis of the number of cytosolic DNA foci revealed that BAK/BAX^{CRISPR} cells contained significantly less cytosolic DNA than cells transduced using an empty vector (Empty^{CRISPR}) (Figure 3.14 B). Further, I addressed the question of the relationship between mitochondrial apoptotic signalling and SASP. The composition and levels SASP components can be measured using several approaches. One of the techniques used is the enzyme-linked immunosorbent assay (ELISA) which is allows to measure the concentration of proteins, here the secreted components of SASP – IL6 and IL8. ELISA assay revealed that the secretion of both cytokines which levels are highly elevated during DIS, is significantly reduced (Figure 3.14 C and D). Our lab also possess data on a wider range of SASP components. Cytokine array demonstrated that fibroblasts growth factor 2 (FGF-2), granulocyte-macrophage colony stimulating factor (GM-CSF), monocyte chemoattractant protein 3 (MCP-3), vascular endothelial growth factor A (VEGF-A), chemokine (C-X-C motif) ligand 1 (CXCL1), C-X-C motif chemokine ligand 10 (CXCL10) aka Interferon gamma-induced protein 10 (IP-10) and interleukin 5 (IL-5) were down-regulated upon BAK/BAX^{CRISPR} (data not shown). Collectively, this set of experiments showed that during DIS, mtDNA leakage depends on BAK and BAX and that these proteins, presumably by mediating mitochondrial apoptotic stress, regulate SASP during damage-induced senescence.

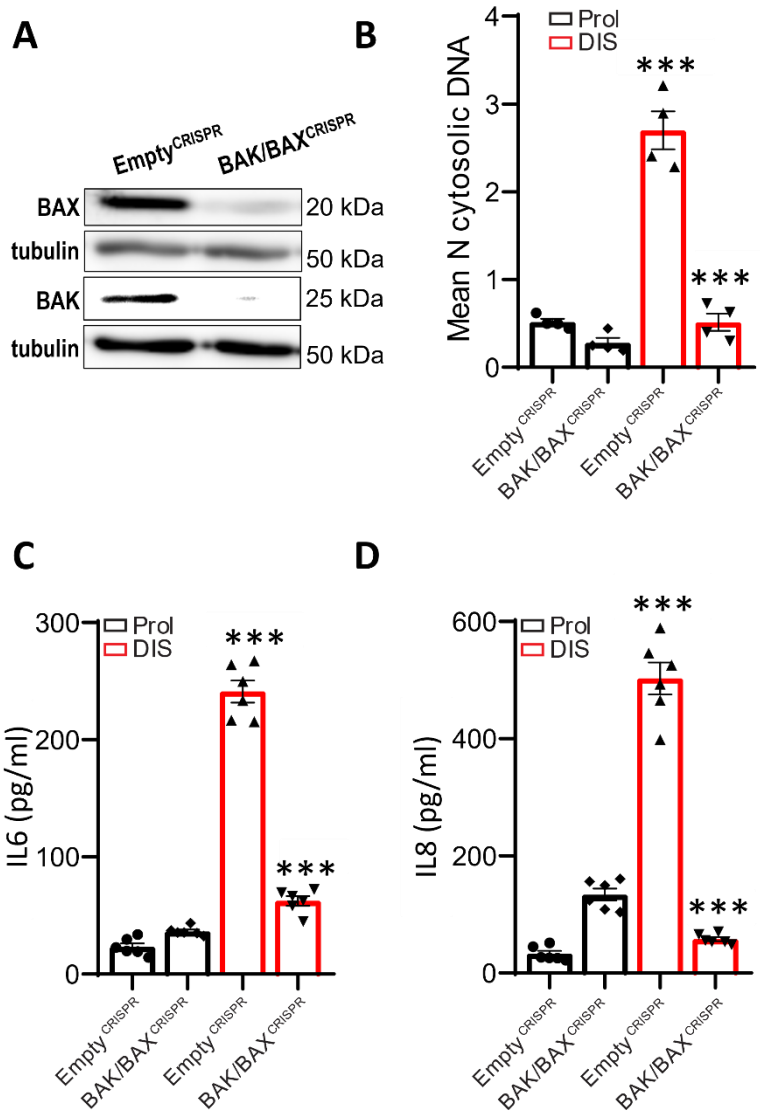

Figure 3.14: Effects of BAK/BAX knock-out on mtDNA leakage and SASP in human embryonic fibroblasts MRC5 during damage-induced senescence

(A) Western blot for BAK and BAX demonstrating knock-out efficiency **(B)** Quantification of the mean number of cytosolic DNA foci, n=4 independent replicates/coverslips. Analysed using Student's t-test: EV Prol vs EC DIS $p<0.0001$, EV DIS vs BAK/BAX DIS $p<0.0001$ **(C)** Concentration of secreted IL6 protein in pg/ml detected using ELISA, n=6 independent replicates/wells. Analysed using Student's t-test: EV Prol vs EC DIS $p<0.001$, EV DIS vs BAK/BAX DIS $p<0.0001$ **(D)** Concentration of secreted IL8 protein in pg/ml detected using ELISA, n=6 independent replicates/wells. Analysed using Student's t-test: EV Prol vs EC DIS $p<0.001$, EV DIS vs BAK/BAX DIS $p<0.0001$. Error bars represent SEM. Data by James Chapman, my contribution is the optimisation of the lentiviral transduction on primary fibroblasts, and the collaboration during generation of knock-out cells.

3.11 Genetic depletion of BAK and BAX or long-term pharmacological inhibition of BAX exacerbates the SASP in oncogene-induced senescence

Having observed that mitochondrial apoptotic stress takes place during OIS, although to a lesser extent than in DIS, I set out to investigate whether BAK and BAX depletion would result in a similar decrease in mtDNA leakage and SASP in cells induced to OIS. In this set of experiments, I decided to generate both single and double knock-out cells, and assess the role of each protein separately. Therefore, I generated BAK^{CRISPR}, BAX^{CRISPR}, BAK/BAX^{CRISPR} IMR90ER:RAS cells. Western blots showing expression of BAX and BAK are presented in Figure 3.15 A.

The analysis of cytosolic DNA using CLSM approach demonstrated only a subtle decrease in the number of cytosolic DNA foci in BAK/BAX^{CRISPR} cells and no significant decrease in single knock-out cells (Figure 3.15 B). Strikingly, however, the knock-out of each gene as well as the double knock-out resulted in a significant up-regulation of SASP, evaluated as secreted IL-6 and IL-8 (Figure 3.15 C and D).

Upon obtaining the unexpected findings of exacerbated SASP in knock-out cells, I set out to validate these results using a pharmacological approach. I utilised a BAX channel inhibitor (BCB), a pharmacological agent that was demonstrated to block BAX pores and prevent the release of inner membrane proteins such as cytochrome *c* (Bombrun *et al.*, 2003). The treatment with BCB was carried out simultaneously with 4-OHT treatment, initiated at day 0. Similarly to the data obtained on knock-out cells, I found significantly elevated levels of IL8 in BCB treated cells during OIS – analysed via western blotting (Figure 3.15 E).

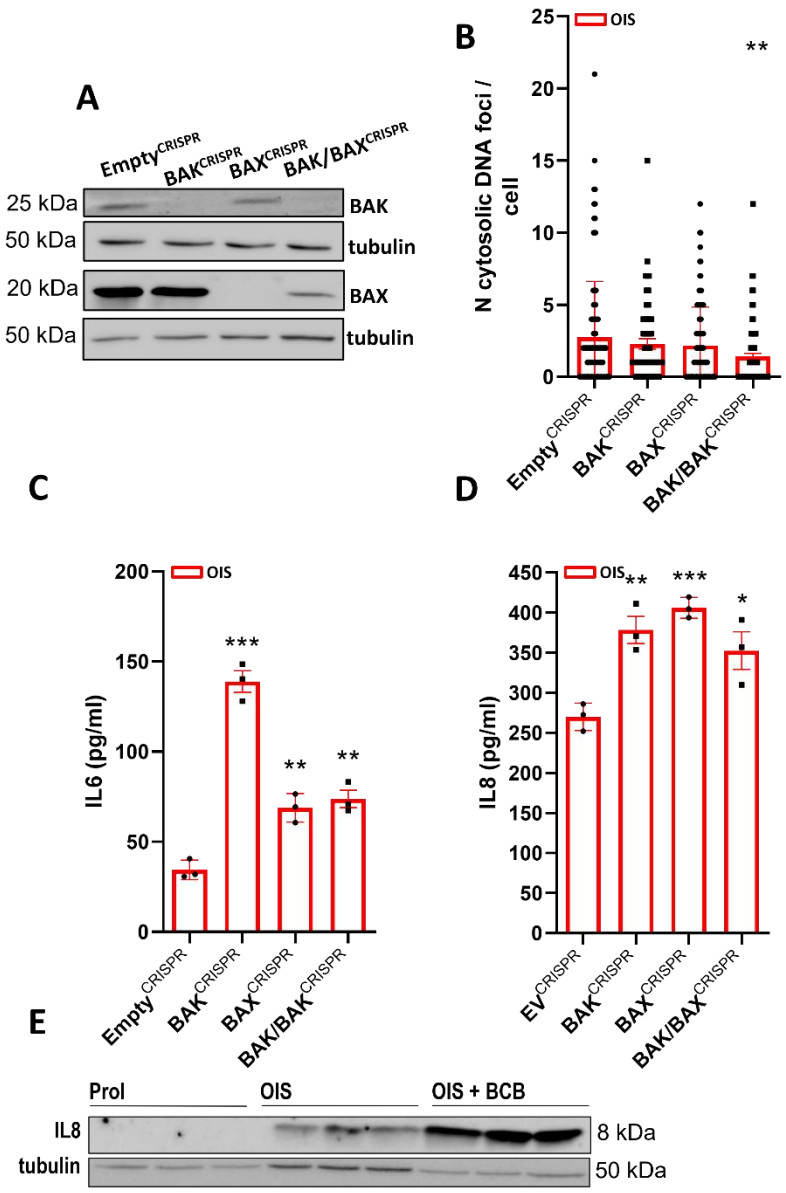

Figure 3.15: Effects of BAK, BAX and BAK/BAX double knock-out and long-term pharmacological inhibition of BAX on mtDNA leakage and SASP in human embryonic fibroblasts IMR90 during oncogene-induced senescence

(A) Western blot for BAK and BAX demonstrating knock-out efficiency **(B)** Quantification of the number of cytosolic DNA foci stained using an anti-DNA antibody, mitochondria stained with TOMM20, upon BAK, BAX and BAK/BAX double knock-out, n=4 independent replicates/coverslips, minimum 59 cells total/condition. Analysed using Mann-Whitney test: OIS EV vs OIS BAK p=0.9544, OIS EV vs OIS BAX p=0.4144, OIS EV vs OIS BAK/BAX p=0.0024 **(C)** Concentration of secreted IL6 protein in pg/ml detected using ELISA, n=3 independent replicates/wells, cytokine undetectable in Prol. Analysed using Student's t-test: EV OIS vs BAK OIS p<0.0001, EV OIS vs BAX OIS p=0.0034, EV OIS vs BAK/BAX OIS p=0.0024 **(D)** Concentration of secreted IL8 protein in pg/ml detected using ELISA, n=3 independent replicates/wells, cytokine undetectable in Prol. Analysed using Student's t-test: EV OIS vs BAK OIS p=0.0053, EV OIS vs BAX OIS p=0.0004, EV OIS vs BAK/BAX OIS p=0.0317 **(E)** Western blot of IL8 in Prol, OIS and OIS upon the treatment with BCB at 2.5 µM concentration initiated at the day of senescence induction. Error bars represent SD for B, error bars represent SEM for C and D.

3.12 Short-term pharmacological inhibition of BAX reduces SASP in oncogene-induced senescence

Having obtained the conflicting results between DIS on MRC5 background and OIS on IMR90 background, I hypothesised that the increase in SASP in BAK/BAX^{CRISPR} cells in OIS (and upon BAX inhibition) could be related to the specific dynamics of OIS induction – which begins by 5 days of hyperproliferation phase, characterised by rapid cell proliferation. Considering the vast non-apoptotic roles of BAK and BAX proteins, it was possible the constitutive knock-out or long-term pharmacological inhibition interfere with processes occurring in this phase. In order to assess the effects of BAX inhibition only after the cells cease to divide, I performed, a delayed short-term BCB treatment. The cells were treated with BCB at day 5 of 4-OHT treatment (instead of day 0) for 5 days as well as at day 9 of 4-OHT treatment for 24h. In this set of experiments, I compared the effect of BCB on OIS alongside DIS. I analysed mRNA abundance of SASP components IL6 and IL8 using a qPCR approach. My data showed that long-term BCB treatment in DIS significantly decreased the expression of IL6 and IL8 (Figure 3.16 A and B). Moreover, in contrast with my previous findings following long-term treatment with BCB, short term BAX inhibition significantly reduced expression of IL8 but, not IL6 (however, a trend for a decrease was observed) (Figure 3.16 A and B). These data suggest that BAK and BAX may play a role during the proliferative phase of of OIS and be required for the normal establishment of this type of senescence. However, SASP can still be reduced by targeting the process of mitochondrial apoptotic stress when the cell-cycle arrest has already been established.

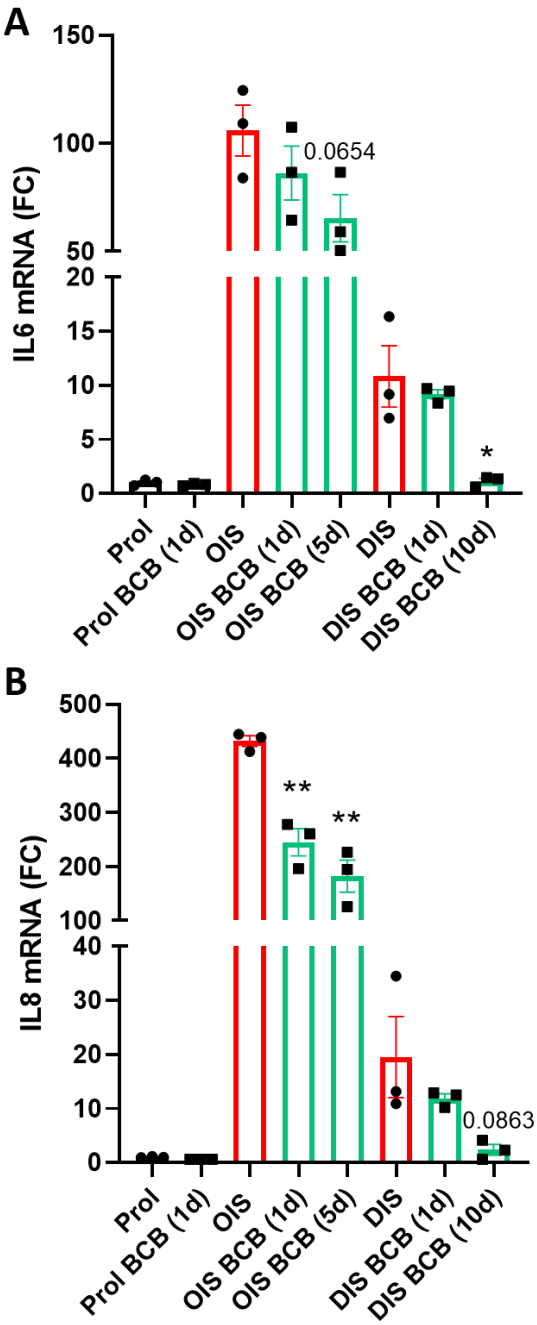

Figure 3.16: Effects of short-term BAX inhibition on SASP and senescence markers in human embryonic fibroblasts IMR90 during oncogene-induced and damage-induced senescence

(A) IL6 mRNA levels via qPCR normalised to RSP16 using Delta-Delta method, n=3 independent replicates/wells. Analysed using Student's t-test: OIS vs OIS BCB(1d) p=0.3142, OIS vs OIS BCB(5d) p=0.0654, DIS vs DIS BCB(1d) p=0.5935, DIS vs DIS BCB(10d) p=0.0270 **(B)** IL8 mRNA levels via qPCR normalised to RSP16 using Delta-Delta method, n=3 independent replicates/wells. Analysed using Student's t-test: OIS vs OIS BCB(1d) p=0.0022, OIS vs OIS BCB(5d) p=0.0.0013, DIS vs DIS BCB(1d) p=0.3704, DIS vs DIS BCB(10d) p=0.0863. Error bars represent SEM.

3.13 mtDNA and vesicles containing activated BAX are secreted by senescent cells

Having observed mitochondrial apoptotic stress and in particular, increased levels of cytosolic DNA in damage-induced senescence, I became interested whether this process may exert systemic effects. mtDNA and other mitochondrial components have been described as DAMPs (Grazioli *et al.*, 2018). By secretion of mtDNA, senescent cells could contribute to the pool of circulating pro-inflammatory factors, beyond the established SASP factors.

By performing immunofluorescent staining for activated BAX (BAX6A7) and TOMM20, I observed that senescent cells were associated with vesicles which were positive for BAX6A7 and TOMM20 (Figure 3.17 A). I quantified BAX6A7 positive vesicles and found that their number was significantly higher during DIS than in proliferating controls (Figure 3.17 B). To evaluate whether mtDNA is enriched in the culture media, I cultured young and senescent cells in fresh media for 24 hours and extracted DNA from the conditioned media. Subsequently, I performed a qPCR to detect mtDNA (D-loop region) in eluted DNA samples. By utilizing a standard curve obtained using serial dilutions of an oligonucleotide with a corresponding sequence to the detected DNA fragment, I was able to express the results as mtDNA copy number present in a microlitre of media. I found that senescent cells had significantly more abundant extracellular mtDNA than their proliferating counterparts (Figure 3.17 C). I performed a similar analysis of secreted mtDNA content in culture media of different senescent cell types. As the subsequent experiments were conducted earlier (in the course of my thesis research), and the standard curve method had not been optimised, the following results are expressed as the fold change difference between proliferating and senescent cells. Consistently, I detected higher levels of mtDNA in the media of senescent human adult lung fibroblasts (obtained from lung biopsies) (Figure 3.17 D). Similarly, higher level of mtDNA were detected in media from mouse adult fibroblasts (MAFs) (Figure 3.17 E). It was previously shown that EVs from senescent cells contribute to paracrine effects of senescent cells (Borghesan *et al.*, 2019). Having detected increased levels of mtDNA in conditioned media from senescent cells, I became interested whether mtDNA could be contained in extracellular vesicles. I purified EVs from senescent conditioned media using a protocol based on ultra-centrifugation. Significantly elevated levels of mtDNA were detected 3 days upon senescence induction (Figure 3.17 F). The experiment should be repeated at the established stage of senescence (10 days) in the future. Collectively, these data indicate that mtDNA can be found extracellularly and at higher concentrations in senescent cells.

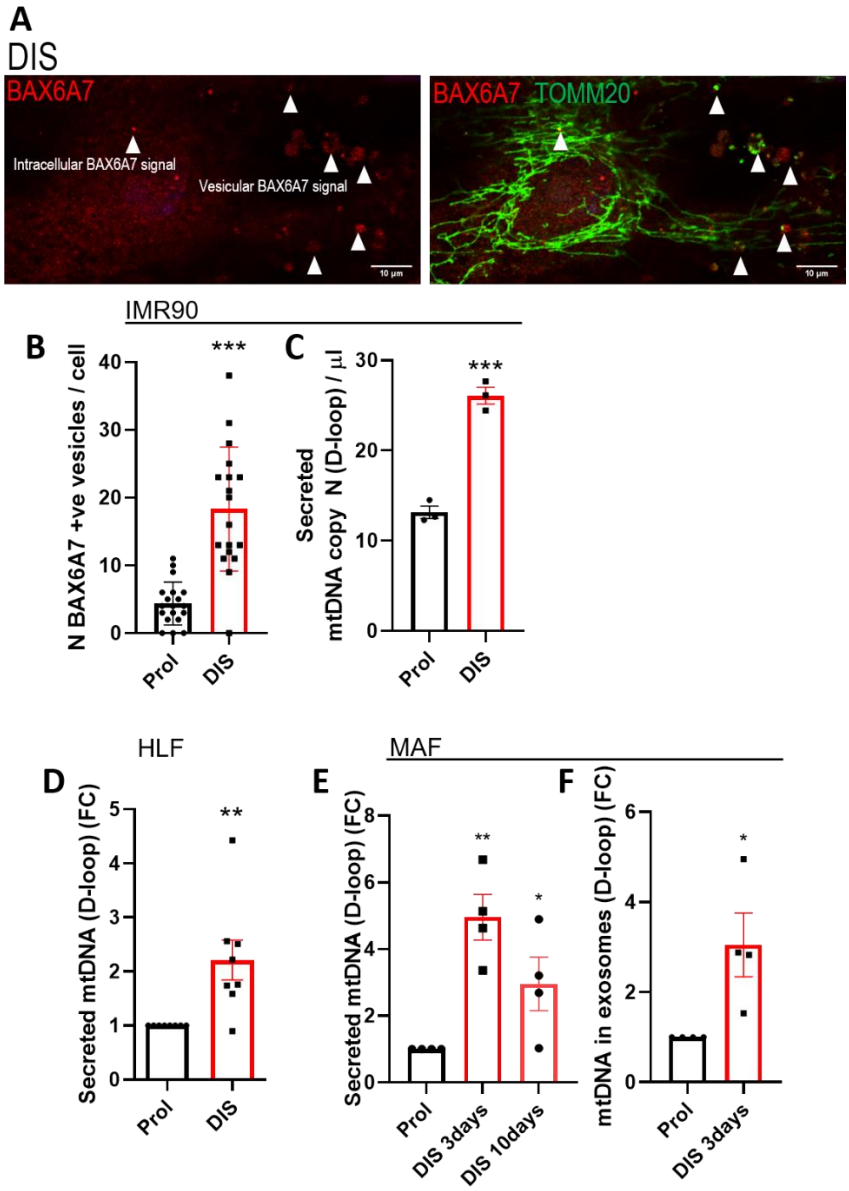

Figure 3.17: Detection of secreted mtDNA and activated BAX during damage-induced senescence

(A) Example CLSM image of extracellular vesicles stained with BAX6A7, marker of activated BAX and TOMM20, marker of mitochondria. A cell in DIS at 10 days post γ-irradiation. **(B)** Quantification of the number of BAX6A7-positive vesicles/1 cell, mitochondria stained using anti-TOMM20 antibody. N=minimum 18cells/condition, analysed using Student's t-test: Prol vs DIS: $p<0.0001$ **(C)** Concentration of mtDNA D-loop in conditioned media in human embryonic fibroblasts IMR90 in DIS via PCR, expressed as copy number per µl of media based on a standard curve, n=3 independent replicates/wells, Student's t-test: Prol vs DIS $p=0.0004$ **(D)** mtDNA D-loop in conditioned media of human adult lung fibroblasts expressed as fold changed quantified using Power method, n=8 independent replicates (8 patients), Student's t-test: Prol vs DIS $p=0.0055$ **(E)** mtDNA D-loop in conditioned media in mouse adult skin fibroblasts upon induction of DIS, 3 and 10 days post irradiation, expressed as fold change quantified using Power method, n=4 independent replicates (4 mice), Student's t-test: Prol vs DIS 3days $p=0.0012$, Prol vs DIS 10days $p=0.0496$ **(F)** mtDNA in exosomes isolated from cellular media in mouse adult skin fibroblasts upon induction of DIS, 3 days post irradiation, expressed as fold change quantified using Power method, n=4 independent replicates/cells derived from

4 mice, Student's t-test: Prol vs DIS 3days p=0.0274. Error bars represent SD for B, error bars represent SEM for C, D, E F.

3.14 Circulating mtDNA in mice does not correlate with age or cellular senescence burden

The findings of an increased mtDNA content in the cytosol, as well as in the secreted form during cellular senescence, expanded my interests to include animal models of high cellular senescence burden. Senescent cells are consistently observed to accumulate during life-span (Karin *et al.*, 2019), therefore I set out to examine whether circulating mtDNA changes as a function of age in mice. I performed a DNA isolation from mouse plasma samples collected from the facial vein and measured the content of mtDNA by qPCR. To express the data as absolute values, I used a standard curve based on serial dilutions of an oligonucleotide matched in sequence to the fragment amplified in the qPCR reaction (as in the case of mtDNA detected in culture media of IMR90 fibroblasts, described above). Further, I calculated the mtDNA copy number per volume of plasma. I optimised the method using a low number of samples first, eventually performing an analysis on total 23 plasma samples collected from female mice at 2-3 and 23 months of age. Analysis of mtDNA content in these samples did not indicate any statistically significant differences occurring with age (Figure 3.18 A). To test whether a more profound age-effects may be observable for males, I used mice at a different age range - 2.5 and 13-15 months of age (available at that time). In these groups, I detected an opposite difference towards our expectation – a decrease of mtDNA concentration in the older age group (Figure 3.18 B). In order to optimise the method and exclude possible technical problems with blood cells lysis during the procedure of blood collection from the facial vein, I used an alternative method for blood draw. The total blood was collected from inferior vena cava in anesthetised mice. DNA was extracted from 100µl of plasma instead of 40µl as in the case of facial draws. This optimisation step did not allow for detection of differences in mtDNA copy number per volume of plasma and again indicated an opposite trend (Figure 3.18 C). Alternatively, I used a model of induced pulmonary fibrosis. Recently, I co-authored a research article which demonstrated that bleomycin-induced lung fibrosis, associated with high cellular senescence burden, can be ameliorated by elimination of senescent cells using senolytic interventions (Schafer *et al*., 2017). Using the same experimental setting, I investigated whether bleomycin-induced lung fibrosis was associated with changes in circulating mtDNA. Furthermore, I set out to establish whether the clearance of senescent cells – in the transgenic mouse model, INK-ATTAC, achieved by administration of AP20187 or alternatively, using a senolytic cocktail of dasatinib and quercetin (DQ), may affect the levels of circulating mtDNA.

My results showed no statistically significant differences between any of the studied groups (Figure 3.18 D). Next, I utilised db/db mouse model of type 2 diabetes mellitus (T2DM) and obesity driven by a mutation in the gene encoding the leptin receptor, leading to leptin deficiency and a lack of satiety (Alpers *et al.*, 2011). Previously, the db/db mice were characterised by an increased senescent cells number in adipose tissue (Tchkonia *et al.*, 2010). However, similarly to my previous attempts, I did not detect increased circulating levels of mtDNA (Figure 3.18 E). All data together suggest that circulating mtDNA is a highly variable biomarker in mice. These data do not support the hypothesis that mtDNA in plasma is associated with age and cellular senescence-related conditions in mice.

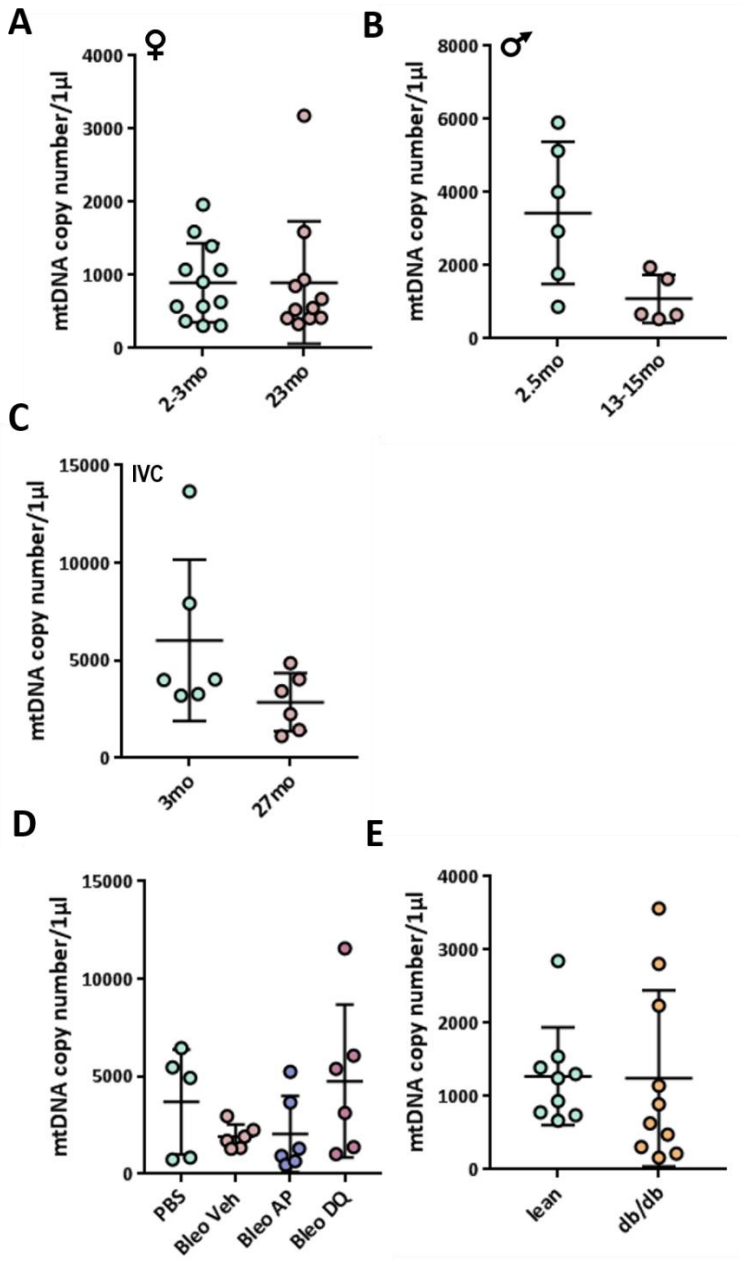

Figure 3.18: Circulating mtDNA in mouse plasma

(A) Content of mtDNA D-loop region detected by qPCR, expressed as copy number per µl of plasma based on a standard curve. DNA isolated from 40µl of mouse plasma collected from facial vein. Analysed using Mann-Whitney test: 2-3mo vs 23mo p=0.6505 **(B)** Content of mtDNA D-loop region detected by qPCR, expressed as copy number per µl of plasma based on a standard curve. DNA isolated from 40µl of mouse plasma collected from facial vein. Analysed using Student's t-test: 2.5mo vs 12-15mo p=0.0305 **(C)** Content of mtDNA D-loop region detected by qPCR, expressed as copy number per µl of plasma based on a standard curve. DNA isolated from 100µl of mouse plasma collected from inferior vena cava. Analysed using Mann-Whitney test: 3mo vs 27mo p=0.2403 **(D)** Content of mtDNA D-loop region detected by qPCR, expressed as copy number per µl of plasma based on a standard curve. DNA isolated from 40 µl of mouse plasma collected from facial vein. Blood was collected from 2.5–8 months old mice upon PBS or 2 U kg−1 bleomycin treatment through aerosolised intratracheal delivery, and upon AP and D/Q treatment. Analysed using 1-way ANOVA, Tukey's multiple comparison test: PBS vs Bleo VEH p=0.6737, PBS vs Bleo AP p=0.7231, PBS vs Bleo DQ p=0.9013, Bleo VEH vs Bleo AP p=0.9997, Bleo VEH vs Bleo DQ p=0.2577, Bleo AP vs Bleo DQ p=0.2950 **(E)** Content of mtDNA

D-loop region detected by qPCR, expressed as copy number per µl of eluate based on a standard curve. DNA isolated from 40µl of mouse plasma collected from facial vein of db/+ heterozygous (lean) and db/db homozygous mice at 3-5 months of age. Analysed using Mann-Whitney test: lean vs db/db p=0.3154. Error bars represent SD.

3.15 Circulating mtDNA in humans does not correlate with frailty score in humans

In contrasts to my results on circulating mtDNA in mouse, mtDNA in plasma has been found as a biomarker of age in humans (Pinti *et al.*, 2014). Authors reported that mtDNA concentration in plasma increases with age, as well as investigated the link between circulating mtDNA and the levels of pro-inflammatory factors. They reported a positive association between mtDNA copy number and cytokines, such as TNF-α, IL6, RANTES, and IL1.

Having identified mtDNA as a component of senescence-associated secretome in human cells, I decided to assess whether the content of circulating mtDNA associates with the clinical parameters of frailty in humans. Frailty is defined as "a clinically recognizable state of increased vulnerability resulting from aging-associated decline in reserve and function across multiple physiologic systems such that the ability to cope with daily or acute stressors is comprised" (Xue, 2011). Multiple studies pinpoint the link between frailty and the burden of cellular senescence (LeBrasseur *et al.*, 2015; Lehmann *et al.*, 2018). In order to assess mtDNA as a biomarker of frailty, I utilised plasma samples from patients between 65 and 94 years old, diagnosed with severe aortic stenosis (AS) and scheduled for surgical or transcatheter aortic valve replacement, treated at Mayo Clinic, Rochester in the years 2013 and 2015. This cohort of patient was previously utilised in a study published by the members of Dr LeBrassuer's laboratory (Schafer *et al.*, 2016). Frailty index score was calculated according to the Cardiovascular Health Study (CHS) criteria (Fried *et al.*, 2001). Clinical parameters of frailty included: weak grip strength, slow walk speed, self-report of low endurance and energy, unintended weight loss and low physical activity. Apart from the frailty index score obtained for these patients, their plasma was characterised in terms of circulating proinflammatory cytokines, which were previously associated with cellular senescence. The list of analysed cytokines is indicated in Materials and Methods section.

I set out to analyse the level of mtDNA represented by D-loop fragment in plasma samples from 93 patients. Subsequently, I performed a correlation analysis between circulating mtDNA levels and the frailty index score, body mass index (BMI) as well as circulating cytokine levels in the bloodstream of the patients. Figure 3.19 A represents data obtained during optimisation of the method on 20 subjects (test samples). I performed DNA extraction from 400 µl of plasma measured mtDNA by qPCR in 2 independent experiments (technical replicates of

DNA extraction). I analysed the correlation of the results obtained in these two independent trials and concluded that the method allows for reliable detection of circulating mtDNA (Figure 3.19 A). Subsequently, I performed DNA extraction followed by qPCR analysis on all 93 samples from the frailty cohort. I did not find a positive association between mtDNA in plasma of the patients and their frailty score (Figure 3.19 B), neither with the BMI (Figure 3.19 C). The lack of correlation was confirmed by multiple linear regression analysis which took into account BMI and gender as potential confounding factors, showing no significant effects of gender and BMI (Appendix, Figure 3). The frailty score displayed a positive and significant correlation with mtDNA when only females were considered (Figure 3.19 D). The correlation was not found to be positive for males, neither for females when their BMI was taken into account (data not shown). However, multiple linear regression analysis of the data obtained for female subjects when BMI was included as a confounding factor revealed the correlation was not significant ($p=0.0514$) (Appendix Figure 3). Among pro-inflammatory cytokines, plasminogen activator inhibitor-2, PAI2, a cytokine robustly associated with cellular senescence (Hsieh *et al.*, 2017; Sossey-Alaoui *et al.*, 2019; West *et al.*, 1996) was positively and significantly correlated with the levels of circulating mtDNA (Figure 3.19 E).

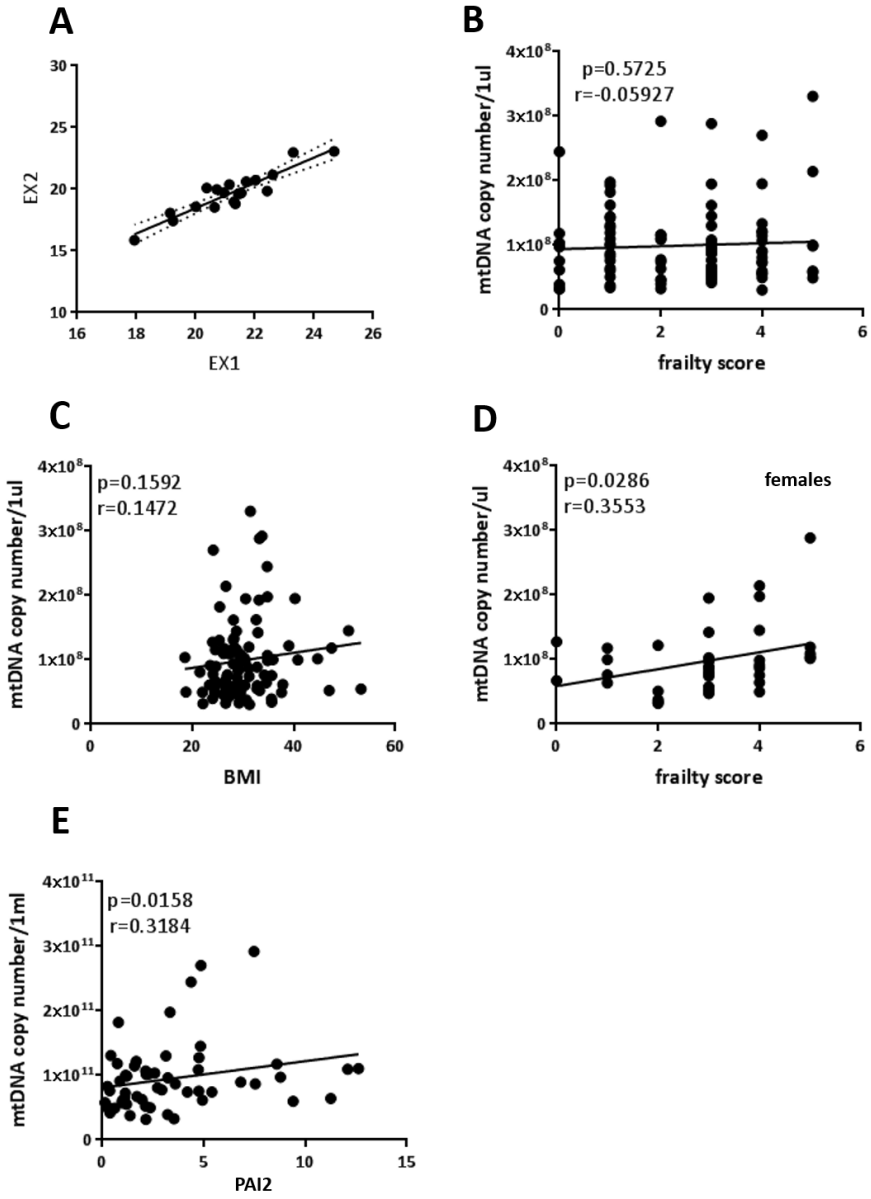

Figure 3.19: Circulating mtDNA in human plasma

(A) Optimisation of mtDNA detection in human plasma. Correlation of Ct values for D-loop region of human mtDNA in plasma samples obtained between two technical replicates (independent DNA extractions), n=20 subjects between 27 and 79 years of age. **(B)** Correlation of mtDNA D-loop concentration in human plasma detected via qPCR expressed as mtDNA D-loop region copy number in 1µl of plasma with frailty score, n=93 subjects, mixed gender **(C)** Correlation of mtDNA D-loop concentration in human plasma detected via qPCR, expressed as mtDNA D-loop region copy number in 1µl of plasma and with BMI, n=93 subjects, mixed gender **(D)** Correlation of mtDNA D-loop in human plasma detected via qPCR expressed as mtDNA D-loop region copy number in 1µl of plasma with frailty score, n=38, females **(E)** Correlation of mtDNA D-loop concentration with concentration of PAI2 in human plasma, n=93 subjects, mixed gender.

3.16 Conclusions

Experimental results presented in this chapter support the hypothesis that mitochondrial apoptotic stress occurs in cellular senescence. I utilised three models of cellular senescence: replicative, damage-induced and oncogene-induced senescence, as well as cells derived from two species. I found that each of the studied systems displayed features of mitochondrial apoptotic cascade. I performed a thorough analysis of the subsequent steps of mitochondrial apoptotic cascade: activation of pro-apoptotic BAK and BAX, formation of mitochondrially localised BAX pores, cytosolic presence of cytochrome *c*, TFAM and mtDNA and finally, caspase-3 activation in human embryonic fibroblast models. Each measure provided consistent and complimentary with each other evidence that the sub-lethal apoptotic signalling takes place at the minority of mitochondria in senescent cells. I found that in the case of DIS, approximately 60 percent of cells contain at least one foci of activated BAX that co-localises with mitochondria, indicating that the majority of cells in this model of senescence experience mitochondrial apoptotic stress. I observed that mitochondria characterised by activated BAX signal are most frequently disassociated from the main mitochondrial network that, in this model of senescence, is hyper-fused. A relatively minor sub-population of fragmented mitochondria in DIS was positive for the mitochondrial fission signal, indicating a mechanism by which dysfunctional mitochondria may separate from the healthy counterparts.

A comparative analysis of damage- and oncogene-induced senescence showed that the same type of cells induced to senescence by two different means, may result in mitochondrial apoptotic stress affecting the cells to a different degree. DIS model was characterised by significantly higher mitochondrial apoptotic stress markers than OIS, including the number of cells positive for BAX signal at mitochondria, leakage of cytochrome *c* and mtDNA as well as caspase-3 activation. Among the population of cells induced to OIS, a significantly higher percentage of cells contained pores of activated BAX when compared to proliferating controls. However, unlike in the case of DIS, only approximately 30 percent of all cells – a minority of them, displayed this feature. In the future, it would be worth addressing the consequences of the observed differences in the degree of mitochondrial apoptotic stress between two models of senescence, for example, by testing their sensitivity to MOMP and apoptosis-inducing stimuli, such as inhibition of BCL-2 family proteins.

In the model of DIS, genetic knock-out of BAK and BAX, the mediators of apoptotic cascade, demonstrated a mechanistic link between their function and the downstream process of mtDNA leakage. The knock-out resulted in a significantly lower leakage of mtDNA into the

cytoplasm of senescent cells. Moreover, depletion of BAK and BAX ameliorated the SASP, indicating that mitochondrial apoptotic stress is a driver of the pro-inflammatory phenotype of senescent cells.

In the model of OIS, genetic knock-out of BAK and BAX as well as pharmacological inhibition of BAX initiated at the day of senescence induction resulted in an unexpected, opposite impact on the SASP, namely its significant exacerbation. Tailoring the pharmacological inhibition to the specificities of OIS, by postponing the treatment onset to the day when cells quit the hyperproliferation phase, allowed to exert the beneficial anti-SASP effect also in the model of OIS. This indicated that mitochondrial apoptotic stress may also contribute to the regulation of SASP in this model of senescence.

Several lines of evidence indicated that mtDNA is being detected in the cytosol of senescent cells. Next, I addressed whether senescent cells are able to secrete mtDNA to their environment, therefore exerting a potential paracrine and eventually organismal effect. Studying various cell types induced to DIS invariably demonstrated that in culture media of senescent cells, the concentration of mtDNA is higher than in that of proliferating cells. Microscopic analysis of cells positive for activated BAX provided additional evidence that senescent cells are a source of extracellular vesicles that contain markers of mitochondrial apoptotic stress. These observations lead to a conclusion that senescent cells are indeed a source of extracellular mtDNA.

In order to address whether secretion of mtDNA by senescent cells may play a role beyond cell culture conditions and associate with the burden of cellular senescence *in vivo*, I looked at circulating mtDNA levels in several mouse models known to harbour increased numbers of senescent cells. The analysis of murine plasma in terms of mtDNA concentrations indicated that mtDNA is not a strong biomarker in the context of ageing as well as in conditions, such as idiopathic pulmonary fibrosis and obesity in mice.

I took a similar approach of analysing circulating mtDNA in human plasma, in a cohort of individuals characterised in terms of frailty and levels of pro-inflammatory cytokines in the blood. The results showed a lack of a positive correlation between mtDNA in plasma of the patients and the frailty index score. However, circulating mtDNA displayed a positive and significant correlation with the frailty index score when females were considered separately. Circulating mtDNA levels were also positively and significantly correlated with plasma levels of PAI2.

3.17 Discussion

Senescent cells are viable cells that bear a high damage load concerning various types of macromolecules, such as damaged DNA, misfolded, oxidised or cross-linked proteins, products of glycation (advanced glycation products, AGEs), or aggregates formed of lipids, metals and misfolded proteins (known as lipofuscin) (Ogrodnik, Salmonowicz, & Gladyshev, 2019). Mitochondria of senescent cells are considered dysfunctional and characterised by a decreased membrane potential (Chapman *et al.*, 2019; Korolchuk *et al.*, 2017), increased production of ROS (Moiseeva *et al.*, 2009; Passos *et al.*, 2010), as well as impaired mitochondrial retrograde signalling that leads to decreased amount of proteins constituting the ETC - despite the initial mitochondrial network expansion (Dalle Pezze *et al.*, 2014, Vizioli *et al.*, 2020). Moreover, senescent cells, by continuing to grow after ceasing to divide, become significantly larger in size (Mitsui *et al.*, 1976). In consequence, senescent cells suffer from insufficient biosynthesis of RNA and protein as for the cell volume, cytoplasm dilution and disturbed intracellular transport (Neurohr *et al.*, 2019). All these findings indicate that senescent cells harbour various dysfunctions. Yet, despite them being present in a cell in combination, senescent cells are strikingly resistant to apoptosis due to a layer of death-inhibitory mechanisms in the form of abundant BCL-2 proteins, primarily BCL-W and BCL-XL, and potentially other, unexplored players (Wang *et al.*, 2006; Yosef *et al.*, 2016; Zhu *et al.*, 2015).

It remained an open question whether the anti-apoptotic mechanisms may prove insufficient to a degree when potent apoptotic triggers are present in abundance. My thesis research shows that senescent cells, despite the strong pro-survival signalling that effectively prevents from the full-blown apoptosis, do display features of a limited mitochondrial apoptotic stress. The phenomenon consists of all the subsequent stages of apoptotic cascade: BAK and BAX activation, formation of BAX pores at mitochondria, leakage of intermembrane proteins, such as cytochrome *c*, leakage of the matrix components, such as mtDNA and TFAM, and finally caspase-3 activation. In the light of other studies that reported miMOMP not leading to cell death (Brokatzky *et al.*, 2019; Ichim *et al.*, 2015), or even recovery from the brink of apoptosis in the process of anastasis (Sun *et al.*, 2017), my observations of the limited mitochondrial apoptotic stress in the context of high apoptotic resistance, may not appear as a paradox. The finding of the limited mitochondrial apoptotic stress in cellular senescence adds yet another piece of evidence indicating that the apoptotic cascade is not always a point of no return.

So far, markers of mitochondrial apoptotic stress were detected upon the treatment with low dose of BH3-mimetic compound, ABT-737, that primes to apoptosis by inhibiting anti-apoptotic BCL-2 family proteins, specifically BCL-2, BCL-W and BCL-XL. This phenomenon that centres around mitochondrial outer membrane permeabilisation (MOMP) is referred to as minority MOMP, or miMOMP (Ichim *et al*., 2015). Authors of this study demonstrated the presence of cytochrome *c* in the cytosolic fraction detected via western blot as well as increased levels of cleaved caspases, such as caspase-3, caspase-7 and caspase-9, also via western blot. Moreover, they detected the entry of a fluorescently labelled (using green fluorescent protein, GFP) cytosolic protein, specifically FK506 binding protein (FKBP), into the mitochondria – referred to as CytoGFP, which served as a method to demonstrate the permeabilisation of the OMM (Ichim *et al*., 2015). Another study that investigated the role of miMOMP in response to microbial infection with viruses (modified vaccinia virus Ankara (MVA), influenza virus A), intracellular bacteria (*Chlamydia trachomatis* and *Salmonella typhimurium*), and a protozoan (*Toxoplasma gondii*), concluded about the occurrence of same phenomenon, termed as sub-lethal apoptotic signalling, by assessing the levels of phosphorylated histone 2A (γH2Ax) by western blot, an indicator of DNA damage level that in this context is inflicted by the effector caspases; immuno-staining of cytochrome *c* and TOMM20; measuring the activity of caspase-3 using a reporter assay and finally, by assessing the levels of the pro-inflammatory cytokines upon the microbial infection in the context of BAK and BAX deficiency (Brokatzky *et al.*, 2019). Both studies used a multi-method approach, however none addressed the question of BAX activation directly, the first of the events within the apoptotic cascade. Thus far, the only studies that demonstrated BAX activation, taking advantage of the available antibody tool that recognises activated BAX by binding to the 6A7 epitope or utilizing size-exclusion chromatography approaches, belonged to field of apoptosis (Riley *et al.*, 2018; Zhang *et al.*, 2005; Zhou *et al.*, 2007). Data presented in this thesis combined with other data from our laboratory, such as detection of cytochrome *c* and TFAM in the cytosolic fraction via western blotting, increased levels of γH2Ax and activation of other than caspase-3 caspases using western blotting in senescent cells (data not included in this thesis), collectively constitute the most robust and extensive analysis of the sub-lethal apoptotic signalling thus far.

Additionally, the importance of these findings lies in their relatively physiological context. I observed increased markers of mitochondrial apoptotic stress in three models of cellular senescence, namely damage-, oncogene-induced and replicative senescence. Until 2019, when Brokatzky and colleagues published their work of sub-lethal apoptotic signalling

upon pathogen invasion, this phenomenon was known only in the context of pharmacological interventions. Findings of my thesis indicate that this new type of mitochondrial stress may be a more common mechanism during various cellular stress- and damage responses.

Ichim and colleagues, who investigated miMOMP upon ABT-737 treatment, found that cells displaying features of apoptotic signalling, possess only approximately 3 percent of affected mitochondria, *i.e.* mitochondria positive for the CytoGFP (Ichim *et al*., 2015). In my studies, I did not set out to measure the volume of permeabilised mitochondria, however, such an approach would be an interesting future direction.

In this study, I show that around 65 percent of cells in DIS are positive for activated BAX co-localising with mitochondria, which informs that the majority of senescent cells experience this kind of stress. In contrast, the study by Ichim *et al.* (2015) found approximately 5 percent of cells positive for mitochondria containing CytoGFP signal. However, this report investigated only the short-term effects of ABT-737 – 3 hours – while in our setting, the time-point of interest was primarily 10 days after the induction of cellular senescence.

Interestingly, my additional data indicate that the initial, short-term (8 hours) consequence of γ-irradiation, is the appearance of a sub-population of the cells in culture displaying a significant wide-spread activated BAX signal at the majority of mitochondria (Figure 3.2 B) and elevated numbers of cytosolic DNA foci (data not shown). As little cell death is generally observed upon 20Gy dose of irradiation, these cells presumably survive MOMP and renew their mitochondrial pool. The finding of widespread BAX activation as a direct consequence of γ-irradiation that does not induce cell death stands as a fascinating finding on its own. It would be worth investigating the processes of mitochondrial degradation and repopulation in this context in the future. My findings indicate that prior to becoming senescent and displaying features of limited apoptotic signalling, cells might be undergoing a process similar to anastasis (Sun *et al.,* 2017) and the mitochondrial apoptotic stress observed at later time-points (10 days) might constitute the unresolved damage that occurred initially.

My data demonstrate the presence of mitochondria containing a signal of activated BAX. However, I do not present evidence that these mitochondria are permeabilised, for example, being characterized by lower mitochondrial membrane potential, lack cytochrome *c* or are in the process of mtDNA release. I did not find evidence of IMM herniation by EM. A broader characterisation of mitochondria containing BAX6A7 signal should be extended for final conclusions of mtDNA release being mediated by BAX6A7 pores.

The mitochondria that are positive for activated BAX and mtDNA leakage are often found at the cell periphery. Such mitochondria are frequently separated from the otherwise highly interconnected network. Two explanations of this observation may be considered. Firstly, mitochondrial hyper-fusion is seen as an adaptive pro-survival response against stress. It has been observed to occur in the models of damage-induced and replicative senescence (Dalle Pezze *et al*., 2014) and upon exposure to a number of other stressful stimuli, such as pharmacological iron chelating that also leads to cellular senescence (Yoon *et al*., 2006), UV irradiation, block of transcription by actinomycin D, and block of translation by cycloheximide (Tondera *et al*., 2009). Potentially, mitochondria that fail to interconnect with the rest of the network, experience a higher load of stress, for example do not maintain a sufficient membrane potential, and undergo a "small apoptosis". This explanation would add to the understanding of why mitochondrial network becomes elongated in the conditions of cellular senescence, hypothetically, as an additional anti-apoptotic mechanism.

On the other hand, my preliminary data based on p-DRP1(Ser616) staining indicates that the fission process could occur secondarily to the very first steps of apoptotic cascade, such as mitochondrial translocation of BAX. During apoptosis, when BAX translocates to mitochondria forming discrete foci observed by anti-BAX antibody staining, these later become the scission sites and co-localise with mitochondrial dynamics machinery, such as DRP1 protein (Karbowski *et al.*, 2002). McArthur et al. (2018) later tested the sequence of events within apoptotic cascade, demonstrating cytochrome *c* release precedes mitochondrial fragmentation. With regards to the requirement of mitochondrial fission for the process, over-expression of the dominant-negative mutant of DRP1 that leads to mitochondrial hyper-fusion, was shown to limit the loss of mitochondrial membrane potential and cytochrome *c* release during apoptosis (Frank *et al.*, 2001), indicating that fission might facilitate the process. Subsequent studies, however, questioned this conclusion. The current consensus states that mitochondrial fragmentation accompanies, however, is not required for the apoptotic cascade (Gillies *et al.*, 2014; McArthur *et al.*, 2018; Oettinghaus *et al.*, 2016; Riley *et al.*, 2018). It was also shown to be mechanistically independent from MOMP, being independently regulated by Bcl-2 family proteins (Sheridan *et al.*, 2008). Among the most recent reports, Riley *et al.* (2018) demonstrated no difference in the degree of mtDNA release between control and DRP1 deficient cells (Riley *et al*., 2018). McArthur *et al.* (2018) also showed that DRP1 deficiency did not prevent from mtDNA release during apoptosis, however, this process was limited in some of their studied cell lines (McArthur *et al*., 2018). Collectively, DRP1-dependent

mitochondrial fission during apoptosis is a part of the apoptotic process, however, depending on the apoptotic stimuli and cell line, this process may be of higher or lesser importance. On the other hand, McArthur *et al.* (2018) utilised also MFN1 and MFN2 double knock-out cells and OPA1 knock-out cells characterised by mitochondrial fragmentation. These mutants were shown to be slightly more sensitive to apoptosis induced by ABT-737 (McArthur *et al*., 2018), standing in line with the concept that fragmentation facilitates mitochondrial apoptotic cascade. In the context of cellular senescence where – at least in DIS – mitochondrial network is hyperfused, a fission signal might limit the propagation of the apoptotic signal among all the mitochondria. If that was true, the maintenance of cellular fission capacity could be seen as a critical anti-apoptotic mechanism. In order to address the question whether it is mitochondrial fusion or fission that prevents the spread of mitochondrial apoptotic stress in the context of interconnected mitochondria of senescent cells, interfering with mitochondrial fusion and fission machineries followed by the assessment of mitochondrial apoptotic stress and sensitivity to apoptosis, would be required.

My data also demonstrate that the two commonly studied models of senescence – DIS and OIS – differ in terms of the degree of mitochondrial apoptotic stress. This comparative analysis was motivated by my preliminary observation that among the cells induced to OIS, it is "even more difficult to spot" the markers of the elusive process of sub-lethal apoptotic signalling than in DIS. All utilised assays – quantification of the number of cells positive for activated BAX signal at mitochondria, measurement of co-localisation between cytochrome *c* and TOMM20, detection of cytosolic mtDNA via cellular fractionation/qPCR and via CLSM, and finally measuring caspase-3 cleavage by western blotting, pinpoint that mitochondrial apoptotic stress is more advanced in DIS than in OIS. My attempts to better understand differences in mitochondrial biology between these two models eventually developed into a separate chapter of this thesis (*Chapter 4*). Generally, the two models differ in terms of the initial trigger that drives cellular senescence. Both models are known to bear a high nuclear DNA damage load that mediates the phenotypes of senescence (Bartkova *et al.*, 2006; Di Micco *et al.*, 2006; Hewitt *et al.*, 2012; Passos *et al.*, 2010). However, γ-irradiation also inflicts a direct damage to other organelles, including mitochondria (Kam & Banati, 2013), while mitochondrial dysfunction in OIS is presumably a secondary effect (Moiseeva *et al*., 2009). Among the immediate consequences of γ-irradiation, there are the formation of free radicals that damage mitochondria, for example, peroxidise the lipids constituting the mitochondrial membranes; mitochondrial swelling; and permeabilisation of cellular membranes, presumably

also mitochondrial membranes (Hannig *et al.*, 2000; Kam & Banati, 2013; Kam, McNamara, *et al.*, 2013; Shadyro *et al.*, 2002). In conclusion, the mitochondria of cells damaged by ionizing radiation directly – in contrast to cells induced to OIS - are primed to dysfunction, as the trigger itself is linked to the inherent, wide-spread damage.

The genetic depletion of BAK and BAX in cells induced to DIS, as well as BAX inhibition using BCB in the same model of senescence, robustly show that mitochondrial apoptotic stress mediated by BAK and BAX is pro-inflammatory. Both interventions very efficiently reduce the transcription and secretion of the pro-inflammatory cytokines, such as IL6 and IL8, as well as other factors. The degree of SASP suppression using both approaches points out that the process of mitochondrial apoptotic stress is of key importance. These results are extremely valuable as a continuation of the former project carried out by my lab colleague, Clara Correia-Melo and others, who demonstrated that mitochondria are required for the SASP. This proof-of-principle study utilised a model of full mitochondrial depletion via Parkin-mediated mitophagy and showed the lack of SASP, despite the normal development of other senescence features, such as cell cycle arrest, in cells deprived of mitochondria (Correia-Melo *et al*., 2016). Based on the results presented in this thesis, we are able to conclude that the mitochondrial apoptotic stress is one of the main drivers of the pro-inflammatory phenotype of cells undergoing damage-induced senescence.

Several downstream processes of BAK and BAX activation and formation of the mitochondrial pores, may be implicated in mediating SASP. Depletion of BAK and BAX in the model of DIS is associated with significantly lower levels of cytosolic mtDNA. Also in OIS, a slight but significant reduction of mtDNA was observed in the double knock-out cells. Similar effects were obtained upon pharmacological inhibition of BAX by BCB, studied independently by myself in DIS on IMR90 background (data not shown) and in DIS on MRC5 and MAFs background, by my lab colleagues. Therefore, reduced levels of cytosolic mtDNA could be responsible for the reduction in the SASP. The mechanism mediating this effect might concern the signalling via cytosolic DNA sensors, such as cGAS-STING pathway, previously shown to control the SASP (Dou *et al*., 2017, Gluck *et al*., 2017). As our lab's data on BAK/BAX depletion or inhibition indicate a very strong suppression of SASP in the model of DIS, and independently, depletion of both cGAS or STING result in a similarly strong reduction of SASP (Dou *et al*., 2017, Gluck *et al*., 2017, James Chapman, unpublished), potentially, these two processes are mechanistically linked. In order to address whether that is the case, it would be critical to assess the activation of cGAS-STING pathway upon BAK/BAX knock-out or

inhibition. In fact, this constituted one of my significant efforts during the PhD studies that, thus far, did not bring the most convincing results. There are several ways to assess the activation of cGAS-STING pathway, such as: measuring the levels of the secondary messenger, cGAMP, detection of STING dimerisation or phosphorylation at serine-366. Moreover, measuring downstream events within the pathway, such as IRF3 phosphorylation at serine-396, nuclear translocation of IRF3 or detection of TBK1 phosphorylation at serine-172, may serve as additional proof of pathway activation (with the notion that these components of the pathway may be activated independently from cGAS-STING) (Chen *et al.*, 2016). A number of these indicators of cGAS-STING activation have been demonstrated in the context of cellular senescence. STING dimerisation has been shown at 6 and 8 days post OIS induction as well as in etoposide-induced senescence in IMR90 fibroblasts (Dou *et al*., 2017). Phosphorylation of IRF3 and TBK1 has was detected in TIG-3 human embryonic fibroblasts undergoing replicative senescence and OIS (Takahashi *et al*., 2018). Increased levels of p-STING, increased percentage of micronuclei-positive cells with STING puncta, P-IRF3 at Serine-395 and TBK1 at Serine-172 have all been identified in senescent cells induced by telomeric DNA double-stand breaks (Abdisalaam *et al.*, 2020). I attempted to measure several of the above-listed readouts of cGAS-STING activation in the context of BAX inhibition. The only one that allowed to successfully detect activated cGAS-STING pathway in senescence was the phosphorylation of IRF3 (the data is included in Appendix Figure 1). Moreover, the treatment with BCB of cells induced to DIS on MRC5 background, led to a detectable reduction in the levels of p-IRF3 (Appendix Figure 1 B). This preliminary analysis may serve as a basis for future efforts aimed at demonstrating the direct link between the process of mtDNA leakage and its detection by the cytosolic DNA sensing pathway, cGAS-STING, during cellular senescence. Potentially, also other pathways could be engaged in mediating the pro-inflammatory effect of mtDNA, for example, NLRP3 inflammasome (Schimada *et al*., 2012). Finally, the contribution of cytosolic mtDNA versus cytosolic DNA of a different origin to the activation of cytosolic DNA sensing pathways remains to be elucidated. Studies thus far pointed out the key role of CCFs (Dou *et al*., 2017, Gluck *et al*., 2017, Vizioli *et al*., 2020) and retrotransposons-derived DNA (De Cecco *et al*., 2019) in driving SASP. Considering these studies, as well as the data presented in this thesis, senescent cells potentially employ multiple mechanisms assuring their pro-inflammatory phenotype. Their engagement may, however, depend on senescence model, cell type as well as studied time-point. One of the potential experimental approaches that would reveal the contribution of specific cytosolic DNA to the

activation of DNA sensing pathway, such as cGAS-STING, could include immunoprecipitation of DNA sensors of interest (for example, cGAS) followed by a qPCR or sequencing of bound DNA. This is a direction our lab is currently heading towards with the aim to better understand SASP regulation by cytosolic DNA.

Another potential mechanism driving the SASP via mitochondrial apoptotic stress is the activation of caspases. During the process of apoptosis, caspases were shown to actually dampen the pro-inflammatory signalling that could develop in consequence of mtDNA release, as the pharmacological caspase inhibition or genetic depletion of caspase-9, Apaf-1, or caspase-3/7 led to secretion of IFN-β by the dying cells (White *et al*., 2014, Rongvaux *et al*., 2014). This mechanism is considered to prevent apoptotic cells to trigger a host immune response. However, this is true when caspases are activated at a lethal level. In contrast, during sub-lethal caspase activation, caspases cause mild DNA damage inflicted by caspase-activated DNase (CAD) – a process of a pro-inflammatory nature (Ichim *et al*., 2015, Brokatzky *et al*., 2019). This is in line with data from our lab, which shows that pan-caspase inhibitor treatment of senescent cells reduces the SASP. Interestingly, DNA damage leads to the formation of CCFs and cGAS-STING pathway activation. Presumably, by limiting caspase activation upon genetic deletion of BAK/BAX or their pharmacological inhibition, the reduction of SASP could be mediated by decreased caspase activation and inhibition of CCFs formation. This would stand in line with several recent reports demonstrating the formation of CCFs in senescent cells and their role in activating cGAS-STING pathway (Dou *et al*., 2017, Gluck *et al*., 2017, Takahashi *et al*., 2018).

Studying the model of OIS in the context of BAK and BAX deficiency, revealed that this model of senescence is fundamentally different from DIS. Among several interventions I performed, only the short-term and late-onset pharmacological inhibition of BAX resulted in the suppression of SASP. The genetic knock-out as well as the pharmacological inhibition initiated at the day of senescence induction resulted in an opposite effect – a significant exacerbation of SASP. A hint to explain this discrepancy may be found by considering the additional, non-canonical functions of BAK and BAX (Gross *et al.*, 2017). First, BAK and BAX were demonstrated to mediate normal fusion of mitochondria in healthy, *i.e.* non-apoptotic, cells (Karbowski *et al.*, 2006). Two reports indicate that BAX does so by interacting with MFN2 (Hoppins *et al.*, 2011; Karbowski *et al.*, 2006). BAK is also known to interact with mitochondrial fusion proteins. During apoptosis, BAK disassociates from MFN2 and enhances the interaction with MFN1 – process that facilitates mitochondrial fragmentation (Brooks *et al.*,

2007). These studies indicate that the two mediators of the mitochondrial apoptotic stress, BAK and BAX, are involved in mitochondrial dynamics. Their depletion – especially during the hyperproliferation phase that OIS undergo – may induce additional mitochondrial perturbations that lead to an exacerbated pro-inflammatory response. My data included in Appendix Figure 2 A and B of unbiased mitochondrial network morphology analysis (Mitochondrial Network Analysis, MiNA) (Valente *et al.*, 2017) points out that especially BAK single knock-out but also BAX and BAK/BAX knock-out cells have more fragmented mitochondrial networks when comparing to EV controls. My data from subsequent Chapter 4 indicate that mitochondrial fragmentation itself does not drive the SASP in the context of senescence, however, the observed changes may be linked to other mitochondrial dysfunctions that exacerbate the SASP.

Another key mitochondrial role affected by the lack of, in this case BAX only, is the energy metabolism. It was shown that BAX deficient cells (a cancer cell line, HCT-116 and primary mouse hepatocytes) were characterised by reduced oxygen consumption and ATP levels balanced out by increased glycolysis (Boohaker *et al.*, 2011). This study also demonstrated that a fraction of mitochondrial BAX is localised to the inner mitochondrial membrane – a finding that supports BAX role in regulating mitochondrial respiration. If BAX deficiency is associated with a glycolytic shift, it is conceivable that in the context of OIS – a type of senescence induced by oncogene activation that is linked to reliance on glucose metabolism for cell growth, especially during the initial hyperproliferative phase (Vander Heiden *et al.*, 2009) – BAX deficiency could potentially prevent cells from entering senescence or facilitate senescence escape. In support of this, stand the results included in Appendix Figure 2. Namely, I observed a tendency for a smaller cell size upon BAX and double BAK/BAX knock-out, no effect in case of single BAK knock-out (Appendix Figure 2 C); a significantly smaller nucleus size, however, only for the double mutant (Appendix Figure 2 D); and finally, a trend for an increased number of proliferating, *i.e.* Ki67 positive, cells detected via immuno-staining for single knock-out cells (a stronger trend for BAX than BAK knock-out) and a significant increase for the double knock-out cells: from 10 percent in control OIS cells to above 20 percent in double knock-out OIS cells (Appendix Figure 2 E). Whether the prevention or escape from cellular senescence may lead to a strengthened pro-inflammatory secretome, remains an open question. However, in the case of BAK mutant, which did not seem to be changed in respect to these measures as BAX and BAK/BAX mutants, SASP was also significantly elevated. Potentially, these are additional phenotypes, related to BAX deficiency, that do not explain the SASP exacerbation.

The roles of BAK and BAX span beyond functions directly related to mitochondria. For example, BAK/BAX deficiency leads to decreased resting calcium (Ca^{2+}) in ER due to increased Ca^{2+} leak and an increase in the phosphorylation state of the inositol trisphosphate receptor type 1 (IP3R-1) (Oakes *et al.*, 2005; Scorrano *et al.*, 2003). This is mediated by the increased interaction of IP3R-1 and BCL-2 upon BAK/BAX depletion – an example demonstrating how cell death signalling mechanisms are interlinked. BAK and BAX also play a role in the unfolded protein response, by directly interacting with the ER transmembrane protein, inositol-requiring enzyme 1α (IRE1α) that mediates the initiation of UPR (Hetz *et al.*, 2006). A double BAK/BAX knock-out in mice, in the context of ER stress induced by tunicamycin, leads to an extensive tissue damage of the liver and decreased expression of the IRE1 substrate X-box–binding protein 1 as well as its target genes (Hetz *et al*., 2006). These additional insights into BAK and BAX biology visualise the complexity of the potential consequences of their knock-out and multitude of avenues worth following to truly understand the mechanisms behind the observed effects.

The following work presented in this chapter revolved around the potential organismal consequences of mitochondrial apoptotic stress, in particular, mtDNA leakage and its subsequent fate - mtDNA secretion by senescent cells. I studied several types of human and mouse fibroblasts in the state of DIS and found elevated concentration of mtDNA upon senescence induction. Interestingly, I also observed increased numbers of vesicular structures associated with senescent cells while imaging cells stained with anti-BAX and anti-TOMM20 antibodies. These vesicles contained activated BAX signal and an OMM signal – TOMM20, suggesting that cells might be shedding the debris consisting of mitochondria that underwent apoptotic stress. Elimination of intracellular waste by the means of exocytosis is a widely accepted concept (Bang *et al.*, 2012). There is now a growing literature indicating mtDNA is being found in the form of exosomes (Ariyoshi *et al.*, 2019; Soltész *et al.*, 2019; Torralba *et al.*, 2018). Moreover, other mitochondrial components, such as TFAM, voltage-dependent anion-selective channel 1 (VDAC1), humanin and mtDNA-derived mRNA sequences, including those for NADH dehydrogenase 2 (ND2), cytochrome oxidase subunit 2 (CO2) have been found in exosomes (Wang, Weidling, *et al.*, 2020). Interestingly, whole functional or dysfunctional mitochondria are being found to be secreted and re-utilized or degraded by recipient cells (Liu *et al.*, 2021). To my knowledge, no study so far reported the presence of activated BAX in the extracellular vesicles. This novel observation of activated BAX secretion in the form of vesicles would be worth following up in the future, addressing the mechanism of

their formation. Potential follow-up experiments would include 1) confirmation of the presence of mitochondria in extracellular vesicles – assessing their ultrastructure and protein composition would allow to discriminate whether the detected signal derives from mitochondrial debris or intact/dysfunctional mitochondria, 2) interference with mitochondrial fission machinery testing whether it is involved in generation of mitochondria packaged into vesicles, 3) interference with vesicle trafficking, particularly exocytosis to test whether secretion of BAX6A7-positive vesicles can be reduced. An interesting question that remains to be answered is whether other than apoptotic cells might release apoptotic bodies-like vesicles?

While studying mouse fibroblasts, I also found elevated levels of mtDNA in the exosomal fraction in cells 3 days post senescence induction. This analysis should be extended by studying the 10 day time-point with regards to exosomal mtDNA to match my other analyses, as well as additional assays confirming the successful isolation of intact exosomes, such as transmission electron microscopy (TEM) for visualisation of exosomes, exosome counting using an instrument for nanoparticle tracking analysis, and a western blot analysis of exosome protein markers such as CD63, CD81 and others (Kowal *et al.*, 2016). Interestingly, exosomal mtDNA in the context of irradiation has been investigated by others (Ariyoshi *et al*., 2019). This study also focused on rather short-term effects of ionizing radiation, such as 24 hours or 72 hours and reports the by-stander effect of irradiated cells on healthy cells in the form of increased nuclear DNA damage, similarly to the by-stander effect observed in the context of established senescence (10 days post irradiation) - induced by the same method (Nelson *et al.*, 2012). Importantly, authors of the article demonstrate that this is the DNA contained in the cell culture media that has the most powerful by-stander inducing effect rather than the RNA and protein constituents. Moreover, the authors show mtDNA requirement for DNA damage induction. Finally, they also report highly and significantly elevated levels of mtDNA in exosomes of irradiated mice (Ariyoshi *et al*., 2019). These findings stand in line with my analyses which point out that the irradiation model – DIS – is characterised by the highest degree of mitochondrial apoptotic stress.

In contrast to the irradiation model presented in the study by Ariyoshi and colleagues (2019), normal ageing or even senescence burden conditions in mice, such as pulmonary fibrosis or severe obesity, were not characterised by increased levels of circulating mtDNA, according to my analyses. Interestingly, our collaborators who consulted the method with our laboratory, obtained contrasting results and detected increased circulating mtDNA in plasma of old mice (Iske *et al.*, 2020). Authors of this paper utilised mice at 18 months of age as the “old

group", which presents as a difference. Old mice in my study were either 23-27 months of age, or in the case of males, younger - 14 months of age. Moreover, the authors of this paper demonstrated that a treatment with a senolytic cocktail, dasatinib + quercetin, results in a significantly decreased levels of plasma mtDNA. Notably, the authors utilised only five mice per each condition and were able to detect the described differences. Considering my own difficulties in obtaining the results, I wish to see this effect independently reproduced.

Further, I decided to explore whether mtDNA could serve as a biomarker of cellular senescence in humans. Using a relatively narrow age group of patients within my cohort of patients with severe aortic stenosis, represented however, by patients of low frailty index score - indicating a good general health status, and medium to high frailty index score - indicating a poor health status, was designed to allow for exclusion of the chronological age factor, accounting rather for the biological age or senescent cells' burden. No positive corelation of mtDNA levels and frailty score was found in the whole cohort. When females were analysed separately, the association was also insignificant (according to multiple linear regression analysis), however the p-value of 0.0514 indicates studying a larger cohort of females could be worthwhile in the future. In general, based on these results, circulating mtDNA levels are not a strong biomarker of frailty. In order to finally conclude about the association of mtDNA with frailty, a study on a larger cohort should be carried out.

Collectively, my analyses of circulating mtDNA content in plasma in mice and humans generally indicate that mtDNA is not a strong biomarker of age or cellular senescence burden. According to the study by Pinti *et al.* (2014), who found a positive and significant association between circulating mtDNA and age, mtDNA is, however, an extremely variable trait. The authors were able to find an association of mtDNA content with age using a large cohort of more than 800 patients. Moreover, a significant association was observed only upon excluding the youngest group of the subjects (Pinti *et al*., 2014). The higher content of circulating mtDNA in the youngest group suggests that factors other than cellular senescence may have an impact on mtDNA concentration in plasma. In support of this, stand several other publications. For example, a study by Soltesz *et al.* (2019) show that despite the successful and reliable detection of mtDNA in peripheral blood, in cell-free plasma and in exosomes isolated from plasma, there is no difference between the healthy control group (72 patients) and patients with atrial fibrillation (60 patients). Authors also report no positive association between this trait and sex or age (Solteszet *al*., 2019). Other report shows no correlation of circulating mtDNA and the levels of IL6 (Kageyama *et al.*, 2018). In fact, these authors also report lower levels of mtDNA

in patients with the major depression disorder, a disease generally known for its association with organismal inflammation (Kageyama *et al.*, 2018). Moreover, even though cell-free circulating DNA is being extensively studied as a potential biomarker of cancer, some studies show that it is the nuclear DNA rather than mtDNA which is associated with cancer (Kohler *et al.*, 2009). In fact, this study reported a significantly decreased levels of mtDNA in cancer patients. In contrast, increased circulating mtDNA levels were associated with acute myocardial ischemia (Sudakov *et al.*, 2017), stroke, trauma and sepsis (Schwarzenbach *et al.*, 2011). Finally, an interesting study demonstrated that acute psychological stress exerted by "simulated public speaking task, consisting of 2 min of preparation for a speech defending themselves against an alleged transgression (shoplifting or traffic violation) followed by 3 min of videotaped speech delivery while directly facing an evaluator wearing a white lab coat" leads to significantly elevated levels of circulating mtDNA (Trumpff *et al.*, 2019). If psychological stress in this form may have such consequences, it is a strong voice suggesting that circulating mtDNA is a feature that may be affected by factors extremely difficult to control, preventing from its use as a biomarker unless in the context of very severe conditions such as mechanical trauma or sepsis.

3.18 Study limitations

One major limitation of this study is the lack of measures of apoptosis in the studied conditions. Even though senescent cells are generally known to be apoptotic resistant, it is not clear, for example, whether OIS and DIS might differ in this respect, which might affect some of the studied features of mitochondrial apoptotic stress. The majority of them were analysed by immunofluorescence/microscopy techniques, which allows to ascertain that the analysed cells are not apoptotic (for example, contain intact nucleus and cytoplasm). On the other hand, the measurement of oligomerised BAX and BAK or caspase-3 cleavage concerns the whole cell populations and its increase might reflect an ongoing apoptosis (even to a small degree) rather than senescence. In order to make confident conclusions regarding all the studied features of mitochondrial apoptotic stress, it would be important to determine whether the population of senescent cells contains more cells at the stage of advanced apoptosis. In fact, I assessed cell survival between Prolif, OIS and DIS by flow cytometry using SYTOX™ Green (Thermo Fisher Scientific, S7020) and found a significantly higher percentage of dead cells in the conditions of DIS than Prolif and OIS (data not shown). However, the method based on flow cytometry has an important disadvantage related to cell size. Cells in DIS are significantly

larger than proliferating cells or cells in OIS (*as described in Chapter 4*). It is possible that rapid cell movement within the capillary of the flow cytometer is causing an additional stress and cell death of larger cells. Moreover, senescent cells may be more fragile that could also contribute to a higher risk of cell death during the experiment. A more suitable approach to measure features of advanced cell death, as well as other phenotypes that might be influenced by cell handling and exacerbated through the breakage of fragile sub-compartments (sub-cellular fractionation followed by qPCR) should rely on or be complemented with microscopy techniques, for example quantification of morphological features of apoptosis via confocal microscopy, single cell readouts for caspase activity using immunofluorescence, or terminal deoxynucleotidyl transferase dUTP nick end labelling (TUNEL) assay.

In Figure 3.4, I present images of cytosolic cytochrome *c*. Other studies that investigated the phenomenon of miMOMP and cytochrome *c* leakage, observed the lack of cytochrome c signal in mitochondria rather than cytochrome *c* in the form of cytosolic puncta (Brokatzky *et al*., Ichim *et al*., 2015). In order to confirm the specificity of the observed foci, future studies should attempt to replicate the observation using an alternative antibody or relying on expression of fluorescently tagged cytochrome *c*.

Data presented in Figure 3.5 was obtained with a small number of MRC5 cells. This is due to the fact that my main focus during the PhD research concerned IMR90 cells. However, our lab possesses additional data on MRC5 fibroblasts collected by others, confirming the observations presented in Figure 3.5. Microscopic images of TFAM/DNA/mitochondria labelling as in Figure 3.6 (only a representative image shown) was also analysed quantitatively by others. I would also like to highlight that data presented in Figure 3.8 has not been quantitatively analysed yet. Therefore, the data in the form presented in the thesis, may be considered preliminary. Data presented in Figure 3.11 concern only a limited number of cells (mtDNA leakage in OIS), however, the same analysis on additional biological replicates is presented in Figure 3.13 (4 independent replicates) as a part of the comparative analysis of mitochondrial apoptotic stress.

Data in Figure 3.7 demonstrates a qPCR analysis of cytosolic levels of mtDNA. Simultaneously, I performed a qPCR analysis of a nuclear gene - haemoglobin (HGB). This experiment did not allow to detect nuclear DNA in the cytosolic fraction. Considering, however, a significantly lower copy number of HGB gene and mtDNA in a cell, this analysis is not sufficient to state about the purity of cytosolic fraction.

Data included in Figure 3.15 concern cells induced to senescence (OIS) and lack proliferating controls. In the case of Figure 3.15 B, the reason for not including proliferating controls was a technical problem during samples' collection. In the case of Figure 3.15 C and D, ELISA analysis was initially performed on proliferating cells, however, the values were below the detectable range. Further, when optimising ELISA assay for cells in OIS (high SASP required samples' dilution), I did not include proliferating controls.

Data presented in Figure 3.15 (ELISA analysis of OIS cells upon BAK/BAX knock-out and BCB treatment were collected at Newcastle University (Newcastle upon Tyne, UK), while data presented in Figure 3.16 (qPCR analysis of IL6 and IL8 in IMR90 upon BCB treatment) were obtained at Mayo Clinic (Rochester, US). Ideally, as these were two related experiments, the same methodology should be utilised. Minimally, a control of OIS cells treated with BCB from the day of senescence induction should be included in Figure 3.16 as a positive control of SASP up-regulation upon this interventions (as shown in Figure 3.15 E).

Data presented in Figure 3.17 A and B should be considered preliminary and require additional analysis. Data presented in 3.17 D was not controlled for the cell number by myself, as the samples were primarily collected for other analyses of conditioned media by the members of Dr Nathan LeBrasseur laboratory.

Chapter 4 Results – Comparative analysis of oncogene- and damage-induced senescence with the focus on mitochondria and the role of mitochondrial network structure in the regulation of SASP

4.1 Introduction

Various kinds of stresses may induce a response programme in the form of cellular senescence. Evidence indicates that senescence triggered by different stimuli share certain key pathways, such as development of a secretory phenotype (SASP), engagement of cytosolic DNA sensing pathway, cGAS-STING in mediating SASP (Dou *et al*., 2017; Gluck *et al*., 2017; Takahashi *et al*., 2018), and apoptotic resistance depending on BCL-2 family of proteins (Yosef *et al*., 2016). However, not all senescence-associated phenotypes are universal, for instance mitochondrial metabolism of fatty acids differs considerably between replicative senescence and OIS (Quijano *et al*,. 2012). Despite that, not many studies have focused on understanding the differences and have mostly focused on the similarities. In fact, studies have attempted to identify a common signature of cellular senescence (Casella *et al.*, 2019; Hernandez-Segura *et al.*, 2017), however, evidence is mounting that senescence varies depending on the inducing stimuli as well as cell-type (Coppe *et al.*, 2008; Itahana *et al.*, 2004; Kosar *et al.*, 2011; Nelson *et al.*, 2014; Quijano *et al.*, 2012; Wiley, Velarde, *et al.*, 2016). Furthermore, data shows that the efficacy of senolytics compounds depends on the cell type and sometimes, the senescence model (Kirkland & Tchkonia, 2017; Yosef *et al.*, 2016; Zhu *et al.*, 2017). A comparative rather than a unifying approach is needed for a better understanding of the heterogeneity of senescent cells (Roy *et al.*, 2020). A distinction of these aspects of senescence programme that regulate SASP or grant apoptotic resistance may help identify better senomorphic and senolytic therapeutic strategies which take into consideration mechanisms driving different types of senescent cells.

In my previous chapter, I found that oncogene-induced senescence driven via RAS activation and damage-induced senescence triggered by γ-irradiation differ in terms of a) the extent of mitochondrial apoptotic stress and b) the effects of BAK/BAX genetic depletion or pharmacological inhibition on the SASP. The existing literature also reported several key differences between the models, such as the levels of secreted SASP factors. Specifically, OIS was found to be characterised by a higher expression of SASP components, such as IL6 and IL8, than DIS (Coppe *et al*., 2008; Takahashi *et al*., 2018). Given that mitochondria have been shown to be key regulators of the SASP (Correia-Melo *et al*., 2016; Vizioli *et al*., 2019), I

hypothesised that differences in mitochondrial function between OIS and DIS may explain dissimilarities in the levels of SASP.

In order to investigate this, I proceeded to characterise the two types of senescence: OIS and DIS, induced in cells of the same type, human embryonic fibroblasts, IMR90. I set out to perform an analysis of the known senescence markers, followed by a line of investigations into mitochondrial function between the two models in order to identify processes responsible for the differences described thus far.

4.2 OIS and DIS cells are indistinguishable in terms of several canonical senescence markers, such as expression levels of β-galactosidase, lamin-B1, p21, and p16 as well as the degree of DDR

Cells undergoing senescence acquire characteristic features, one of them being the increased activity of a lysosomal hydrolase, senescence-associated β-galactosidase (SA-β-gal) (Dimri *et al.*, 1995; Kurz *et al.*, 2000; Lee *et al.*, 2006). I set out to determine whether human embryonic fibroblasts, IMR90, induced to senescence via oncogene-activation and γ-irradiation differ in respect to this senescence marker. I utilised IMR90ER:RAS cells and induced them to OIS and DIS alongside, and collected at the exactly same time-points post senescence induction, *i.e.* 10 days. SA-β-gal may be detected using a cytochemical staining which provides a substrate for β-galactosidase (β-Gal), X-Gal, that upon cleavage occurring at a specific pH (6.0), gives a blue-pigmented product (Dimri *et al.*, 1995). The representative images in Figure 4.1 A inform about the level of SA-β-gal activity in control and senescent cells. Additionally, I measured the levels of transcripts of galactosidase beta 1 (GLB1) and β-Gal**.** GLB1 gene encodes two proteins, β-Gal and an elastin binding protein. The mRNA is alternatively spliced into two products, one of them being β-Gal. This analysis revealed a significant increase in the expression of GLB1 as well as the product of its splicing, β-Gal, in senescence. However, no difference was identified between the two models of senescence (Figure 4.1 B and C).

Next, I set out to analyse other canonical markers of cellular senescence. The loss of lamin B1 has been described to depend on the activation of either the p53 or RB tumour suppressor pathway and occur via a decrease in its mRNA stability (Freund *et al.*, 2012; Shimi *et al.*, 2011). Other studies also point out the autophagic degradation of lamin B1 at the protein level as a mechanism in maintaining its low levels – a process of key importance for the cell cycle arrest (Dou *et al.*, 2015; Shimi *et al.*, 2011). When analysed by western blotting, the levels of lamin B1 become virtually undetectable in senescence. Consistently, both DIS and OIS on

IMR90 background robustly decreased the expression of lamin-B1 at the protein level (Figure 4.1 D).

DNA damage response (DDR) mediated by p53-p21 and a p16INK4a pathways orchestrate cell cycle arrest by regulating cyclin complexes and RB tumour suppressor protein. I assessed the levels of p21 (Figure 4.1 D), p16 (Figure 4.1 E) and the number of γH2A.x foci as a readout of DDR (Figure 4.1 F). Representative images used to quantify the number of γH2A.x foci can be found in Figure 4.3 D. All these markers behaved similarly across the two studied models of senescence - a robust increase was observed when compared to proliferating cells, however, the levels of all markers did not differ between OIS and DIS.

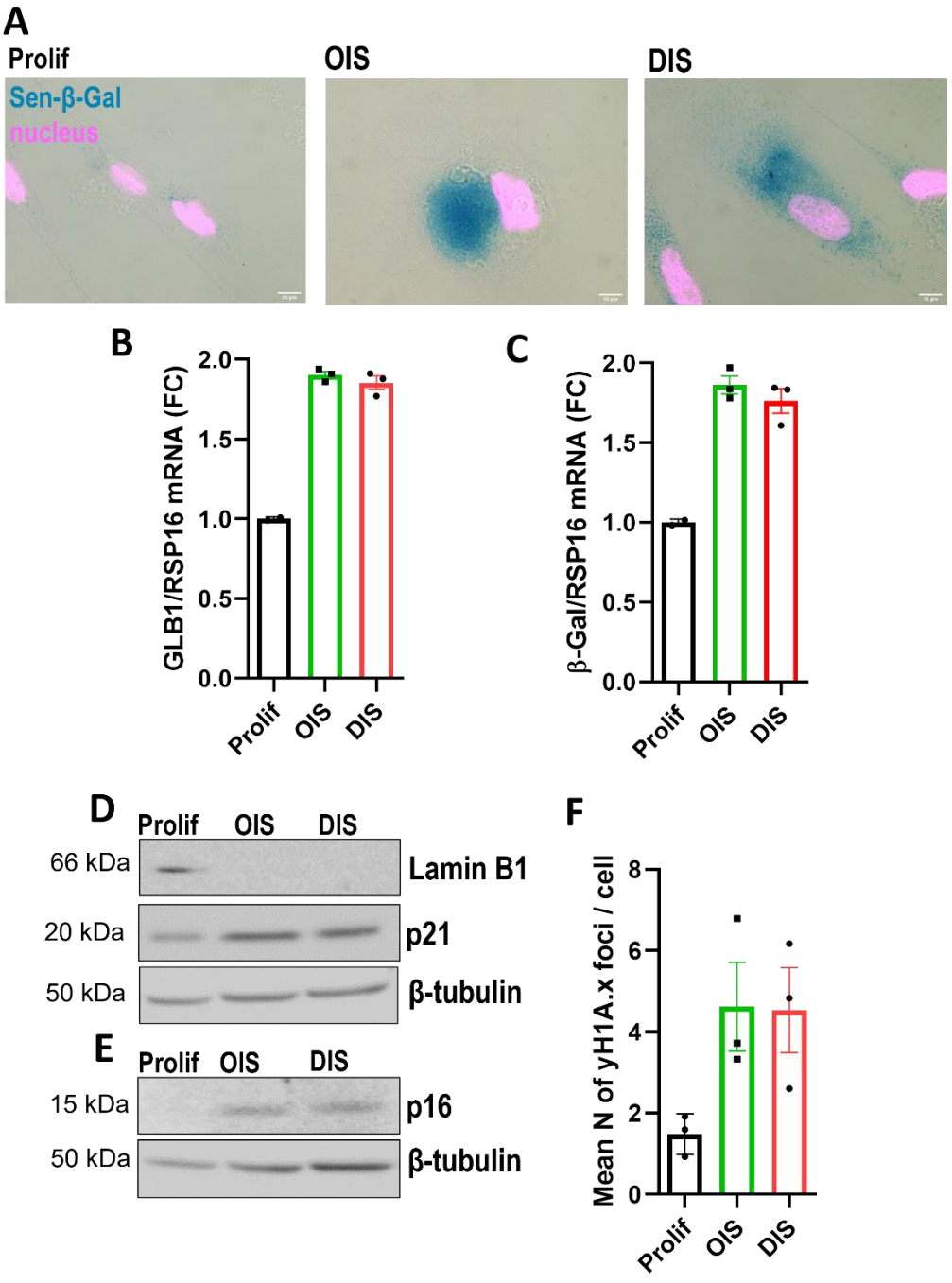

Figure 4.1: Comparative analysis of Sen-β-Gal, cell cycle arrest and DDR markers in human embryonic fibroblasts IMR90 in proliferating conditions, OIS and DIS

(A) Representative bright field microscopy images of Sen-β-Gal staining depicting characteristic morphologies of cells induced to OIS (rounded) and DIS (elongated). Scale bar represent 10μm. **(B)** GLB1 mRNA levels via qPCR normalised to RSP16 using Delta-Delta Ct method, n=2 for Prolif, n=3 for OIS and DIS independent replicates/wells **(C)** β-Gal mRNA levels via qPCR normalised to RSP16 using Delta-Delta Ct methods, n=2 for Prolif, n=3 for OIS and DIS **(D)** Representative western blots of Lamin B1 and p21 levels, n=3 independent replicates/wells **(E)** Representative western blots of p16 levels, n=3 independent replicates/wells **(F)** Quantification of the mean number of DNA damage foci immuno-stained for yH2A.x, n=3 independent replicates/coverslips, minimum 15cells/replicate, 1-way ANOVA Tukey's multiple comparison test: Prolif vs OIS p=0.1024, Prolif vs DIS p=0.1112, OIS vs DIS p=0.9977. Error bars represent SEM.

4.3 DIS and OIS differ in terms of cell size, the number of CCFs and the expression of anti-apoptotic BCL-2 proteins

Cells entering cellular senescence change morphologically, *i.e.* they become larger and flattened (Ben-Porath *et al.*, 2005; Cho *et al.*, 2004; Neurohr *et al.*, 2019). I measured the whole cell surface area as well as nucleus surface area. Both OIS and DIS were found to be significantly larger than control cells (Figure 4.2 A). Similarly, senescent cells contained larger nuclei (Figure 4.2 B). Interestingly, cells in DIS were found to be also significantly larger than OIS, in terms of both parameters (Figure 4.2 A and B). Notably, the shape of cells in OIS and DIS was observed to be distinct, where a typical cell induced to OIS acquires a more rounded morphology, while a cell in DIS an elongated, oblong or fusiform shape (Figure 4.1 A).

Having previously observed a higher level of cytosolic mtDNA in DIS when compared to OIS (*Chapter 3*), I decided to quantify the number of cytosolic chromatin foci (CCFs). DDR marker γH2A.x, a heterochromatin marker in the form of an epigenetic modification to the histone H3K27me3, and DNA (marked with DAPI) are used to visualise CCFs. CCF have been proposed to be major regulators of the SASP during senescence, via the cGAS-Sting pathway. (Ivanov *et al.*, 2013; Gluck *et al.*, 2017). Consistently with the published data, I found an increase of the number of CCFs in senescence, however, in this experiment, it was statistically significant only for the model of DIS (Figure 4.2 C and D). The difference in the number of CCFs between OIS and DIS was not statistically significant. The results suggest that the model of DIS is characterised by a higher abundance of cytosolic DNA, both in terms of mtDNA (*as described in Chapter 3*) and CCFs (Figure 4.2 C and D).

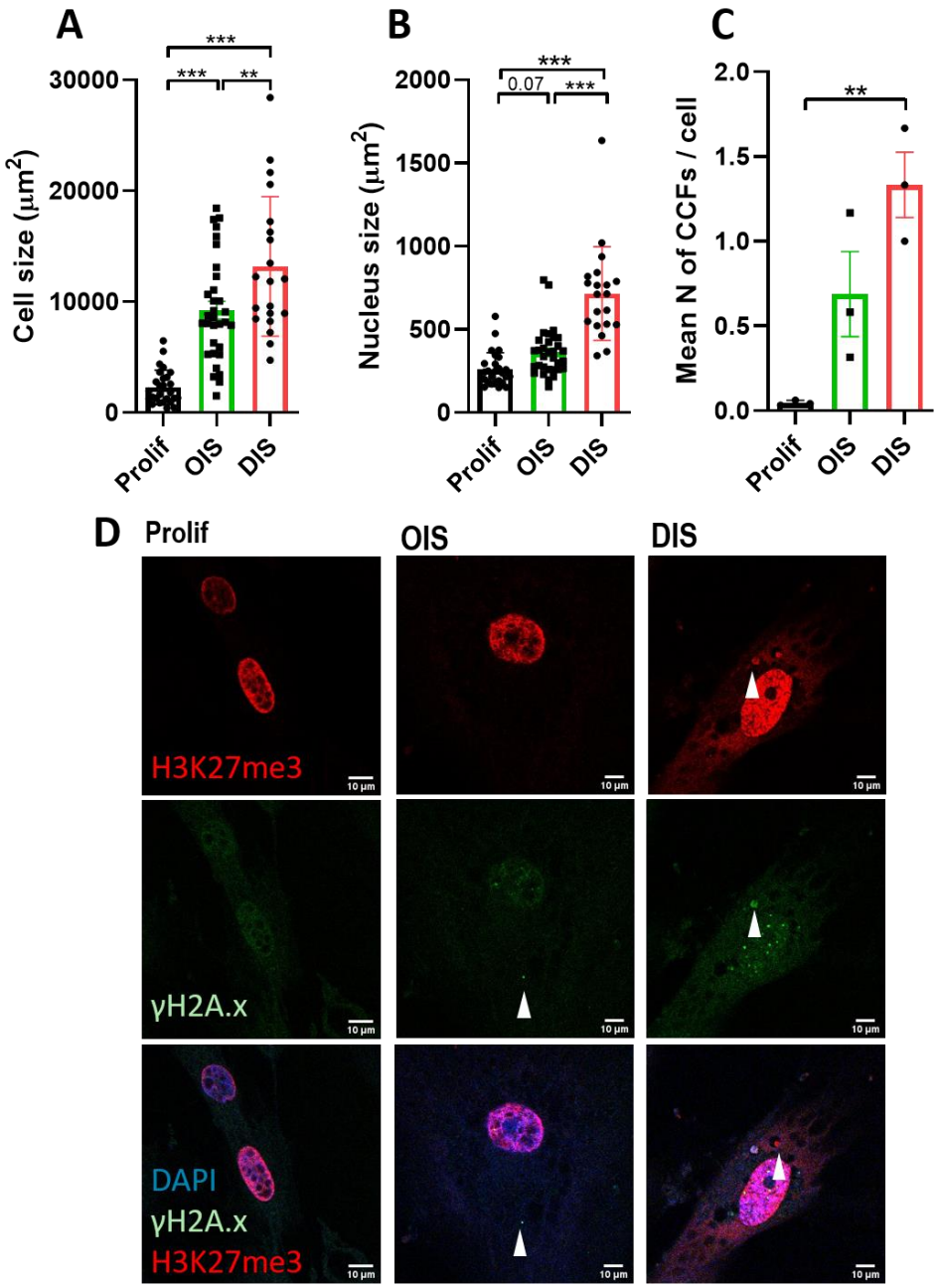

Figure 4.2: Comparative analysis of cell size and CCFs abundance in human embryonic fibroblasts IMR90 in proliferating conditions, OIS and DIS

(A) Cell size in µm^2 , n=minimum 20 cells/condition, pool from 2 independent replicates/coverslips, 1-way ANOVA Tukey's multiple comparison test: Prolif vs OIS p<0.0001, Prolif vs DIS p<0.0001, OIS vs DIS p=0.0062 **(B)** Nucleus size in µm^2, n=minimum 20 cells, pool from 2 independent replicates/coverslips, 1-way ANOVA, Tukey's multiple comparison test: Prolif vs OIS p=0.0744, Prolif vs DIS p<0.0001, OIS vs DIS p<0.0001 **(C)** Quantification of the mean number of CCFs immuno-stained for DNA damage marker γH2A.x, heterochromatin marker H3K27me3 and DNA stained with DAPI, n=3 independent replicates/coverslips, minimum 15cells/replicate, 1-way ANOVA Tukey's multiple comparison test: Prolif vs OIS p=0.1038, Prolif vs DIS p=0.006, OIS vs DIS p=0.1028 **(D)** Representative fluorescence images of DNA damage marker γH2A.x, heterochromatin marker H3K27me3 and DNA stained with DAPI, used for the quantification of γH2A.x foci number and CCFs number, scale bars represent 10µm.

Considering that cells in DIS experience a higher level of apoptotic stress as well as more abundant cytosolic DNA in the form of CCFs, I asked a question whether this model is also characterised by a stronger anti-apoptotic signalling to counteract the pro-apoptotic features. Yosef and colleagues (2016) demonstrate expression levels of a range of BCL-2 family members in IMR90 cells induced to DIS, replicative senescence and OIS. However, these authors do not provide a quantification that would allow to compare the results between senescence models (Yosef *et al*., 2016). I decided to quantify the levels of two BCL-2 proteins, BCL-W and BFL1 in a western blot analysis. The choice of assessed proteins was dictated by the reagents availability. The two studied models of senescence were found to differ in terms of the levels of BCL-W and BFL1, where DIS displays significantly higher levels of BCL-W when compared to both non-senescent cells as well as OIS (Figure 4.3 A and C), while OIS strongly upregulates BFL1 when compared to non-senescent cells and DIS (Figure 4.3 B and C). These data indicate there are senescence models' specificities in terms of anti-apoptotic management, and the levels of BCL-2 proteins are not a direct reflection of the extent of mitochondrial apoptotic stress or the number of CCFs.

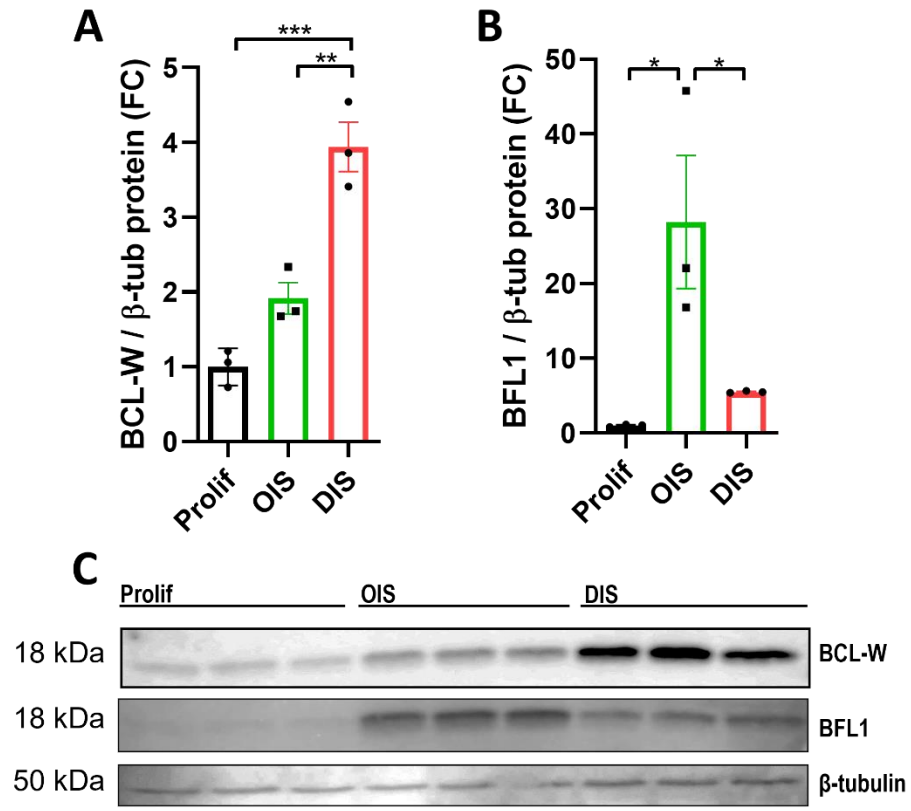

Figure 4.3 Comparative analysis of anti-apoptotic siganlling in human embryonic fibroblasts IMR90 in proliferating conditions, OIS and DIS

(A) BCL-W protein levels via western blot normalised to β-tubulin, FC means fold change when compared to Prolif control, n=3 independent replicates/wells, 1-way ANOVA Tukey's multiple comparison test: Prolif vs OIS p=0.0791, Prolif vs DIS p=0.0003, OIS vs DIS p=0.0024 **(B)** BFL1 protein levels via western blot normalised to β-tubulin, FC means fold change when compared to Prolif control, n=3 independent replicates/wells, 1-way ANOVA Tukey's multiple comparison test: Prolif vs OIS p=0.0225, Prolif vs DIS p=0.8160, OIS vs DIS p=0.0468 **(C)** BCL-W and BFL1 protein levels via western blot, n=3 independent replicate/wells. Error bars represent SEM.

4.4 OIS is characterised by a higher than DIS expression and secretion of several key SASP factors

As described before, SASP composition and strength differ between senescence models (Coppe *et al*., 2008; Takahashi *et al*., 2018). These reports consistently identified higher levels of po-inflammatory cytokines, such as IL6 and IL8, in OIS than in DIS. In my next step, I set out to confirm these findings in OIS and DIS induced on IMR90 background. I utilised two methods for assessing the level of SASP factors, namely, the enzyme-linked immunosorbent assay (ELISA) that allows to measure secreted molecules in the cell culture media as well as a qPCR approach to detect mRNA expression levels. The concentration of IL6 and IL8 in cell culture media was approximately a hundred-fold higher in OIS than in DIS (Figure 4.4 A and B), in contrast to another cytokine, belonging to the CXC chemokine family, interferon gamma-induced protein 10 (IP10) that did not differ between OIS and DIS (Figure 4.4 C). The increase in IL6 and IL8 at mRNA level was not as striking as their secreted forms, however consistently, OIS was characterised by a significantly stronger induction of IL6 and IL8 expression (Figure 4.4 D and E). I also analysed the expression of matrix metallopeptidase 2 (MMP2), IL10 and TNFα and found all of these SASP factors to be elevated to a higher degree in OIS than DIS, with only the latter one not reaching the statistical significance (Figure 4.4 F, G and H). In summary, consistently with previous reports, many SASP factors are produced at higher levels in the model of OIS than in senescence induced by γ-irradiation.

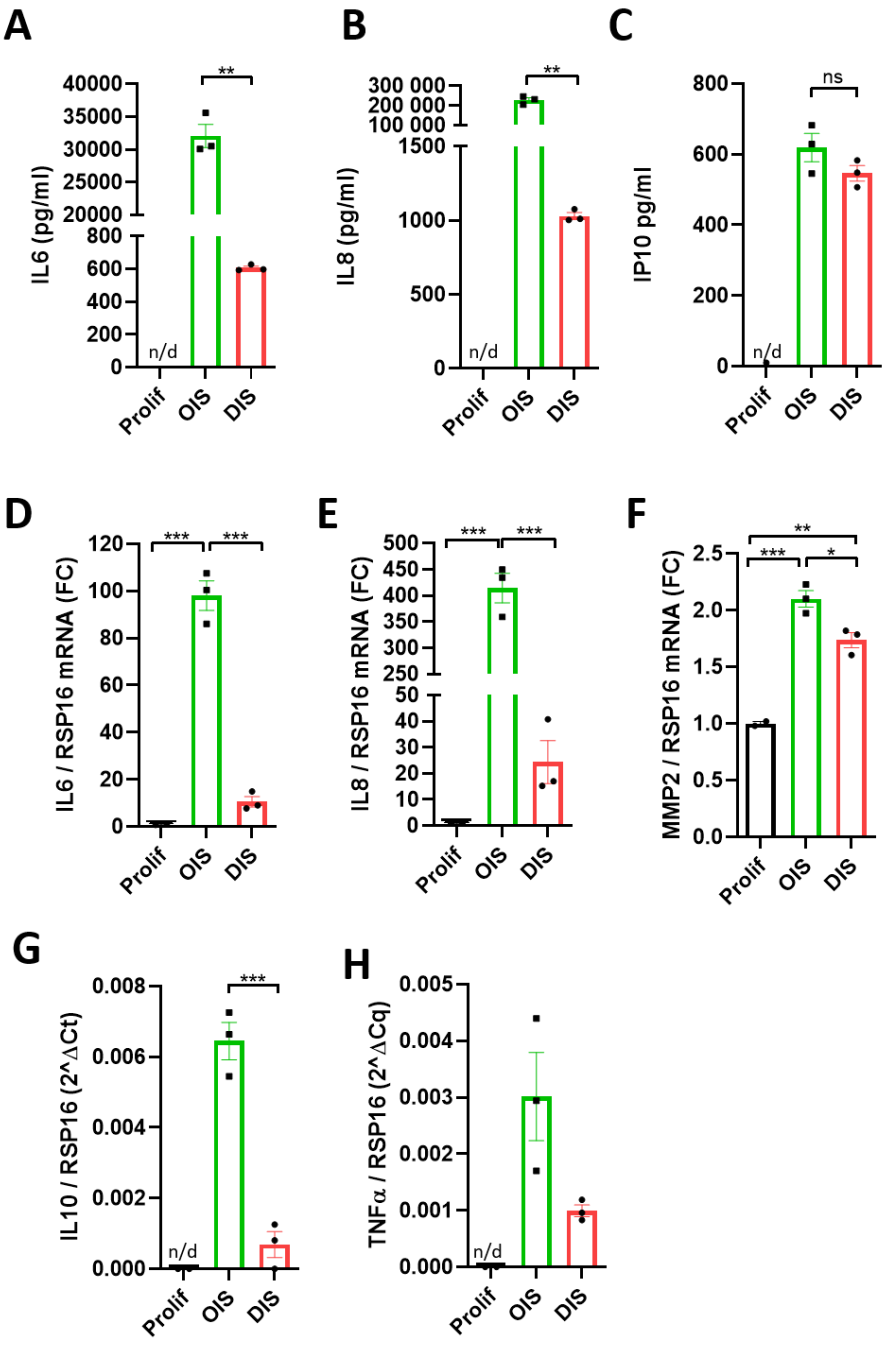

Figure 4.4: SASP profile in human embryonic fibroblasts IMR90 induced to OIS and DIS

(A) Concentration of secreted IL6 protein in pg/ml detected using ELISA, n=3 independent replicates/wells, cytokine undetectable in Prolif conditions, Unpaired t-test with Welsh's correction for unequal SDs: OIS vs DIS p=0.0032 **(B)** Concentration of secreted IL8 protein in pg/ml detected using ELISA, n=3 independent replicates/wells, cytokine undetectable in Prolif conditions, Unpaired t-test with Welsh's correction for unequal SDs: OIS vs DIS p=0.0029 **(C)** Concentration of secreted IP10 protein in pg/ml detected using ELISA, n=3 independent replicates/wells, cytokine undetectable in Prolif conditions, Unpaired t-test: OIS vs DIS p=0.1846 **(D)** IL6 mRNA levels via qPCR normalised to RSP16 using Delta-Delta method, n=2 for Prolif and 3 for OIS and DIS independent replicates/wells, 1-way ANOVA Tukey's multiple comparison's test: Prolif vs OIS p<0.0001, Prolif vs DIS p=0.3947, OIS vs DIS p<0.0001 **(E)** IL8 mRNA levels via qPCR normalised to RSP16 using Delta-Delta method, n=2 for Prolif and 3 for OIS and DIS independent replicates/wells, 1-way ANOVA Tukey's multiple

comparison's test: Prolif vs OIS p<0.0001, Prolif vs DIS p=0.7191, OIS vs DIS p<0.0001 **(F)** MMP2 mRNA levels via qPCR normalised to RSP16 using Delta-Delta method, n=2 for Prolif and 3 for OIS and DIS independent replicates/wells, 1-way ANOVA Tukey's multiple comparison's test: Prolif vs OIS p=0.0002, Prolif vs DIS p=0.0.0017, OIS vs DIS p=0.0215 **(G)** IL10 mRNA levels via qPCR normalised to RSP16 using Delta Ct method, mRNA undetectable in Prolif, n=3 for OIS and DIS independent replicates/wells, Unpaired t-test: OIS vs DIS p=0.0009 **(H)** TNFα mRNA levels via qPCR normalised to RSP16 using Delta Ct method, mRNA undetectable in Prolif, n=3 for OIS and DIS independent replicates/wells, Unpaired t-test: OIS vs DIS p=0.0621. Error bars represent SEM.

4.5 Mitochondrial biogenesis is differentially regulated in oncogene- and damage-induced senescence

Replicative senescence, OIS, DIS as well as other models were all associated with an increase in mitochondrial mass (Ahmad *et al.*, 2015; Correia-Melo *et al.*, 2016; Lee *et al.*, 2006). Damage-induced senescence was also shown to be associated with increased mtDNA copy number, another indicator of mitochondrial biogenesis status (Correia-Melo *et al*., 2016). In contrast to the early stages of DIS development when two key transcriptional co-activators of mitochondrial biogenesis, PGC-1α and PGC-1β, are elevated, a recent report demonstrated that the expression of mitochondrial genes decreases towards the established state of senescence (DIS) (10 days post senescence induction). With regards to OIS, the available published data indicates both biogenesis factors are significantly increased 7 days post senescence induction (Moiseeva *et al*., 2009).

In order to directly compare mitochondrial biogenesis between the two studied senescence variants at the stage of established senescence, I employed a qPCR based approach to assess mtDNA copy number, specifically the relative abundance of D-loop sequence as well as the sequence coding for NADH dehydrogenase 2 (ND2), a subunit of complex I within ETC. I found that the mtDNA copy number is significantly increased in both OIS and DIS. No significant differences were, however, found between the two models of senescence (Figure 4.5 A and B). In contrast, by measuring mitochondrial surface area referred to as mitochondrial footprint – an analysis based on confocal laser scanning microscopy (CLSM) images of mitochondria stained with anti-TOMM20 antibody, I found the cells in DIS possess significantly larger mitochondrial networks than cells in OIS (Figure 4.5 C). Interestingly, the results on mtDNA copy number and mitochondrial network size suggest that the concentration of mtDNA within mitochondrial network is lower in DIS than OIS. To complement the analysis of mitochondrial biogenesis, I set out to test the transcriptional levels of PGC-1α and PGC-1β. As described in section 1.2.3, these transcriptional co-activators induce expression of nuclear encoded mitochondrial genes, including mitochondrial transcriptional factor A (TFAM) that further orchestrates mtDNA replication and expression of mitochondrially encoded genes. I

hypothesised that mitochondrial biogenesis might be more active in OIS than DIS at 10 days' time-point, contributing to a better quality of mitochondria and preventing the mitochondrial apoptotic stress, which I previously showed to be lower in OIS than in DIS (*Chapter 3*). The level of PGC-1α at 10 days post irradiation was significantly increased in DIS only when compared to OIS and not to proliferating controls (Figure 4.5 D). In contrast, PGC-1β was significantly elevated in OIS (approximately by 3-fold) when compared to both proliferating control and DIS. Its levels in DIS matched the non-senescent controls (Figure 4.5 E). By assessing protein levels, I confirmed the up-regulation of PGC-1β (in DIS relative to OIS) as well as one of the nuclear encoded mitochondrial gene products, ubiquinol-cytochrome *c* reductase core protein 2 (UQCRC2) in OIS and not in DIS (Figure 4.5 F and G).

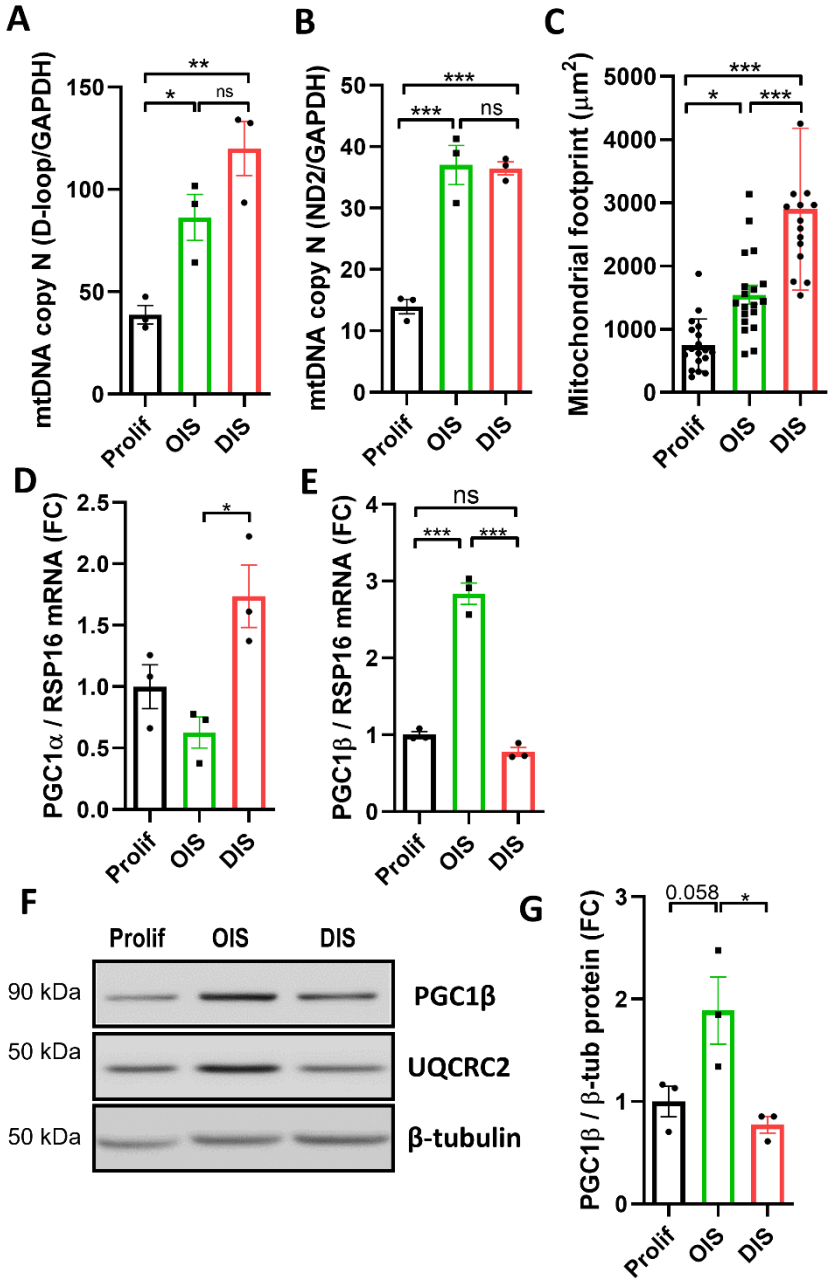

Figure 4.5: Mitochondrial biogenesis in human embryonic fibroblasts IMR90 induced to OIS and DIS

(A) Relative mtDNA D-loop copy number via PCR normalised to GAPDH nuclear gene using Delta Ct method, n=3 independent replicates/wells, 1-way ANOVA Tukey's multiple comparison test: Prolif vs OIS p=0.0405, Prolif vs DIS p=0.0035, OIS vs DIS p=0.1323 **(B)** Relative mtDNA ND2 copy number via PCR normalised to GAPDH nuclear gene using Delta Ct method, n=3 independent replicates/wells, 1-way ANOVA Tukey's multiple comparison test: Prolif vs OIS p=0.0005, Prolif vs DIS p=0.0006, OIS vs DIS p=0.9815 **(C)** Mitochondrial footprint in μm^2 quantified basing on confocal microscopic images of TOMM20 as a mitochondrial marker n=minimum 15 cells across 2 independent replicates/coverslips, 1-way ANOVA Tukey's multiple comparison test: Prolif vs OIS p=0.0130, Prolif vs DIS p<0.0001, OIS vs DIS p<0.0001. **(D)** PGC1-α mRNA levels via qPCR normalised to RSP16 using Delta-Delta method, n=3 independent replicates/wells, 1-way ANOVA Tukey's multiple comparison test: Prolif vs OIS p=0.4138, Prolif vs DIS p=0.0.0794, OIS vs DIS p=0.0156 **(E)** PGC1-β mRNA levels via qPCR normalised to RSP16 using Delta-Delta method, n=3 independent replicates/wells, 1-way ANOVA

Tukey's multiple comparison test: Prolif vs OIS p<0.0001, Prolif vs DIS p=0.2632, OIS vs DIS p<0.0001 **(E)** Representative western blots of PGC1-β and UQCRC2, n=3 independent replicates/wells **(G) D)** PGC1-β protein levels via western blot normalised to β-tubulin, n=3 independent replicates/wells, 1-way ANOVA Tukey's multiple comparison test: Prolif vs OIS p=0.0582, Prolif vs DIS p=0.7438, OIS vs DIS p=0.0236. Error bars represent SEM.

4.6 DIS but not OIS is characterised by increased proton leak

In the next step, I asked whether mitochondria in OIS and DIS differ functionally. I performed an analysis of mitochondrial bioenergetics using a high resolution respirometry (HRR) technique. Oxygraph-2k (Oroboros) allows for assessing the function of the electron transport chain by measuring oxygen consumption. Measurements are made on whole cells in mitochondrial respiration medium without membrane permeabilisation and upon a serial addition of substrates that interfere with ETC complexes, inducing a sequence of "coupling states". Data on oxygen consumption during the specific states draws a picture of the capacity and efficiency of oxidative phosphorylation. All measured "states" described below are expressed after the subtraction of the residual, mitochondrial-independent respiration measured upon addition of ETC inhibitors – antimycin A that inhibits complex III of ETC and rotenone that inhibits complex I of ETC, to the cell suspension.

By performing HRR, I found that both OIS and DIS display higher levels of basal respiration (termed "Basal") (Figure 4.6 A). Due to inter-sample variability, these results are not statistically significant, however the trends are strong. This finding reflects the higher mitochondrial content of senescent cells. Considering the significantly larger mitochondrial network in DIS, it is interesting to notice that the level of Basal respiration in OIS and DIS is similar (p=0.6765) (Figure 4.5 6), indicating the mitochondria are working more efferently in OIS than DIS. As the next step during the respirometry assay, oligomycin A is added in order to inhibit complex V (ATP synthase). This leads to a maximal electrochemical proton gradient and respiration occurring only upon proton exit – or leak - via means other than complex V. Thus, the state is termed as "Leak" indicating non-phosphorylating respiration. The higher it is, the less efficient oxidative phosphorylation. I observed a significant increase in Leak respiration between proliferating control cells and OIS, as well as proliferating control cells and DIS (Figure 4.6 A). Moreover, Leak respiration was significantly higher in DIS than in OIS (Figure 4.6 A). Interestingly, when Leak respiration was normalised to Basal, the results did not differ between non-senescent and OIS cells, indicating that this measure of mitochondrial dysfunction might not be meaningful for OIS, while it was still significantly increased for DIS (Figure 4.6 B). Next, maximum respiration capacity is measured upon the addition of the protonophore,

carbonyl cyanide-4-(trifluoromethoxy)phenylhydrazone (FCCP). It is an uncoupling agent that allows for unrestricted flow of hydrogen ions through the mitochondrial inner membrane leading to a collapse of electrochemical proton potential. Maximum respiration reflects the system capacity to transport protons, which are not restricted to leave intermembrane space via designated systems, such as complex V. I found a trend towards increased maximum respiration for both senescence models (Figure 4.6 A). Upon normalisation to Basal respiration, no difference between the studied systems was observed (Figure 4.6 C). Collectively, these data suggest that at the studied time-point of the senescence induction, oxidative phosphorylation is more efficient for OIS than DIS.

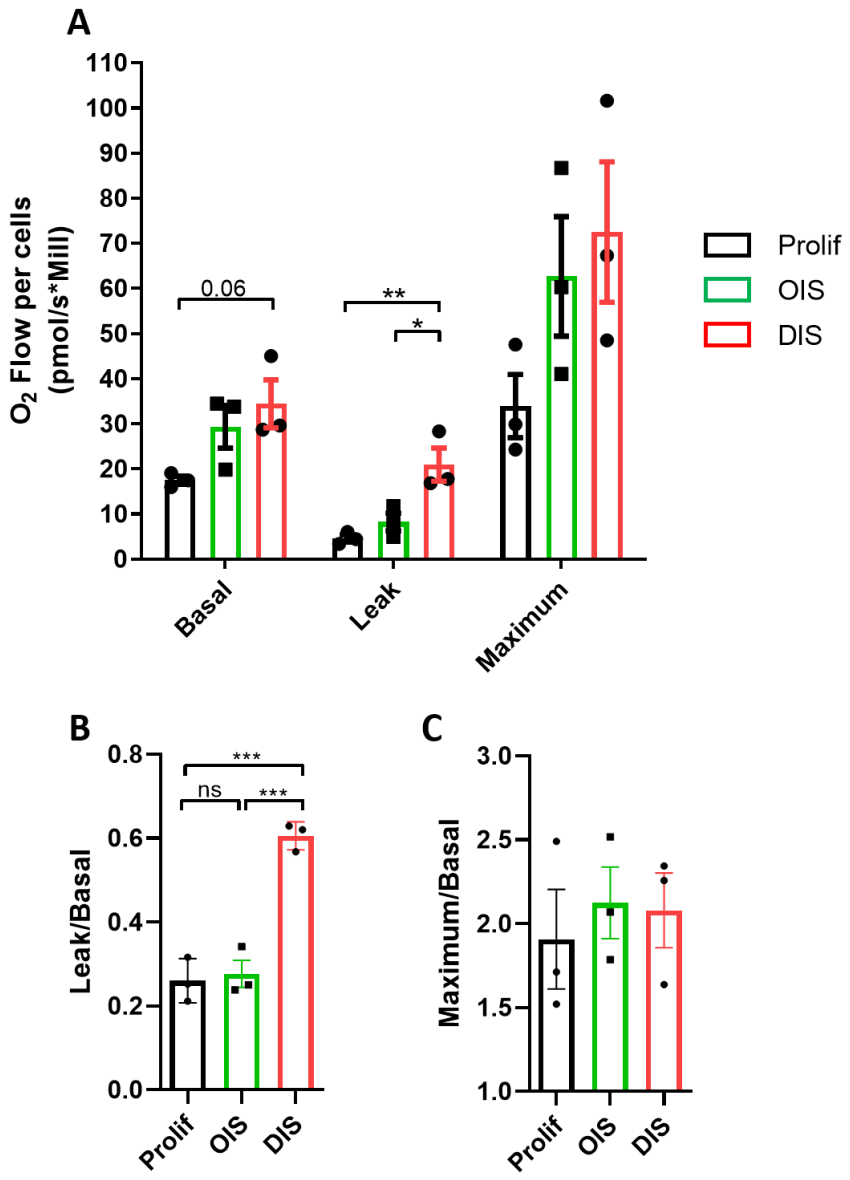

Figure 4.6: Comparative analysis of mitochondrial respiratory function in human embryonic fibroblasts IMR90 induced to OIS and DIS

(A) High resolution respirometry expressed as O_2 Flow in pmoles per second in 1 Million of cells. Basal indicates the basal cellular oxygen consumption, Leak indicates the non-phosphorylating respiration upon addition of oligomycin/inhibition of ATP synthase, Maximum indicates the FCCP uncoupled respiration. For all measurement, residual oxygen consumption, the remaining respiration upon addition of antimycin and rotenone, was subtracted. N=3 independent replicates/flasks of 1 million cells each. Basal respiration analysed using 1-way ANOVA Tukey's multiple comparison test: Prolif vs OIS p=0.1881, Prolif vs DIS p=0.0623, OIS vs DIS p=0.6765. Leak respiration analysed using 1-way ANOVA Tukey's multiple comparison test: Prolif vs OIS p=0.5743, Prolif vs DIS p=0.0077, OIS vs DIS p=0.0242. Maximum respiration analysed using 1-way ANOVA Tukey's multiple comparison test: Prolif vs OIS p=0.3042, Prolif vs DIS p=0.1521, OIS vs DIS p=0.8475 **(B)** Leak/Basal ratio, 1-way ANOVA Tukey's multiple comparison test: Prolif vs OIS p=0.9111, Prolif vs DIS p=0.0003, OIS vs DIS p=0.0004 **(C)** Maximum/Basal ratio, 1-way ANOVA Tukey's multiple comparison test: Prolif vs OIS p=0.8149, Prolif vs DIS p=0.8771, OIS vs DIS p=0.9912. Error bars represent SEM.

4.7 Mitochondrial membrane potential is decreased in both models of senescence

Decreased mitochondrial membrane potential has been independently reported to characterise mitochondria of senescent cells in several models of senescence, such as OIS driven by RAS (Moiseeva *et al*., 2009), DIS induced by γ-irradiation (Passos *et al.*, 2010; Studencka *et al.*, 2017; Vizioli *et al.*, 2020) and replicative senescence (Passos *et al*., 2010). Having observed that mitochondrial dysfunction as assessed by HRR is more severe in DIS than OIS, I hypothesised that mitochondrial membrane potential – a feature directly linked to oxidative phosphorylation capacity, as it reflects the proton gradient generated by ETC complexes, as well as to the proton leak which could decrease it – might differ between the two studied models. To test it, I performed live cell imaging upon the staining with tetramethylrhodamine (TMRE), a red cationic dye entering mitochondria with high mitochondrial membrane potential and nonyl acridine orange (NAO) – a green fluorescent dye whose staining is potential-independent. Confirming the previous findings, senescent cells both in OIS and DIS contained more depolarised mitochondria than non-senescent counterparts. No significant difference was observed, however, between OIS and DIS (Figure 4.7 A and B). Due to a low number of cells analysed in this experiment, the utilised method was not sensitive enough to detect differences between the studied systems. A larger scale experiment would need to be conducted in order to reveal a potential difference.

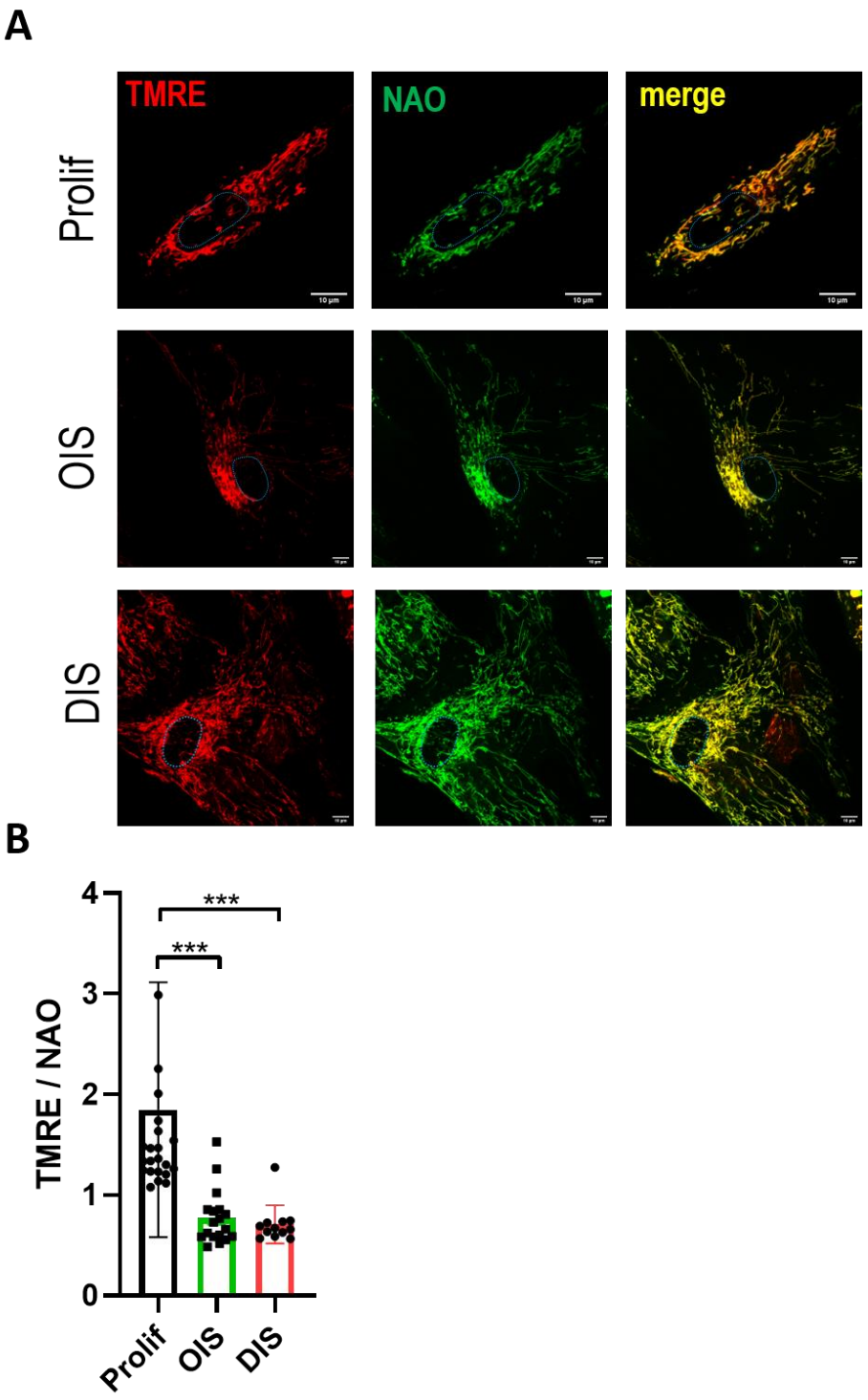

Figure 4.7: Comparative analysis of mitochondrial membrane potential in human embryonic fibroblasts IMR90 induced to OIS and DIS

(A) Representative confocal microscopy images of dual stained cells with TMRE and NAO dyes, nuclei marked with dashed line **(B)** Quantification of TMRE:NAO ratio, n=min 12 cells, 1 glass-bottom dish after conditions optimisation. Analysed using 1-way ANOVA Tukey's multiple comparison test: Prolif vs OIS p=0.0006, Prolif vs DIS p=0.0014, OIS vs DIS p=0.9791. Scale bars represent SD.

4.8 Mitochondrial network is fragmented and dynamic in OIS while hyper-fused and rigid in DIS

Mitochondrial network structure indicates cellular health status. In non-stressed conditions, mitochondrial network maintains an equilibrium of fusion and fission (Berman *et al.*, 2008). A stressor may, however, push fission or fusion processes into one direction, leading to a network's fragmentation or elongation. Thus far, cellular senescence - studied in its damage-induced, mitochondrial dysfunction-induced or replicative variants, was linked to a mitochondrial network elongation (Dalle Pezze *et al.*, 2014; Jendrach *et al.*, 2005; Mai *et al.*, 2010; Yoon *et al.*, 2006). This phenotype is seen as an adaptation to mitochondrial dysfunction. A similar elongated phenotype is observed upon various other cellular stresses that are not acute and powerful enough to induce fragmentation and death (Tondera *et al*., 2009). My data that indicate mitochondrial biogenesis might be still ongoing in OIS at 10 days post senescence induction - in contrast to DIS (Vizioli *et al*., 2019), as well as mitochondrial dysfunction being more advanced in DIS (as measured by mitochondrial bioenergetics and mitochondrial apoptotic stress) led me to ask whether these differences are reflected by the status of mitochondrial network across the studied models.

I performed an analysis of mitochondrial morphology in OIS and DIS by manually assigning a score reflecting the network's status in each analysed cell. Through this, I was able to quantify the number of cells with fragmented, mixed or elongated networks in all studied conditions. The main time-point of interest was 10 days post senescence induction, as the majority of other assays were conducted at the same time. However, in order to exclude the possibility that cells in OIS at 10 days post senescence induction are actually in a less advanced phase of senescence development (considering their cell cycle arrest takes place only after the hyperproliferation phase, *i.e.* 5 days after the onset of the treatment with 4-OHT), I decided to analyse the kinetics of mitochondrial network changes for both models, including a later time-point, 13 days post senescence induction, for OIS. Representative phenotypes of each conditions are presented in Figure 4.8. The quantitative analysis revealed that only a minority of cells in OIS possess hyperfused mitochondria (Figure 4.9 A and B), unlike the cells in DIS that around 5 days post senescence induction, consistently acquire an elongated morphology (Figure 4.10 A and B). Interestingly, according to this analysis (Figure 4.9 B), cells in OIS possess even more fragmented networks than proliferating controls. This striking difference in mitochondrial morphology is associated with differences in mitochondrial dynamics. By conducting live-cell imaging of control and senescent cells, in which mitochondria were visualised using CellLight™ Mitochondria-RFP system, I collected preliminary evidence that

the events of fusion and fission are more frequent in OIS than DIS, and mitochondrial remodelling processes occur in a more diverse and rapid manner in OIS than DIS (Figure 4.11). As depicted in Figure 4.11, in DIS, elongated mitochondria divide and fuse, only minutely changing the structure of the mitochondrial network, while in OIS, fast and long-distanced movement of mitochondria is observed.

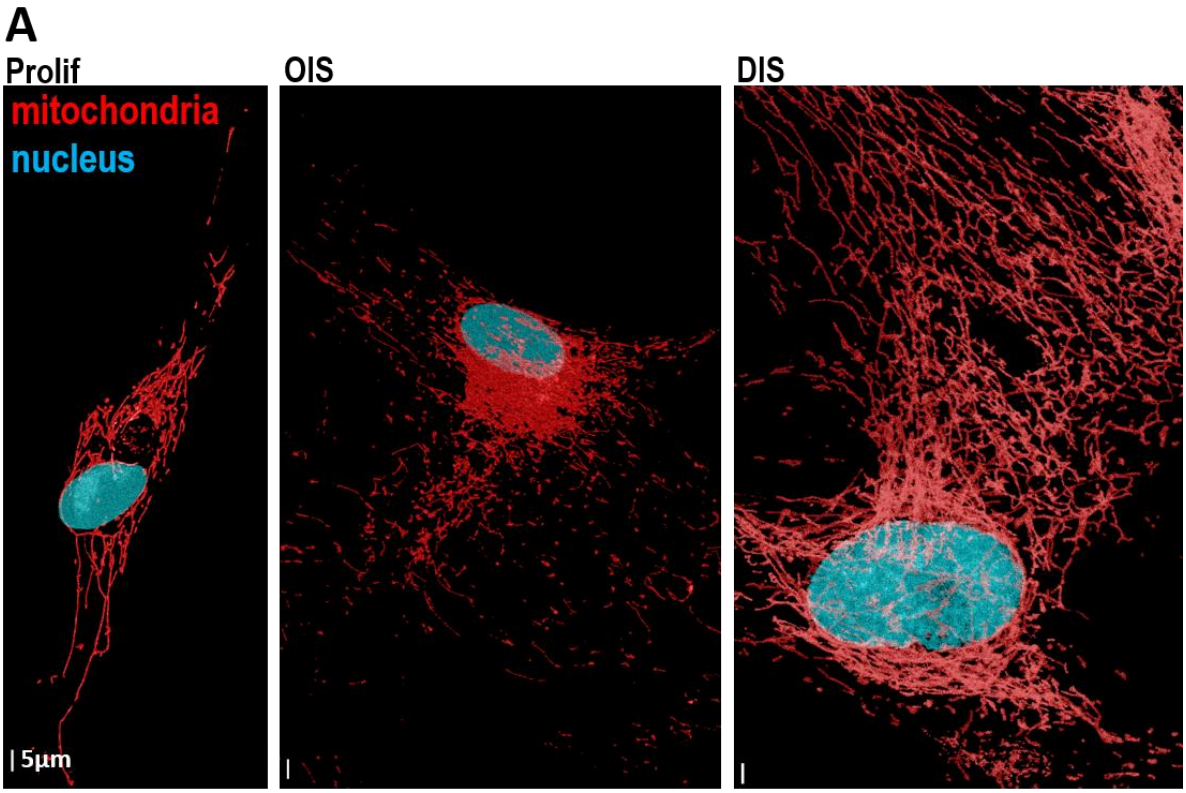

Figure 4.8: Comparative analysis of mitochondrial network structure in human embryonic fibroblasts IMR90 induced to OIS and DIS

(A) Representative confocal microscopy images of mitochondrial networks visualised using CellLight™ Mitochondria-RFP system. Scale bars represent 5µm.

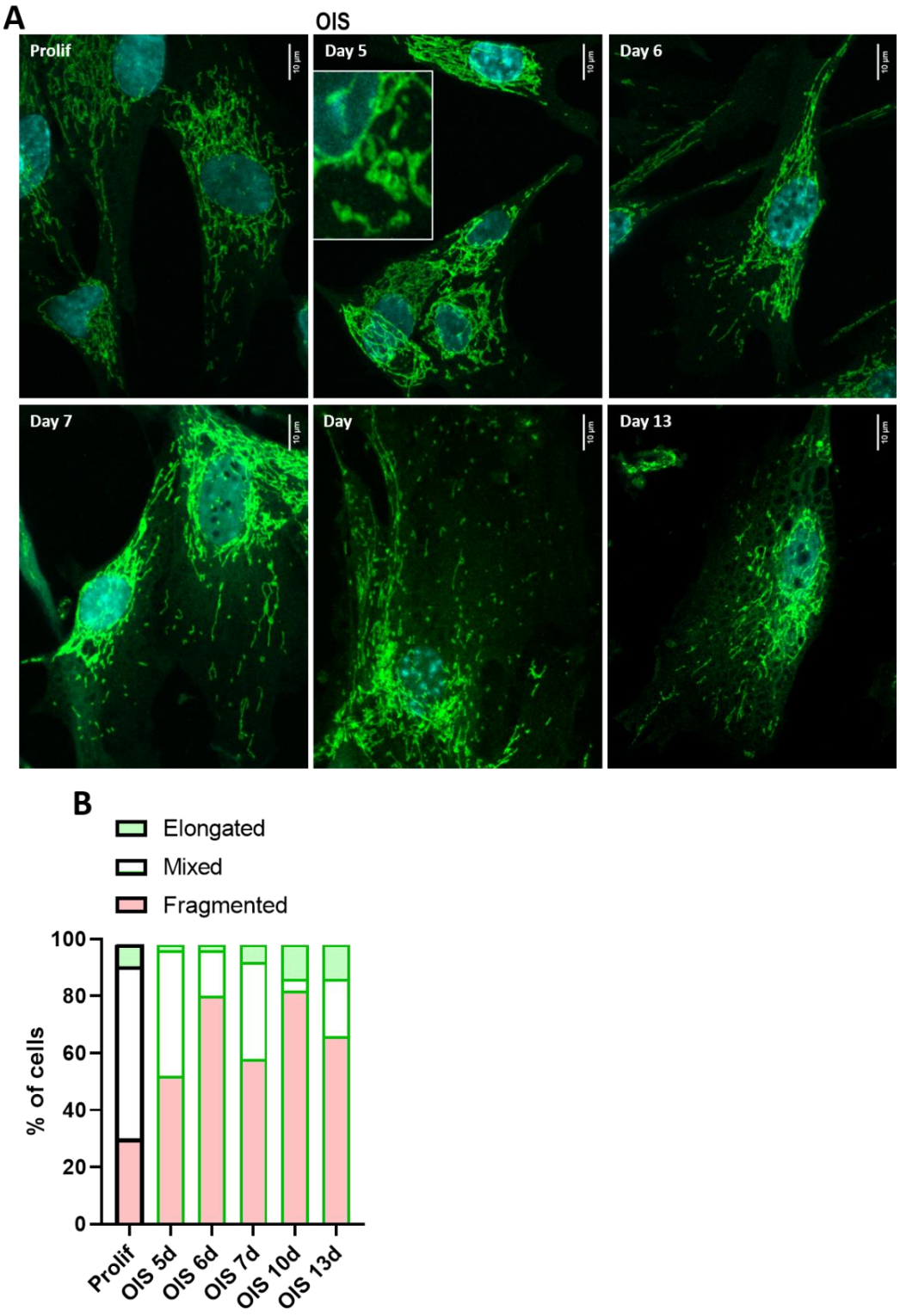

Figure 4.9: Analysis of mitochondrial network structure in human embryonic fibroblasts IMR90 induced to OIS

(A) Representative confocal microscopy images of mitochondrial networks stained using an anti-TOMM20 antibody, nuclei visualised using DAPI. Scale bars represent 10µm. **(B)** Quantification of mitochondrial network structure during the course of oncogene-induced senescence development based on the staining represented in A. N=20 cells/time point. Experiment was independently reproduced 3 times.

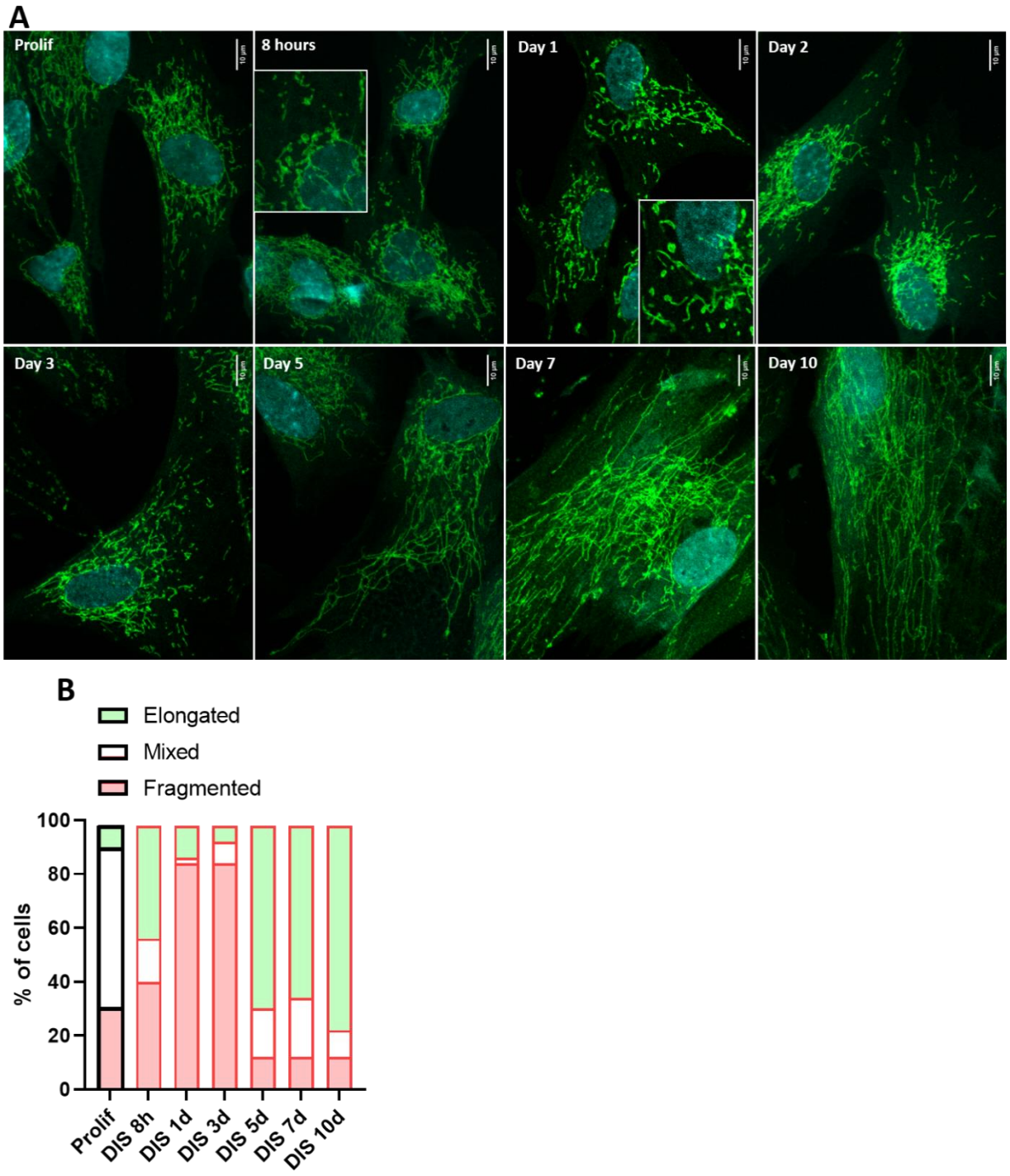

Figure Figure 4.10: Analysis of mitochondrial network structure in human embryonic fibroblasts IMR90 induced to DIS

(A) Representative confocal microscopy images of mitochondrial networks using anti-TOMM20 antibody, nuclei visualised using DAPI. Scale bars represent 10 μm. **(B)** Quantification of mitochondrial network structure during the course of damage-induced senescence development based on the staining represented in A. N=20 cells/time point. Experiment was independently reproduced 3 times.

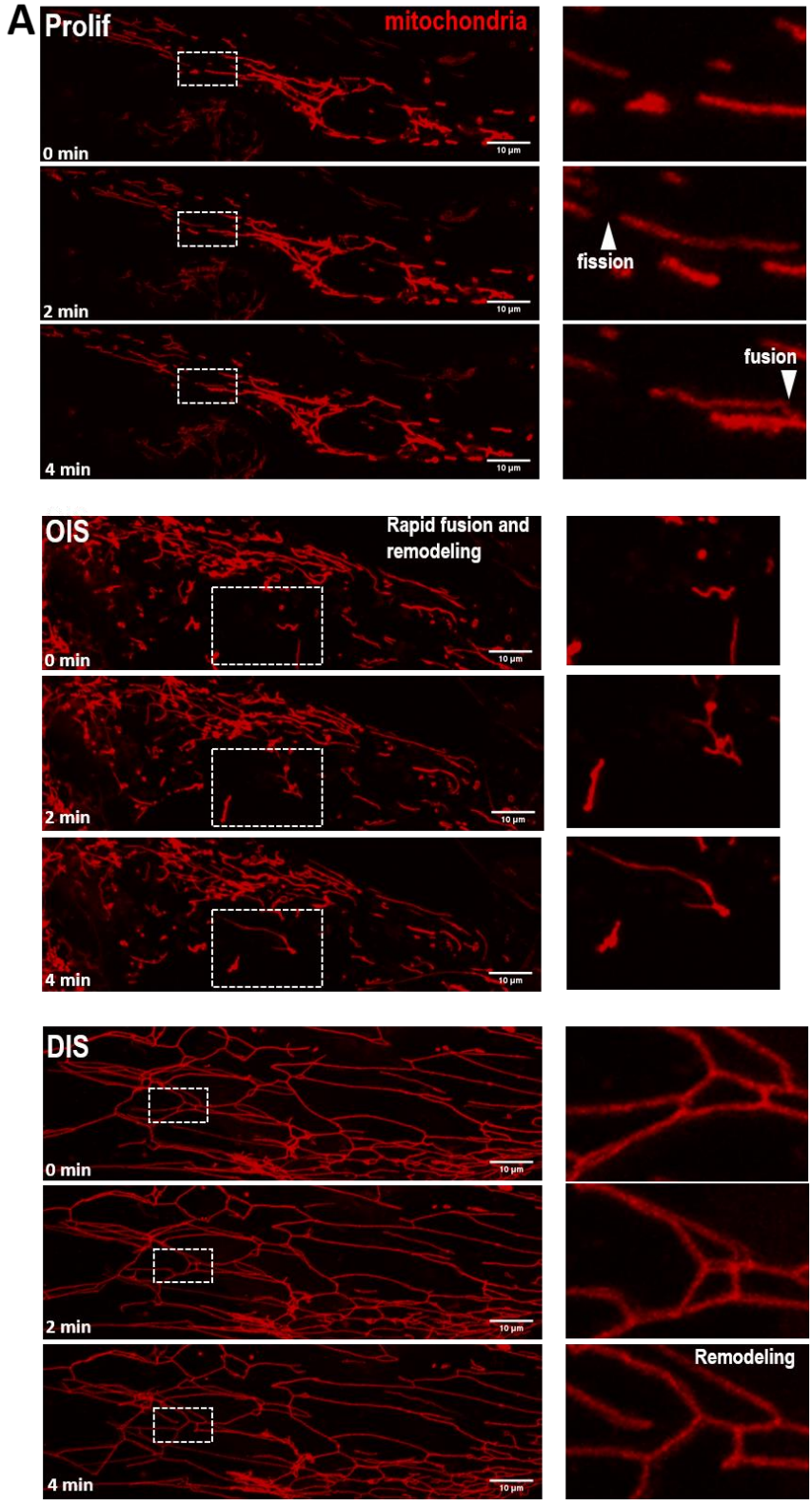

Figure 4.11: Comparative analysis of mitochondrial dynamics in human embryonic fibroblasts IMR90 induced to OIS and DIS

(A) Representative sequences of confocal live-cell images demonstrating the remodelling of mitochondrial networks. Mitochondria visualised using CellLight™ Mitochondria-RFP system.

4.9 Alterations to mitochondrial dynamics factors do not explain the observed differences in terms of mitochondrial network structure

Having observed a novel feature of mitochondria in OIS – their fragmented morphology - that stands in clear contrast with elongated mitochondrial network state in DIS, I set out to analyse the key factors involved in mediating mitochondrial dynamics that might explain the observed difference. First, I considered the possibility that the active RAS signalling in OIS might be directly linked to mitochondrial network status. It was shown that ERK activation – which lies downstream from RAS signalling pathway – in certain conditions, such as reprogramming of induced pluripotent stem cells (Prieto *et al.*, 2016) and tumorigenesis (Kashatus *et al.*, 2015; Serasinghe *et al.*, 2015), mediates phosphorylation of DRP1 at serine 616 (S616) constituting an activating modification. In fact, this process was shown to be necessary for RAS-induced transformation into cancer (Serasinghe *et al.*, 2015). I set out to assess the levels of ERK activation as well as the levels of activating signal in the form of S616 on the fission mediator, DRP1, in OIS and DIS. As expected, the levels of phosphorylated ERK1/2 were higher in OIS than in proliferating controls and DIS (Figure 4.12 A and C), however the difference was not statistically significant. According to the hypothesis, the levels of p-DRP1 in OIS were elevated when compared to non-senescent counterparts (Figure 4.12 B and D). In contrast to the expectations, the levels of p-DRP1 in DIS were even higher than in OIS (Figure 4.12 B and D). This dataset is consistent with previously published literature concerning RAS activation models (Serasinghe *et al*., 2015), however the strikingly elevated levels of p-DRP1 in DIS model do not explain the elongated mitochondrial morphology.

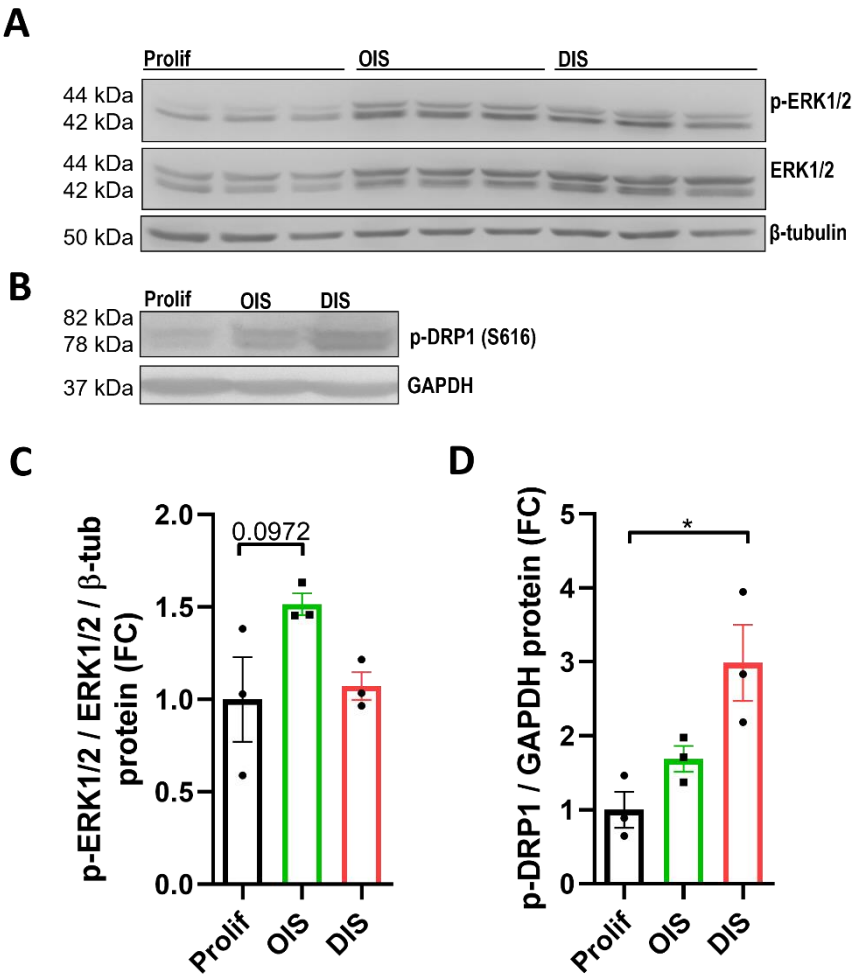

Figure 4.12: Comparative analysis of mediators of mitochondrial dynamics in human embryonic fibroblasts IMR90 induced to OIS and DIS

(A) p-ERK1/2 and ERK1/2 protein levels via western blot, n=3 independent replicates/wells **(B)** Representative western blot of p-DRP1(616) levels, n=3 independent replicates/wells **(C)** Quantification of P-ERK1/2 levels normalised to ERK1/2 and β-tubulin, n=3 independent replicates/wells, 1-way ANOVA Tukey's multiple comparison test: Prolif vs OIS p=0.0972, Prolif vs DIS p=0.9331, OIS vs DIS p=0.1532 **(D)** Quantification of p-DRP1 levels normalised to GAPDH, n=3 independent replicates/wells, 1-way ANOVA Tukey's multiple comparison test: Prolif vs OIS p=0.3913, Prolif vs DIS p=0.0151, OIS vs DIS p=0.0817. Error bars represent SEM.

In the following step, I performed a western blot analysis of the total levels of DRP1 as well as other key players mediating mitochondrial dynamics. The levels of total DRP1 were significantly elevated in both studied models of senescence (Figure 4.13 A and B). The levels of mitochondrial elongation factor, mitofusin 2 (MFN2) did not differ between any studied conditions significantly, however a trend for an increase was observed in the case of DIS (Figure 4.13 A and C). Mitochondrial recruiter of DRP1, FIS1, was previously shown to play a role in cellular senescence, specifically, FIS1 down-regulation was associated with the elongation of mitochondrial network in different senescence settings, *i.e.* an uncommon model of deferoxamine (DFO)-induced senescence in cells of unclear background (Yoon *et al*., 2006) and in γ-irradiation-induced senescence in epithelial cells (Mai *et al*., 2010). In the models of OIS and DIS on fibroblast background, however, no adequate change was observed (Figure 4.13 D and E). In contrast, the fusion mediator, OPA1, was found to be downregulated in DIS comparing to other studied conditions (Figure 4.13 D and F).

Collectively, even though the expected increase in activated ERK1/2 and p-DRP1 was observed in OIS when compared to proliferating controls and might explain why this model of senescence is associated with fragmented mitochondrial network, the opposite was not true for DIS, a senescence model associated with an elongated mitochondrial network. Despite the abundance of mitochondrial fission machinery in DIS, other processes must be responsible for the hyper-fusion of the mitochondrial network.

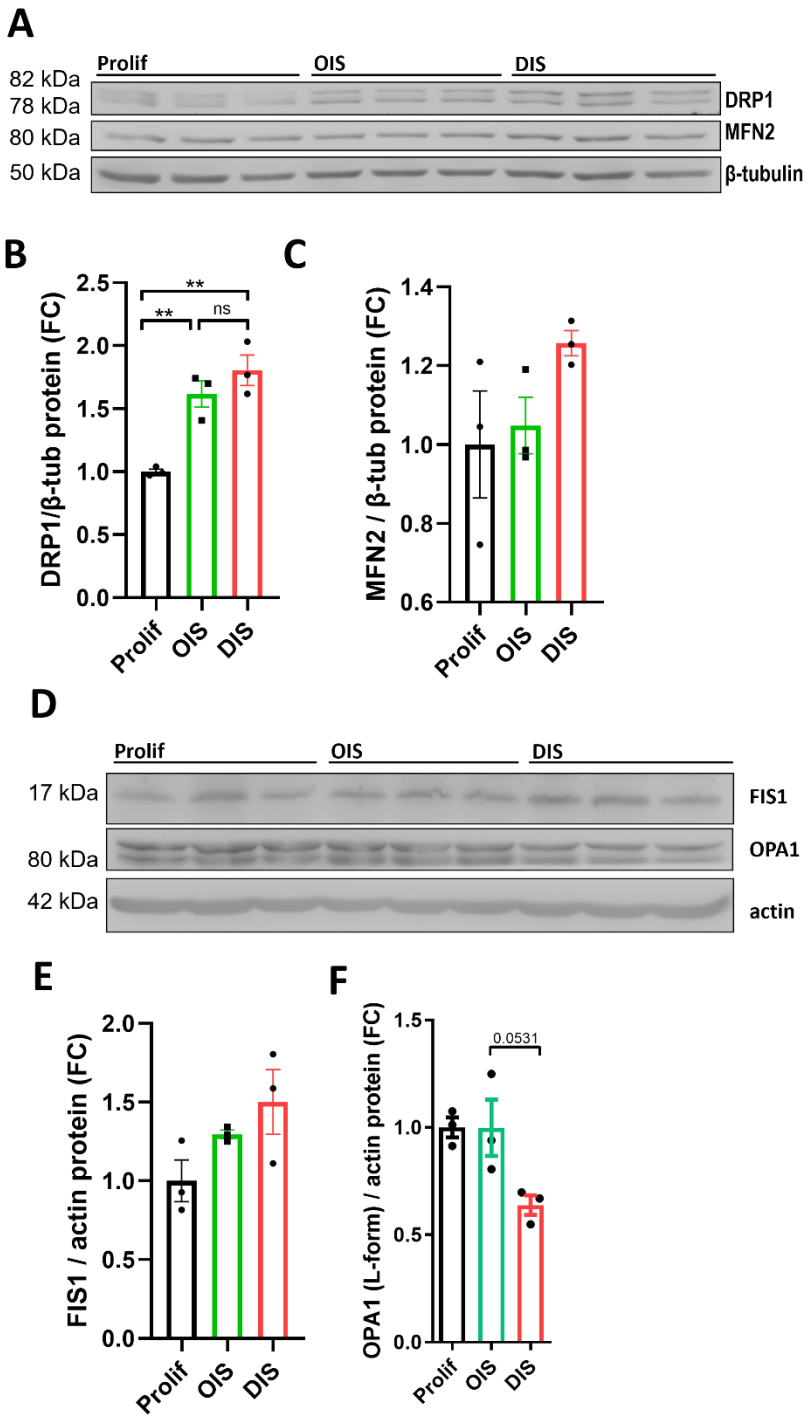

Figure 4.13: Comparative analysis of mediators of mitochondrial dynamics in human embryonic fibroblasts IMR90 induced to OIS and DIS

(A) DRP-1 and MFN2 protein levels via western blot, n=3 independent replicates/wells (**B)** Quantification of DRP1 levels normalised to β-tubulin, n=3 independent replicates/wells, 1-way ANOVA Tukey's multiple comparison test: Prolif vs OIS p=0.0081, Prolif vs DIS p=0.0151, OIS vs DIS p=0.0817 **(C)** Quantification of MFN2 levels normalised to β-tubulin, n=3 independent replicates/wells, 1-way ANOVA Tukey's multiple comparison test: Prolif vs OIS p=0.9267, Prolif vs DIS p=0.1915, OIS vs DIS p=0.3040 **(D)** Representative western blot of FIS1 and OPA1 levels, n=3 independent replicates/wells **(E)** Quantification of FIS1 levels normalised to actin, n=3 independent replicates/wells, 1-way ANOVA Tukey's multiple comparison test: Prolif vs OIS p=0.3660, Prolif vs

DIS p=0.1019, OIS vs DIS p=0.5887, **(F)** Quantification of L-form of OPA1 normalised to actin, n=3 independent replicates/wells, 1-way ANOVA Tukey's multiple comparison test: Prolif vs OIS p=0.9999, Prolif vs DIS p=0.0531, OIS vs DIS p=0.0541. Error bars represent SEM.

4.10 DRP1 knock-down leads to significantly elevated SASP in both OIS and DIS

Having observed the striking differences in mitochondrial network structure in the two most commonly studied systems of cellular senescence, OIS and DIS, I decided to address the question whether mitochondrial morphology is mechanistically linked to SASP. Mitochondria were shown to be key regulators of SASP in the model of DIS (Correia Melo *et al*., 2016, Vizioli *et al*., 2019), however, the same questions was not studied in the context of OIS. In this set of experiments, I hypothesised that silencing mitochondrial fission factor, DRP1, expected to induce mitochondrial fusion, would decrease the SASP in OIS by inducing a similar phenotype in terms of mitochondrial morphology as in DIS. On the other hand, I hypothesised that silencing MFN2 that drives mitochondrial fragmentation, might increase the SASP in DIS by making it resemble OIS in terms of the mitochondrial network.

I performed an siRNA-mediated knock-down of DRP1, using a pool of 4 siRNA sequences. Proliferating cells were collected 5 days after the transfection with siRNA. Both types of senescence were induced 5 days after the transfection and collected 8 days post senescence induction. Knock-down efficiency is demonstrated at 5 days' time-point via western blotting in Figure 4.14 A. An effect of mitochondrial network elongation is also visible basing on CLSM images, where the anti-TOMM20 antibody marks the mitochondria (Figure 4.14 B). Mitochondrial network was severely affected in all conditions (Figure 4.14 B). Mitochondrial network in OIS became denser and more clustered. In DIS, alongside elongated strings (which generally characterize this type of senescence), severe mitochondrial swelling appeared with a degree of mitochondrial fragmentation and formation of circular structures (Figure 4.14 B). Figure 4.14 B contains only representative images, however the phenotype was reproduced in 3 independent experiments. Next, I performed a qPCR analysis of SASP factors expression, IL6 and IL8. DRP1 knock-down led to a very robust exacerbation of IL6 and IL8 expression in all studied conditions, including proliferating cells (Figure 4.15 A and B).

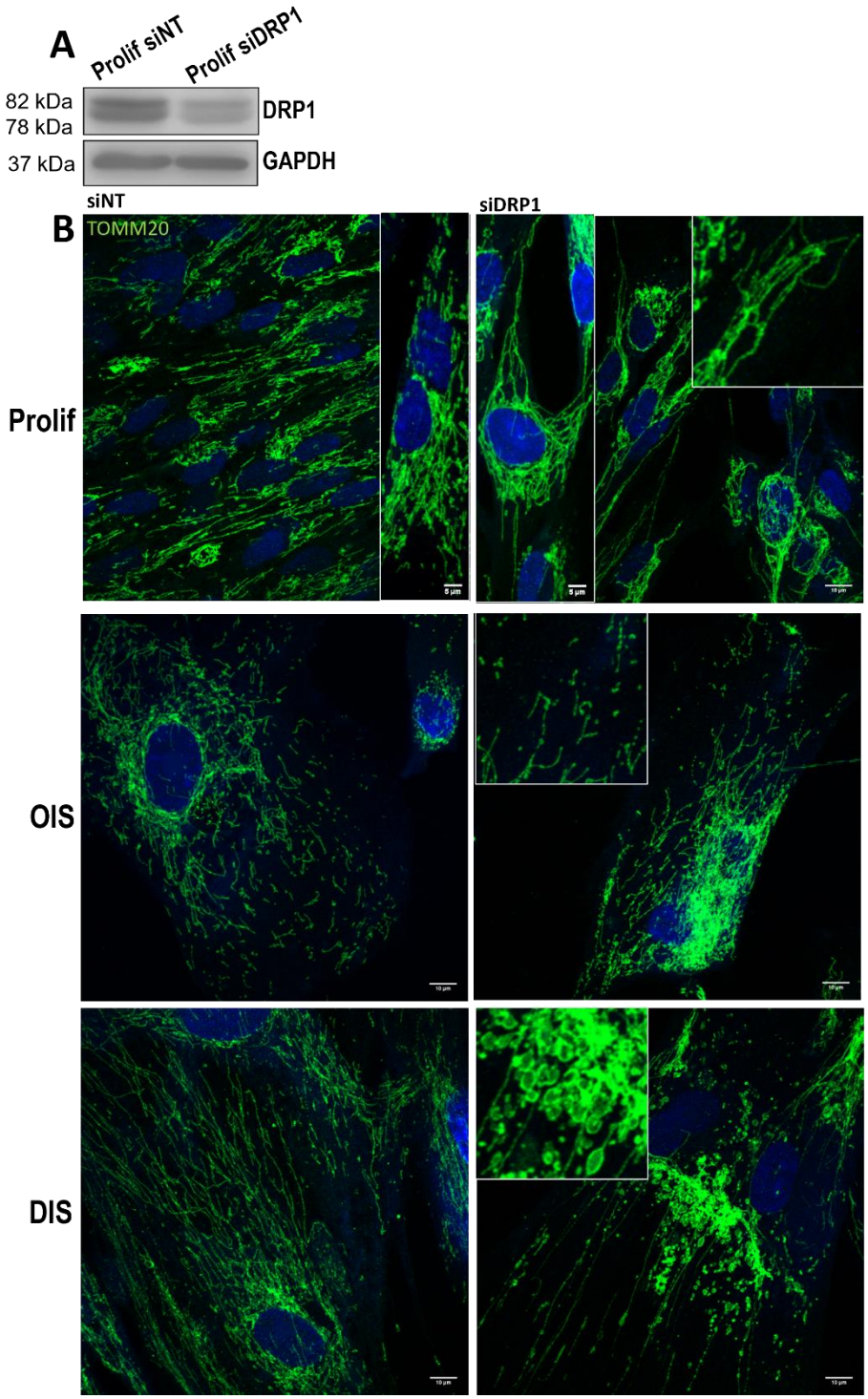

Figure 4.14: Effects of DRP1 knock-down on mitochondrial network in human embryonic fibroblasts IMR90 induced to OIS and DIS

(A) Western blot demonstrating the efficiency of DRP1 knock-down 5 days after transfection **(B)** Representative confocal microscopy images of mitochondrial network stained using anti-TOMM20 antibody in proliferating cells, OIS and DIS upon DRP1 knock-down. Scale bars 10µm.

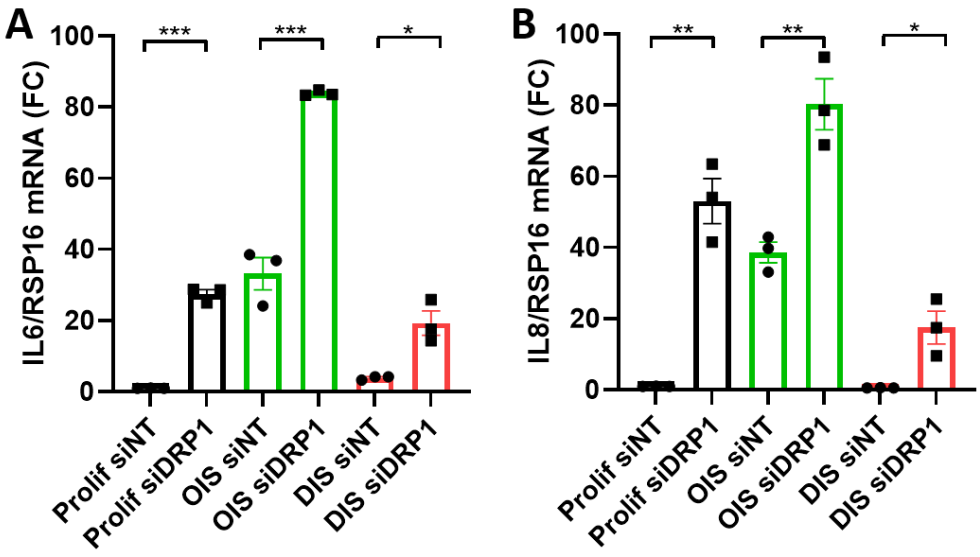

Figure 4.15: Effects of DRP1 knock-down on SASP in human embryonic fibroblasts IMR90 induced to OIS and DIS

(A) IL6 mRNA levels via qPCR normalised to RSP16 using Delta-Delta method. For Prolif, samples were collected 5 days post knock-down. For OIS and DIS, senescence was induced 3 days post knock-down, samples were collected 8 days post senescence induction. N=3 independent replicates/wells, Student's t-test: Prolif siNT vs Prolif siDRP1 $p<0.0001$, OIS siNR vs OIS siDRP1 $p=0.0004$, DIS siNT vs DIS siDRP1 $p=0.0108$ **(B)** IL8 mRNA levels via qPCR normalised to RSP16 using Delta-Delta method. For Prolif, samples were collected 5 days post knock-down. For OIS and DIS, senescence was induced 3 days post knock-down, samples were collected 8 days post senescence induction. N=3 independent replicates/wells, Student's t-test: Prolif siNT vs Prolif siDRP1 $p=0.0012$, OIS siNT vs OIS siDRP1 $p=0.0057$, DIS siNT vs DIS siDRP1 $p=0.0213$. Error bars represent SEM.

4.11 MFN2 knock-down ameliorates SASP in DIS and exacerbated it in OIS

Finally, I performed an siRNA-mediated knock-down of MFN2. The efficiency of the knock-down at the protein level is presented in Figure 4.16 A. Mitochondrial phenotype of network fragmentation was evident in all conditions with the notion that cells in OIS in majority contain already fragmented networks (Figure 4.16 B). The effects upon the expression of IL6 and IL8 differed depending on the conditions. MFN2 knock-down did not elevate IL6 and IL8 in proliferating cells (Figure 4.16 C and D). In OIS, there was a slight increase in terms of IL6 expression and a stronger and significant increase of IL8 expression (Figure 4.16 C and D). Finally, cells in DIS, whose mitochondrial network did not display as severe abnormalities as in the case of DRP1 depletion (mitochondrial swelling), however, also underwent fragmentation, expressed both IL6 and IL8 at significantly lower lever than DIS transfected with nontargeting siRNA (Figure 4.15 C and D). This experiment suggests that mitochondrial elongation in DIS is required for the SASP.

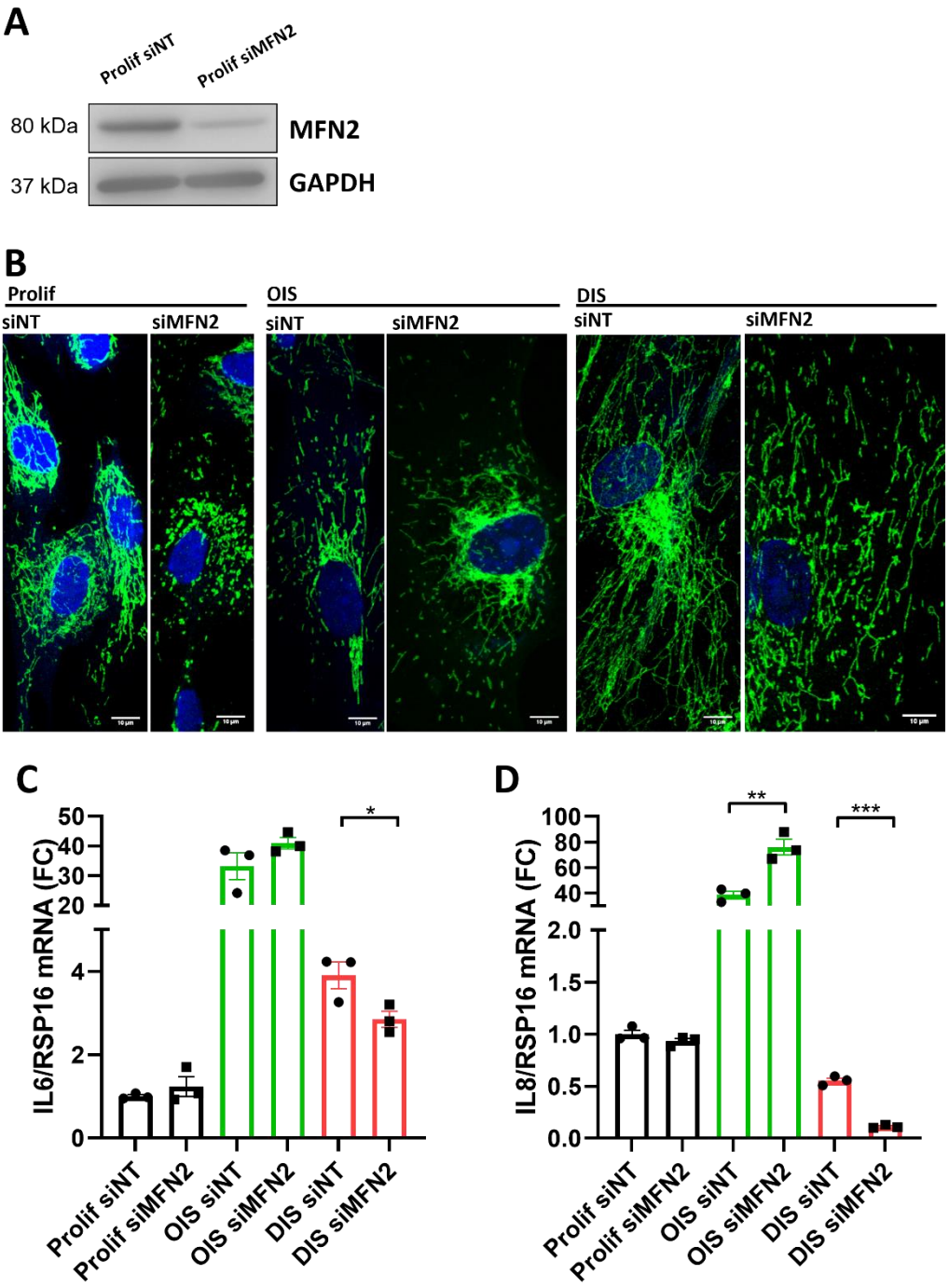

Figure 4.16: Effects of MFN2 knock-down on mitochondrial network and SASP in human embryonic fibroblasts IMR90 induced to OIS and DIS

(A) Western blot demonstrating the efficiency of MFN2 knock-down 5 days after transfection **(B)** Representative confocal microscopy images of mitochondrial network stained using anti-TOMM20 antibody in proliferating cells, OIS and DIS upon the knock-down of MFN2. For Prolif, cells were fixed 5 days post knock-down. For OIS and DIS, senescence was induced 3 days post knock-down, cells were fixed 8 days post senescence induction. Scale bars represent 10µm **(C)** IL6 mRNA levels via qPCR normalised to RSP16 using Delta-Delta method. For Prolif, samples were collected 5 days post knock-down. For OIS and DIS, senescence was induced 3 days post knock-down, samples were collected 8 days post senescence induction. N=3 independent replicates/wells, Student's t-test: Prolif siNT vs Prolif siMFN2 p=0.3876, OIS siNR vs OIS siMFN2 p=1934, DIS siNT vs DIS siMFN2 p=0.0476 **(D)** IL8

mRNA levels via qPCR normalised to RSP16 using Delta-Delta method. For Prolif, samples were collected 5 days post knock-down. For OIS and DIS, senescence was induced 3 days post knock-down, samples were collected 8 days post senescence induction. N=3 independent replicates/wells, Student's t-test: Prolif siNT vs Prolif siMFN2 p=0.2219, OIS siNT vs OIS siMFN2 p=0.0052, DIS siNT vs DIS siMFN2 p<0.0001. Error bars represent SEM.

4.12 Conclusions

The analysis of senescence markers in two most-commonly studied models of cellular senescence, oncogene- and damage-induced senescence, revealed that some aspects of the senescence programme are similar and indistinguishable. These include the expression levels of β-galactosidase, lamin B1, p21, p16 as well as the levels of DDR. In contrast, cells induced to DIS become significantly larger, contain more CCFs and differ in terms of anti-apoptotic regulation when compared to OIS. Moreover, the levels of SASP factors between the two models are critically different, with OIS displaying significantly more powerful SASP. All these encoded within one cell type pushed to enter arguably the same fate. The key novelty that this line of investigation brings is the realisation that the two studied models differ also with regards to the mitochondrial biology.

Cells induced to OIS and DIS were found to contain similar levels of mtDNA measured as mtDNA copy number, however, display significant differences in terms of mitochondrial network size with larger mitochondrial networks characterizing DIS. These data indirectly point out that the concentration of mtDNA within mitochondrial network might be lower in DIS than OIS. Alternatively, the data might indicate the number of mtDNA molecules per nucleoid might be lower in DIS than in OIS. To reach these conclusions, more research is needed, such as the analysis of mtDNA staining intensity when normalised to mitochondrial network size (mitochondrial footprint).

The analysis of mitochondrial biogenesis mediators, PGC-1α and PGC-1β, revealed that cells in DIS express PGC-1α at higher levels than OIS – the difference is not statistically significant when compared to proliferating controls. On the other hand, cells in OIS express 3-times more PGC-1β at mRNA level and approximately 2-times more at the protein level than both proliferating controls and cells in DIS. The differences in mitochondrial network size and biogenesis mediators' expression may seemingly be contradictive. However, according to the literature, mitochondrial biogenesis cessation is to be expected at a later stage of senescence development. Due to mitochondrial dysfunction being of different nature across the two models (*as discussed in section 3.17*), it is possible that at 10 days' time-point, the models are not perfectly matched in terms of the stage of senescence, especially the kinetics of mitochondrial

phenotype. Certainly, however, different mechanisms mediating mitochondrial biogenesis are activated between the models at the studied time-point.

The analysis of mitochondrial respiration of cells in OIS and DIS exposed a more severe mitochondrial dysfunction in cells induced to DIS. Even though both models are characterised by increased Basal respiration, when the Leak respiration is normalised (to Basal), only the cells in DIS display a significantly elevated proton leak. These data suggest the oxidative phosphorylation is less efficient in DIS than in OIS, and, in fact, OIS do not differ from proliferating controls with regards to this measure. Despite the proton leak found in the case of DIS and not OIS, no difference could be detected in terms of mitochondrial membrane potential.

Among the studied mitochondrial processes, the most striking and yet undescribed difference between OIS and DIS concerned the mitochondrial network structure. Cells in OIS acquired a fragmented mitochondrial morphology and maintained the phenotype even beyond the typically studied time-point of 10 days post senescence induction. In contrast, cells in DIS acquired an elongated or hyper-fused phenotype. As a novel finding, I observed the phenotype was acquired not immediately after γ-irradiation, but approximately 5 days later. A preliminary analysis of mitochondrial dynamics additionally pointed out that as opposed to a rigid network of mitochondria in DIS (according to Dalle Pezze *et al*., 2014), mitochondrial in OIS undergo frequent fusion and fission processes.

In my search for an underlying mechanism behind the differences in mitochondrial network structure, I found cells in OIS to possess higher levels of p-ERK1/2 and p-DRP1 than the proliferating controls, which according to the previous reports, might indicate ERK1/2 pathway as a potential mediator of DRP1 pro-fission modification. Unexpectedly, however, cells in DIS were characterised by even higher levels of p-DRP1, as well as similarly to OIS, elevated levels of total DRP1. This finding does not provide a straightforward explanation for the hyper-fused phenotype of mitochondrial network in DIS. Among other mitochondrial dynamics factors, the slight elevation of MFN2 in DIS stands in line with the observed phenotype. Collectively, the simultaneous up-regulation of DRP1 and MFN2 challenges to identify the mechanism responsible for the observed differences in mitochondrial network structure.

Finally, I set out to interfere with mitochondrial networks by silencing DRP1 and independently, MFN2, inducing a hyper-fused or fragmented phenotypes, respectively. I aimed to maintain the mitochondrial phenotypes throughout the process of senescence development in order to analyse their effects upon the SASP. Mitochondrial dysfunction induced by DRP1

knock-down led to high and significant increases in the expression of IL6 and IL8 across all studied conditions. In DIS, where elevated levels of DRP1 and p-DRP1 were observed, mitochondrial network structure was severely affected by DRP1 silencing – mitochondrial network contained swollen mitochondria as well as underwent a degree of fragmentation. This suggests DRP1 is required for the maintenance of mitochondrial network in this model, and the lack of it exacerbates both mitochondrial dysfunction and SASP. On the other hand, MFN2 knock-down ameliorated the SASP in the model of DIS, indicating mitochondrial fusion is needed for the SASP. In the case of OIS, both interventions led to an exacerbated SASP, suggesting mitochondrial dynamics is a key process and its disturbance into any direction is pro-inflammatory. Even though this set of observations provides a rather complex landscape of the relationships between mitochondria and SASP in two studied models, it again points out the two models are fundamentally different, not responding consistently to mitochondrial perturbations.

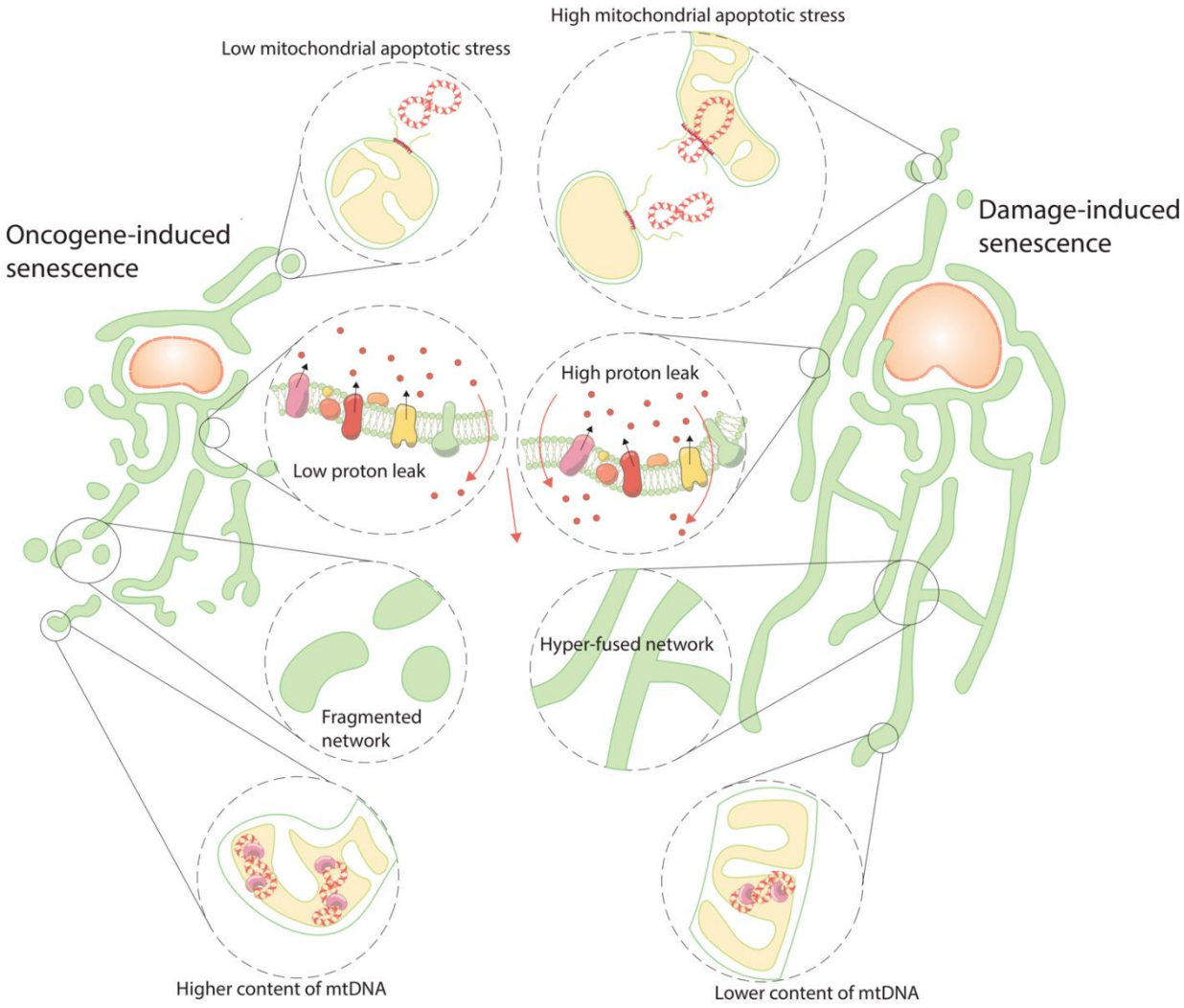

Figure 4.17: A summary of the key differences in mitochondrial biology between oncogene- and damage-induced senescence

DIS is characterised by a higher degree of mitochondrial apoptotic stress than OIS. Respirometry analysis revealed higher proton leak - a measure of OXPHOS system inefficiency, in DIS than in OIS. Mitochondrial network was found to be fragmented in OIS and hyper-fused in DIS. Finally, collected evidence suggests mtDNA content is higher in OIS than in DIS.

4.13 Discussion

While the two most commonly studied models of cellular senescence: oncogene- and damage-induced senescence are often considered to be similar cellular fates, the differences between these models are not surprising, given their very different triggers. The results presented in this chapter revealed several additional differences with regards to mitochondrial biology. The general phenotypes of OIS and DIS overlap in many respects, such as the level of nuclear DNA damage, expression of key cell cycle inhibitors, down-regulation of lamin B1 *etc.*. Among the differences between DIS and OIS, I also observed a differential up-regulation of BCL-2 protein family members, which might be linked to the degree of mitochondrial apoptotic stress characterizing the two studied models (*as shown in Chapter 3*). Further investigations of BCL-2 expression levels and localisation could help to unravel the differences in mitochondrial apoptotic signalling activation. Based on the analyses of mitochondrial morphology and function presented in this chapter, the model of DIS was found to display inefficient oxidative phosphorylation and a hyperfused phenotype of mitochondrial network. In contrast, the model of OIS was not found to suffer from a mitochondrial proton leak and not to acquire a hyper-fused mitochondrial network - in contrast, mitochondrial network in OIS shifts towards fragmentation.

Recently, impaired mitochondrial retrograde signalling was reported for damage-induced senescence (Vizioli *et al*., 2019). At the early stage of senescence development (1 and 3 days after γ-irradiation), gene expression of the mitochondrial biogenesis transcriptional co-activators PGC-1α and PGC-1β, increases. This is associated with increased expression of genes encoding mitochondrial proteins and mitochondrial expansion (Correia-Melo *et al*., 2016). However, the opposite is true when cells reach the established state of cellular senescence - nuclear encoded mitochondrial genes encoding subunits of oxidative phosphorylation complexes become down-regulated (Vizioli *et al*., 2019, transcriptomics data from Correia-Melo *et al*., 2016). This means that despite expanded mitochondrial network, there might be insufficient components to supply mitochondrial biogenesis and maintenance. The two studies together reveal a kinetics of mitochondrial biogenesis in the model of DIS, where initially, it accelerates allowing for mitochondrial expansion (Dalle Pezze *et al*., 2014, Correia-Melo *et al*., 2016) and ceases towards the established state of senescence. At this stage, mitochondria were found to harbour several dysfunctions, such as decreased mitochondrial membrane potential, increased production of mitochondrial ROS, inefficient oxidative phosphorylation (Passos *et al*., 2010, Vizioli *et al*., 2019). Considering that mitophagy might

also be impaired in this model (Dalle Pezze *et al*., 2014, Korolchuk *et al*., 2017), the quality of mitochondria is likely to decrease further due to a lower mitochondrial turn-over.

The same questions have not, however, been addressed for OIS. With regards to mitochondrial retrograde signalling that activates mitochondrial biogenesis, the analysis of mitochondrial biogenesis factors presented in this thesis, indicates that this process is more active in OIS. Even though PGC-1α is not upregulated, PGC-1β is present at levels significantly higher than in proliferating controls and cells in DIS. Moreover, a component of complex III of the ETC, UQCRC2, is not downregulated as shown in the case of DIS at the mRNA level (Vizioli *et al*., 2019). This very basic analysis should be extended by a comparative transcriptomics analysis of the two models. By taking advantage of publicly available data from already published studies, I found some supporting evidence for the statement that OIS is not characterised by an impaired retrograde signalling to the same extent as DIS or at least, at the most commonly studied time-point. For this discussion, I would like to focus on the example of TFAM. TFAM is a key target gene of PGC-1s and a biogenesis mediator, responsible for mtDNA replication and transcription of mitochondrial genes coding for mitochondrial components. In order to compare the levels of this factor between the two models of interest, I checked its expression detected by Affymetrix Human Genome U133 Plus 2.0 Array on IMR90 fibroblasts induced to RAS-driven OIS (Shah et al. 2013, available via Gene Expression Omnibus, NCBI) as well as transcriptomics data from Correia-Melo *et al.* (2016) and Vizioli *et al.* (2019) on MRC5 and IMR90 cells, respectively, induced to DIS. The microarray data on OIS show that TFAM is upregulated 3.5-fold (with p-value of 0.0000147) when compared to non-senescent controls. In support of this finding, Moiseeva *et al.* (2009) also reported a 2.5-fold increase in TFAM at the mRNA level, however at an earlier time-point - 7 days post senescence induction (Moiseeva *et al*., 2009). Based on transcriptomics dataset from Correia-Melo *et al.* (2016) which concerns human embryonic MRC5 fibroblasts induced to DIS, TFAM, was decreased by 2.8-fold in cellular senescence, with a highly significant p-value below 0.0005. These data suggest that, in contrast to DIS, mitochondrial retrograde signalling in OIS is not downregulated at the studied time-point. The difference in TFAM expression levels between OIS and DIS stands in line with my results on the lower abundance of mtDNA within the mitochondrial network in DIS than in OIS. A kinetics experiment assessing mitochondrial biogenesis mediators, mitochondrial mass and mtDNA copy number including later than 10 days' time-points in the case of OIS would be critical to perform in the future. This would allow to make a conclusion whether the sequence of mitochondrial changes in two models of

senescence may be, in fact, similar between the models with differences in kinetics, for example the duration of the two subsequent phases (characterised first by activated and then impaired mitochondrial biogenesis). A direct analysis of mtDNA density using microscopic images of DNA and mitochondria, would also be valuable to make confident conclusions with regards to the number and size of mitochondrial nucleoids.

The results of increased Leak respiration in DIS presented in this thesis, match the existing literature on cellular senescence induced by γ-irradiation as well as replicative senescence (Hutter *et al.*, 2004; Passos *et al.*, 2010). Similar to my data, Hutter and colleagues (2004) first demonstrated that uncoupled respiration (Maximum) is unchanged between the proliferating cells and replicative senescence – indicating that the capacity of oxidative phosphorylation does not differ between the conditions, while the oligomycin-dependent respiration (Leak) is significantly increased for the senescent cells. The same observation was later published for replicative senescence and DIS (Passos *et al*., 2010), as well doxorubicin-induced senescence (Wang *et al*., 2016). With regards to OIS, no report thus far investigated the coupling states in this model, besides the basic measurement of oxygen consumption in the model of BRAFV600E-driven senescence (Kaplon *et al*., 2013). Therefore, my finding of efficient OXPHOS in OIS presents as a novelty. In line are alternative methods assessing mitochondrial function published by others, such as the measurement of increased NAD+/NADH ratio informing on active mitochondrial catabolic pathways in OIS (Kaplon *et al*., 2013) or of the reliance on mitochondrial fatty acid oxidation by cells in OIS (Quijano *et al*., 2012). As to why cells in damage-induced senescence exhibit a proton leak remains an outstanding question. Hutter *et al.* (2004) reported an increase in the protein level of uncoupling protein-2 (UCP-2) in replicatively senescent fibroblasts, however, only when normalised to the cell number and not protein concentration (Hutter *et al*., 2004). Passos *et al.* (2010) also reported an increase in the levels of UCP-2 expression, however, only at 2 days post γ-irradiation. It would be interesting to determine the levels of this and other uncoupling factors across the senescence models in order to determine their role in the partial uncoupling of mitochondrial respiration in DIS. Another question worth addressing in the future concerns the exact mechanism by which a lower supply of mitochondrial constituents – due to impaired retrograde signalling - might contribute to the increased proton leak. Finally, the production of ROS and the resulting, ROS-inflicted damage, should be assessed between the systems to account for it as a potential factor in inducing partial uncoupling in DIS.

The aspects of mitochondrial biology discussed thus far – mitochondrial apoptotic stress, mitochondrial biogenesis and bioenergetic function – indicate the model of OIS potentially suffers from mitochondrial dysfunction to a lesser degree. However, increased ROS production and decreased mitochondrial membrane potential were previously reported in oncogene-induced senescence (Moiseeva *at al.*, 2009). No study, however, performed a comparative analysis of these parameters between OIS and DIS. Potentially, these mitochondrial dysfunctions might also differ in terms of how advanced they are across the models. My analysis of mitochondrial depolarisation indicated no significant difference between OIS and DIS, however, the analysis requires a repetition using a larger number of cells. The variability within proliferating control cells and OIS was higher and might indicate a higher heterogeneity within these cells' populations in terms of mitochondrial membrane potential. Interestingly, the aspect of heterogeneity of mitochondrial membrane potential within replicatively senescent cells has been addressed by Hutter *et al.* (2004). The authors demonstrated that only a sub-population of cells that underwent replicative senescence contained mitochondria with a lower membrane potential. Replicatively senescent cells would be expected to be more heterogenous than cells in DIS - equally treated cells with a high dose of γ-radiation. The question of intercellular heterogeneity in the two models of senescence, OIS and DIS, would constitute as interesting problem for follow-up studies. Moreover, an analysis of intracellular heterogeneity in terms of mitochondrial membrane potential could help to understand whether the active mitochondrial biogenesis, as well as the further discussed aspect of mitochondrial fragmentation in OIS, might contribute to the presence of a sub-population of mitochondria of maintained function, for example higher membrane potential. Interestingly, by utilizing a different mitochondrial dye (JC1, whose emitted fluorescence depends on the membrane potential) in the study by Moiseeva *et al.* (2009), the authors observed that the green fluorescence (indicating low mitochondrial membrane potential) accumulated in the perinuclear region, while peripheral mitochondria remain red (indicating high membrane potential). This might suggest the most dysfunctional mitochondria are found within perinuclear compartment. JC-1 based methodology has been discussed to be more appropriate than rhodamine-based dyes in the context of senescence (Hutter *et al.*, 2004). One limitation of the TMRE/NAO staining presented in this thesis was the need for identification of cells with comparable staining intensity as for the specific microscope settings, indicating the dyes may vary in terms of cellular penetration. Using only one dye (as in the case of JC-1) would be a solution to this potentially biasing problem. In conclusion, even though the data presented here indicate no

difference in mitochondrial membrane potential, the HRR results suggest the difference might exist, therefore a larger scale experiment using TMRE/NAO approach or an alternative method using JC-1 dye should be applied for the final conclusions.

The main finding within this chapter concerns the strikingly contrasting mitochondrial morphologies between the studied models of senescence. Primarily, the reason for network fragmentation is OIS might be a direct result of active RAS – as a component of the MAPK signalling pathway. The effect of constitutively active RAS has been studied in the context of tumorigenic conversion. In order to achieve this outcome and not cellular senescence, an additional oncogene must be introduced, for example, adenovirus early region 1A (E1A) or MYC (Land *et al.*, 1983; Serasinghe *et al.*, 2015). Several articles demonstrated that a robust mitochondrial fragmentation is observed in cells exhibiting active MAPK signalling (Kashatus *et al.*, 2015; Serasinghe *et al.*, 2015). DRP1 was found to be a key factor responsible for mitochondrial fragmentation - a key event in transformation, as a genetic loss or pharmacological inhibition of DRP1 renders cells resistant to transformation and colony formation (Serasinghe *et al*., 2015). Specifically, the DRP1 serine-616 phosphorylation executed by ERK1/2 was identified as a key signal in this context (Kashatus *et al*., 2015). A similar mechanism was identified during induced pluripotent stem (iPS) cells reprogramming, where ERK1/2 is responsible for DRP1 phosphorylation. ERK1/2 activation does not depend on RAS in this context, but occurs via a different mechanism – down-regulation of the MAP kinase phosphatase, dual specificity phosphatase 6 (DUSP6) (Prieto *et al*., 2016). Collectively, a robust evidence demonstrates that DRP1 is a downstream target of MAPK signalling pathway, therefore it likely operates during oncogene-induced senescence driven by RAS. To address the question, I performed a western blot analysis of ERK1/2 as well as its activated version, p-ERK1/2, and p-DRP1 at serine-616 both in OIS and DIS. I expected an increase in both ERK1/2 and DRP1 activation in OIS when compared to proliferating cells and the lack of it in DIS. My data stand in line with the previous reports on MAPK signalling driving mitochondrial fragmentation via p-DRP1. Total levels of ERK1/2 were highly elevated in OIS. This result matches the data presented in Serasinghe *et al.* (2015) who also found it to be increased upon expression of activated RAS. The phosphorylated version of ERK1/2 strongly trended towards an increase in OIS, even when normalised to total ERK1/2 that was increased ($p=0.0972$) (Figure 4.12 A and C). With regards to p-DRP1, 1-way ANOVA Tukey's multiple comparison did not indicate a strong difference between Prolif and OIS due to high variability within DIS. When Prolif and OIS are considered separately, the difference in p-DRP1 levels between Prolif

and in OIS is close to statistical significance (with p=0.0829). These data are in support of MAPK pathway as a potential mediator of the fragmentation phenotype in OIS. In the future, experiments similar to the ones presented in Kashatus *et al.* (2015) would allow to address whether inhibition of the pathway prevents the fragmentation phenotype, for example, pharmacological inhibition of MEK using PD325901. Besides p-DRP1, I also observed an increase in the total DRP1 in OIS. As these two experiments (p-DRP1 and DRP1 western blots) were performed independently, I did not normalize the p-DRP1 to total DRP1 levels – repeating the experiment allowing to normalize p-DRP1 to total DRP1 would be a necessary step in the future. The increase in total DRP1 as well as a trend towards an increase of FIS1 stand in line with the observation of fragmented network in OIS. The levels of a fusion factor, MFN2, were not changed when compared to proliferating controls.

The puzzling result concerned, however, the cells induced to DIS. The general phenotype matched the previous reports, which concordantly find that "senescent cells are typically associated with an overall shift toward more fusion events", which was demonstrated for cells in DIS and replicative senescence on fibroblast and epithelial background (Dalle Pezze *et al.*, 2014; Jendrach *et al.*, 2005; Vasileiou *et al.*, 2019; Ziegler *et al.*, 2015). As a novel observation, I found the cells acquired the elongated phenotypes approximately 5 days post senescence induction. This result matches the kinetics of mitochondrial membrane potential changes demonstrated in the study by Dalle Pezze *et al*. (2014), who showed a gradual decrease from day 5 (Dalle Pezze *et al*., 2014). Presumably, this is also the stage when mitochondrial biogenesis ceases. Among the mechanisms that might mediate the shift towards elongation, I observed a trend for increased levels of MFN2, however, the difference was only slight and not statistically significant. An increase in MFN2 was observed in another model of senescence induced by cigarette smoke exposure, associated with mitochondrial expansion and perinuclear accumulation of mitochondria (Ahmad *et al.*, 2015). With regards to other studies investigating the mechanism of mitochondrial elongation in cellular senescence, reduced expression of DRP1 and FIS1 was reported to be associated with senescence-associated mitochondrial elongation in replicative senescence of epithelial cells (Mai *et al*., 2010). This has not been observed in my experiments using fibroblasts induced to senescence via γ-irradiation. Both factors were up-regulated, with DRP1 reaching statistical significance (p=0.0151) and FIS1 trending (p=0.1019). Moreover, the levels of p-DRP1 were increased significantly when compared to proliferating cells and almost reached the statistical significance (p=0.0817) between OIS and DIS. The levels of p-DRP1 and total DRP1 should be re-tested in a single western blot

experiment, however, basing on the data presented, p-DRP1 seems to be increased in DIS. The results of the simultaneous up-regulation of DRP1 and MFN2 do not allow to equivocally pinpoint the mechanism responsible for mitochondrial hyper-fusion associated with this model of senescence. Generally, the fission machinery is abundant in DIS, but a superior mechanism is probably responsible for the dynamics' shift towards elongation.

In order to consider why the fission machinery might be readily available in the model of DIS despite the phenotype of mitochondrial network hyper-fusion, I would like to recall the result presented in Chapter 3. Namely, I found distinct p-DRP1 foci associated with fragmented mitochondria in the model of DIS, potentially the ones undergoing mitochondrial apoptotic cascade (however, the experiment on the co-localisation of p-DRP1 and activated BAX is missing). This might explain why there might be a need for the fission signal – presumably, to separate severely dysfunctional mitochondrial that are about to engage apoptotic signalling and prevent the spread of the signal across the whole network. If that was true, other inhibitory signals against fission would be required to protect the rest of the network from fragmentation.

A study by Dalle Pezze and colleagues (2014) is one of only several investigating the phenotype of mitochondrial hyper-fusion in cellular senescence (Dalle Pezze *et al*., 2014; Mai *et al*., 2010; Yoon *et al*., 2006). The authors found that the model of DIS, induced by γ-irradiation in human embryonic fibroblasts, MRC5, is characterised by mitochondrial hyper-fusion as well as a decreased rate in the fission and fusion events – similarly to replicatively senescent epithelial (HUVECs) cells (Jendrach *et al*., 2005). The authors did not address the mechanism of the dynamics' shift, however, they considered the consequences of reduced mitochondrial fission and fusion rates, namely the fact that mitochondrial hyper-fusion decreases the available pool of small mitochondria for mitophagy, thereby prevents mitophagy (Dalle Pezze *et al*., 2014). This view is in line with two other studies that addressed the question of mitochondrial hyper-fusion in the context of starvation. There, elongated mitochondria were observed to be spared from degradation and allow for cell survival (Gomes *et al*., 2011; Rambold *et al*., 2011). Here I would like to consider, whether in context of damage-induced cellular senescence, mitochondrial elongation is an anti-autophagic mechanism or might rather be a consequence of impaired autophagy. In the case of OIS, it is generally agreed that autophagy is activated. Specifically, a down-regulation of mTOR 3 days post OIS induction was observed that coincided with autophagy activation that lasted, at least, up to 7 days post senescence induction. Autophagy was found to be required for the provision for nutrients for the massive synthesis of the SASP factors, which additionally may cause endoplasmic

reticulum (ER) stress and an unfolded protein response, managed by autophagy (Young *et al*., 2009; Kwon *et al*., 2011). In the context of OIS, autophagy is considered to promote cellular senescence, as its inhibition was shown to redirect cells to either apoptosis (Huang *et al.*, 2014) or allow for senescence bypass - in the case of OIS driven by BRAF (Liu *et al.*, 2014). On the other hand, in non-senescent conditions, inhibition of autophagy over time induced senescence (Kang *et al*., 2011). The difference results from the type of autophagy that is targeted in these two settings, oncogene-induced autophagy or basal autophagy, respectively. What is the state of autophagy, however, when DIS is induced by other means? In a model of oxidative stress-induced senescence, a dysfunction of autophagy was observed (Tai *et al.*, 2017). The authors observed an impaired autophagy flux with lysosomal dysfunction assessed by degradation of SQSTM1/p62, proportion of the acidic compartment of mRFP-GFP-LC3, as well as the activity of lysosomal proteolytic enzymes (Tai *et al*., 2017). Enhancing or restoring autophagic activity was shown to protect from damage-induced senescence (Dalle Pezze *et al.*, 2014; Han *et al.*, 2016). To my knowledge, no study performed a similar analysis of autophagic function in the model of senescence induced by γ-irradiation. However, it is reasonable to assume autophagic flux in DIS might more closely resemble oxidative-stress induced model rather than OIS. Interestingly, similarly to autophagy induction (for example, by starvation) that is linked to mitochondrial elongation (Gomes *et al*., 2011; Rambold *et al*., 2011), autophagy inhibition also leads to the hyper-fusion phenotype (Navratil *et al.*, 2008). These authors described a formation of giant mitochondria in rat myoblasts upon autophagy inhibition with the use of 3-methyladenine (3MA) that blocks the formation of autophagosomes. Interestingly, these mitochondria were shown to have a low mitochondrial membrane potential and a decreased fusion capacity associated with lower expression of OPA1 (Navratil *et al*., 2008). A similar phenotype was observed in replicatively senescent rat myoblasts. This result stands in line with my finding of decreased levels of OPA1 is DIS (Figure 4.13 D and F). It is not clear whether there is a direct relationship between inhibited autophagy and mitochondrial elongation, or through this intervention, the authors simply induce damage-induced senescence that is associated with mitochondrial elongation. It is possible that there is a direct link - one could speculate that despite the abundance of dynamics machinery, the scarcity of autophagic machinery could signal against fragmentation. If that is not the case, however, the study by Navratil *et al*. (2008) contributes another piece of evidence that highly diverse stressful stimuli may induce senescence, which in the absence of oncogenic signalling, is associate with a mitochondrial shift towards hyper-fusion. It also allows to challenge the view presented in Dalle

Pezze *et al.* (2014) that the hyper-fusion phenotype occurs in order to spare mitochondria from autophagic degradation (as in the case of starvation). Potentially, hyper-fusion might be an adaptation to (a consequence of) "difficult conditions" including autophagic impairment. A decrease in fusion capacity (Dalle Pezze *et al*., 2014; Navratil *et al*., 2008) probably occurs at a later stage, after the elongated network has been formed, however, this question would need to be addressed by a kinetic analysis of mitochondrial dynamics factors, such as OPA1. The authors discuss the possible reasons for the mitochondrial elongation in the contexts of autophagy inhibition and replicative senescence. Interestingly, similarly to my results, the authors observed a lower amount of mtDNA in giant mitochondria than in normal mitochondria (Navratil *et al*., 2008). They assume that if giant mitochondria were formed by fusion of several small mitochondria, that would not be the case, indicating that they are formed by gradual growth of pre-existing mitochondria. It is worthwhile to consider this possibility as an explanation of hyper-fused status of mitochondrial network in DIS, having acquired the new knowledge on the kinetics of mitochondrial biogenesis in senescence (Correia Melo *et al*., 2016). In conclusion, more studies investigating the genesis of hyper-fused mitochondria in cellular senescence and other stress responses are needed.

At the next stage of my work, I set out to evaluate the consequences of mitochondrial network perturbations on the SASP. By inducing mitochondrial fusion through the knock-down of DRP1 and mitochondrial fragmentation by the knock-down of MFN2, I set out to alter the typical mitochondrial phenotypes in the two models of interest and assess how these interventions influenced the expression levels of IL6 and IL8. I observed that DRP1 knock-down robustly enhanced the expression of both cytokines in proliferating cells as well as both models of senescence. In contrast, MFN2 did not affect proliferating cells, enhanced expression of only one of the cytokines (IL8) significantly in OIS, and reduced SASP in DIS. Due to early collection of senescent cells - at 8 days instead of 10 days post senescence induction, the level of IL8 was not yet elevated in the model of DIS. For comparison, SASP levels at 10 days post senescence induction are presented in Figure 4.4 D and E. The decision to collect cells at an earlier time-point resulted from my previous observation that at 8 days post senescence induction, the phenotype of mitochondrial network elongation is already established (Figure 4.10). However, the experiment should be repeated at the time-point of 10 days, when the SASP is "full-blown". It is interesting to juxtapose the finding of MFN2 knock-down effect with the study by Wiley, Velarde *et al.* (2016) on mitochondrial dysfunction-induced cellular senescence (MiDAS). MiDAS induced using several manipulations that compromise mitochondrial

function such as depletion of sirtuin 3 (SIRT3), depletion of mtDNA by continuous treatment with ethidium bromide, interfering with ETC by the treatment with its inhibitors, such as rotenone or antimycin A, was shown to be associated with a distinct SASP lacking IL6 and IL8 expression. Also, cells subjected to γ-irradiation whose mitochondria were simultaneously perturbed (by depletion of SIRT3), did not express these cytokines (Wiley, Velarde *et al*., 2016). The knock-down of MFN2 induced a similar phenotype of senescence with an additional mitochondrial dysfunction, preventing the SASP, at least with regards to the studied cytokines. The full mitochondrial depletion performed by our lab previously (Correia-Melo *et al*., 2016) exerted the same effect of SASP amelioration. This suggests that the formation of giant, elongated mitochondria might be a key process regulating the development of the SASP.

In a striking contrast, the knock-down of DRP1 in DIS led to an even more severe mitochondrial network perturbation – not only in the form of fragmentation but also an extensive swelling, and in some cases, a collapse of the network. Moreover, it significantly exacerbated the SASP. The data suggest that the fission process, even though decreased in frequency in the model of DIS, is of key importance for the network maintenance. Both DRP1 and MFN2 knock-downs in proliferating cells induced evident mitochondrial network alterations, however, only DRP1 changed the inflammatory status. This suggest that a shift towards network fragmentation is generally less "stressful" to the fibroblasts. Primarily, mitochondrial elongation might interfere with cell division, which requires DRP1-mediated fragmentation for an appropriate distribution of mitochondria to the daughter cells; as well as with quality control processes such as mitophagy, contributing to mitochondrial dysfunction. An additional, provocative hypothesis that could help and explain why mitochondrial fragmentation might facilitate mitochondrial health links to my data presented in Chapter 3. I observed increased measures of mitochondrial apoptotic signalling in senescent cells, however interestingly, infrequently the same features were also present in proliferating cells. The percentage of cells with activated BAX on mitochondria within proliferating population was very low, however, the number of apoptotic vesicles that contained activated BAX observed above the cells, even though largely increased in senescent cells, was still noticeable in non-senescent controls. Precisely, it was on average 5 vesicles per cell in proliferating conditions, and up to 20, on average, in DIS (3.17 A and B). This phenomenon is very weakly understood, and more control experiments would be required, especially allowing to exclude the suboptimal culture conditions as a factor affecting the process. Nevertheless, I observed the vesicles in at least 3 independent experiments. Considering these results, it is tempting to speculate that an

apoptotic cascade occurring at a small proportion of mitochondria that undergo fragmentation and are subsequently expelled from the cells in the form of extracellular vesicles, could constitute a cellular quality control process. An analysis of extracellular BAX-positive vesicles upon DRP1 silencing would be necessary to test the hypothesis whether the process of vesicle formation with mitochondrial content is DRP1-dependent.

There is a growing recognition of senescent cells' physiological importance in the diseases of ageing. Senolytics are currently studied in pre-clinical models and in human clinical trials. For these interventions to work efficiently, as well as for trouble-shooting in case of a trial's failure (for example, as in the recent phase II trial of a intra-articular administration of a putative senolytic, UBX0101) (Ellison-Hughes, 2020; Roy *et al.*, 2020), a better understanding of the heterogeneity of senescent cells - its drivers and consequences of various senescence programmes in different tissue contexts, is needed. Importantly, this statement applies to the differences between senescence models but also to the differences between the murine and human systems. The vast majority of review articles describe senescence in a unifying manner, while clearly nuances in mechanisms might cause inconsistent outcomes of senomorphic or senolytic interventions across different organisms. Comparative literature, such as the one by Itahana *et al*. (2004) or research studies with a comparative focus, such as the ones by Nelson *et al.* (2014), might promote this awareness, at the times when shifts from proof of principle studies on mice to humans clinical trials occur in a rapid manner (Hickson *et al.*, 2019). A recent review by Roy *et al.* (2020) listed a number of outstanding questions in the field of senescence, which closely match my own thoughts on this matter, in relation to the findings of this chapter. I will close the discussion by providing a modified list of outstanding questions based on the review article by Roy *et al.* (2020). Firstly, as the science identifies differences between senescence variants, should the definition of senescence be changed accounting for the different triggers leading to different forms of the programme? According to Nelson *et al.* (2014), senescence is not a single unique and unambiguous cell state but rather a collection of related cell states with certain common features, including the irreversible cell cycle arrest and a version of SASP, most often, pro-inflammatory. The authors compare this new view to the case of cell differentiation - "as no single definition of a differentiated cell exist, so there might also be no single definition of a senescent cell" (Nelson *et al.*, 2014). Secondly, how representative are the *in vitro* models of senescence for *in vivo* senescence? For example, is senescence associated mitochondrial hyper-fusion (as observed in the case of DIS and replicative senescence) also true for γ-irradiation induced senescence in tissues (as in Zhu *et al*., 2015),

while oncogene-induced senescence – frequently found in benign lesions or in the tumour neighbourhood (Braig *et al.*, 2005; Michaloglou *et al.*, 2005) – linked to fragmented mitochondrial network? Importantly, are these two settings associated with the striking differences in terms of SASP? Whole body or organ targeted irradiation as well as benign tumours are frequently utilised as *in vivo* senescence models, however, are they similar to senescence induced within various tissues as a function of age in the absence of radiotherapy and tumours – the type of cellular senescence that is responsible for age-related diseases? Finally, when should human tissues and when animal models be used as experimental systems? (Roy *et al.*, 2020) Hopefully, the next decade of research on cellular senescence will bring answers to some of these questions, as well as generate a new, updated version of outstanding problems.

4.14 Study limitations

The major limitation of this project was the use of IMR90ER:RAS fibroblasts to induce both types of cellular senescence. Cells in DIS were induced on the same background as cells in OIS. Initially, this was meant to obtain two senescence models in cells possibly similar to each other in other respects. In the future, a control of non-transduced IMR90 cells should be utilised as a control, equally induced to DIS and OIS and treated with 4-OHT. This would allow to exclude the potential effects of the construct leak (unintentional expression of RAS transgene without the induction by 4-OHT), as well as the potential effects of 4-OHT itself on the studied aspects of cell biology. The utilisation of IMR90 fibroblasts only is also a limitation of the study, as it is impossible to conclude whether the observed differences are true for senescent cells of other backgrounds. Future studies should address mitochondrial biology using a wider variety of cell types.

I provided quantification of GLB1 as well as β-Gal expression via qPCR approach (Figure 4.1 B and C). However, I did not provide quantification of cells positive for Sen-β-Gal staining. This is due to the fact that my proliferating control cells, even though contained meaningfully less staining (Figure 4.1 A), were not absolutely negative in this respect. Less numerous and pronounced Sen-β-Gal crystals can be noticed in proliferating cells (Figure 4.1 A). This is probably an artifact of the staining, related to either incubation time with Sen-β-Gal solution or a slight change in pH. As usually, cells are quantified not in respect to signal intensity but as positive or negative, I decided not to include the analysis.

Data presented in Figure 4.7 were obtained on a limited number of cells. The method's limitation are discussed in section 4.13 Discussion. Data presented in Figure 4.11 were not

analysed quantitatively. A quantitative analysis of mitochondrial fusion/fission rate as well as mitochondrial motility should be analysed in the future. The data presented in the current form should be considered preliminary.

Chapter 5 Results: The role of MxB in regulating mitochondrial function and SASP in damage-induced senescence

5.1 Introduction

Cells upon entering cellular senescence undergo prominent functional and morphological changes. One of the important processes is the release of nuclear chromatin fragments, known as cytosolic chromatin foci (CCFs) (Ivanov *et al*., 2013) that activate cytosolic DNA sensing pathways and mediate the SASP (Dou *et al*., 2017; Gluck *et al*., 2017). Other cellular organelles, including mitochondria, also undergo profound remodelling upon the induction of cellular senescence (*Chapter 4*). Their participation in the regulatory network of SASP has been demonstrated by our lab before (Correia-Melo *et al.*, 2016), pointing out mitochondria as obligatory SASP mediators. The findings of this thesis identify a mechanism that might be the key mitochondrial process driving the SASP, namely the mitochondrial apoptotic stress with the release of mtDNA into the cytoplasm (*Chapter 3*). Apart from these two SASP trigger mechanisms – the formation of CCFs and the release of mtDNA into the cytoplasm – a number of additional innate immunity mechanisms orchestrate SASP. These include the involvement of other damage-associated molecular patterns (DAMPs), such as HMGB1 or acute-phase serum amyloids (A-SAAs), de-repression of retrotransposons, inflammasome activation and even NF-κB signalling pathway itself (Acosta *et al*., 2013, Hari *et al*., 2019, De Cecco *et al*. 2019). These findings point out that the intersection between cellular senescence and innate immunity constitutes a rich source of research directions and will likely advance our understanding of the mechanisms governing the fate of cellular senescence.

In this chapter of my thesis, I directed my focus to the role of myxovirus B resistance protein (MxB) in cellular senescence. Generally, Mx proteins, MxB and myxovirus resistance protein A (MxA), are considered as the first line of defence against viral infections before other mechanisms of the immune system are activated (Steiner *et al.*, 2020). They belong to interferon stimulated genes (ISGs), meaning their expression depends on the interferons, specifically type I and type III of interferons via Janus kinases - signal transducer and activator of transcription (JAK-STAT) signalling pathway (Fackler *et al.*, 2013; Haller *et al.*, 2002; Schneider *et al.*, 2014). In contrast to MxA, however, whose expression is detectable only upon stimulation with exogenous interferon in cell culture conditions, MxB is constitutively expressed, *i.e.* in the absence of the viral invasion (Cao *et al.*, 2020). Mx proteins possess a wide range of ant-iviral activities, where MxA restricts the replication cycle of influenza A virus, tick-borne

thogotovirus, African swine fever virus, hepatitis B and La Crosse virus, while MxB was shown to be involved during human immunodeficiency virus 1 (HIV-1) (Fackler *et al.*, 2013; Goujon *et al.*, 2014; Kane *et al.*, 2013; Liu *et al.*, 2013), herpesviruses (Crameri *et al.*, 2018; Schilling *et al.*, 2018; Staeheli *et al.*, 2018), hepatitis C virus (Yi *et al.*, 2019) and a subset of flaviviruses infections (Buffone *et al.*, 2015; Crameri *et al.*, 2018; Steiner *et al.*, 2020). The mechanisms of their action are diverse, blocking the viral replication cycles at various stages (Steiner *et al*., 2020). MxB is known to reside in the cytoplasm and the nucleus, accumulating, however, at the nuclear pores, restricting the access of the viral genome to the host transcriptional machinery (Cao *et al.*, 2020; Melén *et al.*, 1996). It may be considered an anti-viral guardian of the nucleus, as it was specifically shown to inhibit the nuclear uptake of the HIV-1 virus, however, also the uncoating of viral DNA from the capsid in the case of both HIV-1 and herpesviruses (Crameri *et al*., 2018; Goujon *et al*., 2013; Kane *et al*., 2013; Liu *et al*., 2013). The MxB anti-viral mechanism of action involves binding to the viral capsid via the N-terminal domain and depends on the protein's oligomerisation, occurring via the stalk domain (Buffone *et al*., 2015). The same process is somewhat better understood in the case of MxA, which oligomerisation results in ring-like structures that also constitute inflammasome sensors (Steiner *et al*., 2020). Another important domain in the structure of MxB is the GTPase domain. GTPase domain with the neighbouring bundle signalling elements (BSE) grant MxB a position within dynamin-related family of proteins, similarly to mitochondrial dynamin-related proteins, such as DRP1, mitofusins or OPA1 (Figure 5.1). GTPase domain was shown, however, to be dispensable for the anti-HIV-1 activity (Kane *et al*., 2013). Expression of a dominant negative (GTPase-defective) MxB mutants inhibited nuclear import (King *et al.*, 2004), suggesting MxB is a part of regulatory complexes at the nuclear pores orchestrating cytonuclear trafficking. The same authors demonstrated that MxB depletion induces a cell cycle arrest, pointing out that it plays an important function also in basal conditions (King *et al*., 2004). Finally, there are two isoforms of MxB due to alternative transcription initiation (Melén *et al*., 1996). The N-terminal region containing NLS and responsible for the binding to the viral capsid may be absent, resulting in the short version of MxB (Buffone *et al.*, 2015; Haller *et al.*, 2002).

Recently, MxB was for the first time found to play a house-keeping role in the maintenance of mitochondrial integrity (Cao *et al*., 2020). MxB, previously thought to have cytosolic localisation, was actually found within the mitochondria. MxB knock-down induced features of mitochondrial dysfunction: reduced mitochondrial membrane potential, elevated markers of mitochondrial apoptotic stress, particularly the leakage of mtDNA, as well as a

collapse of mitochondrial structure, in the form of disrupted cristae morphology and robust mitochondrial fragmentation (Cao *et al*., 2020). Considering the role of MxB in regulating mitochondrial apoptotic stress as well as mitochondrial morphology – two features that constituted the subjects of my investigations thus far – I decided to address whether MxB may be involved in a context it has not been studied before, namely during cellular senescence.

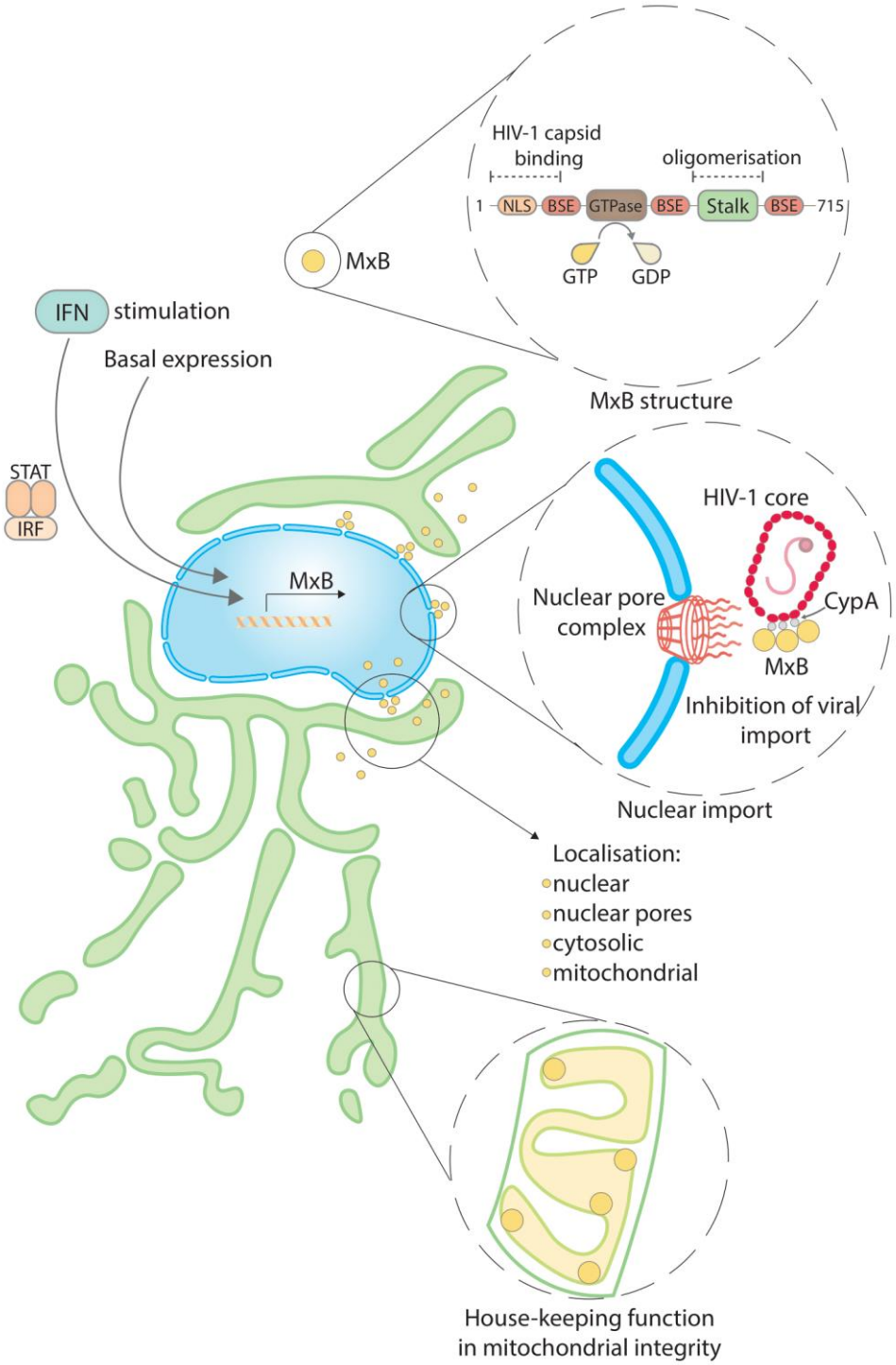

Figure 5.1: The role of MxB as an anti-viral gatekeeper and beyond

The expression of MxB is constitutive, however, may be boosted by interferon (IFN). MxB is localised to 3 sub-cellular compartments, accumulating at the nuclear pore complexes. It is a dynamin-related protein containing nuclear localisation signal (NLS), 3 bundle signalling elements (BSE), GTPase domain and Stalk domain. Among several anti-viral functions, it impedes the nuclear import of human immunodeficiency virus-1 (HIV-1). Binding to HIV-1 occurs via cyclophilin A (CypA). Recently, MxB was found to localise to mitochondria, where it assures the organelle integrity.

5.2 Expression of an anti-viral factor MxB increases in damage-induced senescence and not in oncogene-induced senescence

Based on the recent study showing that MxB regulates mitochondrial function, including mitochondrial apoptotic stress (Cao *et al*., 2020), I set out to determine whether the levels of MxB might change in oncogene- and damage-induced senescence, two models of senescence characterised by different degrees of mitochondrial apoptotic stress (*Chapter 3*) as well as distinct mitochondrial network structures (*Chapter 4*). Considering the observation that MxB depletion leads to mitochondrial apoptotic stress (Cao *et al*., 2020), I hypothesised that MxB might play a protective role in this respect. It is worth noting that mitochondrial apoptotic stress does occur during viral invasions (Brokatzky *et al*., 2019). Is it possible that while performing the anti-viral actions, a subset of MxB proteins is dedicated to translocating to mitochondria and protect them from excessive apoptotic cascade? According to this hypothesis, I expected MxB might be up-regulated in OIS - a model of senescence associated with lower mitochondrial apoptotic signalling, or down-regulated in DIS when compared to proliferating controls.

In order to test this hypothesis, I measured the expression levels of MxB in OIS and DIS. Surprisingly, I found the levels of MxB are significantly elevated only in the model of DIS, at both mRNA (Figure 5.2 A) and protein level (Figure 5.2 B and C). It is worth noting that the higher molecular weight, nuclear isoform is more pronounced than the lower molecular weight isoform (Figure 5.2 C). Having observed the increased levels of MxB in DIS, I asked when during the course of senescence development, MxB becomes up-regulated: immediately upon γ-irradiation or in the established senescence only. The time-course analysis of MxB expression via western blot revealed its expression gradually increases, reaching the highest levels at the 10 days' time-point post irradiation (Figure 5.2 D), also when the SASP factors are known to be at the highest levels in the model of DIS.

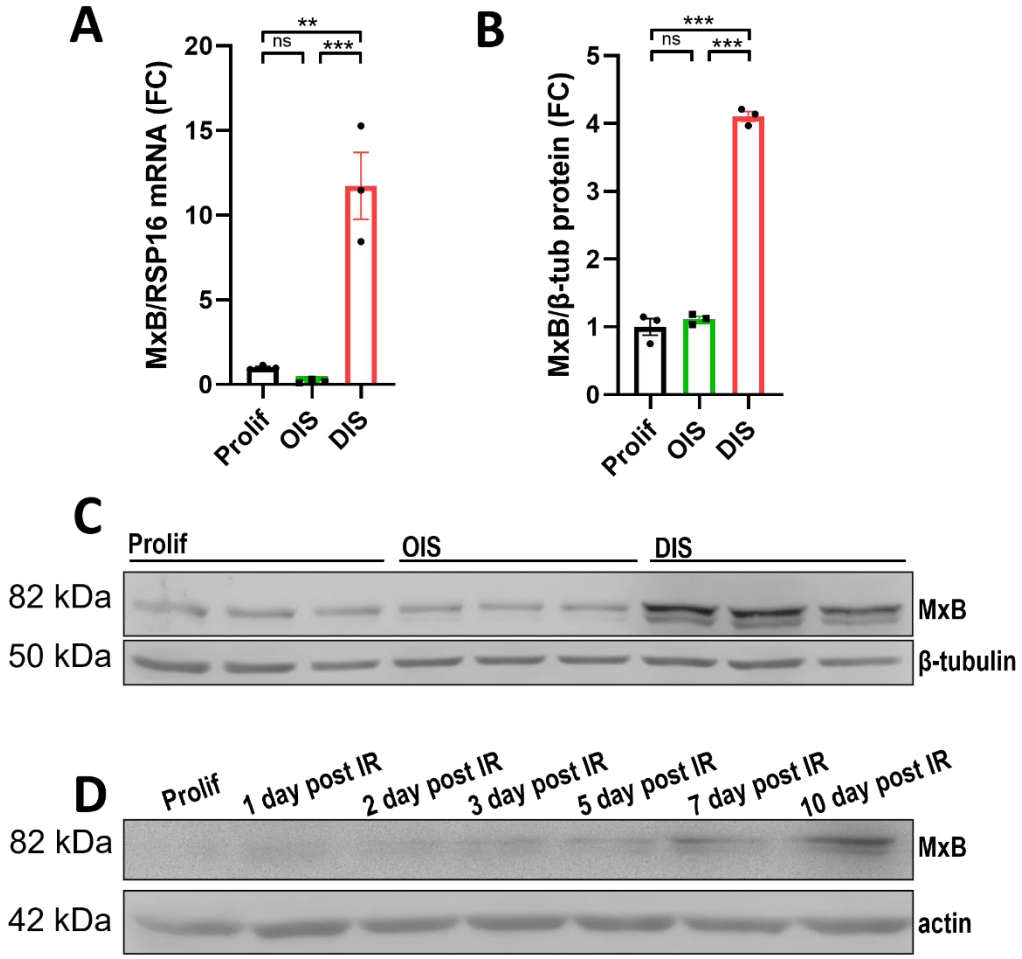

Figure 5.2: MxB expression in OIS and DIS

(A) MxB mRNA levels via qPCR normalised to RSP16 using Delta-Delta Ct method n=3 independent replicates/wells, 1-way ANOVA Tukey's multiple comparison test: Prolif vs OIS p=0.8736, Prolif vs DIS p=0.0014, OIS vs DIS p=0.0009 **(B)** Quantification of MxB protein levels normalised to β-tubulin, n=3 independent replicates/wells, 1-way ANOVA Tukey's multiple comparison test: Prolif vs OIS p=0.6418, Prolif vs DIS p<0.0001, OIS vs DIS p<0.0001 **(C)** MxB protein levels via western blot, n=3 independent replicates/wells **(D)** Time-course of MxB protein levels in DIS via western blot, n=1/time-point. Error bars represent SEM.

5.3 Mitochondrial apoptotic stress and nuclear DNA damage induce MxB expression

Thus far, I observed that elevated MxB expression is associated with damage-induced and not oncogene-induced senescence, indicating that not all types of senescence are universally characterised by this feature. In order to understand what types of cellular stresses may lead to MxB up-regulation, I decided to induce a range of known mitochondrial stresses and test MxB mRNA levels (Figure 5.3 A and B). Having observed a gradual induction of MxB upon γ-irradiation, I chose the time-point of 5 days after irradiation as a positive control for increased MxB expression (Figure 5.3 A) and maintained other stress conditions also for 5 days. The first of the used stimuli was a cell culture medium containing a nutrient cocktail of lactate, pyruvate and octanoic acid, referred to as a hyperlipid medium. The medium was previously used to model non-alcoholic fatty liver disease (NAFLD) *in vitro* (Lyall *et al.*, 2018). Next, I replaced glucose with D-galactose in cell culture media, a known inducer of mitochondrial stress. D-galactose enhances mitochondrial metabolism reflected by a significantly increased oxygen consumption rate (Marroquin *et al.*, 2007). This is due to the inhibited glycolysis and occurs via increased expression of OXPHOS proteins and activities of mitochondrial enzymes (Bustamante *et al.*, 1977; Rossignol *et al.*, 2004). As the next stressor, I used rotenone, an established inhibitor of OXPHOS, specifically of the electron transport from the iron-sulphur centre in complex I to ubiquinone (Palmer *et al.*, 1968). It was also shown to induce a type of cellular senescence referred to as mitochondrial dysfunction-associated senescence (MiDAS) (Wiley *et al.*, 2016). Next, ABT-737 was selected as an inhibitor of anti-apoptotic BCL-2 proteins that induces mitochondrial apoptotic stress (Ichim *et al.*, 2015). ABT-737 allowed to test whether mitochondrial apoptotic stress and not the other changes associated with DIS may be related to MxB expression. On the other hand, I used bleomycin as an alternative senescence inducer that acts through nuclear DNA damage. Even though bleomycin-induced senescence engages mTORC1/PGC-1α/β pathway modulating mitochondrial biogenesis and function, it presumably does not induce a direct, wide-spread mitochondrial damage as in the case of γ-irradiation (Aoshiba *et al.*, 2003; Petrova *et al.*, 2016). Finally, I utilised the same conditions affecting mitochondrial network structure as described in sections 4.10 and 4.11, where I induced DRP1 and MFN2 knock-down. These two conditions allowed to test whether any of the extreme mitochondrial morphologies might be associated with increased MxB expression.

This experiment revealed that next to γ-irradiation that, consistently with previous results, induced the expression of MxB, ABT-737 and bleomycin treatments were the only other conditions associated with the same effect (Figure 5.3 A). Two tested concentrations of each

pharmacological compound generated consistent results, allowing for more confident conclusions on when MxB is induced. In contrast to ABT-737 and bleomycin, the treatment with hyperlipid medium, the stimulation and inhibition of mitochondrial respiratory function, as well as the enforced elongation or fragmentation of mitochondrial network were not associated with MxB induction (Figure 5.3 A and B).

Next, I assessed the levels of two pro-inflammatory cytokines, IL6 and IL8, constituting the typical SASP of cells in DIS. I wanted to learn whether conditions of elevated MxB stand out as particularly pro-inflammatory. In the case of early stage of DIS (5 days post irradiation), IL6 and IL8 were not induced yet (Figure 5.3 C and D). As discussed previously, IL6 and IL8 only become up-regulated at the established stage of DIS. This suggests that the increase in MxB expression precedes the establishment of SASP in this setting. Interestingly, the two other conditions where MxB was up-regulated, ABT-737 and bleomycin, were associated with increased levels of IL6 and IL8 (Figure 5.3 C and D). Among the conditions that did not induce MxB expression, only hyperlipid medium caused elevated expression of one of the cytokines, IL8 (Figure 5.3 D). Interestingly, in the case of ABT-737, the lower concentration led to more dramatic effects in terms of all the measured outcomes – this is in line with the drug's capacity to induce either miMOMP or apoptosis, depending on the concentration. The lower concentration of 10μM was previously established as the miMOMP inducing (Ichim *et al*., 2015, unpublished data by James Chapman). The higher concentration of AB737 (20μM) in my experiment caused a pronounced cell death visible during the microscopic assessment of cultured cells.

In conclusion, next to γ-irradiation, induction of mitochondrial apoptotic stress using ABT-737 and an alternative variant of damage-induced senescence via bleomycin were found to be linked to increased MxB expression as well as the induction of the pro-inflammatory cytokines, IL6 and IL8.

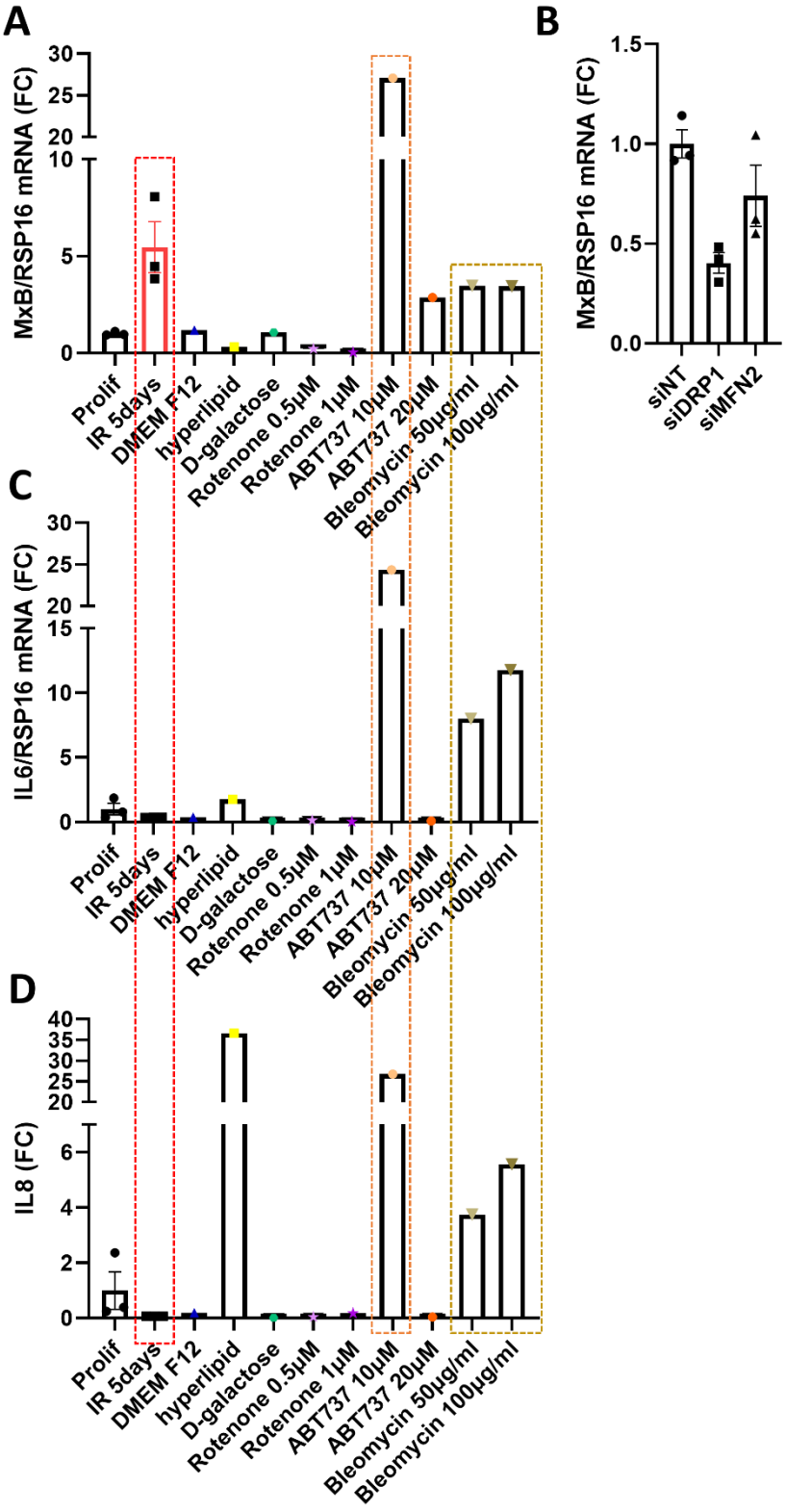

Figure 5.3: Identification of cellular stresses inducing MxB expression

(A) MxB mRNA levels via qPCR normalised to RSP16 using Delta-Delta Ct method upon a 5-day long treatment with the indicated stressors, n=3 independent replicates/wells for Prolif and IR 5days, n=1 for all other stressors, Note: drugs' concentrations indicated in the graph; DMEM, nutrient mixture F12 was used in hyperlipid medium, here, it serves as a control for this condition; D-galactose was used at 10

mM concentration, **(B)** MxB mRNA levels via qPCR normalised to RSP16 using Delta-Delta Ct method upon DRP1 and MFN2 silencing, n=3 independent replicates/wells **(C)** IL6 mRNA levels via qPCR normalised to RSP16 using Delta-Delta Ct method upon a 5-day long treatment with the indicated stressors, n=3 independent replicates/wells for Prolif and IR 5days, n=1 for all other stressors **(D)** IL8 mRNA levels via qPCR normalised to RSP16 using Delta-Delta Ct method upon a 5-day long treatment with the indicated stressors, n=3 independent replicates/wells for Prolif and IR 5days, n=1 for all other stressors. Error bars indicate SEM.

5.4 MxB silencing significantly suppresses the SASP

Having observed MxB up-regulation is associated with the expression of pro-inflammatory cytokines I set out to determine whether MxB is necessary for the SASP in damage-induced senescence. Attempts to completely knock-out MxB did not allow to generate viable cells as reported by others (Cao *et al*., 2020), therefore I employed siRNA-based silencing. I followed the same methodology as previously for DRP1 and MFN2 knock-down experiments (*sections 4.10 and 4.11*). In brief, I performed a transfection with a pool of four siRNA against MxB as well as non-targeting control siRNA mix. I collected the non-senescent cells five days after the transfection. In the case of DIS, I irradiated cells three days post transfection and collected them ten days after senescence induction, equalling thirteen days after the transfection. The efficiency of MxB silencing is demonstrated in Figure 5.4. The upper panel (Figure 5.4 A and B) presents the effect of MxB knock-down at mRNA level. Figure 5.4 C shows the MxB down-regulation at the protein level assessed via western blotting.

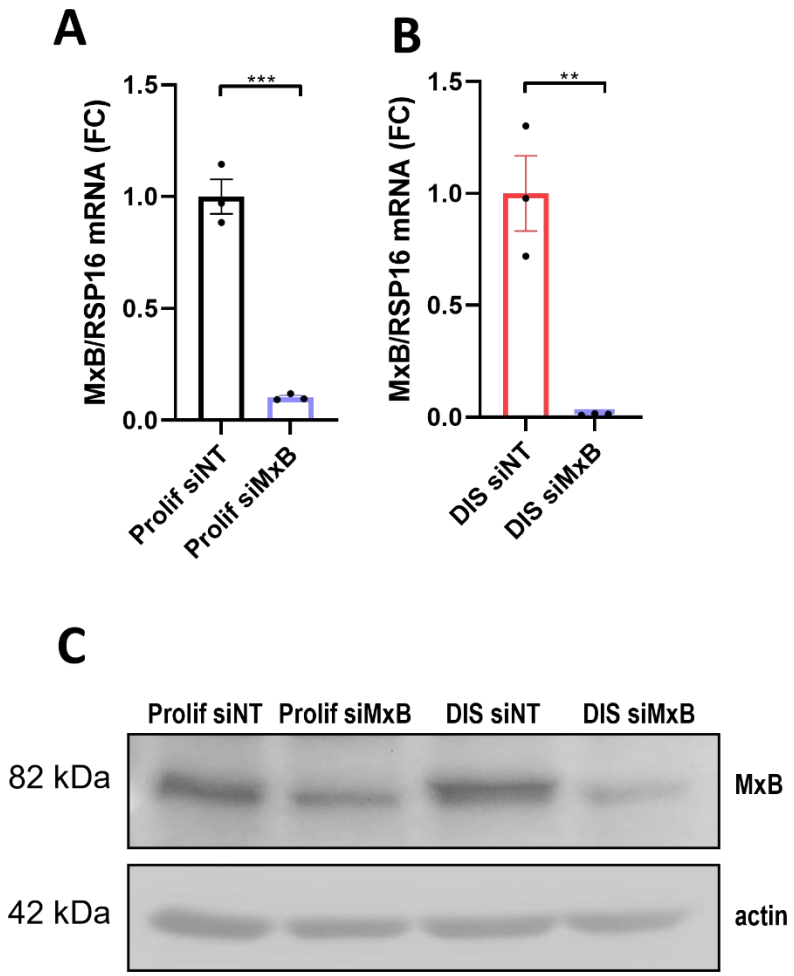

Figure 5.4: Efficiency of MxB knock-down using siRNA pool

(A) MxB mRNA levels via qPCR normalised to RSP16 using Delta-Delta Ct method in proliferating cells, collected 5 days post transfection, n=3 independent experiments/wells, Student's t-test: Prolif siNT vs Prolif siMxB p=0.0003 **(B)** MxB mRNA levels via qPCR normalised to RSP16 using Delta-Delta Ct method in DIS, collected 11 days post transfection (8 days post γ-irradiation), n=3 independent experiments/wells, Student's t-test: DIS siNT vs DIS siMxB p=0.0042 **(C)** MxB protein levels via western blot, collected 6 days post transfection for Prolif, 13 days post transfection (10 days post γ-irradiation) for DIS, n=1 replicate/condition. Error bars represent SEM.

Having obtained viable MxB depleted cells, I analysed the key SASP factors, IL6 and IL8 at 10 days after senescence induction, using a qPCR approach. In proliferating conditions, the changes of IL6 and IL8 expression were minor upon MxB knock-down (Figure 5.5 A and B). Remarkably, upon the induction of senescence, IL6 was down-regulated approximately 20-fold (Figure 5.5 A), and IL8 close to 100-fold (Figure 5.5 B) in MxB knock-down cells. These data, for the first time, demonstrate MxB is a necessary factor for the development of SASP in damage-induced senescence.

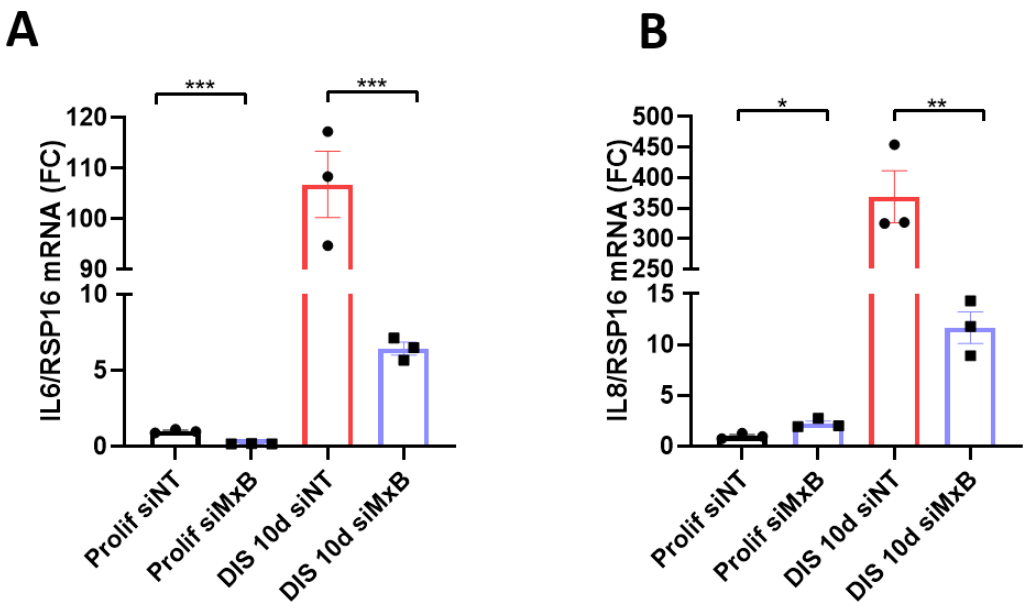

Figure 5.5: SASP upon MxB knock-down in DIS

(A) IL6 mRNA levels via qPCR normalised to RSP16 using Delta-Delta Ct method upon MxB knock-down, cells in DIS collected 10 days post senescence induction, n=3 independent replicates/wells, Student's t-test: Prolif siNT vs Prolif siMxB p=0.0003, DIS siNT vs DIS siMxB p=0.0001 **(B)** IL8 mRNA levels via qPCR normalised to RSP16 using Delta-Delta Ct method upon MxB knock-down, cells in DIS collected 10 days post senescence induction, n=3 independent replicates/wells, Student's t-test: Prolif siNT vs Prolif siMxB p=0.0146, DIS siNT vs DIS siMxB p=0.0.0011. Error bars represent SEM.

5.5 MxB knock-down induces mitochondrial apoptotic stress

Subsequently, I set out to better understand the function of MxB, especially in the context of DIS. First, I investigated the phenotypes related to mitochondria that were previously observed upon MxB knock-down, namely the features of mitochondrial apoptotic stress, previously observed for primary hepatocytes and hepatoma cell lines (Cao *et al*., 2020). I analysed three parameters constituting the mitochondrial apoptotic stress. First, I quantified the percentage of cells containing activated BAX as measured using an anti-BAX6A7 antibody co-localizing with mitochondria marked with anti-TOMM20 antibody. I performed two independent experiments. The results point out that the number of cells with this marker of mitochondrial apoptotic stress is higher upon MxB knock-down in non-senescent conditions (Figure 5.6 A and B). The increase in the number of cells positive for activated BAX in senescent cells was only slight upon MxB depletion (Figure 5.6 A and B). Next, I analysed the level of co-localisation between cytochrome *c* and TOMM20 staining as an indicator of miMOMP (Figure 5.7 A). The analysis suggested a strong effect of MxB knock-down on miMOMP induction in proliferating conditions and no meaningful difference in DIS (Figure 5.7 A). Finally, I quantified the number of extramitochondrial DNA foci stained using an anti-DNA antibody and mitochondria marked using anti-TOMM20 antibody. In accordance to the published results by Cao *et al.* (2020), I observed an increase in the number of cytosolic DNA foci mtDNA upon MxB knock-down that was significant in both proliferating and senescent conditions (Figure 5.7 B and C).

These data point out that mitochondrial apoptotic stress is enhanced in MxB depleted cells, however, upon the induction of senescence that inherently adds to this phenotype, the differences between control and MxB knock-down cells are not as pronounced as in proliferating conditions. An important question that arises is why the SASP is reduced upon MxB knock-down in senescent cells, despite the high mitochondrial apoptotic stress.

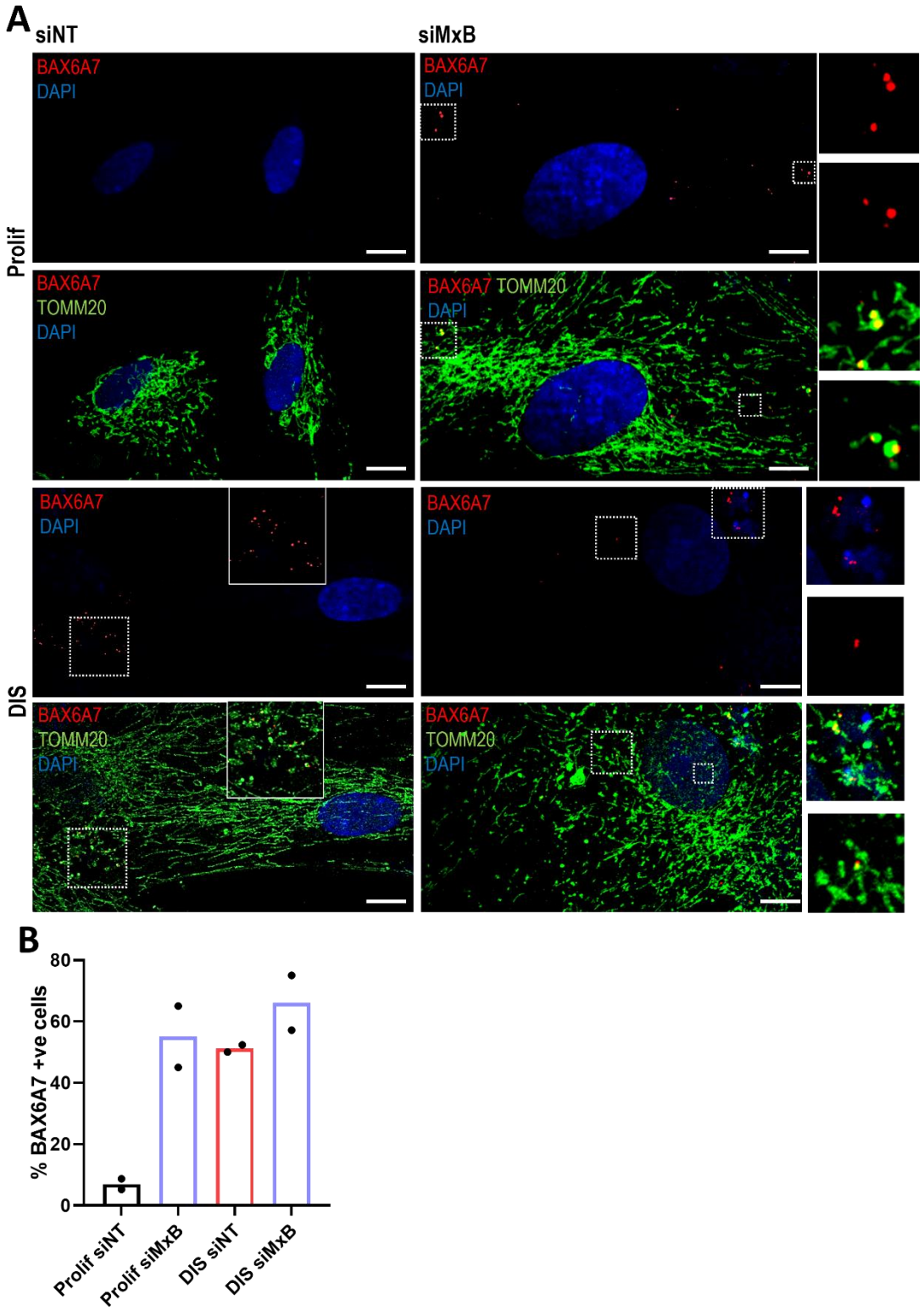

Figure 5.6: Mitochondrial apoptotic stress upon MxB knock-down – BAX activation

(A) Representative CLSM images of activated BAX stained using anti-BAX6A7 antibody and mitochondrial network stained using anti-TOMM20 antibody upon MxB knock-down **(B)** Quantification of BAX6A7 positive cells in proliferating cells and in DIS upon MxB knock-down, collected 6 days post transfection for Prolif, 13 days post transfection (10 days post γ-irradiation) for DIS, n=2 replicates/condition, min 20 cells/replicate. Scale bars 10µm.

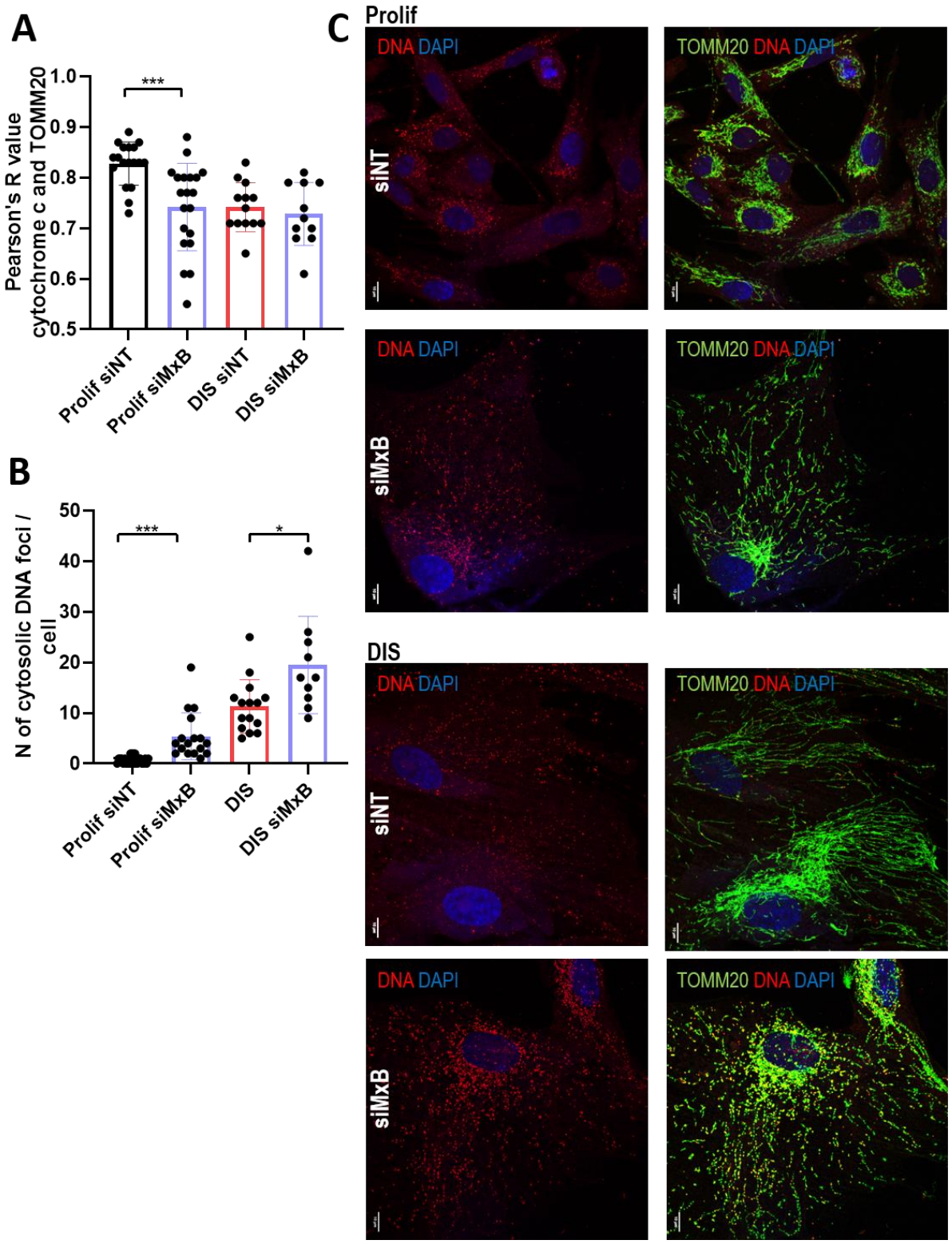

Figure 5.7: Mitochondrial apoptotic stress upon MxB knock-down – cytochrome *c* release and mtDNA leakage

(A) Representative CLSM images of DNA stained using anti-DNA antibody and mitochondrial network stained using anti-TOMM20 antibody upon MxB knock-down **(B)** Analysis of co-localisation between cytochrome *c* and TOMM20 expressed as Pearson's correlation coefficient, n=minimum

11cells/condition. Analysed with Student's t-test: Prolif siNT vs Prolif siMxB p=0.0006, DIS siNT vs DIS siMxB p=0.5593 **(C)** Quantification of the number of cytosolic DNA foci per cell, n=minimum 10 cells/condition. Analysed using Mann-Whitney test: Prolif siNT vs Prolif siMxB p<0.0001, and Student's t-test: DIS siNT vs DIS siMxB p=0.0114. Scale bars 10μm. Error bars represent SD.

5.6 Pan-caspase inhibition does not reverse MxB-dependent SASP suppression

Next, I set out to resolve the paradoxical finding of reduced SASP in conditions of higher apoptotic stress upon MxB knock-down. I hypothesised that the apoptotic signalling after MxB knock-down in the model of damage-induced senescence, even though only slightly elevated, might be sufficient to induce a higher caspase activation and silence the SASP. This hypothesis assumes that there is a threshold of when MOMP may be pro-inflammatory (miMOMP) or anti-inflammatory, such as the widely spread MOMP occurring during apoptosis (White *et al*., 2014). The mechanism of inflammation silencing was recently described, where caspase-3 is responsible for cleaving the key effectors of inflammation, such as cGAS, in human cells to prevent cytokine overproduction (Ning *et al.*, 2019). If MxB knock-down and irradiation had additive effects in terms of mitochondrial apoptotic stress that would cross a certain threshold in these conditions, this might explain the reduction of SASP. I decided to use a pan-caspase inhibitor, QVD, to test whether inhibiting caspases may revert SASP in the context of MxB knock-down.

Previously, our lab showed that pan-caspase inhibitor, QVD at 1μM concentration, reduced SASP in DIS (in human embryonic fibroblasts, MRC5) (unpublished data). In my experiment, the reduction of SASP upon QVD in DIS transfected with non-targeting siRNA was not significant when analysed using Student's t-test (Figure 5.8 A and B). However, when the data were analysed using 1-way ANOVA multiple comparison test, the decrease in both IL6 and IL8 upon QVD treatment in DIS, was significant (p=0.0165 and p=0.0129, respectively). Importantly, the treatment with QVD did not revert the SASP upon MxB knock-down, suggesting another mechanism than the caspase-dependent SASP silencing is in place that leads to the observed effect of SASP amelioration upon MxB knock-down.

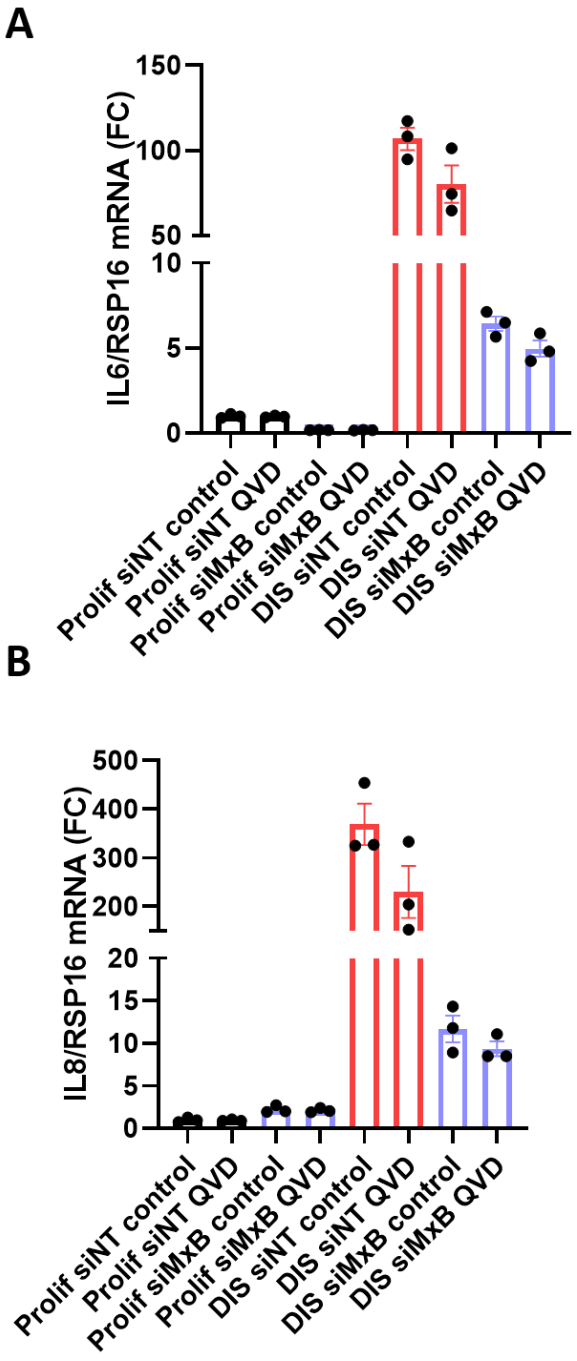

Figure Figure 5.8: SASP upon MxB knock-down and pan-caspase inhibition

(A) IL6 mRNA levels via qPCR normalised to RSP16 using Delta-Delta Ct method upon MxB knock-down and pan-caspase inhibition using QVD at the concentration of 1μM, n=3 independent replicates/wells, Student's t-test: DIS siNT control vs DIS siNT QVD p=0.1052, DIS siMxB control vs DIS siMxB QVD p=0.0849 **(B)** IL68mRNA levels via qPCR normalised to RSP16 using Delta-Delta Ct method upon MxB knock-down and pan-caspase inhibition using QVD at the concentration of 1μM, n=3 independent replicates/wells, Student's t-test: DIS siNT control vs DIS siNT QVD p=0.1134, DIS siMxB control vs DIS siMxB QVD p=0.2640. Error bars represent SEM.

5.7 MxB knock-down prevents mitochondrial hyper-fusion in damage-induced senescence

The data presented so far indicate MxB knock-down exacerbates mitochondrial dysfunction in the form of mitochondrial apoptotic stress and reduces the SASP. In my next steps, I set out to further study the function of MxB, particularly the effect of its depletion of mitochondrial function. First, I analysed mitochondrial network structure in MxB depleted cells. I utilised a method based on manually assigning a score reflecting mitochondrial morphology: fragmented, mixed or elongated. In proliferating conditions, control cells and MxB depleted cells were characterised by similar proportions of fragmented and mixed networks (Figure 5.9 A and B). Notably, in DIS, the lack of the typical hyper-fused phenotype was evident (5.9 A and B). Having observed the striking effect on mitochondrial network in senescent cells, I decided to extend the analysis of mitochondrial morphology in these conditions by employing another method to analyse mitochondria, the MiNA ImageJ plugin. Figure 5.10 A presents mitochondrial skeletons generated upon application of a range of filters (*as described in section 2.4.6*). I measured three parameters of the network allowing for unbiased conclusions on mitochondrial network status, namely the mean length of mitochondrial branches, the mean length of summed branches and the mean number of network branches. Mean branch length trended towards a decrease upon MxB knock-down (Figure 5.10 B), while mean summed branch length (Figure 5.10 C) and mean number of network branches (Figure 5.10 D) were significantly reduced in MxB knock-down cells. Generally, these results stand in line with the manually obtained data. However, additional optimisation of MiNA methodology would allow to better resolve the differences in mitochondrial morphology between control and MxB depleted cells (in regards to mean branch length). The considerations on MiNA optimisation are included in the section 5.12 Discussion.

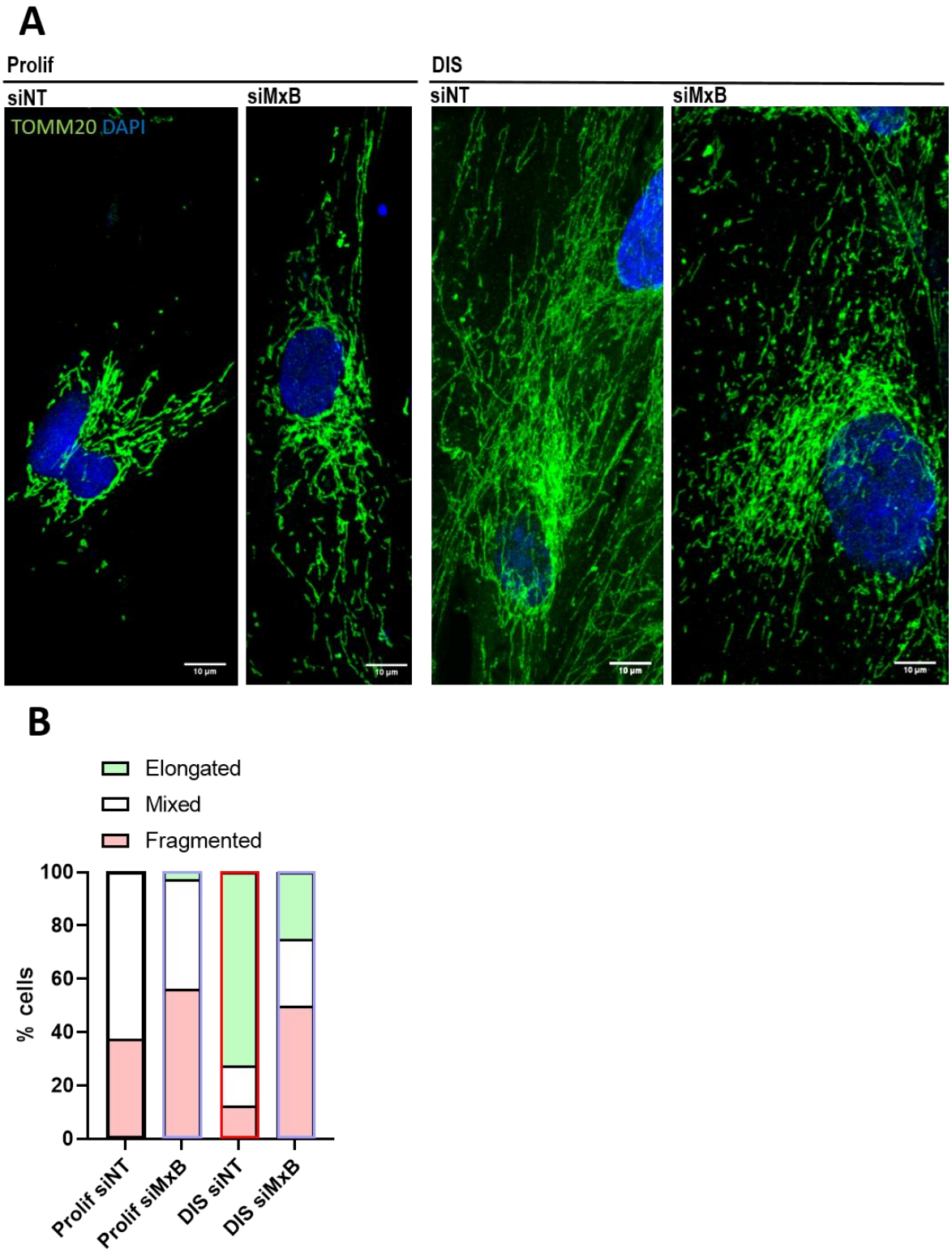

Figure 5.9: Mitochondrial network structure upon MxB knock-down – manual quantification

(A) Representative CLSM microscopy images of mitochondrial networks visualised using anti-TOMM20 antibody, as a mitochondrial marker, **(B)** Quantification of mitochondrial network structure during the course of oncogene-induced senescence development based on the staining represented in A. N=min 40 cells/condition from 3 independent replicates. Scale bars represent SD.

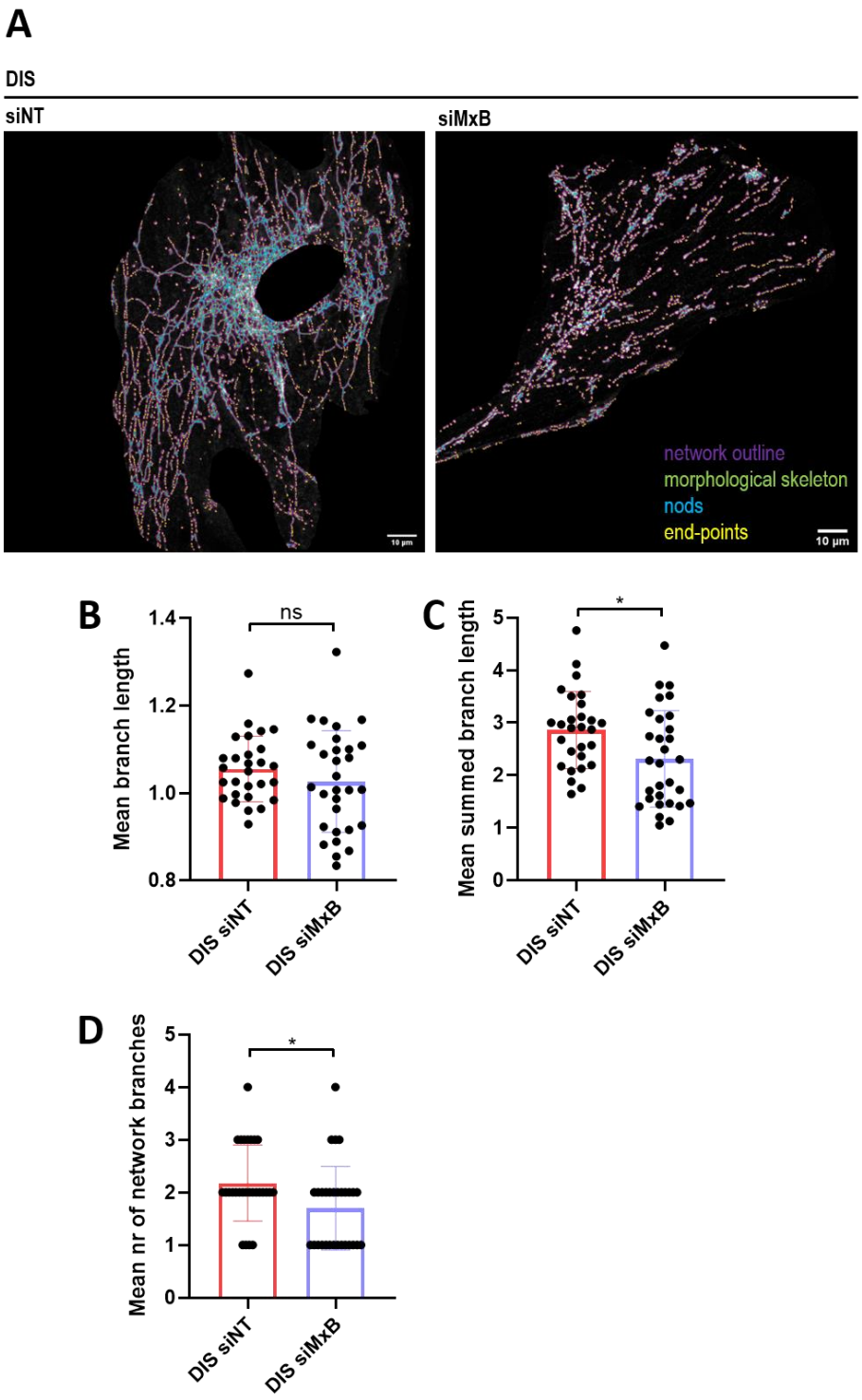

Figure 5.10: Mitochondrial network structure upon MxB knock-down – automated quantification

(A) Representative CLSM microscopy images of mitochondrial networks visualised using anti-TOMM20 antibody, as a mitochondrial marker, upon MiNA processing, **(B)** Measurement of mean branch length using MiNA plugin, n=28-30 cells per condition across 3 biological replicates, Student's t-test: DIS siNT vs DIS siMxB: p=0.2738, **(C)** Measurement of mean summed branch length using MiNA plugin, n=28-30 cells per condition across 3 biological replicates, Student's t-test: DIS siNT vs DIS siMxB: p=0.0158, **(D)** Measurement of mean number of network branches, n=28-30 cells per condition from 3 biological replicates, Student's t-test: DIS siNT vs DIS siMxB: p=0.0124. Scale bars represent 10µm. Error bars represent SD.

5.8 MxB knock-down induces mitochondrial respiratory dysfunction

Next, I set out to assess whether mitochondrial bioenergetics is affected by MxB knock-down, inducing a metabolic imbalance. I employed an alternative methodology for assessing mitochondrial respiratory function to the previously described HRR using O2k system (Oroboros) (*Chapter 4*), namely the Seahorse XF Extracellular Flux Analyser (Seahorse XF, Seahorse Bioscience Inc./Agilent). Among several variants of analyses that might be performed using this system, I used Agilent Seahorse XF Cell Mito Stress Test. One of the main differences between O2k and Seahorse systems (as used in this thesis) concerns the state of cells during the analysis: being either suspended in a medium and stirred, or adherent, growing in dedicated cell culture dishes, respectively. Essentially, both systems inform about oxygen consumption rate (OCR) measured as a decrease of oxygen concentration in the assay medium, in specific coupling states cells are induced into using pharmacological compounds. Similar to O2k, upon the measurement of basal respiration, oligomycin is added to block ATP synthase to assess how much respiration is coupled to ATP production and how much depends on the proton leak. Next, FCCP in added in order to allow for unrestricted proton exit from the inner membrane space to mitochondrial matrix, exposing the respiratory capacity of cells in the conditions of interest. Finally, antimycin A and rotenone are added in order to inhibit electron transport along the ETC, allowing to assess how much of the oxygen is used by processes other than mitochondrial respiration, referred to as non-mitochondrial or residual respiration. Having measured OCR during these four states, I was able to calculate additional parameters characterising mitochondrial respiratory function. Besides the basic parameters described already in Chapter 4: a) basal mitochondrial respiration that is the basal respiration upon the subtraction of residual respiration, b) proton leak that is the oligomycin-independent respiration upon subtraction of residual respiration and c) maximum respiration that is the respiration after the addition of FCCP and upon subtraction of residual respiration, I also calculated d) ATP production, e) coupling efficiency, f) spare respiratory capacity and g) state apparent of mitochondrial respiration. ATP production is calculated upon the subtraction of proton leak from basal respiration. Coupling efficiency is the ratio of ATP production to basal respiration. Spare respiratory capacity is calculated by subtracting basal respiration from maximum respiration. Finally, state apparent is calculated using an equation: State apparent = 4 – (ATP Production / (Maximum respiration – Proton leak)). The higher state apparent informs of a more efficient respiratory system.

The analysis of mitochondrial bioenergetics in proliferating conditions revealed a higher basal respiration and ATP production in MxB knock-down cells (Figure 5.11 A, B and C). MxB knock-down cells are, however, characterised by higher proton leak (Figure 5.11 D). Coupling efficiency was also significantly reduced upon MxB knock-down (Figure 5.11 E). Maximum respiration was increased (Figure 5.11 F), however, the spare respiratory capacity was unchanged in MxB knock-down cells (Figure 5.11 G). These measures indicate inefficient oxidative phosphorylation of MxB depleted cells. Finally, a significantly decreased state apparent confirms the finding of mitochondrial dysfunction (Figure 5.11 H). In conclusion, these data indicate mitochondrial bioenergetics is significantly affected by MxB knock-down. The increased respiration in the presence of system's inefficiency suggest a compensatory response.

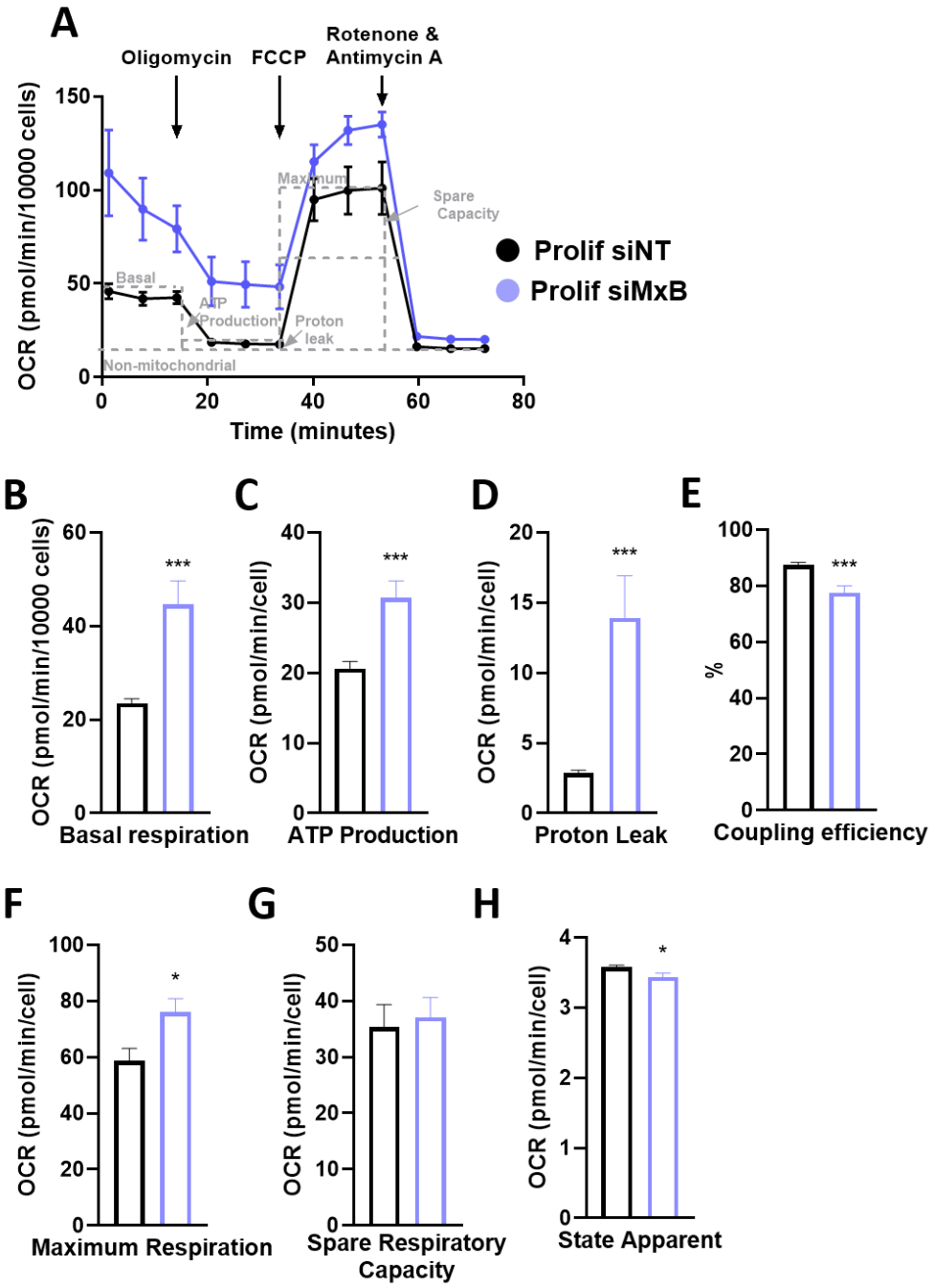

Figure 5.11: Mitochondrial bioenergetics upon MxB knock-down in proliferating conditions

(A) Seahorse analysis of OCR per 10 000 cells in basal conditions and following addition of oligomycin, FCCP, antimycin A and rotenone as indicated, representative of one of two independent experiments consisting of 5 technical replicates each. The following parameters were quantified as described in section 5.8, normalised to cell number and expressed per 10 000 cells. n=2 independent replicates, pool of 5 technical replicates from each independent experiment. Quantification of **(B)** Basal respiration, Student's t-test: Prolif siNT vs Prolif siMxB p=0.002 **(C)** ATP production, Student's t-test: Prolif siNT vs Prolif siMxB p=0.0003 **(D)** Proton leak, Student's t-test: Prolif siNT vs Prolif siMxB p=0.0008 **(E)** Coupling efficiency, Student's t-test: Prolif siNT vs Prolif siMxB p=0.0006 **(F)** Maximum respiration, Student's t-test: Prolif siNT vs Prolif siMxB p=0.0109 **(G)** Spare respiratory capacity, Student's t-test: Prolif siNT vs Prolif siMxB p=07384 and **(H)** State apparent, Student's t-test: Prolif siNT vs Prolif siMxB p=0.0275. Error bars represent SEM.

With regards to senescent cells, basal respiration and ATP production were decreased between control and MxB depleted cells (Figure 5.12 A, B and C). Proton leak was unchanged between the conditions (Figure 5.12 D) probably due to an already higher proton leak characterizing senescent cells (Chapter 4, Figure 4.6). Other parameters, however, such as decreased coupling efficiency (Figure 5.12 E), lower maximum respiration (Figure 5.12 F), lower spare respiratory capacity (Figure 5.12 G), and decreased state apparent pointed out to a higher level of mitochondrial dysfunction upon MxB knock-down. These data indicate that the mitochondrial dysfunction induced by MxB knock-down might initially stimulate a compensatory response, considering the increased basal respiration (proliferating conditions). Upon the second damaging insult towards the mitochondria in the form of γ-irradiation, mitochondrial dysfunction becomes more evident, compromise coupling efficiency further as well as the respiratory capacity of the OXPHOS system.

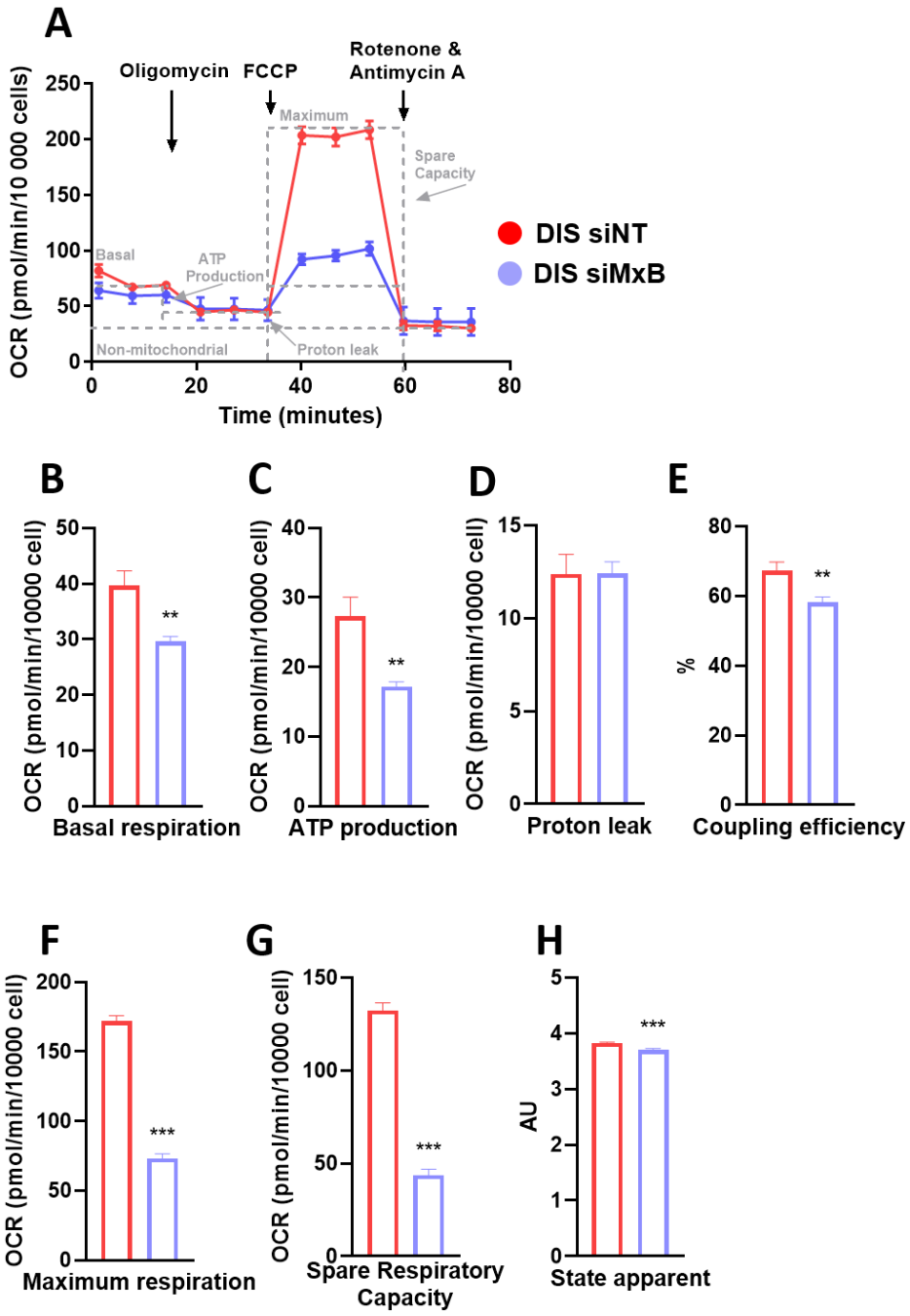

Figure 5.12: Mitochondrial bioenergetics upon MxB knock-down in DIS

(A) Seahorse analysis of OCR per 10 000 cells in basal conditions and following addition of oligomycin, FCCP, antimycin A and rotenone as indicated, performed as one independent experiment consisting of 5 technical replicates each. The following parameters were quantified as described in section 5.8, normalised to cell number and expressed per 10 000 cells. n=1 independent replicates, 5 technical replicates from each independent experiment. Quantification of **(B)** Basal respiration, Student's t-test: DIS siNT vs DIS siMxB p=0.0030 **(C)** ATP production, Student's t-test: DIS siNT vs DIS siMxB p=0.0037 **(D)** Proton leak, Student's t-test: DIS siNT vs DIS siMxB p=0. 9883 **(E)** Coupling efficiency, Student's t-test: DIS siNT vs DIS siMxB p=0.0087 **(F)** Maximum respiration, Student's t-test: DIS siNT vs DIS siMxB p<0.0001 **(G)** Spare respiratory capacity, Student's t-test: DIS siNT vs DIS siMxB p<0.0001 and **(H)** State apparent, Student's t-test: DIS siNT vs DIS siMxB p<0.0001. Error bars represent SEM.

5.9 MxB knock-down drives mitochondrial biogenesis

Having observed significant alterations in mitochondrial bioenergetics in MxB knock-down cells, especially the increased basal respiration in proliferating conditions upon MxB knock-down, I hypothesised that an activation of mitochondrial biogenesis might be responsible for the observed effects. First, I performed an analysis of mitochondrial network size, referred to as mitochondrial footprint, based on CLSM images of mitochondrial marked with anti-TOMM20 antibody, and found the mitochondrial network expands significantly upon MxB knock-down in proliferating conditions (Figure 5.13 A). In the case of DIS, the difference between the control and siMxB transfected cells was not significantly changed (Figure 5.13 A), suggesting that a further network expansion than what is usually observed upon irradiation, might not be attainable by the cell. To complement these data, I also analysed mtDNA copy number using a qPCR based approach to assess the relative abundance of D-loop sequence as well as a ND2. Only a trend for an increase was observed in proliferating conditions, however, the mean values are close to the levels of mtDNA observed in DIS (Figure 5.13 B and C). A further elevation was detected upon MxB knockdown in DIS (Figure 5.13 B and C). Finally, I assessed the transcriptional levels of two key biogenesis mediators, PGC-1α and PGC-1β. Both were significantly elevated when MxB was depleted, in proliferating as well as in DIS conditions (Figure 5.13 D and E). These data point out that MxB knock-down induces mitochondrial biogenesis. Considering the range and severity of mitochondrial dysfunctions caused by MxB knock-down, increased mitochondrial biogenesis suggests that a compensatory response is activated.

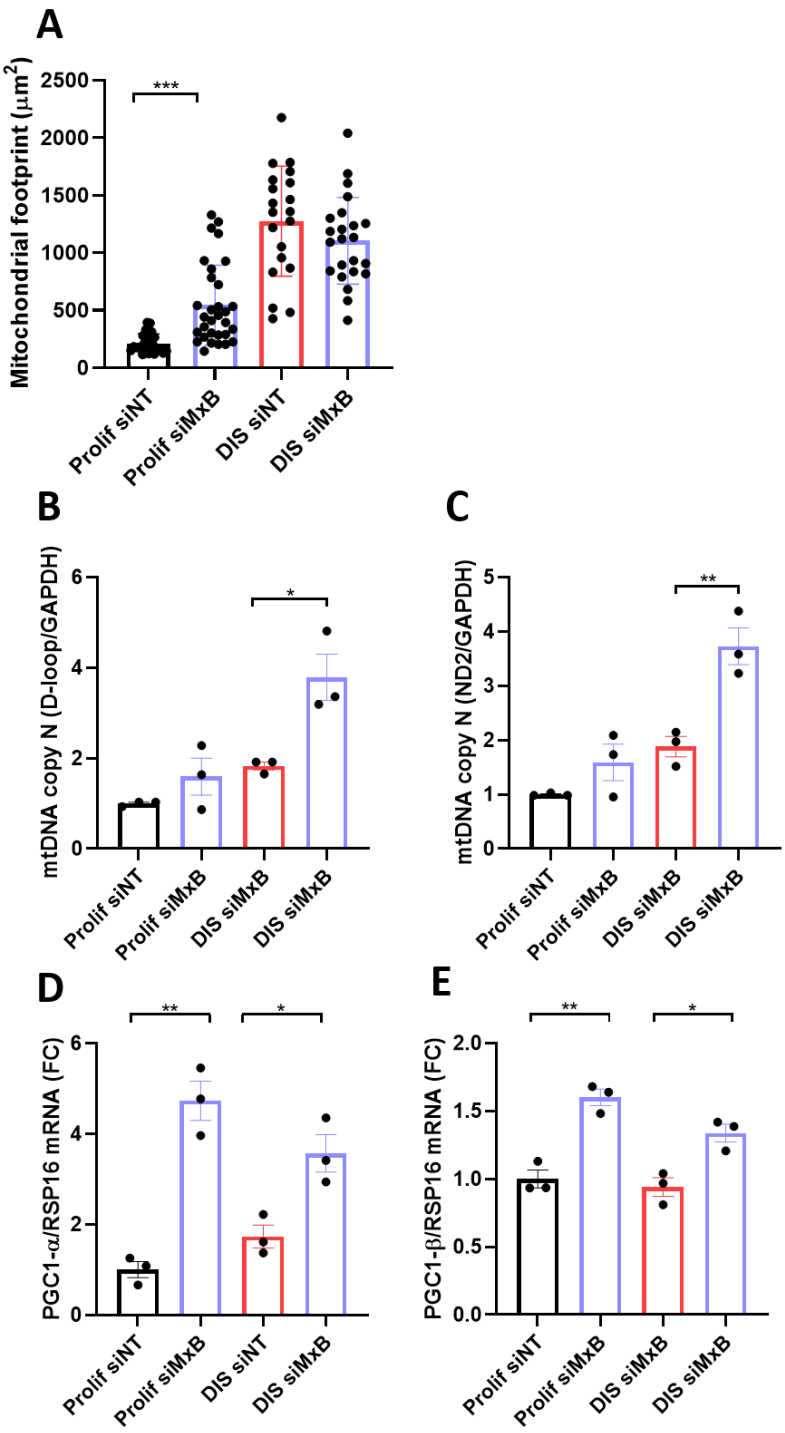

Figure 5.13: Mitochondrial biogenesis upon MxB knock-down in DIS

(A) Mitochondrial footprint in µm2 quantified basing on CLSM images of TOMM20 as a mitochondrial marker n=20-32 cells across 2 independent replicates/coverslips, Mann-Whitney test: Prolif siNT vs siMxB p<0.00001, Student's t-test DIS siNT vs DIS siMxB p=0.1994, **(B)** Relative mtDNA D-loop copy number via PCR normalised to GAPDH nuclear gene using Delta Ct method, n=3 independent replicates/wells, Student's t-test: Prolif siNT vs Prolif siMxB p=0.2204, DIS siNT vs DIS siMxB p=0.0197, **(C)** Relative mtDNA ND2 copy number via PCR normalised to GAPDH nuclear gene using Delta Ct method, n=3 independent replicates/wells, Student's t-test: Prolif siNT vs Prolif siMxB p=0.1519, DIS siNT vs DIS siMxB p=0.0087, **(D)** PGC1-α mRNA levels via qPCR normalised to

RSP16 using Delta-Delta method, n=3 independent replicates/wells, Student's t-test: Prolif siNT vs Prolif siMxB p=0.0013, DIS siNT vs DIS siMxB p=0.0195, **(E)** PGC1-β mRNA levels via qPCR normalised to RSP16 using Delta-Delta method, n=3 independent replicates/wells, Student's t-test: Prolif siNT vs Prolif siMxB p=0.0025, DIS siNT vs DIS siMxB p=00137. Error bars represent SD for A, error bars represent SEM for B-E.

5.10 MxB translocates out of mitochondria and accumulates in the nucleus in damage-induced senescence

Having observed a range of changes to mitochondrial morphology and function upon MxB knock-down, I set out to determine its sub-cellular localisation. MxB was initially found to reside in the nucleus and the cytosol and to accumulate on the outer envelope of the nuclear membrane in proximity to nuclear pores (Mélen *et al*., 1996; Steiner *et al*., 2020). This localisation allows MxB to restrict the viral genome access to the host's transcriptional machinery as well as genome integration (Cao *et al*., 2020). It was also suggested to orchestrate cytonuclear trafficking in basal conditions (King *et al*., 2004). Very recently, MxB was also found to localise to mitochondria, maintaining the cristae structure in human primary hepatocytes and a hepatoma cell lines (Cao *et al*., 2020). It remained to be elucidated whether MxB is also found within mitochondria in the model used throughout these studies, namely human primary fibroblasts, IMR90, and importantly, its fate upon the induction of DIS.

To do this, I performed a sub-cellular fractionation followed by a western blot for MxB, a mitochondrial protein marker, cytochrome *c* oxidase subunit I (COX1) and a cytosolic marker, actin. In proliferating conditions, MxB was found in all three obtained fractions, a fraction enriched in nuclear components (Nuc), cytosolic (Cyto) and mitochondria-enriched fraction (Mito) with the highest levels in the nucleus and mitochondria (Figure 5.14 A). In DIS, the nuclear levels of MxB increased, while its mitochondrial levels decreased (Figure 5.14 A). It is interesting to notice that in WCL there are two bands potentially representing two MxB isoforms, levels of which are equal in proliferating conditions. It is also clear that the longer version is more abundant in the nuclear fraction and the shorter isoform in the cytosolic fraction in proliferating cells. Remarkably, mitochondria seem to contain predominantly the longer isoform, which is in line with the previous report (Cao *et al*., 2020). In senescent cells, the MxB up-regulation concerns mostly the long isoform, as already shown in Figure 5.2. In all fractions, the long isoform is more pronounced, besides the mitochondrial fraction, which seems to be completely deprived of this isoform (Figure 5.14 A). These observations allow for a conclusion that the induction of MxB in cellular senescence by γ-irradiation leads to the accumulation of its longer isoform predominantly in the nucleus. At the same time, mitochondrial MxB translocates out of the mitochondria.

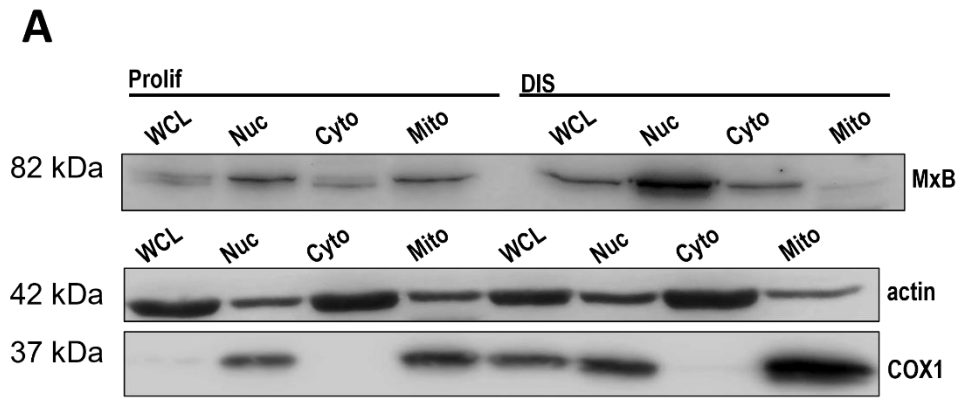

Figure 5.14: MxB subcellular localisation in proliferating cells and in damage-induced senescence

(A) MxB protein levels upon subcellular fractionation into nuclear (Nuc), cytosolic (Cyto) and mitochondria (Mito) compartments, WCL stands for whole cell lysate, actin and cytochrome *c* oxidase subunit I (COX1) serve as loading and purity controls, n=1 subcellular fractionation experiment. Experiment performed in collaboration with Dr Stella Victorelli.

5.11 Conclusions

The data presented in this chapter point out that an anti-viral factor, MxB, whose function was studied almost exclusively in the context of viral infections until very recently is, in fact, an important regulator of mitochondrial function as well as SASP in DIS. First, I found the expression of MxB significantly increases in damage- but not oncogene-induced senescence. This did not confirm my initial hypothesis of a potential protective role of MxB with respect to mitochondrial apoptotic stress. In fact, among various interventions that perturb normal cellular function, these that do or might also induce mitochondrial apoptotic stress were associated with elevated levels of MxB. Next to γ-irradiation, the inhibition of BCL-2 proteins by ABT-737 that leads to the induction of mitochondrial apoptotic stress (Brokatzky *et al*., 2019; Ichim *et al*., 2015,), as well as the induction of another type of DIS via bleomycin, were identified as the stresses that result in the up-regulation of MxB. These two conditions were also associated with elevated production of pro-inflammatory cytokines, IL6 and IL8. A range of other mitochondrial disruptors – stimulation and inhibition of mitochondrial respiration, promoting mitochondrial elongation or fragmentation, as well as changing medium composition to hyper-lipid, in contrast, did not positively affect the expression of MxB.

The depletion of MxB led to several prominent mitochondrial dysfunctions, such as elevated mitochondrial apoptotic stress. In the conditions of DIS that is associated with increased mitochondrial apoptotic stress (*Chapter* 3), the effects of the knock-down in this context were less pronounced. It is worth considering that the cells that survived both irradiation and knock-down must have experienced only such a degree of MOMP that did not lead to cell death. Mitochondrial apoptotic stress observed in MxB depleted senescent cells – only slightly higher than in control senescent cells – might be considered the highest that is still sub-lethal.

Importantly, MxB knock-down also prevented the development of SASP. As the effect was observed simultaneously with high mitochondrial apoptotic stress, I decided to address whether the level of MOMP upon MxB knock-down might have crossed a threshold where it has a silencing effect on SASP. However, the treatment of MxB depleted cells induced to DIS with a pan-caspase inhibitor, did not reverse the SASP suppression, indicating another mechanism is in place that is responsible for this effect. Generally, these findings point out that mitochondrial apoptotic stress may be a SASP trigger as shown in Chapter 3, however, its pro-inflammatory consequences may be overridden by other mechanisms.

Next, I found that MxB knock-down prevented mitochondrial hyper-fusion in damage-induced senescence. Having previously observed that mitochondrial fragmentation led to a

decrease in SASP components expression in DIS, this effect is suspected to be implicated the SASP reduction in the context of MxB.

MxB depletion results in several strong phenotypes with regards to mitochondrial OXPHOS function. I observed a higher mitochondrial respiration (including basal, maximum respiration and spare respiratory capacity) with measures of OXPHOS inefficiency in proliferating conditions, *i.e.* increased proton leak. Senescent MxB depleted cells were either not significantly different from siNT counterparts, as in the case of proton leak or behaved in a seemingly opposite manner, as in the case of basal respiration, maximum respiration and spare respiratory capacity. This apparent discrepancy indicate that MxB is required for the senescence-associated changes to mitochondria. In other words, MxB-dependent mitochondrial dysfunction becomes more severe upon the additional insult in the form of γ-irradiation. These data suggest an additional metabolic defect that is present in MxB depleted cells upon the induction of DIS that may be responsible for the reduction in SASP upon MxB knock-down.

The observed elevation of mitochondrial respiration in proliferating cells co-occurred with mitochondrial network expansion, higher levels of mtDNA copy number and markers of mitochondrial biogenesis, PGC-1α and PGC-1β. In the case of DIS, the network size appeared equal or even slightly smaller upon MxB knock-down, despite the significantly elevated mtDNA levels and mitochondrial biogenesis mediators. This may result from defects in the synthesis of new mitochondria, for example, due to impaired mitochondrial import or the ability to expand of the abnormal mitochondrial membranes (as observed by Cao *et al.* 2020). On the other hand, the unchanged network size despite the activated mitochondrial biogenesis may be a reflection of the fragmented mitochondrial network, taking less space than a hyper-fused network. Interestingly, MxB knock-down does not seem to affect the ability of mitochondria to synthesise new mitochondrial nucleoids, pointing out a potential imbalance in the nuclear-encoded and mitochondrial-encoded mitochondrial constituents.

Finally, the analysis of sub-cellular localisation of MxB in proliferating conditions and upon the induction of DIS, revealed that MxB is present in all studied sub-cellular fractions: nuclei-enriched, cytosolic and mitochondria-enriched fractions. In DIS, MxB markedly accumulated in the nucleus and translocated out of the mitochondria. The last observation is especially interesting in the context of mitochondrial apoptotic stress. Mitochondrial apoptotic stress was shown to be triggered by MxB silencing (Cao *et al.*, 2020). Potentially, however, despite the general increase in the cellular – nuclear - MxB levels, its translocation out of the mitochondria could have the same effect on mitochondrial dysfunction in the conditions of DIS,

as MxB knock-down in proliferating cells. This observation helps to explain the link between MxB and mitochondrial apoptotic stress that is seen in DIS and conditions, such as ABT-737 and bleomycin. There is no protective role of MxB in this respect as my initial hypothesis assumed. It is the MxB translocation out of the mitochondria that might be of critical importance in driving this type of mitochondrial dysfunction. From a more general standpoint, MxB translocation out of the mitochondria may be an additional mechanism that contributes to senescence-associated mitochondrial dysfunction.

Collectively, the data presented in this chapter demonstrate two key directions by which MxB depleted cells are affected. Namely, MxB knock-down induced a severe mitochondrial dysfunction that is associated with a potentially compensatory response in the form of activated mitochondrial biogenesis. Simultaneously, MxB knock-down suppresses the SASP. This occurs despite the high mitochondrial apoptotic stress. The effect of SASP amelioration may result from the changes to mitochondrial network, including the prevention of mitochondrial hyper-fusion, metabolic alterations or continuous mitochondrial biogenesis. On the other hand, and as further discussed, disturbed cytonuclear trafficking due to decreased levels of the nuclear or juxtanuclear MxB at the nuclear pores, might impair the translocation of the transcription factors orchestrating the SASP. These two broad hypotheses are summarised in Figure 5.15. Besides the proposed directions, there might be yet completely undiscovered functions of nuclear MxB, for example its potential involvement in gene expression, that need to be understood for final conclusions on the consequences of MxB depletion in proliferating and stressed/senescent cells.

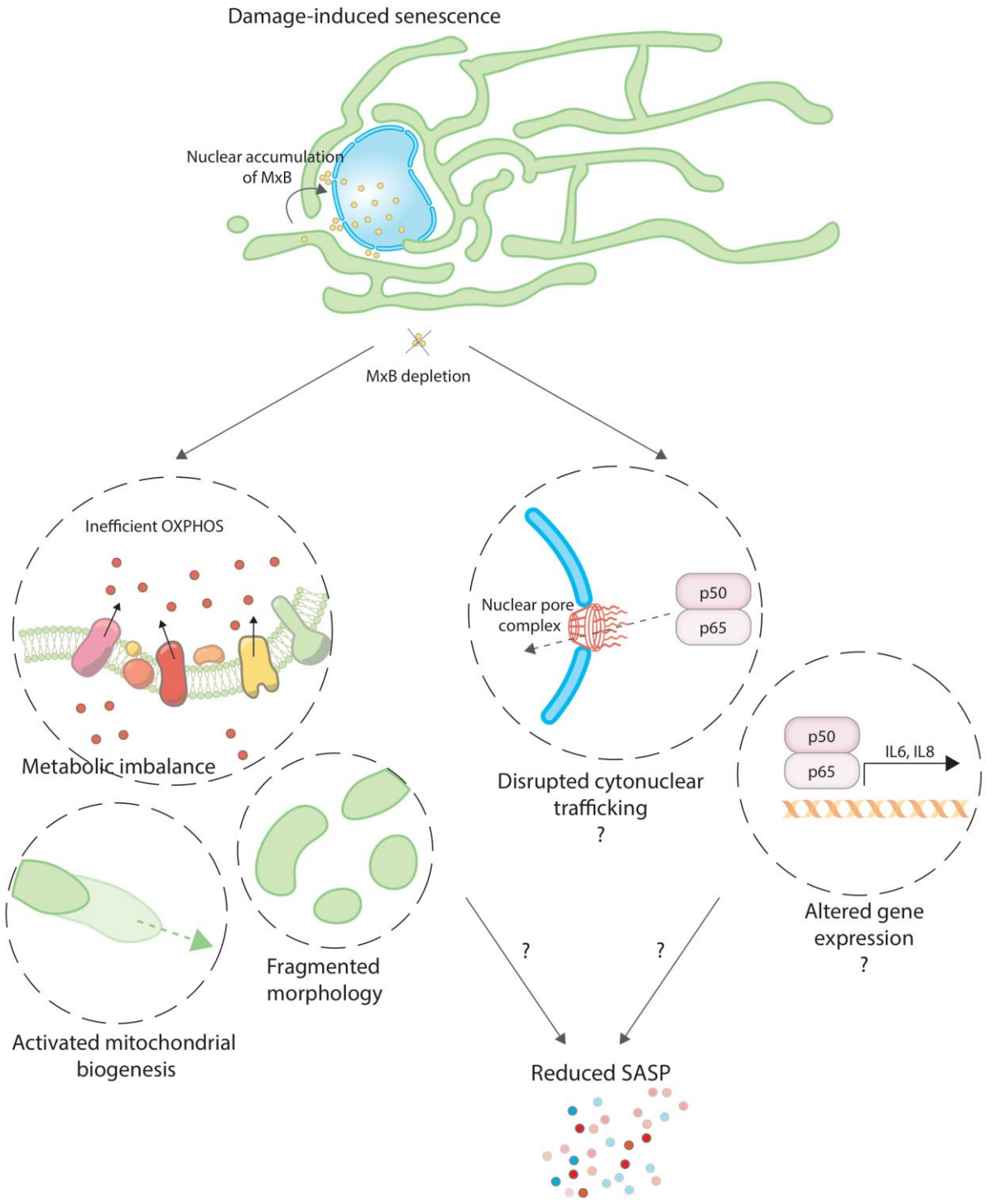

Figure 5.15: Schematic representation of hypotheses explaining the mechanism of SASP reduction upon MxB depletion in DIS

MxB was found to be significantly up-regulated in DIS and to accumulate in the nucleus. MxB depletion induces a range of mitochondrial dysfunctions, including inefficient OXPHOS, mitochondrial network fragmentation and activation of mitochondrial biogenesis. Literature reports on other, non-mitochondrial, however house-keeping functions of MxB, such as the regulation of nuclear import (King *et al.*, 2004). All the depicted processes might be instrumental for the development of the pro-inflammatory phenotype in DIS.

5.12 Discussion

The main novelty presented in this chapter is the fact that a viral resistance factor, MxB, plays a role in cellular stress responses different than viral infections. As previously mentioned, Mx proteins are almost exclusively studied in the context of viral infections (Melén *et al.*, 1996; Miles *et al.*, 2020; Schoggins *et al.*, 2011). Interestingly, the anti-viral function of MxB has not been known until 2013, even though it was discovered as a homolog of MxA back in 1989 (Aebi *et al.*, 1989). The majority of the current literature focuses on the specificity of Mx proteins for different viral species (Crameri *et al.*, 2018), deciphering mechanisms of viral capsid binding (Miles *et al.*, 2020), oligomerisation as a prerequisite for anti-viral activity (Buffone *et al*., 2015), the stages of viral cycle where Mx proteins come to play (Goujon *et al.*, 2014; Kane *et al.*, 2013; Liu *et al.*, 2013; Wang, Niklasch, *et al.*, 2020; Xie *et al.*, 2020), also depending on its sub-cellular localisation (Miles *et al.*, 2020; Steiner *et al.*, 2020; Xie *et al.*, 2020).

Two studies are exceptions from the mainstream research foci. First, King *et al.* (2004) demonstrated a delay in G1/S cell-cycle progression in cells expressing a dominant-negative MxB (in its GTPase domain) as well as in MxB depleted cells. This proved MxB plays an important role in the basal conditions and is required for the normal cell cycle progression - its lack induces a stress response, resembling cellular senescence. Data presented in this chapter, however, point out MxB knock-down does not induce the typical SASP 5 days after the siRNA transfection. Additionally, I set out to address whether mitochondrial apoptotic stress and other mitochondrial dysfunctions that are elevated already 5 days post knock-down (Figure 5.6, 5.7) may lead to increased expression of pro-inflammatory cytokines at a later stage. Data presented in this thesis revealed mitochondrial apoptotic stress was activated early upon γ-irradiation, however the SASP is present only 10 days post the insult. Therefore, I performed an analysis of IL6 and IL8 expression also 10 days after siRNA transfection. And found the increase of these two SASP factors is still minor (Appendix, Figure 4 A and B). In the future, it would be worth addressing a wider range of SASP factors that might be present upon MxB depletion. For example, Wiley *et al.* (2016) who described the phenotype of MiDAS, also reported on an atypical SASP, lacking the IL1α-dependent arm of the SASP. Cells in MiDAS were, however, producing other cytokines, such as TNFα and IL10 (Wiley *et al*., 2016). It would be worth assessing the expression of these factors in MxB depleted cells. Moreover, Wiley *et al.* (2016) demonstrated the addition of sodium pyruvate to the media reverses the MiDAS phenotype and reverts the expression of IL6 and IL8, indicating a metabolic effect is involved. In fact, I have

reproduced the experiment adding sodium pyruvate at 100mM concentration, according to the Wiley *et al.* (2016). I observed improved cell morphology visible during the microscopic assessment of cultured cells. Due to time restriction, I was not able to analyse the collected samples in terms of SASP, however, it would be an interesting question to answer in the future. Despite the lack of SASP consisting of IL6 and IL8, I assessed the proliferation and cell cycle arrest markers confirming MxB knock-down induced a cell cycle arrest (Appendix, Figure 5). I found the percentage of cells positive for a proliferation marker, Ki67, significantly decrease already 5 days post siMxB transfection (Appendix, Figure 5 A and D). I also found significantly elevated levels of p21 transcript assessed via qPCR upon MxB knock-down (Appendix, Figure 5 B). Finally, MxB depleted cells were significantly larger than the control cells (Appendix, Figure 5 C). Of note is also the DNA hetero-chromatinisation observed as regions more intensely stained with DAPI, characteristic to cellular senescence (Kosar *et al*., 2011). Therefore, the conditions labelled as proliferating/"Prolif" in the case of MxB knock-down were clearly compromised in this respect. Collectively, this additional dataset confirms the previously reported observation that MxB has an important house-keeping function, as its depletion leads to a cell cycle arrest, however, as observed here, one that does not lead to a SASP as profound and typical in composition as in other senescence models (Figure 5.4). In the future, it would be worth performing additional analyses of senescence markers, such as senescence-associated β-galactosidase assay, which positively marks senescence cells also in the MiDAS mode (Wiley *et al*., 2016).

The second study that set out to dissect the non-canonical roles of MxB was performed by our collaborators from Dr Mark McNiven's laboratory at Mayo Clinic (Rochester, US), who showed MxB role in mitochondrial function (Cao *et al*., 2020). Assessing the levels of MxB in two models of senescence characterised by different degrees of mitochondrial apoptotic stress did not confirm the initial hypothesis, according to which a model with lower mitochondrial apoptotic stress (OIS) would possess higher levels of MxB. In contrast, the model of DIS with more extensive apoptotic signalling on mitochondria was found to be associated with a significant up-regulation of MxB. My further functional analysis of MxB confirmed the induction of mitochondrial apoptotic stress in the case of proliferating cells - the results standing in line with the report by Cao *et al.* (2020), and a mild exacerbation of the mitochondrial apoptotic stress in senescent cells upon MxB knock-down. These data seemed at first paradoxical, where the lack of MxB induced mitochondrial apoptotic stress and the conditions associated with its high levels exerted by other means (γ-irradiation) were characterised by high

MxB levels. Only the assessment of sub-cellular localisation of MxB provided a potential explanation of these seemingly contradictory results. MxB accumulated predominantly in the nucleus of cells in DIS, while their mitochondria were deprived of it. Therefore, the mitochondrial levels of MxB in both settings are decreased and may be responsible for driving the mitochondrial dysfunction in the form of mitochondrial apoptotic stress.

Cao *et al.* (2020) also demonstrated that MxB is required for the healthy mitochondrial morphology. These authors reported that besides fragmented and "normal" networks, there are additional phenotypes, such as deformed or clustered mitochondria. Based on my microscopic data, I also observed that the fragmented phenotypes were more heterogenous than the effects of MFN2 knock-down presented in Chapter 4, where mitochondria were fragmented but orderly. These observations call for a more precise assessment methods of mitochondrial structures as an indicator of cellular health. Besides manual assessment of mitochondrial network, I employed an approach proposed by Valente *et al.* 2017, describing an unbiased and semi-automatic method for the analysis of mitochondrial network structure, taking advantage of a pair of macros built on existing ImageJ plug-ins (Valente *et al*., 2017) – Mitochondrial Network Analysis (MiNA). The MiNA analysis I performed for this study generally provided a confirmation of a more fragmented network upon MxB knock-down in senescent cells. The differences between control and MxB depleted cells were, however, not as clear as it was anticipated based on microscopic images, at least with respect to mean branch length (Figure 5.10 B). The main pitfall of the analysis I identify is the utilised method to generate the skeleton based on a microscopic image. Namely, the skeleton was generated based on a binary images. It is possible, however, not to use a binary image but base the skeleton on fluorescence intensity itself. This prevents from an artefactual fragmentation of a mitochondrion, whose fluorescence intensity might not be equal throughout its length. That is of relevance especially to cells in DIS that possess long, however often not bright mitochondria (linked to previously discussed cessation of mitochondrial retrograde signalling (Vizioli *et al*., 2020)). In the future, I would like to repeat the analysis by optimising the pre-processing steps, such as skeleton generation using "Ridge detection" plugin in ImageJ.

Cao *et al.* (2020) also described mitochondrial ultrastructure using electron microscopy data, specifically cristae structure. They found mitochondria contain large vacuoles and vesiculated cristae upon MxB knock-down. Importantly, cristae abnormalities were found not only in MxB depleted cells, but also after overexpression of a wild type MxB and GTPase defective, dominant negative MxB (K131A). The two latter interventions led to mitochondria

containing atrophied cristae. This finding allows to consider the potential mitochondrial functions of MxB. Generally, dynamins are known to assemble into oligomers and deform cellular membranes. In the case of dynamin, it forms rings and wraps around the necks of budding vesicles during endocytosis (Anggono *et al.*, 2009). DRP1 executes the mitochondrial outer membrane scission during fission (Kamerkar *et al.*, 2018). Is the role of MxB associated with similar processes concerning the inner mitochondrial membrane? This hypothesis stands in line with the observations that the overexpression of wild type MxB leads to cristae depletion, while its knock-down leads to abundant, vesiculated and swollen cristae. Another key question is whether MxB oligomerises in conditions other than a viral infection, specifically inside of mitochondria. It is interesting to consider the link between mitochondrial structural abnormalities and apoptotic stress induced by MxB depletion. Potentially, the abundance of vesicles formed of mitochondrial inner membrane in MxB depleted cells might explain the increased susceptibility of such mitochondria to enter the apoptotic pathway, and in this case a more advanced release of vesicles containing cytochrome *c* and mtDNA. Moreover, the consequences of the initial dysfunction in the form of activated mitochondrial biogenesis potentially lead to a higher number of abnormal mitochondria and an increased risk for apoptotic cascade initiation. Finally, the higher mtDNA content itself might predispose to its higher amounts in the cytosol.

Mitochondrial changes observed upon MxB depletion presented in this chapter encompass also functional changes in terms of mitochondrial bioenergetics and activated mitochondrial biogenesis. The induction of mitochondrial biogenesis mediators - PGC-1α and PGC-1β in proliferating cells, leads to expansion both in terms of mtDNA copy number, although the difference in this respect is rather mild, and network size as assessed based on microscopic images. The analysis of mitochondrial bioenergetics indicates higher basal and maximum respiration. Cao *et al.* (2020) did not specifically measure mitochondrial biogenesis, however, they also reported an increased total mtDNA copy number (Cao *et al*., 2020). These data indicate MxB knock-down elicits a compensatory mitochondrial biogenesis response. In the conditions of cellular senescence that is normally characterised by an up-regulation of mitochondrial biogenesis and mitochondrial expansion at the early stage and ceasing towards the established stage, I observed the process to still be active even 10 days post senescence induction. Despite that, mitochondrial networks are not able to grow larger than in a typical senescent cell. In contrast, mtDNA copy number increases further. Activation of mitochondrial biogenesis upon MxB knock-down in DIS seems not to be able to compensate for the

exacerbated mitochondrial dysfunction as in the case of proliferating cells, manifesting as a more severe respiratory defect in the Seahorse analysis of mitochondrial respiration. Specifically, basal and maximum respiration that are elevated upon MxB knock-down in proliferating cells, in DIS do not reach the typical phenotypes observed for senescent cells. The lack of mitochondrial hyper-fusion may explain the defect, as this process is considered to facilitate ATP generation in the conditions of stress (Das *et al.*, 2020). In conclusion, MxB knock-down induces mitochondrial dysfunction that is associated with activated mitochondrial biogenesis, presumably as a compensatory mechanism. In DIS, MxB knock-down interferes with the normal mitochondrial adaptation to these conditions.

Next to all the mitochondrial phenotypes observed in MxB depleted cells, these cells were also characterised by reduced SASP upon the induction of senescence. Considering the results of the experiment presented in Figure 5.3, revealing that MxB was induced also upon the treatment with ABT-737 that leads to mitochondrial apoptotic stress, it is possible that the presence of cytosolic mtDNA (or other products of mitochondrial permeabilisation) acts as pathogen-resembling trigger leading to MxB induction and nuclear accumulation, facilitating the inflammatory response. Interestingly, a similar phenotype of MxB up-regulation, accumulation at nuclear envelope as well as mitochondrial fragmentation is observed upon the treatment with interferon (Cao *et al*., 2020). How does MxB facilitate the SASP is still an open question. It remains to be elucidated whether MxB that is observed in the nuclear fraction is nuclear or juxtanuclear. I have attempted to address this question by an immunofluorescence approach using the same antibody as used by the authors of Cao *et al.* (2020) study, however, the staining pattern was dispersed in all studied conditions and I decided not to include the data, considering a technical error (such as the age of the antibody) could have interfered with the detection of MxB expression pattern.

If the nuclear localisation of MxB was at the nuclear pores, it might link the SASP to MxB role in cytonuclear trafficking. King *et al*. (2004), the same authors who demonstrated cell cycle arrest as a consequence of MxB silencing, performed an over-expression of a dominant negative MxB mutant that was defective in GTPase activity. This led to an impaired nuclear import, as assessed by the localisation of a fluorescent reporter protein (c-myc-nucleoplasmin core-SV40 T fused to NLS) (King *et al*., 2004). MxB silencing, however, did not result in the same effect, suggesting MxB is not required, but regulates nuclear import. Interestingly, the GTPase activity seems to be required both for its mitochondrial and nuclear function. This finding of the role of MxB in mediating nuclear import is valuable from the

perspective of my study, as an impaired nuclear import could explain the reduction of the SASP upon MxB knock-down. SASP critically depends on the translocation of various transcription factors from the cytoplasm to the nucleus (Chien *et al.*, 2011). The study by King *et al.* (2004) was performed on various cancer cell lines, therefore the question of cytonuclear trafficking, especially of the SASP transcription factors would be worth addressing in the future in the context of MxB knock-down in human primary fibroblasts, IMR90. Potentially, the nuclear translocation of various factors might be differentially affected, depending on the cell type, efficacy of MxB knock-down as well as the specific protein of interest that undergoes translocation.

Alternatively, the mitochondrial alterations occurring in consequence of MxB depletion, might be blocking the development of the SASP. Among the aspects that might affect the SASP, altered mitochondrial network structure is one of them. Upon MxB knock-down, the typical DIS-associated mitochondrial hyper-fusion was not observed. Both MxB depletion and MFN2 depletion (*presented in Chapter 4*) led to mitochondrial fragmentation and SASP reduction. Secondly, the established state of DIS when SASP is activated, is also associated with the cessation of mitochondrial biogenesis (Vizioli *et al.*, 2019). Data presented in this chapter robustly show that mitochondrial biogenesis is activated to a significantly higher degree upon MxB knock-down even at the stage of established senescence. Whether this process might interfere with the normal development of SASP remains to be addressed. Finally, metabolic alterations due to respiratory defects upon MxB knock-down, affecting the sensing of cellular energetic status, such as AMPK, could be involved. These hypotheses are depicted in Figure 5.15.

In the following paragraph, I would like to move away from the consequences of MxB knock-down and concentrate on the behaviour of MxB in DIS. Data demonstrating a changed sub-cellular localisation of MxB during senescence should be considered with caution and as preliminary, however, they open up an interesting avenue for further studies. I would like to speculate on the potential explanations of the presented observations. The changes in MxB sub-cellular localisation: from mitochondrial to nuclear, indicate MxB might potentially be involved in mediating mitochondrial retrograde signalling. Mitochondrial retrograde signalling is defined as a manner of communication between mitochondria and the nucleus. In the stressful situations, it is responsible for carving an appropriate transcriptional response. The observed changes in MxB distribution resemble the behaviour of certain factors involved in mitochondria-to-nucleus communication axes. ATFS-1 in *C. elegans* serves as a flagship

example as its impaired mitochondrial import leads to nuclear translocation and activation of UPR^{mt} (Nargund *et al.*, 2012). Other proteins of this kind are the G-protein pathway suppressor 2 (GPS2) that becomes translocated to the nucleus in the conditions of mitochondrial stress, such as mitochondrial depolarisation (Cardamone *et al.*, 2018) and mitochondria nuclear retrograde regulator 1 (MNRR1) (Aras *et al.*, 2020). Similar to ATFS-1, GPS2 acts as a transcription factor in the nucleus, specifically, it orchestrates the expression of nuclear-encoded mitochondrial genes. On the other hand, MNRR1 indirectly contributes to a transcriptional response, namely via activating transcription factor 5 (ATF5) (Aras *et al.*, 2020). MxB has not been identified to perform functions directly related to gene expression regulation, however, as previously mentioned, it is involved in the nuclear import (King *et al.*, 2004). Could the mitochondrial driven response affect other processes than gene expression, however, such that control it at a different stage?

Another interesting question concerns the mechanism behind differential sub-cellular localisation of MxB during senescence. Do the same species of MxB that translocate out of mitochondria travel to the nucleus? Or alternatively, is the altered sub-cellular distribution of MxB in senescence a consequence of changed localisation of the newly synthesised proteins solely? If the latter case is true, is the mitochondrial import of MxB blocked in cellular senescence? If that was the case, could it contribute to senescence-associated mitochondrial dysfunction? The dynamic distribution of MxB was studied by Cao *et al.* (2020), who found that MxB is able to drastically change its sub-cellular localisation within hours (up to 12 hours) of live-cell imaging, from cytosolic distribution to the formation of large aggregates, repeatedly disassociating into the cytosol. The assessment of the dynamic behaviour of endogenous fluorescently-tagged MxB upon induction of senescence or another mitochondrial stresses associated with MxB up-regulation, would be worth performing in the future. Importantly, expression of MxB should be endogenous only, as its overexpression was also shown to cause abnormal mitochondrial ultrastructure (Cao *et al.*, 2020).

Another open avenue related to the sub-cellular distribution of MxB concerns the signals mediating its specific localisation. MxB found in mitochondria via western blotting was the long isoform, known to contain the nuclear localisation signal (Melén *et al.*, 1996). Is it however certainly the same, NLS-containing variant? What kind of post-translational modifications may be involved in determining MxB mitochondrial or nuclear localisation? In my study on human primary fibroblasts originating from the lung as well as in the study by Cao and colleagues (2020) on human hepatocytes, hepatoma cell lines and HeLa cancer cell line,

the long isoform was consistently more pronounced, upon senescence induction or interferon stimulation, respectively. In the studies by Goujon *et al.* (2013) and Melén *et al.* (1996) who utilised a glioma or glioblastoma cell lines, the shorter isoform was up-regulated upon interferon treatment. This discrepancy might simply result from the usage of different antibodies, however, a better understanding of the function of both isoforms, especially for house-keeping purposes is required. MxA that shares 63% of amino acid identity with MxB and does not contain NLS, is known to localise to the membranes of the smooth endoplasmic reticulum and Golgi-intermediate compartment (Haller *et al*., 2015). Super-resolution microscopy of the endogenous short isoform would be required to reveal a more precise localisation of MxB short isoform. In the context of mitochondria, the mitochondrial isolates could be treated with proteases to reveal MxB localisation at higher resolution, and specifically assign it to the outer membrane, inner membrane or matrix, as performed by Cao *et al.* (2020). Finally, to better understand MxB function, protein-proximity labelling might be harnessed to investigate MxB interaction partners in basal and senescence conditions (Sears *et al.*, 2019).

The data presented in this chapter provide an additional proof that the mechanisms of innate immunity known from the studies on pathogen invasions, overlap with how cells react to sterile, but damaging insults - such as γ-irradiation. They remind that the cellular repertoire of responses to stress is, to a certain degree, common across exogenous and endogenous insults. After the recent ground-breaking publications describing the involvement of cGAS-STING pathway in cellular senescence as a mediator of SASP (Dou *et al*., 2017; Gluck *et al*., 2017; Takahashi *et al*., 2018) as well as other findings standing at the crossroad between innate immunity and cellular senescence (De Cecco *et al*. 2019; Hari *et al*., 2019), the data included in this chapter constitute a basis for another view-changing discovery in the field of cellular senescence, where an anti-viral factor is a key member of the SASP regulatory network.

5.13 Study limitations

Due to time restrictions, some of the experiments included is this chapter have not been performed a sufficient number of times as for publication standards and should be considered as preliminary. The experiments that require a repetition include: the western blot of sub-cellular localisation of MxB, the western blot of MxB knock-down efficiency as well as the Seahorse analysis of cells induced to DIS. With regards to the sub-cellular localisation of MxB, detection of COX1 in nuclei-enriched fraction presents as a major limitation indicating mitochondrial contamination of this fraction. The conclusions based on this experiment in the

presented form should be considered preliminary. The Seahorse analysis of cells in DIS was performed once using five technical replicates per chosen cell density. Similarly, the analyses of mitochondrial apoptotic stress were not performed 3 independent times as in the case of the analyses presented in Chapter 3. In Figure 5.12 B and C, I show data on mtDNA copy number upon MxB depletion. Having observed a trend for an increase in mtDNA copy number in MxB depleted proliferating cells and mitochondrial expansion observed in microscopic images (Figure 5.12 A), I would like to repeat the qPCR experiments measuring mtDNA copy number for a final conclusion regarding the degree of up-regulation of the mtDNA replication.

The experiment aimed at understanding whether over-active caspases might limit the SASP upon MxB depletion should be controlled for the efficacy of the pan-caspase inhibitor, QVD. As I have not observed a strong reduction of SASP in siNT transfected senescent cells, a control experiment, for example measuring the cell death inhibition using the same batch of QVD, should be included. Additionally, an analysis of caspase-3 activation could be assessed in MxB depleted cells. Data in the presented form, do not allow for final conclusions.

Chapter 6. Discussion

6.1 General conclusions and the impact of the presented results

During my PhD project I investigated the biology of mitochondria in cellular senescence from three interrelated angles. I followed up on the existing knowledge on this topic, specifically the findings demonstrating that a) mitochondria in senescent cells are dysfunctional (Dalle Pezze *et al*., 2014; Korolchuk *et al*., 2017; Passos *et al*., 2010) – or with regards to some aspects, adopted to stress conditions, and b) mitochondria are required for the pro-inflammatory phenotype of senescent cells in damage-induced senescence, as their depletion prevents SASP (Correia-Melo *et al*., 2016) and certain mitochondrial stresses alter its typical composition (Wiley *et al*., 2016). In each chapter of this thesis, I attempted to extend the currently available characterisations of mitochondria in senescent cells and test their mechanistic link with the SASP.

In Chapter 3, I demonstrated that processes occurring at mitochondria during apoptosis, to a much smaller degree also affect senescent cells and in this context are referred to as mitochondrial apoptotic stress. Mitochondrial apoptotic stress consists of the formation of BAK and BAX pores, the release of mitochondrial content, including cytochrome *c* and mtDNA into the cytoplasm and sub-lethal caspase activation. By performing a depletion of BAK and BAX, disabling the formation of the outer mitochondrial membrane pores in human fibroblasts, I demonstrated a reduction in the proinflammatory phenotype in damage-induced senescence. Oncogene-induced senescence characterised by a lower mitochondrial apoptotic stress, and higher SASP, differs from damage-induced senescence in terms of SASP regulation. Genetic depletion of BAK and BAX exacerbated SASP, however, a tailored pharmaceutical BAX inhibition ameliorated the SASP also in this model of senescence. Even though senescent cells were found to secrete mtDNA, the levels of circulating mtDNA did not prove as a reliable biomarker of senescence burden in the organismal context in mice and human.

In Chapter 4, I observed that oncogene- and damage-induced senescence present several distinct phenotypes with respect to mitochondrial function, beyond the degree of mitochondrial apoptotic stress described in Chapter 3. Namely, mitochondria in damage-induced senescence were found to respire less efficiently and acquire a hyper-fused phenotype, while mitochondria in oncogene-induced senescence undergo a more active process of mitochondrial biogenesis and are found in a more fragmented state. The process of mitochondrial fusion directed by DRP1 is highly important in all studied conditions, as DRP1 silencing induced or exacerbated

the pro-inflammatory phenotype in proliferating and senescent cells (OIS and DIS), respectively. Inducing mitochondrial fragmentation by MFN2 silencing, thereby preventing the hyper-fused mitochondrial phenotype in damage-induced senescence, reduced the SASP in this model. Mitochondrial hyper-fusion emerges as a potential key regulator of SASP in damage-induced senescence. In contrast, MFN2 silencing in oncogene-induced senescence leads to an elevated level of SASP. Mitochondria in oncogene-induced senescence seem to be highly sensitive to various types of perturbations, such as constitutive BAK/BAX deletion (*Chapter 3*) and shifts in mitochondrial morphology (*Chapter 4*), responding with SASP elevation.

In Chapter 5, I investigated an anti-viral dynamin-related protein, MxB that plays an essential, house-keeping function in mitochondria (Cao *et al*., 2020). In this chapter, I unravelled additional functions of MxB in the context of cellular senescence. I found its levels significantly increase in damage-induced senescence as well as upon the induction of mitochondrial apoptotic stress. Moreover, MxB was found to reside in mitochondria and the nucleus, and to change its sub-cellular localisation in senescence when it is absent in mitochondria and accumulates in the nucleus. The data presented in this chapter suggest that MxB may be participating in the mitochondria-to-nucleus communication axis. Importantly, it regulates the SASP, as its depletion leads to SASP amelioration. MxB role in the SASP regulation may be indirect, due to the role it plays in maintaining mitochondrial integrity, or direct, considering its function related to nuclear import. The data presented in Chapter 5 also indicates that mitochondrial hyper-fusion might be essential for the SASP in damage-induced senescence.

Collectively, the findings within each chapter provide an extension to our current knowledge on mitochondrial biology in cellular senescence. The data presented in Chapter 3 are awaiting publication and after the key findings on the role of cGAS-STING pathway in cellular senescence (Dou *et al*., 2017; Gluck *et al*., 2017; Takahashi *et al*., 2018), contribute to the understanding of the types of cytosolic nucleic acids that may trigger cGAS-mediated inflammation in cellular senescence. Data presented in Chapter 4 constitute a novel observation and point out an important difference between two commonly studied models of cellular senescence: damage- and oncogene-induced senescence. In fact, these findings suggested the two senescence variants should be treated as distinct cellular fates, and the findings related to mitochondria, metabolism and SASP regulation obtained with the use of one model should not be extrapolated to the other. The mechanisms behind the two distinct mitochondrial network morphologies, especially hyper-fusion in the model of DIS, remain to be studied further. The

data presented in Chapter 5 broaden our understanding of MxB mitochondrial function and its role during cellular stress responses. The alteration of sub-cellular localisation of MxB during senescence presents MxB as a promising candidate to study the mitochondria-to-nucleus communication in the context of cellular senescence. The exact mechanism via which MxB regulates SASP remains to be elucidated. Overall, these findings indicate a novel mechanism within innate immunity repertoire that is harnessed by senescent cells, contributing to their pro-inflammatory profile.

6.2 Are cellular senescence and apoptosis duelling fates?

Cellular senescence and the programmed cell death (apoptosis) are thought to be alternative and opposing cellular fates in response to stress (Childs *et al.*, 2014; Marcotte *et al.*, 2004; Wang, 1995). In the simplest view, the choice between the two fates depends on type of stressful stimuli or its "strength" (e.g. intensity or length). Various genotoxic treatments inducing DNA damage serve as examples of a setting where the fate depends on the dose: a low dose induces cellular senescence and a high dose – apoptosis (Chen, Liu, *et al.*, 2000; Song *et al.*, 2005). Secondly, sensitivity of the specific cell type and their "particular wiring" (e.g. expression profile of proteins related to stress resistance/response), contributes to the fate determination (Childs *et al*., 2014). Mechanistic studies explain aspects of this decision-making process (reviewed in Childs *et al*., 2014). These point to p53 as a core player in the cell fate determination in this context. Whether a cell undergoes senescence or apoptosis depends, among others, on p53 expression levels and kinetics, its post-translational modifications, specifically - the acetylation, as well as the interactions within p53 tetramer - its DNA binding domains, affecting the preferred target genes' expression (Geva-Zatorsky *et al.*, 2006; Kracikova *et al.*, 2013; Murray-Zmijewski *et al.*, 2008; Purvis *et al.*, 2012). Another key determinant of cell fate is the level of p21, which is in an inverse relationship with apoptosis sensitivity (Chen *et al*., 2000; Yosef *et al*., 2017). Additional mechanisms of apoptosis inhibition are executed via overexpression of proteins from BCL-2 family, which prevents the execution of MOMP as well as down-regulation of caspase-3 (Marcotte *et al*., 2004; Wang *et al*., 1995; Zhu *et al*., 2015). These mechanisms are critical for senescent cells' survival, "locking" the decision on entering cellular senescence and inhibiting apoptosis (Yosef *et al*., 2016; Zhu *et al*., 2015).

The findings in this thesis suggest, however, the apoptosis inhibition might not be fully efficient. How the limited apoptotic signalling is possible despite its specific inhibition remains

an unanswered question. One possibility is that mitochondrial dysfunctions might become severe and at the minority of mitochondria, inevitably trigger apoptotic cascade. Secondly, in accordance with the data presented in Figure 3.2 B, mitochondrial apoptotic stress may begin prior to the initiation of the anti-apoptotic signalling – the kinetics of which requires a thorough assessment. Nevertheless, the observation of a limited mitochondrial apoptotic stress during cellular senescence – a seemingly opposite to apoptosis cell fate, calls for a reconsideration of the question asked already several years ago, namely whether these two fates are duelling (Childs *et al*., 2014). My view at the relationship between these processes proposes that cellular senescence and apoptosis are not duelling only at the initial decision-making step. At least at the mitochondria, they remain in a continuous conflict, throughout the life-span of a senescent cell. Mitochondria might be seen as the key cell fate determinants, maintaining the decision of survival despite dysfunction. In a slightly different view, senescence may be the outcome of the conflict between apoptosis and cell survival. Importantly, mitochondrial apoptotic stress seems to be a key for the SASP in damage-induced senescence, meaning senescence requires apoptosis to happen at a considerably smaller scale, for its typical phenotypic manifestation. This, on the other hand, suggests that the fates are not duelling, they are closely intertwined, utilizing the same executory mechanisms.

The pro-apoptotic signalling described in the previous paragraph has been investigated at the relatively early stage of the established senescence. Similarly, the apoptotic resistance has rarely been tracked later than 10 days post senescence induction. Wang *et al.* (2016) performed a study on the late stages of damage-induced senescence (by doxorubicin) and replicative senescence in human foreskin fibroblasts. In the study they compared cells 10 and 21 days post senescence induction, and the passages PD38 and PD50, respectively (Wang *et al.*, 2016). The authors found a considerably higher proportion of apoptosis within the senescent cells' population at the late stage of senescence versus the earlier stage (10 days after senescence induction), established stage using two alternative methods. They observed that the decrease in survival is associated with a significant reduction in mitochondrial membrane potential (D. Wang *et al*., 2016). Fumagalli *et al.* (2014) confirm that at least some cell types and senescence models, for example pre-mature oxidative stress induced senescence in lung fibroblasts WI-38, are characterised by a decreased survival with time, while replicatively senescent fibroblasts BJ are not . This indicates that some cell types might be more prone to the cell death when senescent. Whether the progression of the apoptotic cascade beyond the minority of mitochondria, is directly responsible for the reduced survival of senescent cells in long-term

culture, remains to be determined. If so, the "internal conflict" occurring at the mitochondria - allowing for and restricting apoptotic signaling – may eventually lead to the cell's suicidal death.

6.3 Mitochondrial apoptotic stress – another deleterious process during ageing

Even though the biology of ageing has been flourishing over the past decade, gaining attention of the scientists from different fields, the question of what ageing is, still remains a mystery. Among various theories that contributed to our understating of ageing as of now, I would like to briefly describe the concepts of damage accumulation and deleteriome (Gladyshev, 2013, 2016; Harman, 1972; Orgel, 1973), as the foundations of ageing, as well as discuss where the observed process of mitochondrial apoptotic stress at the minority of mitochondria may be added within this framework of thinking.

The build-up of numerous forms of molecular damage as the fundamental cause of ageing has been discussed for several decades, starting from the views on the specific types of molecular damage – for example as in the case of the oxidative theory of ageing (Harman, 1972). Molecular damage encompasses various changes to the macromolecules as well as the accumulation of the side products of housekeeping processes that are not efficiently repaired or diluted (Ogrodnik, Salmonowicz, & Gladyshev, 2019). In a yet wider understanding, other consequences of "biological imperfectness" make up the deleteriome, an umbrella term, that besides macromolecular damage also concerns the fluctuations in gene expression, metabolite levels, expression of unwanted genetic elements, such as retrotransposons, metabolic remodelling, epigenetic drift *etc*. that all add to "the inherent noise, infidelity, and heterogeneity associated with cellular life" (Gladyshev, 2013).

There is abundant evidence that macromolecular damage and cellular senescence are closely linked, where the first is an inducer of the latter (Gorgoulis *et al.*, 2019; Toussaint *et al.*, 2000; Toussaint *et al.*, 2002). Moreover, many variants of cellular senescence depend on a damage amplification loop, with the induction and maintenance of DNA damage is a key senescence process (DDR-dependent cellular senescence) (Aird *et al*., 2013; Passos *et al*. 2010). This concept is widely accepted, however – to me – it is still astonishing that as a part of a cellular stress response, an already damaged cell needs to maintain a certain damage-level. Maintaining damage limits the proliferation, however it adds to the cell and system's dysfunction. In a recent conceptual piece I co-authored, senescence was discussed from the perspective of additional damage amplification processes, some potentially resulting from

initial damage-induced dysfunction, such as overburdened quality control and degradation systems (Ogrodnik, Salmonowicz, & Gladyshev, 2019).

The results of this thesis point out another mechanism that may clearly be considered as a type of an intracellular damage. Until recently, MOMP has been seen as an all or nothing event – by eliminating a dysfunctional cell, it would not be able to exert long-term consequences (Ichim *et al*., 2015). As of now, multiple studies demonstrate this process – referred to as miMOMP, mitochondrial apoptotic stress, limited apoptotic signalling or mtDNA leakage – is found as a part of various cellular stress responses and innate immunity mechanisms (Brokatzky *et al.*, 2019; Riley *et al.*, 2020; Shimizu *et al.*, 2020; West *et al.*, 2017). These advances point out two detrimental aspects of mitochondrial apoptotic stress from the viewpoint of the ageing theories.

First, mitochondrial apoptotic stress constitutes a damage amplification process, being shown to induce DNA and proteome damage due to caspase activation (Buendia *et al.*, 1999; Ichim *et al.*, 2015). Therefore, it is not only the stochastic damage or the consequences of inefficient repair, drift and system overload that occur with ageing, but also parts of programmed cellular stress responses that may wreak havoc on cellular systems to further contribute to age-related damage accumulation. By using the word "programmed" I need to highlight that by it is not a programmed ageing process, it is just the utilisation of short-term beneficial programmes, of which long-term consequences evolution is blind to.

The second point concerns the umbrella term of deleteriome – besides all the previously mentioned age-related changes, mitochondrial apoptotic stress constitutes an example of a possibly larger group of deleterious events: sub-cellular mis-localisation and compartment mixing. Protein mis-trafficking is widely studied and its consequences linked to diseases, such as cystic fibrosis (Hegde *et al.*, 2019). Here, however, I leave aside trafficking errors and rather speculate on how an event of mitochondrial apoptotic stress with the release of mitochondrial content might affect the cytosolic environment. There is no experimental evidence that I am aware of demonstrating the consequences of this process in the context of ageing. It is possible, however, to envision consequences of mitochondrial content release, including DNA, RNA, proteins such as AIF, cytochrome *c*, SMAC *etc.* on the processes other than sensing of cytosolic DNA, inflammasome or apoptosome assembly (Bao *et al.*, 2007; Shimada *et al.*, 2012; West *et al.*, 2015). One of the possible consequences of mitochondrial inner membrane herniation and rupture could be a localised change in pH. In fact, by utilizing pH-dependent mutants of GFP fluorescence protein, Matsuyama *et al.* (2000) demonstrated that apoptotic stimuli such as BAX

overexpression, treatment with staurosporine or UV irradiation induce mitochondrial alkalinisation and cytosol acidification (Matsuyama *et al.*, 2000). Changes in protein interactions upon the release of mitochondrial content as well as pH changes might temporarily disturb the local homeostasis, impacting on the folding of the cytosolic counterparts. Whether such changes have any significant effects on a cell, remains to be elucidated. Here, I propose that mitochondrial apoptotic stress might have other deleterious consequences and contribute to the increasing deleteriome by a) constituting a damage amplification process and b) contributing to the compartment mixing that may, in turn, affect protein folding and signal transduction.

6.4 Updating the definition of cellular senescence

The findings presented throughout this thesis, reveal a number of key differences in mitochondrial biology and SASP between two commonly studied models of cellular senescence, oncogene- and damage-induced senescence. Even though the awareness of senescence mechanisms' diversity is present in the field's scientific discourse (Hernandez-Segura *et al.*, 2018), my data constitute another reminder that a nomenclature system that will not obscure the diversity, is needed. Various articles, especially review articles, still do not always specify and highlight which senescence type is discussed, especially when discussing metabolic and mitochondrial aspects of the senescence programme (Amaya-Montoya *et al.*, 2020; Gorgoulis *et al.*, 2019; Herranz *et al.*, 2018). This unintentionally promotes ignorance. Paradigms promoting a unified definition of senescence gain great attention both among lay public, as well as scientific community. At the bench, however, biology does not always conform. The potential consequences of findings' extrapolation across senescence variants may have negative consequences at, arguably, the most important stage of biomedical discoveries - clinical trials. A similar problem of nomenclature simplifications has been noticed within the field of cell death, which has advanced coining new terms describing death variants (Fink *et al.*, 2005). The term senescence (from Latin: *senesce,* to grow old) itself will likely not fall out of use, even though the observed phenomenon is in many cases an irreversible stress response or "cellular progeria", often not a simple cellular ageing. The precise description and distinction of cellular senescence pathways in original research and review articles should lead to an even higher awareness of their diversity. The need of finding a common senescence signature that would allow to estimate senescence burden in an organism and assess the efficacy of senomorphic therapies, motivates many researchers (Casella *et al.*, 2019; Hernandez-Segura *et*

al., 2017; Sharpless *et al.*, 2015). This links to the assumption that elimination of any senescent cells will bring desired clinical outcomes, which recently has been questioned (Chu *et al.*, 2020; Grosse *et al.*, 2020). In my opinion, it is worth discussing an alternative view, where specific signatures related to macromolecular damage, signalling pathways and metabolism of senescence variants are sought after, thereby preventing the oversimplification of the remarkable concept of senescence and leading to the better future outcomes of senotherapies.

6.5 Cellular senescence – an anti-viral mechanism?

Cellular senescence has been found to appear in various physiological and pathological settings – playing a role in animal development, tissue remodelling and regeneration, as a tumour suppressor as well as a response to cellular damage (Kowald *et al.*, 2020). The idea that cellular senescence might have evolved as a host anti-viral defence is another fascinating concept that, so far, has only been mentioned in several research articles (Baz-Martínez *et al.*, 2016; He *et al.*, 2017; Reddel, 2010). The premises behind this theory include the fact that certain viruses rely on host's cell proliferation for viral replication (Baz-Martínez *et al.*, 2016; Reddel, 2010) and the fact that the SASP is exactly what infected cells need in order to recruit immune system and counteract the progression of infection (He *et al.*, 2016). In line with this, lie the studies demonstrating that viral infections, such measles virus, HIV-1, Epstein–Barr virus and respiratory syncytial virus (RSV), induce cellular senescence (Chuprin *et al.*, 2013; Malavolta *et al.*, 2020; Martínez *et al.*, 2016). In fact, my observations from multiple rounds of lentiviral transduction on human primary cells, such as MRC5 and IMR90, performed during the research for this thesis, indicate that this procedure itself, induces a cell cycle arrest (transiently, when the procedure is optimised) and enlarged cell morphology (unpublished observations). The fact that some viruses encode oncoproteins that interfere with p53 and RB pathways provides another evidence that counteracting senescence might constitute a viral defence system (He *et al.*, 2017). Moreover, additional literature provides indirect evidence that stress responses to viral infections are convergent with the phenotypes characterising senescence in other settings. These include the canonical elements of the senescence programme, such as elevated nuclear DNA damage (Machida *et al.*, 2010) and SASP (Brokatzky *et al.*, 2019), but also the phenomena described for the first time in this thesis in the context of cellular senescence, namely mitochondrial apoptotic stress (Brokatzky *et al.*, 2019). For example, hepatitis C virus (HCV) infection was shown to induce mitochondrial permeability transition – a prerequisite for mtDNA leakage, followed by increased ROS production, DNA damage and STAT3 activation

(Machida *et al*., 2006). Based on this set of measures, mitochondrial apoptotic stress is likely to occur in these settings. Only last year, another study advanced the characterisation of mitochondrial apoptotic stress in the context of viral, bacterial, and protozoan pathogens (Brokatzky *et al*., 2019). Importantly, similarly to the data presented in this thesis, these authors provided a mechanistic link between BAK/BAX involvement and pro-inflammatory phenotype upon pathogen invasion (Brokatzky *et al*., 2019), pointing out that mitochondrial apoptotic stress might be the key convergent mechanism between sterile and non-sterile cellular stress responses.

Apart from mitochondrial apoptotic stress, alterations to mitochondrial network morphology also occur in virus-infected cells. Whether mitochondrial network shifts towards fusion or fission depends on several factors, such as the length of time after infection and the type of virus (Barbier *et al.*, 2017; Kim *et al.*, 2014; Yu *et al.*, 2015). Also, it is interesting to consider that some of the mitochondrial changes might be innate, anti-viral mechanisms and some viral immune evasion, as viruses are described to specifically interfere with mitochondrial regulatory proteins (Castanier *et al.*, 2010; Shi *et al.*, 2014; Yu *et al.*, 2015). From the perspective of this discussion where I aim to compare cellular senescence to the phenotypes acquired by virus-infected cells, the mitochondrial adaptations that stimulate anti-viral signalling are of interest. In general, it is thought that mitochondrial hyper-fusion mediates anti-viral signalling (Castanier *et al*., 2009; Kim *et al*., 2018). Mitochondrial anti-viral signalling protein (MAVS) is an anti-viral adaptor protein localised to the mitochondrial outer membrane and mitochondria-associated membranes. It becomes activated by cytosolic pathogen recognition receptors, such as retinoic acid-inducible gene I (RIG-I) and melanoma differentiation-associated protein 5 (MDA5) (Kim *et al*., 2018). Upon activation of MAVS, a multimeric signalling complex - MAVS signalosome, is assembled (composed of, among others, TBK1 and IRFs). The MAVS signalosome facilitates the synthesis of interferons. Mitochondrial elongation achieved through silencing of DRP1 enhances anti-viral response via RIG-like receptors and MAVS, while mitochondrial fragmentation through MFN2 and OPA1 knock-down reduces it (Castanier *et al.*, 2010; Kim *et al.*, 2014; Onoguchi *et al.*, 2010). These findings are accordance with my results presented in Chapter 4, where DRP1 knock-down resulted in exacerbated expression of IL6 and IL8, while MFF2 knock-down had an opposite effect. Moreover, mitochondrial hyper-fusion induced by loss of DRP1 was shown to promote NLRP3 inflammasome activation in macrophages (Park *et al.*, 2015). These studies provide additional insight for a better understanding of why mitochondrial hyper-fusion might be

required for SASP in damage-induced senescence. It is puzzling, however, why the treatment with interferon induces the opposite phenotype, namely mitochondrial fragmentation (Cao *et al.*, 2020). Possibly, exogenous interferon levels exert a negative feedback loop, where mitochondrial fragmentation limits further production of MAVS downstream target genes, the interferons. In conclusions, even though the changes to mitochondrial morphology upon viral infections are far from being consistent, the innate mechanisms facilitating pro-inflammatory signalling are convergent with changes observed during damage-induced senescence (Kim *et al.*, 2018).

The data presented in Chapter 5 open a novel avenue for the exploration of innate immunity mechanisms in cellular senescence. An anti-viral protein, MxB, thus far known to be up-regulated solely in virus-related settings, was now also shown to be up-regulated during damage-induced senescence. As of now, it is not clear whether MxB plays a specific role in induction or establishment of senescence or is up-regulated as a "side effect" of other interferon-stimulated genes' overexpression. It has to be stated, however, that the transcriptomic data from Correia-Melo *et al.* (2016) indicate interferon-stimulated genes are not consistently up-regulated in DIS of MRC5. Besides, the work by De Cecco *et al.* (2019) indicates that interferon-stimulated genes are only expressed at late stages of senescence (beyond 30 days post senescence induction) (De Cecco *et al.*, 2019). MxB, however, becomes up-regulated very early upon senescence induction. This suggests that MxB elevation might not be a side effect, but a designated regulatory mechanism of senescence. However, more research is needed to better define the regulation of MxB expression.

In summary, these data and considerations provide another argument pointing out the similarity between cellular senescence and anti-viral responses. In the strict "evolutionary meaning", it is possible that the mechanisms are convergent - or, by having evolved from the same type of cellular stress response, homologous.

6.6 (.6) Ageing – and the burning of it

One of the theories of ageing, known as inflammaging (from Latin *inflammatio*; kindling for setting fire), identifies a progressive, low-grade inflammation or in another definition, a chronic stimulation of innate immune system, as a key process contributing to age-related pathologies (Franceschi *et al.*, 2000). This concept has been discussed and developed over the past two decades and recently, gained even more attention due to severe acute respiratory syndrome coronavirus, SARS-CoV-2, pandemic (Bektas *et al.*, 2020; Malavolta *et al.*, 2020). The world's

eyes turning to inflammation is due to the fact that conditions associated with increased chronic inflammation, such as ageing, diabetes, obesity, hypertension, metabolic syndrome, cancer *etc.* predispose to a severe course of the COVID-19 disease with respiratory failure, septic shock, multiple organ dysfunction and death (Ragab *et al.*, 2020). Mechanistically, in the conditions of elevated basal inflammation, a pathological and uncontrolled inflammatory response is elicited upon viral invasion, referred to as cytokine storm syndrome (CSS) that leads to further tissue damage and organ failure (Bektas *et al.*, 2020; Kelley *et al.*, 2020; Ragab *et al.*, 2020). By looking specifically at the circulating factors, these that characterise inflammaging - IL6, IL8, TNF, C-reactive protein (CRP), IL1 - overlap with the ones that are over-produced during the course of severe COVID-19, such as IL6, TNFα, IL1β, IFNγ, IP-10, CRP (Bektas et al,. 2020). Importantly, not only the pre-existing inflammation as a predisposing factor for the severe course of the disease is discussed in the context of inflammaging. The consequences of the disease are also described as mimicking inflammaging, or even accelerating it and resulting in physical and cognitive decline, commonly referred to as frailty (Bektas *et al*., 2020). These findings indicate that similar mechanisms underlying inflammaging also modulate the course of COVID-19 and its long-term consequences. Apart from acute syndromes as caused by SARS-CoV-2, chronic and persistent pathogen infections, such as cytomegalovirus or bacterial – periodontitis, were also shown to result in elevated inflammation and biological age (Ebersole *et al.*, 2016; Franceschi *et al.*, 2007; Kananen *et al.*, 2015; Koch *et al.*, 2006; Schmaltz *et al.*, 2005).

Cellular senescence has been accepted as one of the key mediators of the chronic inflammation (Franceschi *et al.*, 2017; Furman *et al.*, 2019; Olivieri *et al.*, 2018). Recently, cellular senescence has been discussed also as a key pro-inflammatory process in the context of COVID-19. This is due to the fact that advanced age and chronic, age-related diseases are associated with a high cellular senescence burden (Gorgoulis *et al.*, 2019). Moreover, as described in the section 6.5, cells invaded by the viruses may acquire a senescence-like phenotype, employing a pro-inflammatory phenotype to counteract the infection (Malavolta *et al.*, 2020). Additionally, prolonged cytokine signalling due to virus infection and cellular senescence may induce more cells to enter senescence (da Silva *et al.*, 2019; Nelson *et al.*, 2012). From the clinical perspective, three following points are debated: a) initial cellular senescence burden may affect the course of the COVID-19 (Malavolta *et al*., 2020); b) cellular senescence may be induced by the viral invasion and contribute to inflammation and tissue dysfunction (Malavolta *et al*., 2020); c) cellular senescence arises as a consequence of the viral

disease possibly contributing to the long-term consequences, such as frailty (Bektas *et al*., 2020). For these reasons, cellular senescence becomes a subject of the studies in the context outside of the age-related chronic pathologies, but as phenomenon that mediates severe course of acute conditions that may, however, be targetable.

In this section, I would like to consider what stimuli at the most basic level "fuel" inflammaging and for whose cellular senescence may constitute a "common denominator". Thus far in this thesis, damage-associated molecular patterns (DAMPs) such as leaked mitochondrial content and fragments of damaged mitochondria, including extramitochondrial mtDNA were discussed as the triggers of inflammation in the context of senescence. Senescent cells have already been identified as a source of DAMPs in the context of inflammaging (Franceschi *et al*., 2017). Moreover, exogenous agents such as bacteria and viruses – described in the sections above - belong to pathogen-associated molecular pattern (PAMPs) category of inflammatory triggers. These, however, contribute to inflammation not only by a direct activation of innate immune pathways but also by increasing the level of DAMPs, for example via causing mitochondrial apoptotic stress and DNA damage (Brokatzky *et al*., 2019; West *et al*., 2015) – possibly contributing to senescence development. Besides the DAMPs and PAMPs, there are additional stimuli that drive inflammaging, exact nature of which is beyond the scope of this thesis. In brief, these may include microbiota that change in composition with age and disease, amplifying the pathobionts' counterpart and may constitute another source of PAMPs (Franceschi *et al.*, 2018). Moreover, food contained nutrients, especially when ingested in excess may present as pro-inflammatory stimuli (Franceschi *et al.*, 2018). Obesity and metabolic syndrome have previously been associated with a burden of cellular senescence (Burton *et al.*, 2018; Gorgoulis *et al.*, 2019; Tchkonia *et al.*, 2010), supporting the role of nutrients in driving inflammation via senescence. Notably, both DAMPs and PAMPs are detected by a similar set of innate immune receptors, known as pattern-recognition receptors (PRRs), including TLRs, NOD-like receptors, cGAS and aryl hydrocarbon receptor (AHR) present on the cell surface and in the cytoplasm, activation of which leads to the production of a multitude of pro-inflammatory factors (Franceschi *et al.*, 2018). Some of these innate immunity receptors have been robustly implicated in cellular senescence (Acosta *et al*., 2013; Davalos *et al*., 2013; Dou *et al*., 2017; Gluck *et al*., 2017; Hari *et al*., 2019). The exact composition and strength of the resulting pro-inflammatory phenotype depends on the trigger and is modulated by a multi-layer regulatory network, as described in section 1.1.4.2 in the context of cellular senescence. The fact that a broad range of pro-inflammatory triggers

converge into a more limited range of damage sensors and diverge again into a variety of inflammatory compounds, is described as a "bow tie" architecture of the inflammaging machinery (Franceschi *et al*., 2018). Considering that among each sensor type, for example TLR, there are several variants (10 TLRs in humans) (Barreiro *et al.*, 2009), I would not like to ignore the complexity of each system. However, it is probably safe to state that the sensing systems are to a degree degenerate and less numerous that the potential inputs. Cellular senescence, in general – leaving aside its type-specific nuances – may also be seen as a "node" of the "bow tie". Here I chose to illustrate this concept in the form of a bonfire (inverted "bow tie") (Figure 6.1). Cellular senescence is included in the scheme as a "common denominator" between the inflammatory stimuli and signalling effectors (depicted as a burning coal).

Among the key future perspectives related to the concept of inflammaging and cellular senescence, I would list the following as critical and promising: a) identification of the inflammaging stimuli from a personalised perspective, *i.e.* affecting an individual's inflammatory status, including, among others, immune-biography - a history of lifetime exposure to pro-inflammatory stimuli that affect future inflammatory responses, as well as cellular senescence burden related to a particular conditions, for instance, cigarette smoking or chemotherapy (Franceschi *et al*., 2018) and finally, individual nutrient sensitivities; b) the role of cellular senescence as a common denominator of inflammation resulting from different triggers, beyond the typical age-associated conditions, including acute syndromes such as COVID-19, and finally; c) the role and identity of anti-inflammatory processes that allow the centenarians to thrive despite not being spared from inflammaging (Franceschi *et al*., 2017), so to say "endogenous senostatics".

I hope the results presented in this thesis will help to a) better understand how the pro-inflammatory status of senescent cells develops as well as to design novel senomorphic strategies in might to ameliorate inflammaging; b) increase awareness of the differences between types of senescence that might prove critical for the outcomes of senotherapies and finally, c) broaden the understanding of innate immunity mechanisms employed by senescent cells. Acknowledging that fuelled by diverse stimuli, age-associated inflammatory processes with cellular senescence as a central node, are the common mechanism responsible for ageing as we know it.

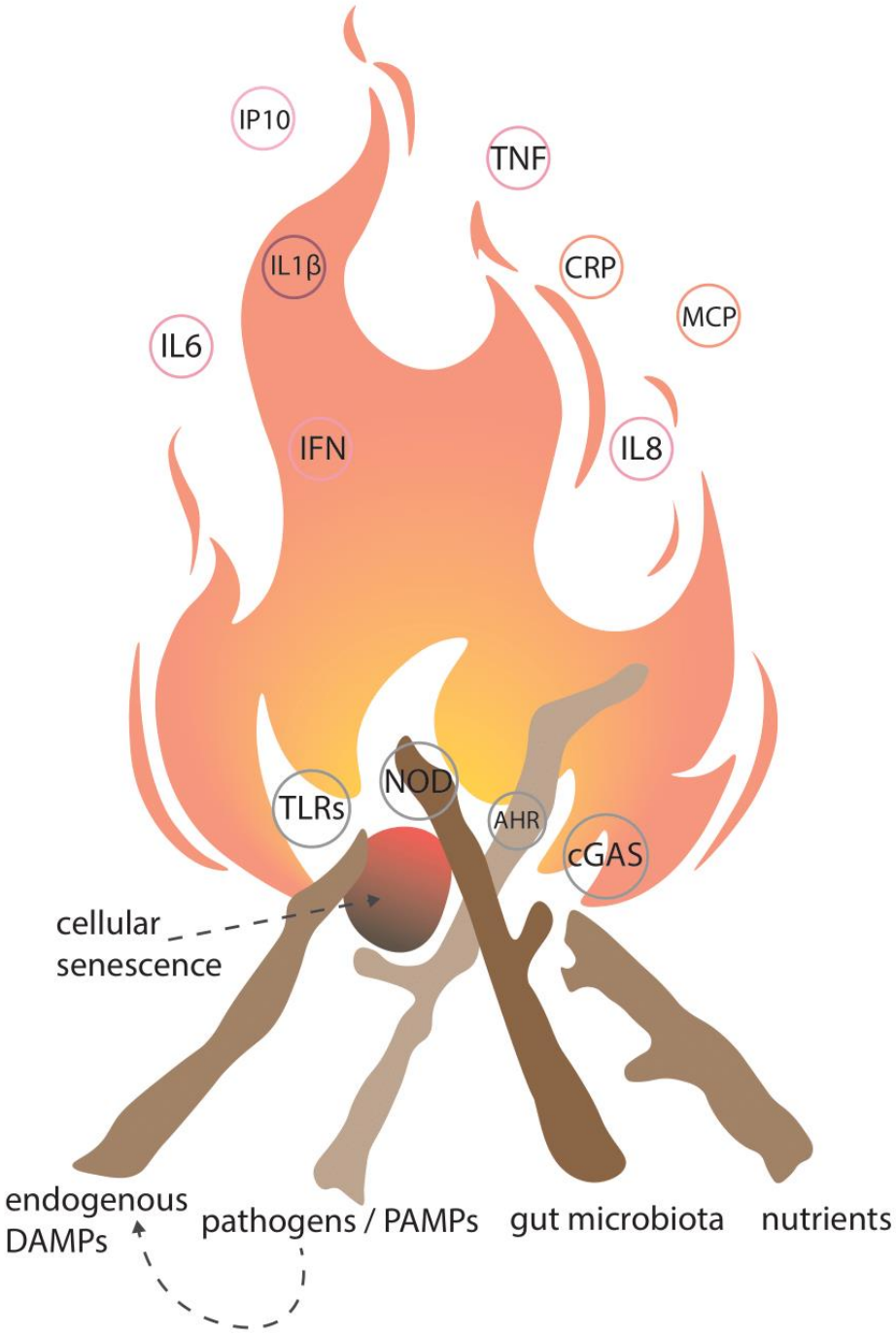

Figure 6.1: Inflammaging

The presence of elevated, low-grade inflammation characterises the ageing process. It results from various triggers: endogenous and exogenous stresses, such as cell/tissue damage, microorganism exposure, including the microbiota and the ingested compounds/nutrients. Cellular senescence may be considered a common mechanism resulting from the exposure to a variety of pro-inflammatory stimuli and mediate the process of inflammation.

Appendix

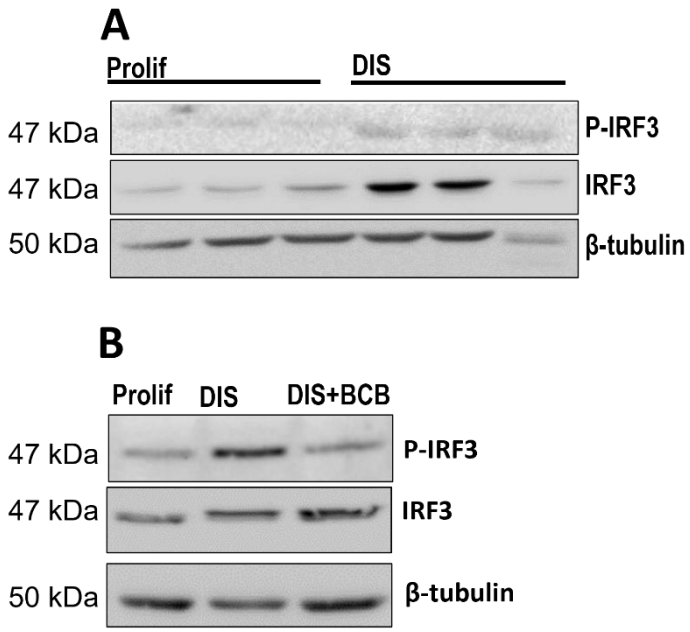

Figure 1: Activation of cGAS-STING pathway in human embryonic fibroblasts, MRC5 and the effects of BAX inhibition

(A) Western blot for P-IRF3 and total IRF3, n=3 independent experiments **(B)** Western blot for P-IRF3 and total IRF3 upon the treatment with BCB at 2.5uM, representative of n=2 independent experiments/wells.

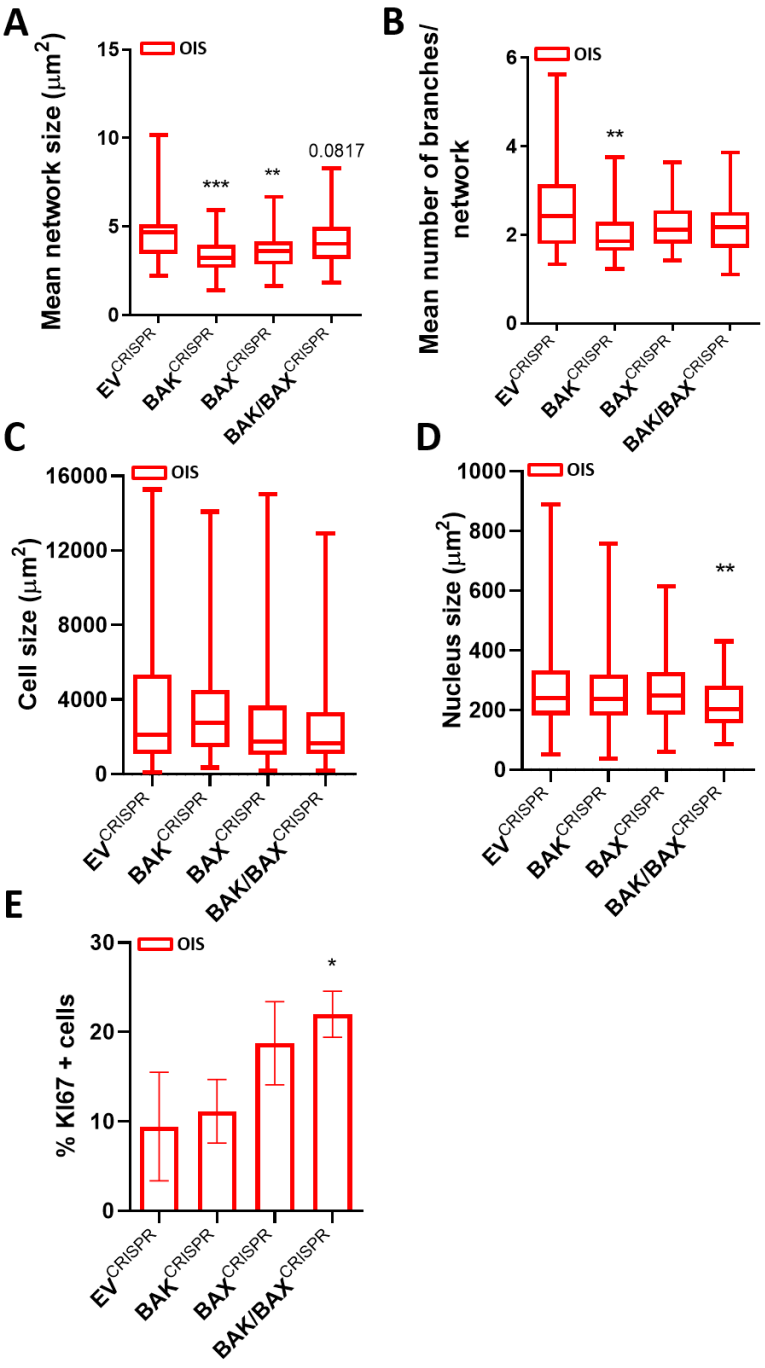

Figure 2: Allometric characterisation of human embryonic fibroblasts in OIS upon BAK/BAX single and double knock-out

(A) Measurement of the mean mitochondrial network size using MiNA plugin, n=minimum 38 cells in total/condition, pool from 2 independent replicates/coverslips. Analysed using Mann-Whitney test: OIS EV vs OIS BAK p=0.0001, OIS EV vs OIS BAX p=0.0070, OIS EV vs OIS BAK/BAX p=0.0817 **(B)** Measurement of the mean numer of branches per mitochondrial network using unbiased MiNA macro, n=minimum 36 cells in total/conditio, pool from 2 independent replicates/coverslips. Analysed using Mann-Whitney test: OIS EV vs OIS BAK p=0.0090, OIS EV vs OIS BAX p=0.2467, OIS EV vs OIS BAK/BAX p=0.1002 **(C)** Cell size in μm^2 , n=minimum 100 cells/condition, pool from 2 independent replicates/coverslips. Analysed using Mann-Whitney test: OIS EV vs OIS BAK p=0.5046, OIS EV vs OIS BAX p=0.2696, OIS EV vs OIS BAK/BAX p=0.1438 **(D)** Nucleus size in μm^2, n=minimum 100

cells, pool from 2 independent replicates/coverslips, 1-way ANOVA. Analysed using Mann-Whitney test: OIS EV vs OIS BAK p=0.9156, OIS EV vs OIS BAX p=0.8046, OIS EV vs OIS BAK/BAX p=0.0039 **(E)** Quantification of the percentage of cells positive for cel proliferation marker, Ki67, n=3 independent experiments/minimum 20 cells/replicate. Analysed using unpaired Student's t-test: OIS EV vs OIS BAK p=0.7489, OIS EV vs OIS BAX p=0.1850, OIS EV vs OIS BAK/BAX p=0.0446. Error bars represent Min to Max for A-D, error bars represent SEM for E.

A

Model	mtDNA copy number/1ul ~ Intercept + Frailty + BMI + Gender				
Analysis of Variance	SS	DF	MS	F (DFn, DFd)	P value
Regression	4.79E+17	7	6.84E+16	F (7, 85) = 0.6978	P=0.6737
Frailty	3.45E+17	5	6.89E+16	F (5, 85) = 0.7031	P=0.6226
BMI	1.83E+17	1	1.83E+17	F (1, 85) = 1.869	P=0.1752
Gender	4.35E+15	1	4.35E+15	F (1, 85) = 0.04433	P=0.8338

B

Model	mtDNA copy number/1ul ~ Intercept + Frailty + BMI				
Analysis of Variance	SS	DF	MS	F (DFn, DFd)	P value
Regression	3.73E+17	2	1.86E+17	F (2, 35) = 2.846	P=0.0716
Frailty	2.66E+17	1	2.66E+17	F (1, 35) = 4.068	P=0.0514
BMI	8.05E+16	1	8.05E+16	F (1, 35) = 1.229	P=0.2752

Figure Figure 3: Circulating mtDNA in human plasma – multiple linear regression analysis

(A) Multiple linear regression analysis of mtDNA D-loop concentration human plasma detected via qPCT, expressed as mtDNA D-loop region copy in 1 µl of plasma and with BMI, n=93 subjects, mixed gender **(B)** Multiple linear regression analysis of mtDNA D-loop concentration human plasma detected via qPCT, expressed as mtDNA D-loop region copy in 1 µl of plasma and with BMI, n=38 subjects, females. SS = sum of squares, DF = degrees of freedom, MS = mean square, F= F-statistics.

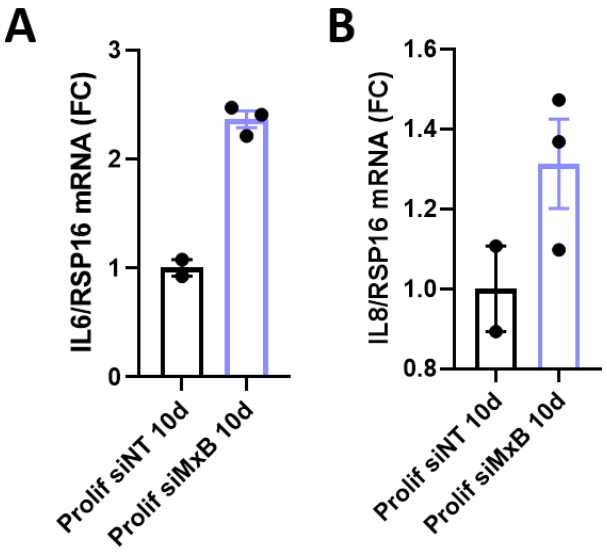

Figure 4: SASP upon MxB knock-down – 10 days after siRNA transfection

(A) IL6 mRNA levels via qPCR normalised to RSP16 using Delta-Delta Ct method upon MxB knock-down, n=2 independent replicates/wells for siNT and 3 independent replicates/wells for siMxB. **(B)** IL8 mRNA levels via qPCR normalised to RSP16 using Delta-Delta Ct method upon MxB knock-down, n=2 independent replicates/wells for siNT and 3 independent replicates/wells for siMxB. Error bars represent SEM. Experiment carried out in collaboration with Dr Stella Victorelli.

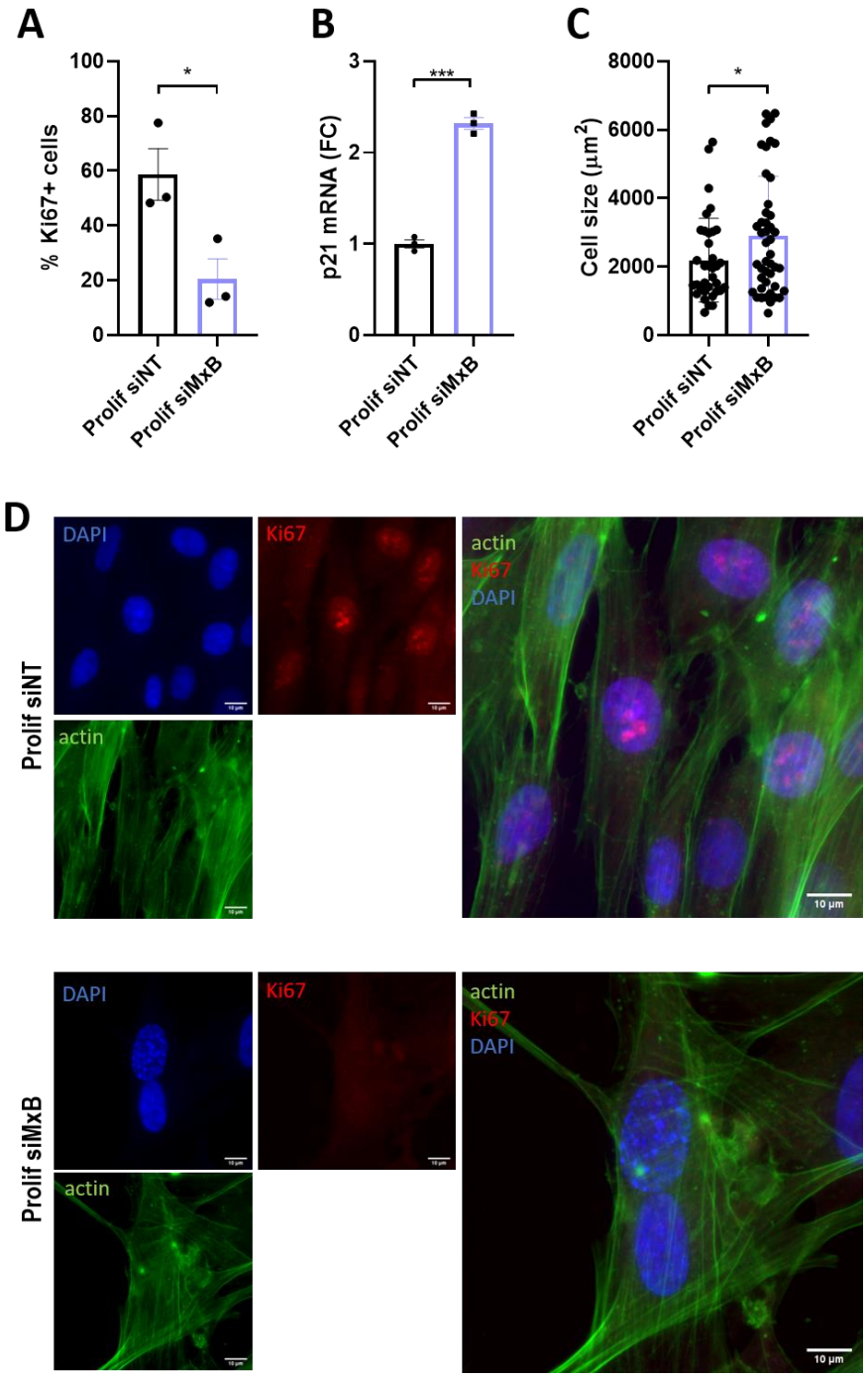

Figure 5: Markers of cell cycle arrest upon MxB knock-down

(A) Quantification of Ki67-positive cells based on immuno-fluorescence staining using an anti-Ki67anibody, a proliferation marker, actin staining using Alexa Fluor™ 488 Phalloidin and nuclei stained with DAPI, n=3 independent replicates/coverslips, at least 500 cells/condition in total, Student's t-test: Prolif siNT vs Prolif siMxB p=0.0331 **(B)** p21 mRNA levels via qPCR normalised to RSP16 using Delta-Delta Ct method upon MxB knock-down, n=3 independent replicates/wells, Student's t-test: Prolif siNT vs Prolif siMxB p<0.0001, **(C)** Cell size in μm^2 , n=minimum 30 cells/conditions in total across 2 independent replicates, **(D)** Representative images of proliferating IMR90 stained using an anti-Ki67antibody, a proliferation marker, actin using Alexa Fluor™ 488 Phalloidin and DAPI. Scale bars represent 10µm. Error bars represent SEM for A and B, error bars represent SD for C. Experiment shown in A and D done in collaboration with Dr Mikolaj Ogrodnik.

References

Abdisalaam, S., Bhattacharya, S., Mukherjee, S., Sinha, D., Srinivasan, K., Zhu, M., . . . Asaithamby, A. (2020). Dysfunctional telomeres trigger cellular senescence mediated by cyclic GMP-AMP synthase. *J Biol Chem, 295*(32), 11144-11160. doi:10.1074/jbc.RA120.012962

Acosta, J. C., Banito, A., Wuestefeld, T., Georgilis, A., Janich, P., Morton, J. P., . . . Gil, J. (2013). A complex secretory program orchestrated by the inflammasome controls paracrine senescence. *Nat Cell Biol, 15*(8), 978-990. doi:10.1038/ncb2784

Acosta, J. C., O'Loghlen, A., Banito, A., Guijarro, M. V., Augert, A., Raguz, S., . . . Gil, J. (2008). Chemokine signaling via the CXCR2 receptor reinforces senescence. *Cell, 133*(6), 1006-1018. doi:10.1016/j.cell.2008.03.038

Aebi, M., Fäh, J., Hurt, N., Samuel, C. E., Thomis, D., Bazzigher, L., . . . Staeheli, P. (1989). cDNA structures and regulation of two interferon-induced human Mx proteins. *Mol Cell Biol, 9*(11), 5062-5072. doi:10.1128/mcb.9.11.5062

Ahmad, T., Sundar, I. K., Lerner, C. A., Gerloff, J., Tormos, A. M., Yao, H., & Rahman, I. (2015). Impaired mitophagy leads to cigarette smoke stress-induced cellular senescence: implications for chronic obstructive pulmonary disease. *Faseb j, 29*(7), 2912-2929. doi:10.1096/fj.14-268276

Ahmed, S., Passos, J. F., Birket, M. J., Beckmann, T., Brings, S., Peters, H., . . . Saretzki, G. (2008). Telomerase does not counteract telomere shortening but protects mitochondrial function under oxidative stress. *J Cell Sci, 121*(Pt 7), 1046-1053. doi:10.1242/jcs.019372

Aird, K. M., Worth, A. J., Snyder, N. W., Lee, J. V., Sivanand, S., Liu, Q., . . . Zhang, R. (2015). ATM couples replication stress and metabolic reprogramming during cellular senescence. *Cell Rep, 11*(6), 893-901. doi:10.1016/j.celrep.2015.04.014

Aird, K. M., Zhang, G., Li, H., Tu, Z., Bitler, B. G., Garipov, A., . . . Zhang, R. (2013). Suppression of nucleotide metabolism underlies the establishment and maintenance of oncogene-induced senescence. *Cell Rep, 3*(4), 1252-1265. doi:10.1016/j.celrep.2013.03.004

Alavi, M. V., & Fuhrmann, N. (2013). Dominant optic atrophy, OPA1, and mitochondrial quality control: understanding mitochondrial network dynamics. *Mol Neurodegener, 8*, 32. doi:10.1186/1750-1326-8-32

Alimonti, A., Nardella, C., Chen, Z., Clohessy, J. G., Carracedo, A., Trotman, L. C., . . . Pandolfi, P. P. (2010). A novel type of cellular senescence that can be enhanced in mouse models and human tumor xenografts to suppress prostate tumorigenesis. *J Clin Invest, 120*(3), 681-693. doi:10.1172/JCI40535

Alpers, C. E., & Hudkins, K. L. (2011). Mouse models of diabetic nephropathy. *Curr Opin Nephrol Hypertens, 20*(3), 278-284. doi:10.1097/MNH.0b013e3283451901

Amaya-Montoya, M., Pérez-Londoño, A., Guatibonza-García, V., Vargas-Villanueva, A., & Mendivil, C. O. (2020). Cellular Senescence as a Therapeutic Target for Age-Related Diseases: A Review. *Adv Ther, 37*(4), 1407-1424. doi:10.1007/s12325-020-01287-0

Andrade-Navarro, M. A., Sanchez-Pulido, L., & McBride, H. M. (2009). Mitochondrial vesicles: an ancient process providing new links to peroxisomes. *Curr Opin Cell Biol, 21*(4), 560-567. doi:10.1016/j.ceb.2009.04.005

Andreeva, L., Hiller, B., Kostrewa, D., Lässig, C., de Oliveira Mann, C. C., Jan Drexler, D., . . . Hopfner, K. P. (2017). cGAS senses long and HMGB/TFAM-bound U-turn DNA by forming protein-DNA ladders. *Nature, 549*(7672), 394-398. doi:10.1038/nature23890

Anggono, V., & Robinson, P. J. (2009). Dynamin. In L. R. Squire (Ed.), *Encyclopedia of Neuroscience* (pp. 725-735). Oxford: Academic Press.

Aoshiba, K., Tsuji, T., & Nagai, A. (2003). Bleomycin induces cellular senescence in alveolar epithelial cells. *Eur Respir J, 22*(3), 436-443. doi:10.1183/09031936.03.00011903

Aras, S., Purandare, N., Gladyck, S., Somayajulu-Nitu, M., Zhang, K., Wallace, D. C., & Grossman, L. I. (2020). Mitochondrial Nuclear Retrograde Regulator 1 (MNRR1) rescues the cellular phenotype of MELAS by inducing homeostatic mechanisms. *Proc Natl Acad Sci U S A, 117*(50), 32056-32065. doi:10.1073/pnas.2005877117

Aravamudan, B., Kiel, A., Freeman, M., Delmotte, P., Thompson, M., Vassallo, R., . . . Prakash, Y. S. (2014). Cigarette smoke-induced mitochondrial fragmentation and dysfunction in human airway smooth muscle. *Am J Physiol Lung Cell Mol Physiol, 306*(9), L840-854. doi:10.1152/ajplung.00155.2013

Ariyoshi, K., Miura, T., Kasai, K., Fujishima, Y., Nakata, A., & Yoshida, M. (2019). Radiation-Induced Bystander Effect is Mediated by Mitochondrial DNA in Exosome-Like Vesicles. *Sci Rep, 9*(1), 9103. doi:10.1038/s41598-019-45669-z

Baar, M. P., Brandt, R. M. C., Putavet, D. A., Klein, J. D. D., Derks, K. W. J., Bourgeois, B. R. M., . . . de Keizer, P. L. J. (2017). Targeted Apoptosis of Senescent Cells Restores Tissue Homeostasis in Response to Chemotoxicity and Aging. *Cell, 169*(1), 132-147 e116. doi:10.1016/j.cell.2017.02.031

Babbar, M., & Sheikh, M. S. (2013). Metabolic Stress and Disorders Related to Alterations in Mitochondrial Fission or Fusion. *Mol Cell Pharmacol, 5*(3), 109-133.

Baker, D. J., Childs, B. G., Durik, M., Wijers, M. E., Sieben, C. J., Zhong, J., . . . van Deursen, J. M. (2016). Naturally occurring p16(Ink4a)-positive cells shorten healthy lifespan. *Nature, 530*(7589), 184-189. doi:10.1038/nature16932

Baker, D. J., Jeganathan, K. B., Cameron, J. D., Thompson, M., Juneja, S., Kopecka, A., . . . van Deursen, J. M. (2004). BubR1 insufficiency causes early onset of aging-associated phenotypes and infertility in mice. *Nat Genet, 36*(7), 744-749. doi:10.1038/ng1382

Baker, D. J., Wijshake, T., Tchkonia, T., LeBrasseur, N. K., Childs, B. G., van de Sluis, B., . . . van Deursen, J. M. (2011). Clearance of p16Ink4a-positive senescent cells delays ageing-associated disorders. *Nature, 479*(7372), 232-236. doi:10.1038/nature10600

Balka, K. R., & De Nardo, D. (2020). Molecular and spatial mechanisms governing STING signalling. *Febs j*. doi:10.1111/febs.15640

Bang, C., & Thum, T. (2012). Exosomes: new players in cell-cell communication. *Int J Biochem Cell Biol, 44*(11), 2060-2064. doi:10.1016/j.biocel.2012.08.007

Banoth, B., & Cassel, S. L. (2018). Mitochondria in innate immune signaling. *Transl Res, 202*, 52-68. doi:10.1016/j.trsl.2018.07.014

Bao, Q., & Shi, Y. (2007). Apoptosome: a platform for the activation of initiator caspases. *Cell Death Differ, 14*(1), 56-65. doi:10.1038/sj.cdd.4402028

Barbier, V., Lang, D., Valois, S., Rothman, A. L., & Medin, C. L. (2017). Dengue virus induces mitochondrial elongation through impairment of Drp1-triggered mitochondrial fission. *Virology, 500*, 149-160. doi:10.1016/j.virol.2016.10.022

Barreiro, L. B., Ben-Ali, M., Quach, H., Laval, G., Patin, E., Pickrell, J. K., . . . Quintana-Murci, L. (2009). Evolutionary dynamics of human Toll-like receptors and their different contributions to host defense. *PLoS Genet, 5*(7), e1000562. doi:10.1371/journal.pgen.1000562

Bartkova, J., Rezaei, N., Liontos, M., Karakaidos, P., Kletsas, D., Issaeva, N., . . . Gorgoulis, V. G. (2006). Oncogene-induced senescence is part of the tumorigenesis barrier imposed by DNA damage checkpoints. *Nature, 444*(7119), 633-637. doi:10.1038/nature05268

Bartoletti-Stella, A., Mariani, E., Kurelac, I., Maresca, A., Caratozzolo, M. F., Iommarini, L., . . . Gasparre, G. (2013). Gamma rays induce a p53-independent mitochondrial biogenesis that is counter-regulated by HIF1alpha. *Cell Death Dis, 4*, e663. doi:10.1038/cddis.2013.187

Basu, A., Lenka, N., Mullick, J., & Avadhani, N. G. (1997). Regulation of murine cytochrome oxidase Vb gene expression in different tissues and during myogenesis. Role of a YY-1 factor-binding negative enhancer. *J Biol Chem, 272*(9), 5899-5908. doi:10.1074/jbc.272.9.5899

Battersby, B. J., & Richter, U. (2013). Why translation counts for mitochondria - retrograde signalling links mitochondrial protein synthesis to mitochondrial biogenesis and cell proliferation. *J Cell Sci, 126*(Pt 19), 4331-4338. doi:10.1242/jcs.131888

Baz-Martínez, M., Da Silva-Álvarez, S., Rodríguez, E., Guerra, J., El Motiam, A., Vidal, A., . . . Rivas, C. (2016). Cell senescence is an antiviral defense mechanism. *Sci Rep, 6*, 37007. doi:10.1038/srep37007

Bektas, A., Schurman, S. H., Franceschi, C., & Ferrucci, L. (2020). A public health perspective of aging: do hyper-inflammatory syndromes such as COVID-19, SARS, ARDS, cytokine storm syndrome, and post-ICU syndrome accelerate short- and long-term inflammaging? *Immun Ageing, 17*, 23. doi:10.1186/s12979-020-00196-8

Ben-Porath, I., & Weinberg, R. A. (2005). The signals and pathways activating cellular senescence. *Int J Biochem Cell Biol, 37*(5), 961-976. doi:10.1016/j.biocel.2004.10.013

Benador, I. Y., Veliova, M., Mahdaviani, K., Petcherski, A., Wikstrom, J. D., Assali, E. A., . . . Shirihai, O. S. (2018). Mitochondria Bound to Lipid Droplets Have Unique Bioenergetics, Composition, and Dynamics that Support Lipid Droplet Expansion. *Cell Metab, 27*(4), 869-885 e866. doi:10.1016/j.cmet.2018.03.003

Berman, S. B., Pineda, F. J., & Hardwick, J. M. (2008). Mitochondrial fission and fusion dynamics: the long and short of it. *Cell Death Differ, 15*(7), 1147-1152. doi:10.1038/cdd.2008.57

Bhaumik, D., Scott, G. K., Schokrpur, S., Patil, C. K., Orjalo, A. V., Rodier, F., . . . Campisi, J. (2009). MicroRNAs miR-146a/b negatively modulate the senescence-associated inflammatory mediators IL-6 and IL-8. *Aging (Albany NY), 1*(4), 402-411. doi:10.18632/aging.100042

Bhola, P. D., Mattheyses, A. L., & Simon, S. M. (2009). Spatial and temporal dynamics of mitochondrial membrane permeability waves during apoptosis. *Biophys J, 97*(8), 2222-2231. doi:10.1016/j.bpj.2009.07.056

Biran, A., & Krizhanovsky, V. (2015). Senescent cells talk frankly with their neighbors. *Cell Cycle, 14*(14), 2181-2182. doi:10.1080/15384101.2015.1056608

Bodnar, A. G., Ouellette, M., Frolkis, M., Holt, S. E., Chiu, C. P., Morin, G. B., . . . Wright, W. E. (1998). Extension of life-span by introduction of telomerase into normal human cells. *Science, 279*(5349), 349-352. doi:10.1126/science.279.5349.349

Bombrun, A., Gerber, P., Casi, G., Terradillos, O., Antonsson, B., & Halazy, S. (2003). 3,6-dibromocarbazole piperazine derivatives of 2-propanol as first inhibitors of cytochrome c release via Bax channel modulation. *J Med Chem, 46*(21), 4365-4368. doi:10.1021/jm034107j

Boohaker, R. J., Zhang, G., Carlson, A. L., Nemec, K. N., & Khaled, A. R. (2011). BAX supports the mitochondrial network, promoting bioenergetics in nonapoptotic cells. *Am J Physiol Cell Physiol, 300*(6), C1466-1478. doi:10.1152/ajpcell.00325.2010

Borghesan, M., Fafián-Labora, J., Eleftheriadou, O., Carpintero-Fernández, P., Paez-Ribes, M., Vizcay-Barrena, G., . . . O'Loghlen, A. (2019). Small Extracellular Vesicles Are Key Regulators of Non-cell Autonomous Intercellular Communication in Senescence via the Interferon Protein IFITM3. *Cell Rep, 27*(13), 3956-3971.e3956. doi:10.1016/j.celrep.2019.05.095

Borghesan, M., Hoogaars, W. M. H., Varela-Eirin, M., Talma, N., & Demaria, M. (2020). A Senescence-Centric View of Aging: Implications for Longevity and Disease. *Trends Cell Biol, 30*(10), 777-791. doi:10.1016/j.tcb.2020.07.002

Braig, M., Lee, S., Loddenkemper, C., Rudolph, C., Peters, A. H., Schlegelberger, B., . . . Schmitt, C. A. (2005). Oncogene-induced senescence as an initial barrier in lymphoma development. *Nature, 436*(7051), 660-665. doi:10.1038/nature03841

Braig, M., Lee, S., Loddenkemper, C., Rudolph, C., Peters, A. H., Schlegelberger, B., . . . Schmitt, C. A. (2005). Oncogene-induced senescence as an initial barrier in lymphoma development. *Nature, 436*(7051), 660-665. doi:10.1038/nature03841

Braig, M., & Schmitt, C. A. (2006). Oncogene-induced senescence: putting the brakes on tumor development. *Cancer Res, 66*(6), 2881-2884. doi:10.1158/0008-5472.CAN-05-4006

Branzei, D., & Foiani, M. (2008). Regulation of DNA repair throughout the cell cycle. *Nat Rev Mol Cell Biol, 9*(4), 297-308. doi:10.1038/nrm2351

Braymer, J. J., & Lill, R. (2017). Iron-sulfur cluster biogenesis and trafficking in mitochondria. *J Biol Chem, 292*(31), 12754-12763. doi:10.1074/jbc.R117.787101

Brokatzky, D., Dörflinger, B., Haimovici, A., Weber, A., Kirschnek, S., Vier, J., . . . Häcker, G. (2019). A non-death function of the mitochondrial apoptosis apparatus in immunity. *EMBO J, 38*(11). doi:10.15252/embj.2018100907

Brooks, C., Wei, Q., Feng, L., Dong, G., Tao, Y., Mei, L., . . . Dong, Z. (2007). Bak regulates mitochondrial morphology and pathology during apoptosis by interacting with mitofusins. *Proc Natl Acad Sci U S A, 104*(28), 11649-11654. doi:10.1073/pnas.0703976104

Brown, T. A., Tkachuk, A. N., Shtengel, G., Kopek, B. G., Bogenhagen, D. F., Hess, H. F., & Clayton, D. A. (2011). Superresolution fluorescence imaging of mitochondrial nucleoids reveals their spatial range, limits, and membrane interaction. *Mol Cell Biol, 31*(24), 4994-5010. doi:10.1128/mcb.05694-11

Brustovetsky, T., Li, T., Yang, Y., Zhang, J. T., Antonsson, B., & Brustovetsky, N. (2010). BAX insertion, oligomerization, and outer membrane permeabilization in brain mitochondria: role of permeability transition and SH-redox regulation. *Biochim Biophys Acta, 1797*(11), 1795-1806. doi:10.1016/j.bbabio.2010.07.006

Buendia, B., Santa-Maria, A., & Courvalin, J. C. (1999). Caspase-dependent proteolysis of integral and peripheral proteins of nuclear membranes and nuclear pore complex proteins during apoptosis. *J Cell Sci, 112 (Pt 11)*, 1743-1753.

Buffone, C., Schulte, B., Opp, S., & Diaz-Griffero, F. (2015). Contribution of MxB oligomerization to HIV-1 capsid binding and restriction. *J Virol, 89*(6), 3285-3294. doi:10.1128/jvi.03730-14

Burd, C. E., Sorrentino, J. A., Clark, K. S., Darr, D. B., Krishnamurthy, J., Deal, A. M., . . . Sharpless, N. E. (2013). Monitoring tumorigenesis and senescence in vivo with a p16(INK4a)-luciferase model. *Cell, 152*(1-2), 340-351. doi:10.1016/j.cell.2012.12.010

Burman, J. L., Pickles, S., Wang, C., Sekine, S., Vargas, J. N. S., Zhang, Z., . . . Youle, R. J. (2017). Mitochondrial fission facilitates the selective mitophagy of protein aggregates. *J Cell Biol, 216*(10), 3231-3247. doi:10.1083/jcb.201612106

Burton, D. G. A., & Faragher, R. G. A. (2018). Obesity and type-2 diabetes as inducers of premature cellular senescence and ageing. *Biogerontology, 19*(6), 447-459. doi:10.1007/s10522-018-9763-7

Bustamante, E., & Pedersen, P. L. (1977). High aerobic glycolysis of rat hepatoma cells in culture: role of mitochondrial hexokinase. *Proc Natl Acad Sci U S A, 74*(9), 3735-3739. doi:10.1073/pnas.74.9.3735

Butow, R. A., & Avadhani, N. G. (2004). Mitochondrial signaling: the retrograde response. *Mol Cell, 14*(1), 1-15. doi:10.1016/s1097-2765(04)00179-0

Campisi, J., & d'Adda di Fagagna, F. (2007). Cellular senescence: when bad things happen to good cells. *Nat Rev Mol Cell Biol, 8*(9), 729-740. doi:10.1038/nrm2233

Cao, H., Krueger, E. W., Chen, J., Drizyte-Miller, K., Schulz, M. E., & McNiven, M. A. (2020). The anti-viral dynamin family member MxB participates in mitochondrial integrity. *Nat Commun, 11*(1), 1048. doi:10.1038/s41467-020-14727-w

Cappello, C., Zwergal, A., Kanclerski, S., Haas, S. C., Kandemir, J. D., Huber, R., . . . Brand, K. (2009). C/EBPbeta enhances NF-kappaB-associated signalling by reducing the level of IkappaB-alpha. *Cell Signal, 21*(12), 1918-1924. doi:10.1016/j.cellsig.2009.08.009

Cardamone, M. D., Tanasa, B., Cederquist, C. T., Huang, J., Mahdaviani, K., Li, W., . . . Perissi, V. (2018). Mitochondrial Retrograde Signaling in Mammals Is Mediated by the Transcriptional Cofactor GPS2 via Direct Mitochondria-to-Nucleus Translocation. *Mol Cell, 69*(5), 757-772.e757. doi:10.1016/j.molcel.2018.01.037

Carroll, B., Nelson, G., Rabanal-Ruiz, Y., Kucheryavenko, O., Dunhill-Turner, N. A., Chesterman, C. C., . . . Korolchuk, V. I. (2017). Persistent mTORC1 signaling in cell senescence results from defects

in amino acid and growth factor sensing. *J Cell Biol, 216*(7), 1949-1957. doi:10.1083/jcb.201610113
Casella, G., Munk, R., Kim, K. M., Piao, Y., De, S., Abdelmohsen, K., & Gorospe, M. (2019). Transcriptome signature of cellular senescence. *Nucleic Acids Res, 47*(14), 7294-7305. doi:10.1093/nar/gkz555
Castanier, C., Garcin, D., Vazquez, A., & Arnoult, D. (2010). Mitochondrial dynamics regulate the RIG-I-like receptor antiviral pathway. *EMBO Rep, 11*(2), 133-138. doi:10.1038/embor.2009.258
Castresana, J., & Saraste, M. (1995). Evolution of energetic metabolism: the respiration-early hypothesis. *Trends Biochem Sci, 20*(11), 443-448. doi:10.1016/s0968-0004(00)89098-2
Certo, M., Del Gaizo Moore, V., Nishino, M., Wei, G., Korsmeyer, S., Armstrong, S. A., & Letai, A. (2006). Mitochondria primed by death signals determine cellular addiction to antiapoptotic BCL-2 family members. *Cancer Cell, 9*(5), 351-365. doi:10.1016/j.ccr.2006.03.027
Chan, S. S., & Copeland, W. C. (2009). DNA polymerase gamma and mitochondrial disease: understanding the consequence of POLG mutations. *Biochim Biophys Acta, 1787*(5), 312-319. doi:10.1016/j.bbabio.2008.10.007
Chapman, J., Fielder, E., & Passos, J. F. (2019). Mitochondrial dysfunction and cell senescence: deciphering a complex relationship. *FEBS Lett, 593*(13), 1566-1579. doi:10.1002/1873-3468.13498
Chaung, W. W., Wu, R., Ji, Y., Dong, W., & Wang, P. (2012). Mitochondrial transcription factor A is a proinflammatory mediator in hemorrhagic shock. *Int J Mol Med, 30*(1), 199-203. doi:10.3892/ijmm.2012.959
Chen, C., Detmer, S. A., Ewald, A. J., Griffin, E. E., Fraser, S. E., & Chan, D. C. (2003). Mitofusins Mfn1 and Mfn2 coordinately regulate mitochondrial fusion and are essential for embryonic development. *J Cell Biol, 160*(2), 189-200. doi:10.1083/jcb.200211046
Chen, C., Edelstein, L. C., & Gelinas, C. (2000). The Rel/NF-kappaB family directly activates expression of the apoptosis inhibitor Bcl-x(L). *Mol Cell Biol, 20*(8), 2687-2695. doi:10.1128/mcb.20.8.2687-2695.2000
Chen, Q., Sun, L., & Chen, Z. J. (2016). Regulation and function of the cGAS-STING pathway of cytosolic DNA sensing. *Nat Immunol, 17*(10), 1142-1149. doi:10.1038/ni.3558
Chen, Q. M., Liu, J., & Merrett, J. B. (2000). Apoptosis or senescence-like growth arrest: influence of cell-cycle position, p53, p21 and bax in H2O2 response of normal human fibroblasts. *Biochem J, 347*(Pt 2), 543-551. doi:10.1042/0264-6021:3470543
Chen, Y., Zhou, Z., & Min, W. (2018). Mitochondria, Oxidative Stress and Innate Immunity. *Front Physiol, 9*, 1487. doi:10.3389/fphys.2018.01487
Chien, Y., Scuoppo, C., Wang, X., Fang, X., Balgley, B., Bolden, J. E., . . . Lowe, S. W. (2011). Control of the senescence-associated secretory phenotype by NF-kappaB promotes senescence and enhances chemosensitivity. *Genes Dev, 25*(20), 2125-2136. doi:10.1101/gad.17276711
Childs, B. G., Baker, D. J., Kirkland, J. L., Campisi, J., & van Deursen, J. M. (2014). Senescence and apoptosis: dueling or complementary cell fates? *EMBO Rep, 15*(11), 1139-1153. doi:10.15252/embr.201439245
Childs, B. G., Baker, D. J., Wijshake, T., Conover, C. A., Campisi, J., & van Deursen, J. M. (2016). Senescent intimal foam cells are deleterious at all stages of atherosclerosis. *Science, 354*(6311), 472-477. doi:10.1126/science.aaf6659
Childs, B. G., Durik, M., Baker, D. J., & van Deursen, J. M. (2015). Cellular senescence in aging and age-related disease: from mechanisms to therapy. *Nat Med, 21*(12), 1424-1435. doi:10.1038/nm.4000
Cho, K. A., Ryu, S. J., Oh, Y. S., Park, J. H., Lee, J. W., Kim, H. P., . . . Park, S. C. (2004). Morphological adjustment of senescent cells by modulating caveolin-1 status. *J Biol Chem, 279*(40), 42270-42278. doi:10.1074/jbc.M402352200

Choubey, D., & Panchanathan, R. (2016). IFI16, an amplifier of DNA-damage response: Role in cellular senescence and aging-associated inflammatory diseases. *Ageing Res Rev, 28*, 27-36. doi:10.1016/j.arr.2016.04.002

Chu, C. T., Ji, J., Dagda, R. K., Jiang, J. F., Tyurina, Y. Y., Kapralov, A. A., . . . Kagan, V. E. (2013). Cardiolipin externalization to the outer mitochondrial membrane acts as an elimination signal for mitophagy in neuronal cells. *Nat Cell Biol, 15*(10), 1197-1205. doi:10.1038/ncb2837

Chu, X., Wen, J., & Raju, R. P. (2020). Rapid senescence-like response after acute injury. *Aging Cell, 19*(9), e13201. doi:10.1111/acel.13201

Chuprin, A., Gal, H., Biron-Shental, T., Biran, A., Amiel, A., Rozenblatt, S., & Krizhanovsky, V. (2013). Cell fusion induced by ERVWE1 or measles virus causes cellular senescence. *Genes Dev, 27*(21), 2356-2366. doi:10.1101/gad.227512.113

Cipriano, R., Kan, C. E., Graham, J., Danielpour, D., Stampfer, M., & Jackson, M. W. (2011). TGF-beta signaling engages an ATM-CHK2-p53-independent RAS-induced senescence and prevents malignant transformation in human mammary epithelial cells. *Proc Natl Acad Sci U S A, 108*(21), 8668-8673. doi:10.1073/pnas.1015022108

Colell, A., Ricci, J. E., Tait, S., Milasta, S., Maurer, U., Bouchier-Hayes, L., . . . Green, D. R. (2007). GAPDH and autophagy preserve survival after apoptotic cytochrome c release in the absence of caspase activation. *Cell, 129*(5), 983-997. doi:10.1016/j.cell.2007.03.045

Collado, M., & Serrano, M. (2005). The senescent side of tumor suppression. *Cell Cycle, 4*(12), 1722-1724. doi:10.4161/cc.4.12.2260

Collins, L. V., Hajizadeh, S., Holme, E., Jonsson, I. M., & Tarkowski, A. (2004). Endogenously oxidized mitochondrial DNA induces in vivo and in vitro inflammatory responses. *J Leukoc Biol, 75*(6), 995-1000. doi:10.1189/jlb.0703328

Coppe, J. P., Desprez, P. Y., Krtolica, A., & Campisi, J. (2010). The senescence-associated secretory phenotype: the dark side of tumor suppression. *Annu Rev Pathol, 5*, 99-118. doi:10.1146/annurev-pathol-121808-102144

Coppe, J. P., Patil, C. K., Rodier, F., Sun, Y., Munoz, D. P., Goldstein, J., . . . Campisi, J. (2008). Senescence-associated secretory phenotypes reveal cell-nonautonomous functions of oncogenic RAS and the p53 tumor suppressor. *PLoS Biol, 6*(12), 2853-2868. doi:10.1371/journal.pbio.0060301

Cormenier, J., Martin, N., Desle, J., Salazar-Cardozo, C., Pourtier, A., Abbadie, C., & Pluquet, O. (2018). The ATF6alpha arm of the Unfolded Protein Response mediates replicative senescence in human fibroblasts through a COX2/prostaglandin E2 intracrine pathway. *Mech Ageing Dev, 170*, 82-91. doi:10.1016/j.mad.2017.08.003

Correia-Melo, C., Marques, F. D., Anderson, R., Hewitt, G., Hewitt, R., Cole, J., . . . Passos, J. F. (2016). Mitochondria are required for pro-ageing features of the senescent phenotype. *EMBO J, 35*(7), 724-742. doi:10.15252/embj.201592862

Cosentino, K., & García-Sáez, A. J. (2017). Bax and Bak Pores: Are We Closing the Circle? *Trends Cell Biol, 27*(4), 266-275. doi:10.1016/j.tcb.2016.11.004

Courtois-Cox, S., Jones, S. L., & Cichowski, K. (2008). Many roads lead to oncogene-induced senescence. *Oncogene, 27*(20), 2801-2809. doi:10.1038/sj.onc.1210950

Crameri, M., Bauer, M., Caduff, N., Walker, R., Steiner, F., Franzoso, F. D., . . . Pavlovic, J. (2018). MxB is an interferon-induced restriction factor of human herpesviruses. *Nat Commun, 9*(1), 1980. doi:10.1038/s41467-018-04379-2

Crawford, E. D., & Wells, J. A. (2011). Caspase substrates and cellular remodeling. *Annu Rev Biochem, 80*, 1055-1087. doi:10.1146/annurev-biochem-061809-121639

d'Adda di Fagagna, F. (2008). Living on a break: cellular senescence as a DNA-damage response. *Nat Rev Cancer, 8*(7), 512-522. doi:10.1038/nrc2440

d'Adda di Fagagna, F., Reaper, P. M., Clay-Farrace, L., Fiegler, H., Carr, P., Von Zglinicki, T., . . . Jackson, S. P. (2003). A DNA damage checkpoint response in telomere-initiated senescence. *Nature, 426*(6963), 194-198. doi:10.1038/nature02118

Da Cruz, S., Parone, P. A., Gonzalo, P., Bienvenut, W. V., Tondera, D., Jourdain, A., . . . Martinou, J. C. (2008). SLP-2 interacts with prohibitins in the mitochondrial inner membrane and contributes to their stability. *Biochim Biophys Acta, 1783*(5), 904-911. doi:10.1016/j.bbamcr.2008.02.006

da Silva, P. F. L., Ogrodnik, M., Kucheryavenko, O., Glibert, J., Miwa, S., Cameron, K., . . . von Zglinicki, T. (2019). The bystander effect contributes to the accumulation of senescent cells in vivo. *Aging Cell, 18*(1), e12848. doi:10.1111/acel.12848

Dalle Pezze, P., Nelson, G., Otten, E. G., Korolchuk, V. I., Kirkwood, T. B., von Zglinicki, T., & Shanley, D. P. (2014). Dynamic modelling of pathways to cellular senescence reveals strategies for targeted interventions. *PLoS Comput Biol, 10*(8), e1003728. doi:10.1371/journal.pcbi.1003728

Dankort, D., Filenova, E., Collado, M., Serrano, M., Jones, K., & McMahon, M. (2007). A new mouse model to explore the initiation, progression, and therapy of BRAFV600E-induced lung tumors. *Genes Dev, 21*(4), 379-384. doi:10.1101/gad.1516407

Das, R., & Chakrabarti, O. (2020). Mitochondrial hyperfusion: a friend or a foe. *Biochem Soc Trans, 48*(2), 631-644. doi:10.1042/bst20190987

Datta, S. R., Dudek, H., Tao, X., Masters, S., Fu, H., Gotoh, Y., & Greenberg, M. E. (1997). Akt phosphorylation of BAD couples survival signals to the cell-intrinsic death machinery. *Cell, 91*(2), 231-241. doi:10.1016/s0092-8674(00)80405-5

Davalos, A. R., Kawahara, M., Malhotra, G. K., Schaum, N., Huang, J., Ved, U., . . . Campisi, J. (2013). p53-dependent release of Alarmin HMGB1 is a central mediator of senescent phenotypes. *J Cell Biol, 201*(4), 613-629. doi:10.1083/jcb.201206006

De Cecco, M., Ito, T., Petrashen, A. P., Elias, A. E., Skvir, N. J., Criscione, S. W., . . . Sedivy, J. M. (2019). L1 drives IFN in senescent cells and promotes age-associated inflammation. *Nature, 566*(7742), 73-78. doi:10.1038/s41586-018-0784-9

de Lange, T. (2002). Protection of mammalian telomeres. *Oncogene, 21*(4), 532-540. doi:10.1038/sj.onc.1205080

Del Dotto, V., Fogazza, M., Carelli, V., Rugolo, M., & Zanna, C. (2018). Eight human OPA1 isoforms, long and short: What are they for? *Biochim Biophys Acta Bioenerg, 1859*(4), 263-269. doi:10.1016/j.bbabio.2018.01.005

Demaria, M., Ohtani, N., Youssef, S. A., Rodier, F., Toussaint, W., Mitchell, J. R., . . . Campisi, J. (2014). An essential role for senescent cells in optimal wound healing through secretion of PDGF-AA. *Dev Cell, 31*(6), 722-733. doi:10.1016/j.devcel.2014.11.012

Deshmukh, M., Kuida, K., & Johnson, E. M., Jr. (2000). Caspase inhibition extends the commitment to neuronal death beyond cytochrome c release to the point of mitochondrial depolarization. *J Cell Biol, 150*(1), 131-143. doi:10.1083/jcb.150.1.131

Dhanwani, R., Takahashi, M., & Sharma, S. (2018). Cytosolic sensing of immuno-stimulatory DNA, the enemy within. *Curr Opin Immunol, 50*, 82-87. doi:10.1016/j.coi.2017.11.004

Dhir, A., Dhir, S., Borowski, L. S., Jimenez, L., Teitell, M., Rötig, A., . . . Proudfoot, N. J. (2018). Mitochondrial double-stranded RNA triggers antiviral signalling in humans. *Nature, 560*(7717), 238-242. doi:10.1038/s41586-018-0363-0

Dhomen, N., Reis-Filho, J. S., da Rocha Dias, S., Hayward, R., Savage, K., Delmas, V., . . . Marais, R. (2009). Oncogenic Braf induces melanocyte senescence and melanoma in mice. *Cancer Cell, 15*(4), 294-303. doi:10.1016/j.ccr.2009.02.022

Di Leonardo, A., Linke, S. P., Clarkin, K., & Wahl, G. M. (1994). DNA damage triggers a prolonged p53-dependent G1 arrest and long-term induction of Cip1 in normal human fibroblasts. *Genes Dev, 8*(21), 2540-2551. doi:10.1101/gad.8.21.2540

Di Micco, R., Fumagalli, M., Cicalese, A., Piccinin, S., Gasparini, P., Luise, C., . . . d'Adda di Fagagna, F. (2006). Oncogene-induced senescence is a DNA damage response triggered by DNA hyper-replication. *Nature, 444*(7119), 638-642. doi:10.1038/nature05327

Dikic, I., & Elazar, Z. (2018). Mechanism and medical implications of mammalian autophagy. *Nat Rev Mol Cell Biol, 19*(6), 349-364. doi:10.1038/s41580-018-0003-4

Dimri, G. P., Lee, X., Basile, G., Acosta, M., Scott, G., Roskelley, C., . . . et al. (1995). A biomarker that identifies senescent human cells in culture and in aging skin in vivo. *Proc Natl Acad Sci U S A, 92*(20), 9363-9367. doi:10.1073/pnas.92.20.9363

Dou, Z., Ghosh, K., Vizioli, M. G., Zhu, J., Sen, P., Wangensteen, K. J., . . . Berger, S. L. (2017). Cytoplasmic chromatin triggers inflammation in senescence and cancer. *Nature, 550*(7676), 402-406. doi:10.1038/nature24050

Dou, Z., Xu, C., Donahue, G., Shimi, T., Pan, J. A., Zhu, J., . . . Berger, S. L. (2015). Autophagy mediates degradation of nuclear lamina. *Nature, 527*(7576), 105-109. doi:10.1038/nature15548

Dunphy, G., Flannery, S. M., Almine, J. F., Connolly, D. J., Paulus, C., Jonsson, K. L., . . . Unterholzner, L. (2018). Non-canonical Activation of the DNA Sensing Adaptor STING by ATM and IFI16 Mediates NF-kappaB Signaling after Nuclear DNA Damage. *Mol Cell, 71*(5), 745-760 e745. doi:10.1016/j.molcel.2018.07.034

Ebersole, J. L., Graves, C. L., Gonzalez, O. A., Dawson, D., 3rd, Morford, L. A., Huja, P. E., . . . Wallet, S. M. (2016). Aging, inflammation, immunity and periodontal disease. *Periodontol 2000, 72*(1), 54-75. doi:10.1111/prd.12135

Edlich, F., Banerjee, S., Suzuki, M., Cleland, M. M., Arnoult, D., Wang, C., . . . Youle, R. J. (2011). Bcl-x(L) retrotranslocates Bax from the mitochondria into the cytosol. *Cell, 145*(1), 104-116. doi:10.1016/j.cell.2011.02.034

Ellison-Hughes, G. M. (2020). First evidence that senolytics are effective at decreasing senescent cells in humans. *EBioMedicine, 56*, 102473. doi:10.1016/j.ebiom.2019.09.053

Enriquez, J. A., Martinez-Azorin, F., Garesse, R., Lopez-Perez, M. J., Perez-Martos, A., Bornstein, B., & Montoya, J. (1998). [Human mitochondrial genetic system]. *Rev Neurol, 26 Suppl 1*, S21-26. Retrieved from https://www.ncbi.nlm.nih.gov/pubmed/9810587

Escobar-Henriques, M., & Langer, T. (2014). Dynamic survey of mitochondria by ubiquitin. *EMBO Rep, 15*(3), 231-243. doi:10.1002/embr.201338225

Fackler, O. T., & Keppler, O. T. (2013). MxB/Mx2: the latest piece in HIV's interferon puzzle. *EMBO Rep, 14*(12), 1028-1029. doi:10.1038/embor.2013.172

Faitg, J., Leduc-Gaudet, J. P., Reynaud, O., Ferland, G., Gaudreau, P., & Gouspillou, G. (2019). Effects of Aging and Caloric Restriction on Fiber Type Composition, Mitochondrial Morphology and Dynamics in Rat Oxidative and Glycolytic Muscles. *Front Physiol, 10*, 420. doi:10.3389/fphys.2019.00420

Falkenberg, M. (2018). Mitochondrial DNA replication in mammalian cells: overview of the pathway. *Essays Biochem, 62*(3), 287-296. doi:10.1042/ebc20170100

Fang, C., Wei, X., & Wei, Y. (2016). Mitochondrial DNA in the regulation of innate immune responses. *Protein Cell, 7*(1), 11-16. doi:10.1007/s13238-015-0222-9

Fink, S. L., & Cookson, B. T. (2005). Apoptosis, pyroptosis, and necrosis: mechanistic description of dead and dying eukaryotic cells. *Infect Immun, 73*(4), 1907-1916. doi:10.1128/iai.73.4.1907-1916.2005

Fiorucci, G., & Hall, A. (1988). All three human ras genes are expressed in a wide range of tissues. *Biochim Biophys Acta, 950*(1), 81-83. doi:10.1016/0167-4781(88)90076-0

Franceschi, C., Bonafè, M., Valensin, S., Olivieri, F., De Luca, M., Ottaviani, E., & De Benedictis, G. (2000). Inflamm-aging. An evolutionary perspective on immunosenescence. *Ann N Y Acad Sci, 908*, 244-254. doi:10.1111/j.1749-6632.2000.tb06651.x

Franceschi, C., Capri, M., Monti, D., Giunta, S., Olivieri, F., Sevini, F., . . . Salvioli, S. (2007). Inflammaging and anti-inflammaging: a systemic perspective on aging and longevity emerged from studies in humans. *Mech Ageing Dev, 128*(1), 92-105. doi:10.1016/j.mad.2006.11.016

Franceschi, C., Garagnani, P., Parini, P., Giuliani, C., & Santoro, A. (2018). Inflammaging: a new immune-metabolic viewpoint for age-related diseases. *Nat Rev Endocrinol, 14*(10), 576-590. doi:10.1038/s41574-018-0059-4

Franceschi, C., Garagnani, P., Vitale, G., Capri, M., & Salvioli, S. (2017). Inflammaging and 'Garb-aging'. *Trends Endocrinol Metab, 28*(3), 199-212. doi:10.1016/j.tem.2016.09.005

Frank, S., Gaume, B., Bergmann-Leitner, E. S., Leitner, W. W., Robert, E. G., Catez, F., . . . Youle, R. J. (2001). The role of dynamin-related protein 1, a mediator of mitochondrial fission, in apoptosis. *Dev Cell, 1*(4), 515-525. doi:10.1016/s1534-5807(01)00055-7

Freund, A., Laberge, R. M., Demaria, M., & Campisi, J. (2012). Lamin B1 loss is a senescence-associated biomarker. *Mol Biol Cell, 23*(11), 2066-2075. doi:10.1091/mbc.E11-10-0884

Freund, A., Orjalo, A. V., Desprez, P. Y., & Campisi, J. (2010). Inflammatory networks during cellular senescence: causes and consequences. *Trends Mol Med, 16*(5), 238-246. doi:10.1016/j.molmed.2010.03.003

Freund, A., Patil, C. K., & Campisi, J. (2011). p38MAPK is a novel DNA damage response-independent regulator of the senescence-associated secretory phenotype. *EMBO J, 30*(8), 1536-1548. doi:10.1038/emboj.2011.69

Fried, L. P., Tangen, C. M., Walston, J., Newman, A. B., Hirsch, C., Gottdiener, J., . . . McBurnie, M. A. (2001). Frailty in older adults: evidence for a phenotype. *J Gerontol A Biol Sci Med Sci, 56*(3), M146-156. doi:10.1093/gerona/56.3.m146

Fruman, D. A., Chiu, H., Hopkins, B. D., Bagrodia, S., Cantley, L. C., & Abraham, R. T. (2017). The PI3K Pathway in Human Disease. *Cell, 170*(4), 605-635. doi:10.1016/j.cell.2017.07.029

Fu, M., St-Pierre, P., Shankar, J., Wang, P. T., Joshi, B., & Nabi, I. R. (2013). Regulation of mitophagy by the Gp78 E3 ubiquitin ligase. *Mol Biol Cell, 24*(8), 1153-1162. doi:10.1091/mbc.E12-08-0607

Furman, D., Campisi, J., Verdin, E., Carrera-Bastos, P., Targ, S., Franceschi, C., . . . Slavich, G. M. (2019). Chronic inflammation in the etiology of disease across the life span. *Nat Med, 25*(12), 1822-1832. doi:10.1038/s41591-019-0675-0

Garcia, D., & Shaw, R. J. (2017). AMPK: Mechanisms of Cellular Energy Sensing and Restoration of Metabolic Balance. *Mol Cell, 66*(6), 789-800. doi:10.1016/j.molcel.2017.05.032

Gaspari, M., Larsson, N. G., & Gustafsson, C. M. (2004). The transcription machinery in mammalian mitochondria. *Biochim Biophys Acta, 1659*(2-3), 148-152. doi:10.1016/j.bbabio.2004.10.003

Gavathiotis, E., Reyna, D. E., Davis, M. L., Bird, G. H., & Walensky, L. D. (2010). BH3-triggered structural reorganization drives the activation of proapoptotic BAX. *Mol Cell, 40*(3), 481-492. doi:10.1016/j.molcel.2010.10.019

Geva-Zatorsky, N., Rosenfeld, N., Itzkovitz, S., Milo, R., Sigal, A., Dekel, E., . . . Alon, U. (2006). Oscillations and variability in the p53 system. *Mol Syst Biol, 2*, 2006.0033. doi:10.1038/msb4100068

Gillies, L. A., & Kuwana, T. (2014). Apoptosis regulation at the mitochondrial outer membrane. *J Cell Biochem, 115*(4), 632-640. doi:10.1002/jcb.24709

Gladyshev, V. N. (2013). The origin of aging: imperfectness-driven non-random damage defines the aging process and control of lifespan. *Trends Genet, 29*(9), 506-512. doi:10.1016/j.tig.2013.05.004

Gladyshev, V. N. (2016). Aging: progressive decline in fitness due to the rising deleteriome adjusted by genetic, environmental, and stochastic processes. *Aging Cell, 15*(4), 594-602. doi:10.1111/acel.12480

Gluck, S., Guey, B., Gulen, M. F., Wolter, K., Kang, T. W., Schmacke, N. A., . . . Ablasser, A. (2017). Innate immune sensing of cytosolic chromatin fragments through cGAS promotes senescence. *Nat Cell Biol, 19*(9), 1061-1070. doi:10.1038/ncb3586

Gomes, L. C., Di Benedetto, G., & Scorrano, L. (2011). During autophagy mitochondria elongate, are spared from degradation and sustain cell viability. *Nat Cell Biol, 13*(5), 589-598. doi:10.1038/ncb2220

Gonzalez-Meljem, J. M., Apps, J. R., Fraser, H. C., & Martinez-Barbera, J. P. (2018). Paracrine roles of cellular senescence in promoting tumourigenesis. *Br J Cancer, 118*(10), 1283-1288. doi:10.1038/s41416-018-0066-1

Gopalakrishnan, L., & Scarpulla, R. C. (1994). Differential regulation of respiratory chain subunits by a CREB-dependent signal transduction pathway. Role of cyclic AMP in cytochrome c and COXIV gene expression. *J Biol Chem, 269*(1), 105-113.

Gordaliza-Alaguero, I., Canto, C., & Zorzano, A. (2019). Metabolic implications of organelle-mitochondria communication. *EMBO Rep, 20*(9), e47928. doi:10.15252/embr.201947928
Gorgoulis, V., Adams, P. D., Alimonti, A., Bennett, D. C., Bischof, O., Bishop, C., . . . Demaria, M. (2019). Cellular Senescence: Defining a Path Forward. *Cell, 179*(4), 813-827. doi:10.1016/j.cell.2019.10.005
Gorgoulis, V. G., & Halazonetis, T. D. (2010). Oncogene-induced senescence: the bright and dark side of the response. *Curr Opin Cell Biol, 22*(6), 816-827. doi:10.1016/j.ceb.2010.07.013
Goujon, C., Moncorgé, O., Bauby, H., Doyle, T., Barclay, W. S., & Malim, M. H. (2014). Transfer of the amino-terminal nuclear envelope targeting domain of human MX2 converts MX1 into an HIV-1 resistance factor. *J Virol, 88*(16), 9017-9026. doi:10.1128/jvi.01269-14
Grazioli, S., & Pugin, J. (2018). Mitochondrial Damage-Associated Molecular Patterns: From Inflammatory Signaling to Human Diseases. *Front Immunol, 9*, 832. doi:10.3389/fimmu.2018.00832
Griffith, J. K., Bryant, J. E., Fordyce, C. A., Gilliland, F. D., Joste, N. E., & Moyzis, R. K. (1999). Reduced telomere DNA content is correlated with genomic instability and metastasis in invasive human breast carcinoma. *Breast Cancer Res Treat, 54*(1), 59-64. doi:10.1023/a:1006128228761
Gross, A., & Katz, S. G. (2017). Non-apoptotic functions of BCL-2 family proteins. *Cell Death Differ, 24*(8), 1348-1358. doi:10.1038/cdd.2017.22
Grosse, L., Wagner, N., Emelyanov, A., Molina, C., Lacas-Gervais, S., Wagner, K. D., & Bulavin, D. V. (2020). Defined p16(High) Senescent Cell Types Are Indispensable for Mouse Healthspan. *Cell Metab, 32*(1), 87-99 e86. doi:10.1016/j.cmet.2020.05.002
Guo, B., Zhai, D., Cabezas, E., Welsh, K., Nouraini, S., Satterthwait, A. C., & Reed, J. C. (2003). Humanin peptide suppresses apoptosis by interfering with Bax activation. *Nature, 423*(6938), 456-461. doi:10.1038/nature01627
Guo, H., Callaway, J. B., & Ting, J. P. (2015). Inflammasomes: mechanism of action, role in disease, and therapeutics. *Nat Med, 21*(7), 677-687. doi:10.1038/nm.3893
Hall, B. M., Balan, V., Gleiberman, A. S., Strom, E., Krasnov, P., Virtuoso, L. P., . . . Gudkov, A. V. (2016). Aging of mice is associated with p16(Ink4a)- and beta-galactosidase-positive macrophage accumulation that can be induced in young mice by senescent cells. *Aging (Albany NY), 8*(7), 1294-1315. doi:10.18632/aging.100991
Haller, O., & Kochs, G. (2002). Interferon-induced mx proteins: dynamin-like GTPases with antiviral activity. *Traffic, 3*(10), 710-717. doi:10.1034/j.1600-0854.2002.31003.x
Han, X., Tai, H., Wang, X., Wang, Z., Zhou, J., Wei, X., . . . Xiao, H. (2016). AMPK activation protects cells from oxidative stress-induced senescence via autophagic flux restoration and intracellular NAD(+) elevation. *Aging Cell, 15*(3), 416-427. doi:10.1111/acel.12446
Hance, N., Ekstrand, M. I., & Trifunovic, A. (2005). Mitochondrial DNA polymerase gamma is essential for mammalian embryogenesis. *Hum Mol Genet, 14*(13), 1775-1783. doi:10.1093/hmg/ddi184
Hannig, J., Zhang, D., Canaday, D. J., Beckett, M. A., Astumian, R. D., Weichselbaum, R. R., & Lee, R. C. (2000). Surfactant sealing of membranes permeabilized by ionizing radiation. *Radiat Res, 154*(2), 171-177. doi:10.1667/0033-7587(2000)154[0171:ssompb]2.0.co;2
Hari, P., Millar, F. R., Tarrats, N., Birch, J., Quintanilla, A., Rink, C. J., . . . Acosta, J. C. (2019). The innate immune sensor Toll-like receptor 2 controls the senescence-associated secretory phenotype. *Sci Adv, 5*(6), eaaw0254. doi:10.1126/sciadv.aaw0254
Harley, C. B., Futcher, A. B., & Greider, C. W. (1990). Telomeres shorten during ageing of human fibroblasts. *Nature, 345*(6274), 458-460. doi:10.1038/345458a0
Harman, D. (1972). The biologic clock: the mitochondria? *J Am Geriatr Soc, 20*(4), 145-147. doi:10.1111/j.1532-5415.1972.tb00787.x
Hayflick, L. (1965). The Limited in Vitro Lifetime of Human Diploid Cell Strains. *Exp Cell Res, 37*, 614-636. doi:10.1016/0014-4827(65)90211-9

Hayflick, L., & Moorhead, P. S. (1961). The serial cultivation of human diploid cell strains. *Exp Cell Res, 25*, 585-621. doi:10.1016/0014-4827(61)90192-6

He, S., & Sharpless, N. E. (2017). Senescence in Health and Disease. *Cell, 169*(6), 1000-1011. doi:10.1016/j.cell.2017.05.015

Hegde, R. S., & Zavodszky, E. (2019). Recognition and Degradation of Mislocalized Proteins in Health and Disease. *Cold Spring Harb Perspect Biol, 11*(11). doi:10.1101/cshperspect.a033902

Herbig, U., & Sedivy, J. M. (2006). Regulation of growth arrest in senescence: telomere damage is not the end of the story. *Mech Ageing Dev, 127*(1), 16-24. doi:10.1016/j.mad.2005.09.002

Hernandez-Segura, A., de Jong, T. V., Melov, S., Guryev, V., Campisi, J., & Demaria, M. (2017). Unmasking Transcriptional Heterogeneity in Senescent Cells. *Curr Biol, 27*(17), 2652-2660 e2654. doi:10.1016/j.cub.2017.07.033

Hernandez-Segura, A., Nehme, J., & Demaria, M. (2018). Hallmarks of Cellular Senescence. *Trends Cell Biol, 28*(6), 436-453. doi:10.1016/j.tcb.2018.02.001

Herranz, N., Gallage, S., Mellone, M., Wuestefeld, T., Klotz, S., Hanley, C. J., . . . Gil, J. (2015). mTOR regulates MAPKAPK2 translation to control the senescence-associated secretory phenotype. *Nat Cell Biol, 17*(9), 1205-1217. doi:10.1038/ncb3225

Herranz, N., & Gil, J. (2018). Mechanisms and functions of cellular senescence. *J Clin Invest, 128*(4), 1238-1246. doi:10.1172/jci95148

Hetz, C., Bernasconi, P., Fisher, J., Lee, A. H., Bassik, M. C., Antonsson, B., . . . Korsmeyer, S. J. (2006). Proapoptotic BAX and BAK modulate the unfolded protein response by a direct interaction with IRE1alpha. *Science, 312*(5773), 572-576. doi:10.1126/science.1123480

Hewitt, G., Jurk, D., Marques, F. D., Correia-Melo, C., Hardy, T., Gackowska, A., . . . Passos, J. F. (2012). Telomeres are favoured targets of a persistent DNA damage response in ageing and stress-induced senescence. *Nat Commun, 3*, 708. doi:10.1038/ncomms1708

Hickson, L. J., Langhi Prata, L. G. P., Bobart, S. A., Evans, T. K., Giorgadze, N., Hashmi, S. K., . . . Kirkland, J. L. (2019). Senolytics decrease senescent cells in humans: Preliminary report from a clinical trial of Dasatinib plus Quercetin in individuals with diabetic kidney disease. *EBioMedicine, 47*, 446-456. doi:10.1016/j.ebiom.2019.08.069

Hoare, M., Ito, Y., Kang, T. W., Weekes, M. P., Matheson, N. J., Patten, D. A., . . . Narita, M. (2016). NOTCH1 mediates a switch between two distinct secretomes during senescence. *Nat Cell Biol, 18*(9), 979-992. doi:10.1038/ncb3397

Holt, I. J., & Reyes, A. (2012). Human mitochondrial DNA replication. *Cold Spring Harb Perspect Biol, 4*(12). doi:10.1101/cshperspect.a012971

Hoppins, S., Edlich, F., Cleland, M. M., Banerjee, S., McCaffery, J. M., Youle, R. J., & Nunnari, J. (2011). The soluble form of Bax regulates mitochondrial fusion via MFN2 homotypic complexes. *Mol Cell, 41*(2), 150-160. doi:10.1016/j.molcel.2010.11.030

Horn, A., & Jaiswal, J. K. (2020). Splitting up to heal: mitochondrial shape regulates signaling for focal membrane repair. *Biochem Soc Trans, 48*(5), 1995-2002. doi:10.1042/BST20200120

Horn, A., Raavicharla, S., Shah, S., Cox, D., & Jaiswal, J. K. (2020). Mitochondrial fragmentation enables localized signaling required for cell repair. *J Cell Biol, 219*(5). doi:10.1083/jcb.201909154

Hsieh, H. H., Chen, Y. C., Jhan, J. R., & Lin, J. J. (2017). The serine protease inhibitor serpinB2 binds and stabilizes p21 in senescent cells. *J Cell Sci, 130*(19), 3272-3281. doi:10.1242/jcs.204974

Hsu, Y. T., Wolter, K. G., & Youle, R. J. (1997). Cytosol-to-membrane redistribution of Bax and Bcl-X(L) during apoptosis. *Proc Natl Acad Sci U S A, 94*(8), 3668-3672. doi:10.1073/pnas.94.8.3668

Hu, Q., Ren, J., Wu, J., Li, G., Wu, X., Liu, S., . . . Li, J. (2017). Elevated Levels of Plasma Mitochondrial DNA Are Associated with Clinical Outcome in Intra-Abdominal Infections Caused by Severe Trauma. *Surg Infect (Larchmt), 18*(5), 610-618. doi:10.1089/sur.2016.276

Huang, Y. H., Yang, P. M., Chuah, Q. Y., Lee, Y. J., Hsieh, Y. F., Peng, C. W., & Chiu, S. J. (2014). Autophagy promotes radiation-induced senescence but inhibits bystander effects in human breast cancer cells. *Autophagy, 10*(7), 1212-1228. doi:10.4161/auto.28772

Huggins, C. J., Malik, R., Lee, S., Salotti, J., Thomas, S., Martin, N., . . . Johnson, P. F. (2013). C/EBPgamma suppresses senescence and inflammatory gene expression by heterodimerizing with C/EBPbeta. *Mol Cell Biol, 33*(16), 3242-3258. doi:10.1128/MCB.01674-12

Huttemann, M., Lee, I., Samavati, L., Yu, H., & Doan, J. W. (2007). Regulation of mitochondrial oxidative phosphorylation through cell signaling. *Biochim Biophys Acta, 1773*(12), 1701-1720. doi:10.1016/j.bbamcr.2007.10.001

Hutter, E., Renner, K., Pfister, G., Stöckl, P., Jansen-Dürr, P., & Gnaiger, E. (2004). Senescence-associated changes in respiration and oxidative phosphorylation in primary human fibroblasts. *Biochem J, 380*(Pt 3), 919-928. doi:10.1042/bj20040095

Ichim, G., Lopez, J., Ahmed, S. U., Muthalagu, N., Giampazolias, E., Delgado, M. E., . . . Tait, S. W. G. (2015). Limited mitochondrial permeabilization causes DNA damage and genomic instability in the absence of cell death. *Mol Cell, 57*(5), 860-872. doi:10.1016/j.molcel.2015.01.018

Innes, A. J., & Gil, J. (2019). IMR90 ER:RAS: A Cell Model of Oncogene-Induced Senescence. *Methods Mol Biol, 1896*, 83-92. doi:10.1007/978-1-4939-8931-7_9

Irvine, K. M., Skoien, R., Bokil, N. J., Melino, M., Thomas, G. P., Loo, D., . . . Powell, E. E. (2014). Senescent human hepatocytes express a unique secretory phenotype and promote macrophage migration. *World J Gastroenterol, 20*(47), 17851-17862. doi:10.3748/wjg.v20.i47.17851

Iske, J., Seyda, M., Heinbokel, T., Maenosono, R., Minami, K., Nian, Y., . . . Tullius, S. G. (2020). Senolytics prevent mt-DNA-induced inflammation and promote the survival of aged organs following transplantation. *Nat Commun, 11*(1), 4289. doi:10.1038/s41467-020-18039-x

Itahana, K., Campisi, J., & Dimri, G. P. (2004). Mechanisms of cellular senescence in human and mouse cells. *Biogerontology, 5*(1), 1-10. doi:10.1023/b:bgen.0000017682.96395.10

Ivanov, A., Pawlikowski, J., Manoharan, I., van Tuyn, J., Nelson, D. M., Rai, T. S., . . . Adams, P. D. (2013). Lysosome-mediated processing of chromatin in senescence. *J Cell Biol, 202*(1), 129-143. doi:10.1083/jcb.201212110

Jackson, S. P., & Bartek, J. (2009). The DNA-damage response in human biology and disease. *Nature, 461*(7267), 1071-1078. doi:10.1038/nature08467

Jain, A., & Holthuis, J. C. M. (2017). Membrane contact sites, ancient and central hubs of cellular lipid logistics. *Biochim Biophys Acta Mol Cell Res, 1864*(9), 1450-1458. doi:10.1016/j.bbamcr.2017.05.017

James, E. L., Michalek, R. D., Pitiyage, G. N., de Castro, A. M., Vignola, K. S., Jones, J., . . . Parkinson, E. K. (2015). Senescent human fibroblasts show increased glycolysis and redox homeostasis with extracellular metabolomes that overlap with those of irreparable DNA damage, aging, and disease. *J Proteome Res, 14*(4), 1854-1871. doi:10.1021/pr501221g

Jaul, E., & Barron, J. (2017). Age-Related Diseases and Clinical and Public Health Implications for the 85 Years Old and Over Population. *Front Public Health, 5*, 335. doi:10.3389/fpubh.2017.00335

Jendrach, M., Pohl, S., Vöth, M., Kowald, A., Hammerstein, P., & Bereiter-Hahn, J. (2005). Morpho-dynamic changes of mitochondria during ageing of human endothelial cells. *Mech Ageing Dev, 126*(6-7), 813-821. doi:10.1016/j.mad.2005.03.002

Jeon, O. H., Kim, C., Laberge, R. M., Demaria, M., Rathod, S., Vasserot, A. P., . . . Elisseeff, J. H. (2017). Local clearance of senescent cells attenuates the development of post-traumatic osteoarthritis and creates a pro-regenerative environment. *Nat Med, 23*(6), 775-781. doi:10.1038/nm.4324

Jin, S. M., Lazarou, M., Wang, C., Kane, L. A., Narendra, D. P., & Youle, R. J. (2010). Mitochondrial membrane potential regulates PINK1 import and proteolytic destabilization by PARL. *J Cell Biol, 191*(5), 933-942. doi:10.1083/jcb.201008084

Jones, A. W., Yao, Z., Vicencio, J. M., Karkucinska-Wieckowska, A., & Szabadkai, G. (2012). PGC-1 family coactivators and cell fate: roles in cancer, neurodegeneration, cardiovascular disease

and retrograde mitochondria-nucleus signalling. *Mitochondrion, 12*(1), 86-99. doi:10.1016/j.mito.2011.09.009

Jung, S. H., Hwang, H. J., Kang, D., Park, H. A., Lee, H. C., Jeong, D., . . . Lee, J. S. (2019). mTOR kinase leads to PTEN-loss-induced cellular senescence by phosphorylating p53. *Oncogene, 38*(10), 1639-1650. doi:10.1038/s41388-018-0521-8

Jurk, D., Wilson, C., Passos, J. F., Oakley, F., Correia-Melo, C., Greaves, L., . . . von Zglinicki, T. (2014). Chronic inflammation induces telomere dysfunction and accelerates ageing in mice. *Nat Commun, 2*, 4172. doi:10.1038/ncomms5172

Kageyama, Y., Kasahara, T., Kato, M., Sakai, S., Deguchi, Y., Tani, M., . . . Kato, T. (2018). The relationship between circulating mitochondrial DNA and inflammatory cytokines in patients with major depression. *J Affect Disord, 233*, 15-20. doi:10.1016/j.jad.2017.06.001

Kam, W. W., & Banati, R. B. (2013). Effects of ionizing radiation on mitochondria. *Free Radic Biol Med, 65*, 607-619. doi:10.1016/j.freeradbiomed.2013.07.024

Kam, W. W., McNamara, A. L., Lake, V., Banos, C., Davies, J. B., Kuncic, Z., & Banati, R. B. (2013). Predicted ionisation in mitochondria and observed acute changes in the mitochondrial transcriptome after gamma irradiation: a Monte Carlo simulation and quantitative PCR study. *Mitochondrion, 13*(6), 736-742. doi:10.1016/j.mito.2013.02.005

Kamerkar, S. C., Kraus, F., Sharpe, A. J., Pucadyil, T. J., & Ryan, M. T. (2018). Dynamin-related protein 1 has membrane constricting and severing abilities sufficient for mitochondrial and peroxisomal fission. *Nat Commun, 9*(1), 5239. doi:10.1038/s41467-018-07543-w

Kananen, L., Nevalainen, T., Jylhävä, J., Marttila, S., Hervonen, A., Jylhä, M., & Hurme, M. (2015). Cytomegalovirus infection accelerates epigenetic aging. *Exp Gerontol, 72*, 227-229. doi:10.1016/j.exger.2015.10.008

Kane, M., Yadav, S. S., Bitzegeio, J., Kutluay, S. B., Zang, T., Wilson, S. J., . . . Bieniasz, P. D. (2013). MX2 is an interferon-induced inhibitor of HIV-1 infection. *Nature, 502*(7472), 563-566. doi:10.1038/nature12653

Kang, H. T., Lee, K. B., Kim, S. Y., Choi, H. R., & Park, S. C. (2011). Autophagy impairment induces premature senescence in primary human fibroblasts. *PLoS One, 6*(8), e23367. doi:10.1371/journal.pone.0023367

Kanki, T., Ohgaki, K., Gaspari, M., Gustafsson, C. M., Fukuoh, A., Sasaki, N., . . . Kang, D. (2004). Architectural role of mitochondrial transcription factor A in maintenance of human mitochondrial DNA. *Mol Cell Biol, 24*(22), 9823-9834. doi:10.1128/mcb.24.22.9823-9834.2004

Kaplon, J., Zheng, L., Meissl, K., Chaneton, B., Selivanov, V. A., Mackay, G., . . . Peeper, D. S. (2013). A key role for mitochondrial gatekeeper pyruvate dehydrogenase in oncogene-induced senescence. *Nature, 498*(7452), 109-112. doi:10.1038/nature12154

Karbowski, M., Lee, Y. J., Gaume, B., Jeong, S. Y., Frank, S., Nechushtan, A., . . . Youle, R. J. (2002). Spatial and temporal association of Bax with mitochondrial fission sites, Drp1, and Mfn2 during apoptosis. *J Cell Biol, 159*(6), 931-938. doi:10.1083/jcb.200209124

Karbowski, M., Norris, K. L., Cleland, M. M., Jeong, S. Y., & Youle, R. J. (2006). Role of Bax and Bak in mitochondrial morphogenesis. *Nature, 443*(7112), 658-662. doi:10.1038/nature05111

Karbowski, M., & Youle, R. J. (2011). Regulating mitochondrial outer membrane proteins by ubiquitination and proteasomal degradation. *Curr Opin Cell Biol, 23*(4), 476-482. doi:10.1016/j.ceb.2011.05.007

Karin, O., Agrawal, A., Porat, Z., Krizhanovsky, V., & Alon, U. (2019). Senescent cell turnover slows with age providing an explanation for the Gompertz law. *Nat Commun, 10*(1), 5495. doi:10.1038/s41467-019-13192-4

Käser, M., & Langer, T. (2000). Protein degradation in mitochondria. *Semin Cell Dev Biol, 11*(3), 181-190. doi:10.1006/scdb.2000.0166

Kashatus, J. A., Nascimento, A., Myers, L. J., Sher, A., Byrne, F. L., Hoehn, K. L., . . . Kashatus, D. F. (2015). Erk2 phosphorylation of Drp1 promotes mitochondrial fission and MAPK-driven tumor growth. *Mol Cell, 57*(3), 537-551. doi:10.1016/j.molcel.2015.01.002

Kelley, W. J., Zemans, R. L., & Goldstein, D. R. (2020). Cellular senescence: friend or foe to respiratory viral infections? *Eur Respir J, 56*(6). doi:10.1183/13993003.02708-2020

Kim, S. J., Syed, G. H., Khan, M., Chiu, W. W., Sohail, M. A., Gish, R. G., & Siddiqui, A. (2014). Hepatitis C virus triggers mitochondrial fission and attenuates apoptosis to promote viral persistence. *Proc Natl Acad Sci U S A, 111*(17), 6413-6418. doi:10.1073/pnas.1321114111

King, M. C., Raposo, G., & Lemmon, M. A. (2004). Inhibition of nuclear import and cell-cycle progression by mutated forms of the dynamin-like GTPase MxB. *Proc Natl Acad Sci U S A, 101*(24), 8957-8962. doi:10.1073/pnas.0403167101

Kirkland, J. L., & Tchkonia, T. (2017). Cellular Senescence: A Translational Perspective. *EBioMedicine, 21*, 21-28. doi:10.1016/j.ebiom.2017.04.013

Kirkland, J. L., & Tchkonia, T. (2020). Senolytic drugs: from discovery to translation. *J Intern Med, 288*(5), 518-536. doi:10.1111/joim.13141

Kirkland, J. L., Tchkonia, T., Zhu, Y., Niedernhofer, L. J., & Robbins, P. D. (2017). The Clinical Potential of Senolytic Drugs. *J Am Geriatr Soc, 65*(10), 2297-2301. doi:10.1111/jgs.14969

Koch, S., Solana, R., Dela Rosa, O., & Pawelec, G. (2006). Human cytomegalovirus infection and T cell immunosenescence: a mini review. *Mech Ageing Dev, 127*(6), 538-543. doi:10.1016/j.mad.2006.01.011

Kohler, C., Radpour, R., Barekati, Z., Asadollahi, R., Bitzer, J., Wight, E., . . . Zhong, X. Y. (2009). Levels of plasma circulating cell free nuclear and mitochondrial DNA as potential biomarkers for breast tumors. *Mol Cancer, 8*, 105. doi:10.1186/1476-4598-8-105

Korolchuk, V. I., Miwa, S., Carroll, B., & von Zglinicki, T. (2017). Mitochondria in Cell Senescence: Is Mitophagy the Weakest Link? *EBioMedicine, 21*, 7-13. doi:10.1016/j.ebiom.2017.03.020

Kosar, M., Bartkova, J., Hubackova, S., Hodny, Z., Lukas, J., & Bartek, J. (2011). Senescence-associated heterochromatin foci are dispensable for cellular senescence, occur in a cell type- and insult-dependent manner and follow expression of p16(ink4a). *Cell Cycle, 10*(3), 457-468. doi:10.4161/cc.10.3.14707

Kowal, J., Arras, G., Colombo, M., Jouve, M., Morath, J. P., Primdal-Bengtson, B., . . . Théry, C. (2016). Proteomic comparison defines novel markers to characterize heterogeneous populations of extracellular vesicle subtypes. *Proc Natl Acad Sci U S A, 113*(8), E968-977. doi:10.1073/pnas.1521230113

Kowald, A., Passos, J. F., & Kirkwood, T. B. L. (2020). On the evolution of cellular senescence. *Aging Cell, 19*(12), e13270. doi:10.1111/acel.13270

Kracikova, M., Akiri, G., George, A., Sachidanandam, R., & Aaronson, S. A. (2013). A threshold mechanism mediates p53 cell fate decision between growth arrest and apoptosis. *Cell Death Differ, 20*(4), 576-588. doi:10.1038/cdd.2012.155

Krizhanovsky, V., Yon, M., Dickins, R. A., Hearn, S., Simon, J., Miething, C., . . . Lowe, S. W. (2008). Senescence of activated stellate cells limits liver fibrosis. *Cell, 134*(4), 657-667. doi:10.1016/j.cell.2008.06.049

Kuilman, T., Michaloglou, C., Mooi, W. J., & Peeper, D. S. (2010). The essence of senescence. *Genes Dev, 24*(22), 2463-2479. doi:10.1101/gad.1971610

Kuilman, T., Michaloglou, C., Vredeveld, L. C., Douma, S., van Doorn, R., Desmet, C. J., . . . Peeper, D. S. (2008). Oncogene-induced senescence relayed by an interleukin-dependent inflammatory network. *Cell, 133*(6), 1019-1031. doi:10.1016/j.cell.2008.03.039

Kuilman, T., & Peeper, D. S. (2009). Senescence-messaging secretome: SMS-ing cellular stress. *Nat Rev Cancer, 9*(2), 81-94. doi:10.1038/nrc2560

Kukat, C., Wurm, C. A., Spåhr, H., Falkenberg, M., Larsson, N. G., & Jakobs, S. (2011). Super-resolution microscopy reveals that mammalian mitochondrial nucleoids have a uniform size and

frequently contain a single copy of mtDNA. *Proc Natl Acad Sci U S A, 108*(33), 13534-13539. doi:10.1073/pnas.1109263108
Kurz, D. J., Decary, S., Hong, Y., & Erusalimsky, J. D. (2000). Senescence-associated (beta)-galactosidase reflects an increase in lysosomal mass during replicative ageing of human endothelial cells. *J Cell Sci, 113 (Pt 20)*, 3613-3622.
Laberge, R. M., Sun, Y., Orjalo, A. V., Patil, C. K., Freund, A., Zhou, L., . . . Campisi, J. (2015). MTOR regulates the pro-tumorigenic senescence-associated secretory phenotype by promoting IL1A translation. *Nat Cell Biol, 17*(8), 1049-1061. doi:10.1038/ncb3195
Lackner, L. L. (2019). The Expanding and Unexpected Functions of Mitochondria Contact Sites. *Trends Cell Biol, 29*(7), 580-590. doi:10.1016/j.tcb.2019.02.009
Ladoukakis, E. D., & Zouros, E. (2017). Evolution and inheritance of animal mitochondrial DNA: rules and exceptions. *J Biol Res (Thessalon), 24*, 2. doi:10.1186/s40709-017-0060-4
Land, H., Parada, L. F., & Weinberg, R. A. (1983). Cellular oncogenes and multistep carcinogenesis. *Science, 222*(4625), 771-778. doi:10.1126/science.6356358
Lang, B. F., Gray, M. W., & Burger, G. (1999). Mitochondrial genome evolution and the origin of eukaryotes. *Annu Rev Genet, 33*, 351-397. doi:10.1146/annurev.genet.33.1.351
Laplante, M., & Sabatini, D. M. (2009). An emerging role of mTOR in lipid biosynthesis. *Curr Biol, 19*(22), R1046-1052. doi:10.1016/j.cub.2009.09.058
Larribere, L., Wu, H., Novak, D., Galach, M., Bernhardt, M., Orouji, E., . . . Utikal, J. (2015). NF1 loss induces senescence during human melanocyte differentiation in an iPSC-based model. *Pigment Cell Melanoma Res, 28*(4), 407-416. doi:10.1111/pcmr.12369
Lartigue, L., Medina, C., Schembri, L., Chabert, P., Zanese, M., Tomasello, F., . . . De Giorgi, F. (2008). An intracellular wave of cytochrome c propagates and precedes Bax redistribution during apoptosis. *J Cell Sci, 121*(Pt 21), 3515-3523. doi:10.1242/jcs.029587
Lau, L., Porciuncula, A., Yu, A., Iwakura, Y., & David, G. (2019). Uncoupling the Senescence-Associated Secretory Phenotype from Cell Cycle Exit via Interleukin-1 Inactivation Unveils Its Protumorigenic Role. *Mol Cell Biol, 39*(12). doi:10.1128/MCB.00586-18
Leboucher, G. P., Tsai, Y. C., Yang, M., Shaw, K. C., Zhou, M., Veenstra, T. D., . . . Weissman, A. M. (2012). Stress-induced phosphorylation and proteasomal degradation of mitofusin 2 facilitates mitochondrial fragmentation and apoptosis. *Mol Cell, 47*(4), 547-557. doi:10.1016/j.molcel.2012.05.041
LeBrasseur, N. K., Tchkonia, T., & Kirkland, J. L. (2015). Cellular Senescence and the Biology of Aging, Disease, and Frailty. *Nestle Nutr Inst Workshop Ser, 83*, 11-18. doi:10.1159/000382054
Lee, B. Y., Han, J. A., Im, J. S., Morrone, A., Johung, K., Goodwin, E. C., . . . Hwang, E. S. (2006). Senescence-associated beta-galactosidase is lysosomal beta-galactosidase. *Aging Cell, 5*(2), 187-195. doi:10.1111/j.1474-9726.2006.00199.x
Lee, J. Y., Kapur, M., Li, M., Choi, M. C., Choi, S., Kim, H. J., . . . Yao, T. P. (2014). MFN1 deacetylation activates adaptive mitochondrial fusion and protects metabolically challenged mitochondria. *J Cell Sci, 127*(Pt 22), 4954-4963. doi:10.1242/jcs.157321
Lee, S. M., Dho, S. H., Ju, S. K., Maeng, J. S., Kim, J. Y., & Kwon, K. S. (2012). Cytosolic malate dehydrogenase regulates senescence in human fibroblasts. *Biogerontology, 13*(5), 525-536. doi:10.1007/s10522-012-9397-0
Lehmann, J., Baar, M. P., & de Keizer, P. L. J. (2018). Senescent Cells Drive Frailty through Systemic Signals. *Trends Mol Med, 24*(11), 917-918. doi:10.1016/j.molmed.2018.09.003
Little, J. P., Simtchouk, S., Schindler, S. M., Villanueva, E. B., Gill, N. E., Walker, D. G., . . . Klegeris, A. (2014). Mitochondrial transcription factor A (Tfam) is a pro-inflammatory extracellular signaling molecule recognized by brain microglia. *Mol Cell Neurosci, 60*, 88-96. doi:10.1016/j.mcn.2014.04.003
Liu, C., & Lin, J. D. (2011). PGC-1 coactivators in the control of energy metabolism. *Acta Biochim Biophys Sin (Shanghai), 43*(4), 248-257. doi:10.1093/abbs/gmr007

Liu, D., Gao, Y., Liu, J., Huang, Y., Yin, J., Feng, Y., . . . Gao, J. (2021). Intercellular mitochondrial transfer as a means of tissue revitalization. *Signal Transduction and Targeted Therapy, 6*(1), 65. doi:10.1038/s41392-020-00440-z

Liu, D., & Hornsby, P. J. (2007). Senescent human fibroblasts increase the early growth of xenograft tumors via matrix metalloproteinase secretion. *Cancer Res, 67*(7), 3117-3126. doi:10.1158/0008-5472.CAN-06-3452

Liu, G. Y., & Sabatini, D. M. (2020). mTOR at the nexus of nutrition, growth, ageing and disease. *Nat Rev Mol Cell Biol, 21*(4), 183-203. doi:10.1038/s41580-019-0199-y

Liu, H., He, Z., & Simon, H. U. (2014). Autophagy suppresses melanoma tumorigenesis by inducing senescence. *Autophagy, 10*(2), 372-373. doi:10.4161/auto.27163

Liu, J. Y., Souroullas, G. P., Diekman, B. O., Krishnamurthy, J., Hall, B. M., Sorrentino, J. A., . . . Sharpless, N. E. (2019). Cells exhibiting strong p16 (INK4a) promoter activation in vivo display features of senescence. *Proc Natl Acad Sci U S A, 116*(7), 2603-2611. doi:10.1073/pnas.1818313116

Liu, Z., Pan, Q., Ding, S., Qian, J., Xu, F., Zhou, J., . . . Liang, C. (2013). The interferon-inducible MxB protein inhibits HIV-1 infection. *Cell Host Microbe, 14*(4), 398-410. doi:10.1016/j.chom.2013.08.015

Longhese, M. P., Anbalagan, S., Martina, M., & Bonetti, D. (2012). The role of shelterin in maintaining telomere integrity. *Front Biosci (Landmark Ed), 17*, 1715-1728. doi:10.2741/4014

Lopes-Paciencia, S., Saint-Germain, E., Rowell, M. C., Ruiz, A. F., Kalegari, P., & Ferbeyre, G. (2019). The senescence-associated secretory phenotype and its regulation. *Cytokine, 117*, 15-22. doi:10.1016/j.cyto.2019.01.013

Lopez-Otin, C., Blasco, M. A., Partridge, L., Serrano, M., & Kroemer, G. (2013). The hallmarks of aging. *Cell, 153*(6), 1194-1217. doi:10.1016/j.cell.2013.05.039

Lopez, J., & Tait, S. W. G. (2015). Mitochondrial apoptosis: killing cancer using the enemy within. *British journal of cancer, 112*(6), 957-962. doi:10.1038/bjc.2015.85

Lorenzini, A., Tresini, M., Mawal-Dewan, M., Frisoni, L., Zhang, H., Allen, R. G., . . . Cristofalo, V. J. (2002). Role of the Raf/MEK/ERK and the PI3K/Akt(PKB) pathways in fibroblast senescence. *Exp Gerontol, 37*(10-11), 1149-1156. doi:10.1016/s0531-5565(02)00133-x

Lyall, M. J., Cartier, J., Thomson, J. P., Cameron, K., Meseguer-Ripolles, J., O'Duibhir, E., . . . Drake, A. J. (2018). Modelling non-alcoholic fatty liver disease in human hepatocyte-like cells. *Philos Trans R Soc Lond B Biol Sci, 373*(1750). doi:10.1098/rstb.2017.0362

Machida, K., McNamara, G., Cheng, K. T., Huang, J., Wang, C. H., Comai, L., . . . Lai, M. M. (2010). Hepatitis C virus inhibits DNA damage repair through reactive oxygen and nitrogen species and by interfering with the ATM-NBS1/Mre11/Rad50 DNA repair pathway in monocytes and hepatocytes. *J Immunol, 185*(11), 6985-6998. doi:10.4049/jimmunol.1000618

MacVicar, T., & Langer, T. (2016). OPA1 processing in cell death and disease - the long and short of it. *J Cell Sci, 129*(12), 2297-2306. doi:10.1242/jcs.159186

Mai, S., Klinkenberg, M., Auburger, G., Bereiter-Hahn, J., & Jendrach, M. (2010). Decreased expression of Drp1 and Fis1 mediates mitochondrial elongation in senescent cells and enhances resistance to oxidative stress through PINK1. *J Cell Sci, 123*(Pt 6), 917-926. doi:10.1242/jcs.059246

Malavolta, M., Giacconi, R., Brunetti, D., Provinciali, M., & Maggi, F. (2020). Exploring the Relevance of Senotherapeutics for the Current SARS-CoV-2 Emergency and Similar Future Global Health Threats. *Cells, 9*(4). doi:10.3390/cells9040909

Mannava, S., Moparthy, K. C., Wheeler, L. J., Natarajan, V., Zucker, S. N., Fink, E. E., . . . Nikiforov, M. A. (2013). Depletion of deoxyribonucleotide pools is an endogenous source of DNA damage in cells undergoing oncogene-induced senescence. *Am J Pathol, 182*(1), 142-151. doi:10.1016/j.ajpath.2012.09.011

Marcotte, R., Lacelle, C., & Wang, E. (2004). Senescent fibroblasts resist apoptosis by downregulating caspase-3. *Mech Ageing Dev, 125*(10-11), 777-783. doi:10.1016/j.mad.2004.07.007

Marroquin, L. D., Hynes, J., Dykens, J. A., Jamieson, J. D., & Will, Y. (2007). Circumventing the Crabtree effect: replacing media glucose with galactose increases susceptibility of HepG2 cells to mitochondrial toxicants. *Toxicol Sci, 97*(2), 539-547. doi:10.1093/toxsci/kfm052

Martens, A., Schmid, B., Akintola, O., & Saretzki, G. (2019). Telomerase Does Not Improve DNA Repair in Mitochondria upon Stress but Increases MnSOD Protein under Serum-Free Conditions. *Int J Mol Sci, 21*(1). doi:10.3390/ijms21010027

Martin, S. J., Henry, C. M., & Cullen, S. P. (2012). A perspective on mammalian caspases as positive and negative regulators of inflammation. *Mol Cell, 46*(4), 387-397. doi:10.1016/j.molcel.2012.04.026

Martínez-Redondo, V., Pettersson, A. T., & Ruas, J. L. (2015). The hitchhiker's guide to PGC-1α isoform structure and biological functions. *Diabetologia, 58*(9), 1969-1977. doi:10.1007/s00125-015-3671-z

Martínez, I., García-Carpizo, V., Guijarro, T., García-Gomez, A., Navarro, D., Aranda, A., & Zambrano, A. (2016). Induction of DNA double-strand breaks and cellular senescence by human respiratory syncytial virus. *Virulence, 7*(4), 427-442. doi:10.1080/21505594.2016.1144001

Martinou, J. C., Desagher, S., & Antonsson, B. (2000). Cytochrome c release from mitochondria: all or nothing. *Nat Cell Biol, 2*(3), E41-43. doi:10.1038/35004069

Maruta, H., & Burgess, A. W. (1994). Regulation of the Ras signalling network. *Bioessays, 16*(7), 489-496. doi:10.1002/bies.950160708

Mason, D. X., Jackson, T. J., & Lin, A. W. (2004). Molecular signature of oncogenic ras-induced senescence. *Oncogene, 23*(57), 9238-9246. doi:10.1038/sj.onc.1208172

Matsuda, N., & Tanaka, K. (2010). Uncovering the roles of PINK1 and parkin in mitophagy. *Autophagy, 6*(7), 952-954. doi:10.4161/auto.6.7.13039

Matsuyama, S., Llopis, J., Deveraux, Q. L., Tsien, R. Y., & Reed, J. C. (2000). Changes in intramitochondrial and cytosolic pH: early events that modulate caspase activation during apoptosis. *Nat Cell Biol, 2*(6), 318-325. doi:10.1038/35014006

May, A. I., Devenish, R. J., & Prescott, M. (2012). The many faces of mitochondrial autophagy: making sense of contrasting observations in recent research. *Int J Cell Biol, 2012*, 431684. doi:10.1155/2012/431684

Maya-Mendoza, A., Ostrakova, J., Kosar, M., Hall, A., Duskova, P., Mistrik, M., . . . Bartek, J. (2015). Myc and Ras oncogenes engage different energy metabolism programs and evoke distinct patterns of oxidative and DNA replication stress. *Mol Oncol, 9*(3), 601-616. doi:10.1016/j.molonc.2014.11.001

Mazurek, S., Zwerschke, W., Jansen-Durr, P., & Eigenbrodt, E. (2001). Effects of the human papilloma virus HPV-16 E7 oncoprotein on glycolysis and glutaminolysis: role of pyruvate kinase type M2 and the glycolytic-enzyme complex. *Biochem J, 356*(Pt 1), 247-256. doi:10.1042/0264-6021:3560247

McArthur, K., Whitehead, L. W., Heddleston, J. M., Li, L., Padman, B. S., Oorschot, V., . . . Kile, B. T. (2018). BAK/BAX macropores facilitate mitochondrial herniation and mtDNA efflux during apoptosis. *Science, 359*(6378). doi:10.1126/science.aao6047

McBride, H. M., Neuspiel, M., & Wasiak, S. (2006). Mitochondria: more than just a powerhouse. *Curr Biol, 16*(14), R551-560. doi:10.1016/j.cub.2006.06.054

McClintock, B. (1941). The Stability of Broken Ends of Chromosomes in Zea Mays. *Genetics, 26*(2), 234-282. Retrieved from https://www.ncbi.nlm.nih.gov/pubmed/17247004

McKinney, E. A., & Oliveira, M. T. (2013). Replicating animal mitochondrial DNA. *Genet Mol Biol, 36*(3), 308-315. doi:10.1590/s1415-47572013000300002

Melber, A., & Haynes, C. M. (2018). UPR(mt) regulation and output: a stress response mediated by mitochondrial-nuclear communication. *Cell Res, 28*(3), 281-295. doi:10.1038/cr.2018.16

Melén, K., Keskinen, P., Ronni, T., Sareneva, T., Lounatmaa, K., & Julkunen, I. (1996). Human MxB protein, an interferon-alpha-inducible GTPase, contains a nuclear targeting signal and is

localized in the heterochromatin region beneath the nuclear envelope. *J Biol Chem, 271*(38), 23478-23486. doi:10.1074/jbc.271.38.23478

Meyne, J., Ratliff, R. L., & Moyzis, R. K. (1989). Conservation of the human telomere sequence (TTAGGG)n among vertebrates. *Proc Natl Acad Sci U S A, 86*(18), 7049-7053. doi:10.1073/pnas.86.18.7049

Michaloglou, C., Vredeveld, L. C., Soengas, M. S., Denoyelle, C., Kuilman, T., van der Horst, C. M., . . . Peeper, D. S. (2005). BRAFE600-associated senescence-like cell cycle arrest of human naevi. *Nature, 436*(7051), 720-724. doi:10.1038/nature03890

Miles, R. J., Kerridge, C., Hilditch, L., Monit, C., Jacques, D. A., & Towers, G. J. (2020). MxB sensitivity of HIV-1 is determined by a highly variable and dynamic capsid surface. *Elife, 9*. doi:10.7554/eLife.56910

Mitsui, Y., & Schneider, E. L. (1976). Increased nuclear sizes in senescent human diploid fibroblast cultures. *Exp Cell Res, 100*(1), 147-152. doi:10.1016/0014-4827(76)90336-0

Miwa, S., Lawless, C., & von Zglinicki, T. (2008). Mitochondrial turnover in liver is fast in vivo and is accelerated by dietary restriction: application of a simple dynamic model. *Aging Cell, 7*(6), 920-923. doi:10.1111/j.1474-9726.2008.00426.x

Mizushima, N., Levine, B., Cuervo, A. M., & Klionsky, D. J. (2008). Autophagy fights disease through cellular self-digestion. *Nature, 451*(7182), 1069-1075. doi:10.1038/nature06639

Moiseeva, O., Bourdeau, V., Roux, A., Deschenes-Simard, X., & Ferbeyre, G. (2009). Mitochondrial dysfunction contributes to oncogene-induced senescence. *Mol Cell Biol, 29*(16), 4495-4507. doi:10.1128/MCB.01868-08

Morris, D. L., Kastner, D. W., Johnson, S., Strub, M. P., He, Y., Bleck, C. K. E., . . . Tjandra, N. (2019). Humanin induces conformational changes in the apoptosis regulator BAX and sequesters it into fibers, preventing mitochondrial outer-membrane permeabilization. *J Biol Chem, 294*(50), 19055-19065. doi:10.1074/jbc.RA119.011297

Munoz-Espin, D., Canamero, M., Maraver, A., Gomez-Lopez, G., Contreras, J., Murillo-Cuesta, S., . . . Serrano, M. (2013). Programmed cell senescence during mammalian embryonic development. *Cell, 155*(5), 1104-1118. doi:10.1016/j.cell.2013.10.019

Murray-Zmijewski, F., Slee, E. A., & Lu, X. (2008). A complex barcode underlies the heterogeneous response of p53 to stress. *Nat Rev Mol Cell Biol, 9*(9), 702-712. doi:10.1038/nrm2451

Myrianthopoulos, V., Evangelou, K., Vasileiou, P. V. S., Cooks, T., Vassilakopoulos, T. P., Pangalis, G. A., . . . Gorgoulis, V. G. (2019). Senescence and senotherapeutics: a new field in cancer therapy. *Pharmacol Ther, 193*, 31-49. doi:10.1016/j.pharmthera.2018.08.006

Nacarelli, T., Liu, P., & Zhang, R. (2017). Epigenetic Basis of Cellular Senescence and Its Implications in Aging. *Genes (Basel), 8*(12). doi:10.3390/genes8120343

Nagata, S. (2005). DNA degradation in development and programmed cell death. *Annu Rev Immunol, 23*, 853-875. doi:10.1146/annurev.immunol.23.021704.115811

Nakahira, K., Haspel, J. A., Rathinam, V. A., Lee, S. J., Dolinay, T., Lam, H. C., . . . Choi, A. M. (2011). Autophagy proteins regulate innate immune responses by inhibiting the release of mitochondrial DNA mediated by the NALP3 inflammasome. *Nat Immunol, 12*(3), 222-230. doi:10.1038/ni.1980

Nargund, A. M., Pellegrino, M. W., Fiorese, C. J., Baker, B. M., & Haynes, C. M. (2012). Mitochondrial import efficiency of ATFS-1 regulates mitochondrial UPR activation. *Science, 337*(6094), 587-590. doi:10.1126/science.1223560

Navratil, M., Terman, A., & Arriaga, E. A. (2008). Giant mitochondria do not fuse and exchange their contents with normal mitochondria. *Exp Cell Res, 314*(1), 164-172. doi:10.1016/j.yexcr.2007.09.013

Nelson, D. M., McBryan, T., Jeyapalan, J. C., Sedivy, J. M., & Adams, P. D. (2014). A comparison of oncogene-induced senescence and replicative senescence: implications for tumor suppression and aging. *Age (Dordr), 36*(3), 9637. doi:10.1007/s11357-014-9637-0

Nelson, G., Wordsworth, J., Wang, C., Jurk, D., Lawless, C., Martin-Ruiz, C., & von Zglinicki, T. (2012). A senescent cell bystander effect: senescence-induced senescence. *Aging Cell, 11*(2), 345-349. doi:10.1111/j.1474-9726.2012.00795.x

Neurohr, G. E., Terry, R. L., Lengefeld, J., Bonney, M., Brittingham, G. P., Moretto, F., . . . Amon, A. (2019). Excessive Cell Growth Causes Cytoplasm Dilution And Contributes to Senescence. *Cell, 176*(5), 1083-1097.e1018. doi:10.1016/j.cell.2019.01.018

Nicholls, T. J., & Minczuk, M. (2014). In D-loop: 40 years of mitochondrial 7S DNA. *Exp Gerontol, 56*, 175-181. doi:10.1016/j.exger.2014.03.027

Ning, X., Wang, Y., Jing, M., Sha, M., Lv, M., Gao, P., . . . Jiang, Z. (2019). Apoptotic Caspases Suppress Type I Interferon Production via the Cleavage of cGAS, MAVS, and IRF3. *Mol Cell, 74*(1), 19-31.e17. doi:10.1016/j.molcel.2019.02.013

Nissanka, N., Bacman, S. R., Plastini, M. J., & Moraes, C. T. (2018). The mitochondrial DNA polymerase gamma degrades linear DNA fragments precluding the formation of deletions. *Nat Commun, 9*(1), 2491. doi:10.1038/s41467-018-04895-1

Oakes, S. A., Scorrano, L., Opferman, J. T., Bassik, M. C., Nishino, M., Pozzan, T., & Korsmeyer, S. J. (2005). Proapoptotic BAX and BAK regulate the type 1 inositol trisphosphate receptor and calcium leak from the endoplasmic reticulum. *Proc Natl Acad Sci U S A, 102*(1), 105-110. doi:10.1073/pnas.0408352102

Oettinghaus, B., D'Alonzo, D., Barbieri, E., Restelli, L. M., Savoia, C., Licci, M., . . . Scorrano, L. (2016). DRP1-dependent apoptotic mitochondrial fission occurs independently of BAX, BAK and APAF1 to amplify cell death by BID and oxidative stress. *Biochim Biophys Acta, 1857*(8), 1267-1276. doi:10.1016/j.bbabio.2016.03.016

Ogrodnik, M., Miwa, S., Tchkonia, T., Tiniakos, D., Wilson, C. L., Lahat, A., . . . Jurk, D. (2017). Cellular senescence drives age-dependent hepatic steatosis. *Nat Commun, 8*, 15691. doi:10.1038/ncomms15691

Ogrodnik, M., Salmonowicz, H., & Gladyshev, V. N. (2019). Integrating cellular senescence with the concept of damage accumulation in aging: Relevance for clearance of senescent cells. *Aging Cell, 18*(1), e12841. doi:10.1111/acel.12841

Ogrodnik, M., Salmonowicz, H., Jurk, D., & Passos, J. F. (2019). Expansion and Cell-Cycle Arrest: Common Denominators of Cellular Senescence. *Trends Biochem Sci, 44*(12), 996-1008. doi:10.1016/j.tibs.2019.06.011

Ohtsuji, M., Katsuoka, F., Kobayashi, A., Aburatani, H., Hayes, J. D., & Yamamoto, M. (2008). Nrf1 and Nrf2 play distinct roles in activation of antioxidant response element-dependent genes. *J Biol Chem, 283*(48), 33554-33562. doi:10.1074/jbc.M804597200

Olivieri, F., Prattichizzo, F., Grillari, J., & Balistreri, C. R. (2018). Cellular Senescence and Inflammaging in Age-Related Diseases. *Mediators Inflamm, 2018*, 9076485. doi:10.1155/2018/9076485

Olsen, C. L., Gardie, B., Yaswen, P., & Stampfer, M. R. (2002). Raf-1-induced growth arrest in human mammary epithelial cells is p16-independent and is overcome in immortal cells during conversion. *Oncogene, 21*(41), 6328-6339. doi:10.1038/sj.onc.1205780

Omori, S., Wang, T. W., Johmura, Y., Kanai, T., Nakano, Y., Kido, T., . . . Nakanishi, M. (2020). Generation of a p16 Reporter Mouse and Its Use to Characterize and Target p16(high) Cells In Vivo. *Cell Metab, 32*(5), 814-828 e816. doi:10.1016/j.cmet.2020.09.006

Onoguchi, K., Onomoto, K., Takamatsu, S., Jogi, M., Takemura, A., Morimoto, S., . . . Fujita, T. (2010). Virus-infection or 5'ppp-RNA activates antiviral signal through redistribution of IPS-1 mediated by MFN1. *PLoS Pathog, 6*(7), e1001012. doi:10.1371/journal.ppat.1001012

Orgel, L. E. (1973). Ageing of clones of mammalian cells. *Nature, 243*(5408), 441-445. doi:10.1038/243441a0

Orjalo, A. V., Bhaumik, D., Gengler, B. K., Scott, G. K., & Campisi, J. (2009). Cell surface-bound IL-1alpha is an upstream regulator of the senescence-associated IL-6/IL-8 cytokine network. *Proc Natl Acad Sci U S A, 106*(40), 17031-17036. doi:10.1073/pnas.0905299106

Ott, M., Robertson, J. D., Gogvadze, V., Zhivotovsky, B., & Orrenius, S. (2002). Cytochrome c release from mitochondria proceeds by a two-step process. *Proc Natl Acad Sci U S A, 99*(3), 1259-1263. doi:10.1073/pnas.241655498

Pahl, H. L. (1999). Activators and target genes of Rel/NF-kappaB transcription factors. *Oncogene, 18*(49), 6853-6866. doi:10.1038/sj.onc.1203239

Pahl, H. L. (1999). Signal transduction from the endoplasmic reticulum to the cell nucleus. *Physiol Rev, 79*(3), 683-701. doi:10.1152/physrev.1999.79.3.683

Pajvani, U. B., Trujillo, M. E., Combs, T. P., Iyengar, P., Jelicks, L., Roth, K. A., . . . Scherer, P. E. (2005). Fat apoptosis through targeted activation of caspase 8: a new mouse model of inducible and reversible lipoatrophy. *Nat Med, 11*(7), 797-803. doi:10.1038/nm1262

Palmer, A. K., Xu, M., Zhu, Y., Pirtskhalava, T., Weivoda, M. M., Hachfeld, C. M., . . . Kirkland, J. L. (2019). Targeting senescent cells alleviates obesity-induced metabolic dysfunction. *Aging Cell, 18*(3), e12950. doi:10.1111/acel.12950

Palmer, G., Horgan, D. J., Tisdale, H., Singer, T. P., & Beinert, H. (1968). Studies on the respiratory chain-linked reduced nicotinamide adenine dinucleotide dehydrogenase. XIV. Location of the sites of inhibition of rotenone, barbiturates, and piericidin by means of electron paramagnetic resonance spectroscopy. *J Biol Chem, 243*(4), 844-847.

Papa, L., & Germain, D. (2011). Estrogen receptor mediates a distinct mitochondrial unfolded protein response. *J Cell Sci, 124*(Pt 9), 1396-1402. doi:10.1242/jcs.078220

Park, S., Won, J. H., Hwang, I., Hong, S., Lee, H. K., & Yu, J. W. (2015). Defective mitochondrial fission augments NLRP3 inflammasome activation. *Sci Rep, 5*, 15489. doi:10.1038/srep15489

Pascal, T., Debacq-Chainiaux, F., Chretien, A., Bastin, C., Dabee, A. F., Bertholet, V., . . . Toussaint, O. (2005). Comparison of replicative senescence and stress-induced premature senescence combining differential display and low-density DNA arrays. *FEBS Lett, 579*(17), 3651-3659. doi:10.1016/j.febslet.2005.05.056

Passos, J. F., Nelson, G., Wang, C., Richter, T., Simillion, C., Proctor, C. J., . . . von Zglinicki, T. (2010). Feedback between p21 and reactive oxygen production is necessary for cell senescence. *Mol Syst Biol, 6*, 347. doi:10.1038/msb.2010.5

Passos, J. F., Saretzki, G., Ahmed, S., Nelson, G., Richter, T., Peters, H., . . . von Zglinicki, T. (2007). Mitochondrial dysfunction accounts for the stochastic heterogeneity in telomere-dependent senescence. *PLoS Biol, 5*(5), e110. doi:10.1371/journal.pbio.0050110

Pazmandi, K., Agod, Z., Kumar, B. V., Szabo, A., Fekete, T., Sogor, V., . . . Bacsi, A. (2014). Oxidative modification enhances the immunostimulatory effects of extracellular mitochondrial DNA on plasmacytoid dendritic cells. *Free Radic Biol Med, 77*, 281-290. doi:10.1016/j.freeradbiomed.2014.09.028

Petrova, N. V., Velichko, A. K., Razin, S. V., & Kantidze, O. L. (2016). Small molecule compounds that induce cellular senescence. *Aging Cell, 15*(6), 999-1017. doi:10.1111/acel.12518

Pfanner, N., Warscheid, B., & Wiedemann, N. (2019). Mitochondrial proteins: from biogenesis to functional networks. *Nat Rev Mol Cell Biol, 20*(5), 267-284. doi:10.1038/s41580-018-0092-0

Piantadosi, C. A., & Suliman, H. B. (2006). Mitochondrial transcription factor A induction by redox activation of nuclear respiratory factor 1. *J Biol Chem, 281*(1), 324-333. doi:10.1074/jbc.M508805200

Pinti, M., Cevenini, E., Nasi, M., De Biasi, S., Salvioli, S., Monti, D., . . . Cossarizza, A. (2014). Circulating mitochondrial DNA increases with age and is a familiar trait: Implications for "inflamm-aging". *Eur J Immunol, 44*(5), 1552-1562. doi:10.1002/eji.201343921

Platnich, J. M., & Muruve, D. A. (2019). NOD-like receptors and inflammasomes: A review of their canonical and non-canonical signaling pathways. *Arch Biochem Biophys, 670*, 4-14. doi:10.1016/j.abb.2019.02.008

Ploumi, C., Daskalaki, I., & Tavernarakis, N. (2017). Mitochondrial biogenesis and clearance: a balancing act. *Febs j, 284*(2), 183-195. doi:10.1111/febs.13820

Pluquet, O., Pourtier, A., & Abbadie, C. (2015). The unfolded protein response and cellular senescence. A review in the theme: cellular mechanisms of endoplasmic reticulum stress signaling in health and disease. *Am J Physiol Cell Physiol, 308*(6), C415-425. doi:10.1152/ajpcell.00334.2014

Poveda-Huertes, D., Matic, S., Marada, A., Habernig, L., Licheva, M., Myketin, L., . . . Vögtle, F. N. (2020). An Early mtUPR: Redistribution of the Nuclear Transcription Factor Rox1 to Mitochondria Protects against Intramitochondrial Proteotoxic Aggregates. *Mol Cell, 77*(1), 180-188.e189. doi:10.1016/j.molcel.2019.09.026

Prieto, J., León, M., Ponsoda, X., Sendra, R., Bort, R., Ferrer-Lorente, R., . . . Torres, J. (2016). Early ERK1/2 activation promotes DRP1-dependent mitochondrial fission necessary for cell reprogramming. *Nat Commun, 7*, 11124. doi:10.1038/ncomms11124

Primo, L. M. F., & Teixeira, L. K. (2019). DNA replication stress: oncogenes in the spotlight. *Genet Mol Biol, 43*(1 suppl 1), e20190138. doi:10.1590/1678-4685gmb-2019-0138

Puigserver, P., Wu, Z., Park, C. W., Graves, R., Wright, M., & Spiegelman, B. M. (1998). A cold-inducible coactivator of nuclear receptors linked to adaptive thermogenesis. *Cell, 92*(6), 829-839. doi:10.1016/s0092-8674(00)81410-5

Purvis, J. E., Karhohs, K. W., Mock, C., Batchelor, E., Loewer, A., & Lahav, G. (2012). p53 dynamics control cell fate. *Science, 336*(6087), 1440-1444. doi:10.1126/science.1218351

Qin, Q., Jin, J., He, F., Zheng, Y., Li, T., Zhang, Y., & He, J. (2018). Humanin promotes mitochondrial biogenesis in pancreatic MIN6 β-cells. *Biochem Biophys Res Commun, 497*(1), 292-297. doi:10.1016/j.bbrc.2018.02.071

Quijano, C., Cao, L., Fergusson, M. M., Romero, H., Liu, J., Gutkind, S., . . . Finkel, T. (2012). Oncogene-induced senescence results in marked metabolic and bioenergetic alterations. *Cell Cycle, 11*(7), 1383-1392. doi:10.4161/cc.19800

Ragab, D., Salah Eldin, H., Taeimah, M., Khattab, R., & Salem, R. (2020). The COVID-19 Cytokine Storm; What We Know So Far. *Front Immunol, 11*, 1446. doi:10.3389/fimmu.2020.01446

Rambold, A. S., Kostelecky, B., Elia, N., & Lippincott-Schwartz, J. (2011). Tubular network formation protects mitochondria from autophagosomal degradation during nutrient starvation. *Proc Natl Acad Sci U S A, 108*(25), 10190-10195. doi:10.1073/pnas.1107402108

Rashi-Elkeles, S., Elkon, R., Weizman, N., Linhart, C., Amariglio, N., Sternberg, G., . . . Shiloh, Y. (2006). Parallel induction of ATM-dependent pro- and antiapoptotic signals in response to ionizing radiation in murine lymphoid tissue. *Oncogene, 25*(10), 1584-1592. doi:10.1038/sj.onc.1209189

Reddel, R. R. (2010). Senescence: an antiviral defense that is tumor suppressive? *Carcinogenesis, 31*(1), 19-26. doi:10.1093/carcin/bgp274

Rehm, M., Huber, H. J., Hellwig, C. T., Anguissola, S., Dussmann, H., & Prehn, J. H. (2009). Dynamics of outer mitochondrial membrane permeabilization during apoptosis. *Cell Death Differ, 16*(4), 613-623. doi:10.1038/cdd.2008.187

Riedl, S. J., & Shi, Y. (2004). Molecular mechanisms of caspase regulation during apoptosis. *Nat Rev Mol Cell Biol, 5*(11), 897-907. doi:10.1038/nrm1496

Rigby, R. E., Webb, L. M., Mackenzie, K. J., Li, Y., Leitch, A., Reijns, M. A., . . . Jackson, A. P. (2014). RNA:DNA hybrids are a novel molecular pattern sensed by TLR9. *EMBO J, 33*(6), 542-558. doi:10.1002/embj.201386117

Riley, J. S., Quarato, G., Cloix, C., Lopez, J., O'Prey, J., Pearson, M., . . . Tait, S. W. (2018). Mitochondrial inner membrane permeabilisation enables mtDNA release during apoptosis. *EMBO J, 37*(17). doi:10.15252/embj.201899238

Riley, J. S., & Tait, S. W. (2020). Mitochondrial DNA in inflammation and immunity. *EMBO Rep, 21*(4), e49799. doi:10.15252/embr.201949799

Rizzuto, R., De Stefani, D., Raffaello, A., & Mammucari, C. (2012). Mitochondria as sensors and regulators of calcium signalling. *Nat Rev Mol Cell Biol, 13*(9), 566-578. doi:10.1038/nrm3412

Robbins, P. D., Jurk, D., Khosla, S., Kirkland, J. L., LeBrasseur, N. K., Miller, J. D., . . . Niedernhofer, L. J. (2020). Senolytic Drugs: Reducing Senescent Cell Viability to Extend Health Span. *Annu Rev Pharmacol Toxicol*. doi:10.1146/annurev-pharmtox-050120-105018

Rodier, F., Coppe, J. P., Patil, C. K., Hoeijmakers, W. A., Munoz, D. P., Raza, S. R., . . . Campisi, J. (2009). Persistent DNA damage signalling triggers senescence-associated inflammatory cytokine secretion. *Nat Cell Biol, 11*(8), 973-979. doi:10.1038/ncb1909

Roe, A. J., & Qi, X. (2018). Drp1 phosphorylation by MAPK1 causes mitochondrial dysfunction in cell culture model of Huntington's disease. *Biochem Biophys Res Commun, 496*(2), 706-711. doi:10.1016/j.bbrc.2018.01.114

Rongvaux, A., Jackson, R., Harman, C. C., Li, T., West, A. P., de Zoete, M. R., . . . Flavell, R. A. (2014). Apoptotic caspases prevent the induction of type I interferons by mitochondrial DNA. *Cell, 159*(7), 1563-1577. doi:10.1016/j.cell.2014.11.037

Roper, J. M., Mazzatti, D. J., Watkins, R. H., Maniscalco, W. M., Keng, P. C., & O'Reilly, M. A. (2004). In vivo exposure to hyperoxia induces DNA damage in a population of alveolar type II epithelial cells. *Am J Physiol Lung Cell Mol Physiol, 286*(5), L1045-1054. doi:10.1152/ajplung.00376.2003

Rossignol, R., Gilkerson, R., Aggeler, R., Yamagata, K., Remington, S. J., & Capaldi, R. A. (2004). Energy substrate modulates mitochondrial structure and oxidative capacity in cancer cells. *Cancer Res, 64*(3), 985-993. doi:10.1158/0008-5472.can-03-1101

Roy, A. L., Sierra, F., Howcroft, K., Singer, D. S., Sharpless, N., Hodes, R. J., . . . Anderson, J. M. (2020). A Blueprint for Characterizing Senescence. *Cell, 183*(5), 1143-1146. doi:10.1016/j.cell.2020.10.032

Rufini, A., Tucci, P., Celardo, I., & Melino, G. (2013). Senescence and aging: the critical roles of p53. *Oncogene, 32*(43), 5129-5143. doi:10.1038/onc.2012.640

Rutter, J., & Hughes, A. L. (2015). Power(2): the power of yeast genetics applied to the powerhouse of the cell. *Trends Endocrinol Metab, 26*(2), 59-68. doi:10.1016/j.tem.2014.12.002

Ryu, S. J., Oh, Y. S., & Park, S. C. (2007). Failure of stress-induced downregulation of Bcl-2 contributes to apoptosis resistance in senescent human diploid fibroblasts. *Cell Death Differ, 14*(5), 1020-1028. doi:10.1038/sj.cdd.4402091

Salminen, A., Kauppinen, A., & Kaarniranta, K. (2012). Emerging role of NF-kappaB signaling in the induction of senescence-associated secretory phenotype (SASP). *Cell Signal, 24*(4), 835-845. doi:10.1016/j.cellsig.2011.12.006

Salotti, J., & Johnson, P. F. (2019). Regulation of senescence and the SASP by the transcription factor C/EBPbeta. *Exp Gerontol, 128*, 110752. doi:10.1016/j.exger.2019.110752

Santarosa, M., Del Col, L., Tonin, E., Caragnano, A., Viel, A., & Maestro, R. (2009). Premature senescence is a major response to DNA cross-linking agents in BRCA1-defective cells: implication for tailored treatments of BRCA1 mutation carriers. *Mol Cancer Ther, 8*(4), 844-854. doi:10.1158/1535-7163.MCT-08-0951

Scarpulla, R. C. (2006). Nuclear control of respiratory gene expression in mammalian cells. *J Cell Biochem, 97*(4), 673-683. doi:10.1002/jcb.20743

Scarpulla, R. C. (2008). Nuclear control of respiratory chain expression by nuclear respiratory factors and PGC-1-related coactivator. *Ann N Y Acad Sci, 1147*, 321-334. doi:10.1196/annals.1427.006

Schafer, B., Quispe, J., Choudhary, V., Chipuk, J. E., Ajero, T. G., Du, H., . . . Kuwana, T. (2009). Mitochondrial outer membrane proteins assist Bid in Bax-mediated lipidic pore formation. *Mol Biol Cell, 20*(8), 2276-2285. doi:10.1091/mbc.e08-10-1056

Schafer, M. J., Atkinson, E. J., Vanderboom, P. M., Kotajarvi, B., White, T. A., Moore, M. M., . . . LeBrasseur, N. K. (2016). Quantification of GDF11 and Myostatin in Human Aging and Cardiovascular Disease. *Cell Metab, 23*(6), 1207-1215. doi:10.1016/j.cmet.2016.05.023

Schafer, M. J., White, T. A., Iijima, K., Haak, A. J., Ligresti, G., Atkinson, E. J., . . . LeBrasseur, N. K. (2017). Cellular senescence mediates fibrotic pulmonary disease. *Nat Commun, 8*, 14532. doi:10.1038/ncomms14532

Schafer, M. J., Zhang, X., Kumar, A., Atkinson, E. J., Zhu, Y., Jachim, S., . . . LeBrasseur, N. K. (2020). The senescence-associated secretome as an indicator of age and medical risk. *JCI Insight, 5*(12). doi:10.1172/jci.insight.133668

Schilling, M., Bulli, L., Weigang, S., Graf, L., Naumann, S., Patzina, C., . . . Kochs, G. (2018). Human MxB Protein Is a Pan-herpesvirus Restriction Factor. *J Virol, 92*(17). doi:10.1128/jvi.01056-18

Schindler, S. M., Frank, M. G., Annis, J. L., Maier, S. F., & Klegeris, A. (2018). Pattern recognition receptors mediate pro-inflammatory effects of extracellular mitochondrial transcription factor A (TFAM). *Mol Cell Neurosci, 89*, 71-79. doi:10.1016/j.mcn.2018.04.005

Schmaltz, H. N., Fried, L. P., Xue, Q. L., Walston, J., Leng, S. X., & Semba, R. D. (2005). Chronic cytomegalovirus infection and inflammation are associated with prevalent frailty in community-dwelling older women. *J Am Geriatr Soc, 53*(5), 747-754. doi:10.1111/j.1532-5415.2005.53250.x

Schneider, W. M., Chevillotte, M. D., & Rice, C. M. (2014). Interferon-stimulated genes: a complex web of host defenses. *Annu Rev Immunol, 32*, 513-545. doi:10.1146/annurev-immunol-032713-120231

Schoggins, J. W., Wilson, S. J., Panis, M., Murphy, M. Y., Jones, C. T., Bieniasz, P., & Rice, C. M. (2011). A diverse range of gene products are effectors of the type I interferon antiviral response. *Nature, 472*(7344), 481-485. doi:10.1038/nature09907

Schwarzenbach, H., Hoon, D. S., & Pantel, K. (2011). Cell-free nucleic acids as biomarkers in cancer patients. *Nat Rev Cancer, 11*(6), 426-437. doi:10.1038/nrc3066

Scorrano, L., Oakes, S. A., Opferman, J. T., Cheng, E. H., Sorcinelli, M. D., Pozzan, T., & Korsmeyer, S. J. (2003). BAX and BAK regulation of endoplasmic reticulum Ca2+: a control point for apoptosis. *Science, 300*(5616), 135-139. doi:10.1126/science.1081208

Sears, R. M., May, D. G., & Roux, K. J. (2019). BioID as a Tool for Protein-Proximity Labeling in Living Cells. *Methods Mol Biol, 2012*, 299-313. doi:10.1007/978-1-4939-9546-2_15

Sebastián, D., Palacín, M., & Zorzano, A. (2017). Mitochondrial Dynamics: Coupling Mitochondrial Fitness with Healthy Aging. *Trends Mol Med, 23*(3), 201-215. doi:10.1016/j.molmed.2017.01.003

Sebastian, T., Malik, R., Thomas, S., Sage, J., & Johnson, P. F. (2005). C/EBPbeta cooperates with RB:E2F to implement Ras(V12)-induced cellular senescence. *EMBO J, 24*(18), 3301-3312. doi:10.1038/sj.emboj.7600789

Sedlackova, L., & Korolchuk, V. I. (2019). Mitochondrial quality control as a key determinant of cell survival. *Biochim Biophys Acta Mol Cell Res, 1866*(4), 575-587. doi:10.1016/j.bbamcr.2018.12.012

Serasinghe, M. N., Wieder, S. Y., Renault, T. T., Elkholi, R., Asciolla, J. J., Yao, J. L., . . . Chipuk, J. E. (2015). Mitochondrial division is requisite to RAS-induced transformation and targeted by oncogenic MAPK pathway inhibitors. *Mol Cell, 57*(3), 521-536. doi:10.1016/j.molcel.2015.01.003

Serrano, M., Lin, A. W., McCurrach, M. E., Beach, D., & Lowe, S. W. (1997). Oncogenic ras provokes premature cell senescence associated with accumulation of p53 and p16INK4a. *Cell, 88*(5), 593-602. doi:10.1016/s0092-8674(00)81902-9

Shadyro, O. I., Yurkova, I. L., & Kisel, M. A. (2002). Radiation-induced peroxidation and fragmentation of lipids in a model membrane. *Int J Radiat Biol, 78*(3), 211-217. doi:10.1080/09553000110104065

Shah, P. P., Donahue, G., Otte, G. L., Capell, B. C., Nelson, D. M., Cao, K., . . . Berger, S. L. (2013). Lamin B1 depletion in senescent cells triggers large-scale changes in gene expression and the chromatin landscape. *Genes Dev, 27*(16), 1787-1799. doi:10.1101/gad.223834.113

Sharma, A., Smith, H. J., Yao, P., & Mair, W. B. (2019). Causal roles of mitochondrial dynamics in longevity and healthy aging. *EMBO Rep, 20*(12), e48395. doi:10.15252/embr.201948395

Sharpless, N. E., Bardeesy, N., Lee, K. H., Carrasco, D., Castrillon, D. H., Aguirre, A. J., . . . DePinho, R. A. (2001). Loss of p16Ink4a with retention of p19Arf predisposes mice to tumorigenesis. *Nature, 413*(6851), 86-91. doi:10.1038/35092592

Sharpless, N. E., & Sherr, C. J. (2015). Forging a signature of in vivo senescence. *Nat Rev Cancer, 15*(7), 397-408. doi:10.1038/nrc3960

Sheridan, C., Delivani, P., Cullen, S. P., & Martin, S. J. (2008). Bax- or Bak-Induced Mitochondrial Fission Can Be Uncoupled from Cytochrome c Release. *Molecular Cell, 31*(4), 570-585. doi:https://doi.org/10.1016/j.molcel.2008.08.002

Shi, C. S., Qi, H. Y., Boularan, C., Huang, N. N., Abu-Asab, M., Shelhamer, J. H., & Kehrl, J. H. (2014). SARS-coronavirus open reading frame-9b suppresses innate immunity by targeting mitochondria and the MAVS/TRAF3/TRAF6 signalosome. *J Immunol, 193*(6), 3080-3089. doi:10.4049/jimmunol.1303196

Shimada, K., Crother, T. R., Karlin, J., Dagvadorj, J., Chiba, N., Chen, S., . . . Arditi, M. (2012). Oxidized mitochondrial DNA activates the NLRP3 inflammasome during apoptosis. *Immunity, 36*(3), 401-414. doi:10.1016/j.immuni.2012.01.009

Shimi, T., Butin-Israeli, V., Adam, S. A., Hamanaka, R. B., Goldman, A. E., Lucas, C. A., . . . Goldman, R. D. (2011). The role of nuclear lamin B1 in cell proliferation and senescence. *Genes Dev, 25*(24), 2579-2593. doi:10.1101/gad.179515.111

Shimizu, M., Okuno, T., Kinoshita, M., Sumi, H., Fujimura, H., Yamashita, K., . . . Mochizuki, H. (2020). Mitochondrial DNA enhance innate immune responses in neuromyelitis optica by monocyte recruitment and activation. *Sci Rep, 10*(1), 13274. doi:10.1038/s41598-020-70203-x

Shpilka, T., & Haynes, C. M. (2018). The mitochondrial UPR: mechanisms, physiological functions and implications in ageing. *Nat Rev Mol Cell Biol, 19*(2), 109-120. doi:10.1038/nrm.2017.110

Simmons, J. D., Lee, Y. L., Mulekar, S., Kuck, J. L., Brevard, S. B., Gonzalez, R. P., . . . Richards, W. O. (2013). Elevated levels of plasma mitochondrial DNA DAMPs are linked to clinical outcome in severely injured human subjects. *Ann Surg, 258*(4), 591-596; discussion 596-598. doi:10.1097/SLA.0b013e3182a4ea46

Solt, L. A., & May, M. J. (2008). The IkappaB kinase complex: master regulator of NF-kappaB signaling. *Immunol Res, 42*(1-3), 3-18. doi:10.1007/s12026-008-8025-1

Soltész, B., Urbancsek, R., Pös, O., Hajas, O., Forgács, I. N., Szilágyi, E., . . . Nagy, B. (2019). Quantification of peripheral whole blood, cell-free plasma and exosome encapsulated mitochondrial DNA copy numbers in patients with atrial fibrillation. *J Biotechnol, 299*, 66-71. doi:10.1016/j.jbiotec.2019.04.018

Song, J., Yoon, D., Christensen, R. D., Horvathova, M., Thiagarajan, P., & Prchal, J. T. (2015). HIF-mediated increased ROS from reduced mitophagy and decreased catalase causes neocytolysis. *J Mol Med (Berl), 93*(8), 857-866. doi:10.1007/s00109-015-1294-y

Song, Y. S., Lee, B. Y., & Hwang, E. S. (2005). Dinstinct ROS and biochemical profiles in cells undergoing DNA damage-induced senescence and apoptosis. *Mech Ageing Dev, 126*(5), 580-590. doi:10.1016/j.mad.2004.11.008

Sossey-Alaoui, K., Pluskota, E., Szpak, D., & Plow, E. F. (2019). The Kindlin2-p53-SerpinB2 signaling axis is required for cellular senescence in breast cancer. *Cell Death Dis, 10*(8), 539. doi:10.1038/s41419-019-1774-z

Soto-Gamez, A., Quax, W. J., & Demaria, M. (2019). Regulation of Survival Networks in Senescent Cells: From Mechanisms to Interventions. *J Mol Biol, 431*(15), 2629-2643. doi:10.1016/j.jmb.2019.05.036

Soubannier, V., McLelland, G. L., Zunino, R., Braschi, E., Rippstein, P., Fon, E. A., & McBride, H. M. (2012). A vesicular transport pathway shuttles cargo from mitochondria to lysosomes. *Curr Biol, 22*(2), 135-141. doi:10.1016/j.cub.2011.11.057

Spinelli, J. B., & Haigis, M. C. (2018). The multifaceted contributions of mitochondria to cellular metabolism. *Nat Cell Biol, 20*(7), 745-754. doi:10.1038/s41556-018-0124-1

Sprenger, H. G., & Langer, T. (2019). The Good and the Bad of Mitochondrial Breakups. *Trends Cell Biol, 29*(11), 888-900. doi:10.1016/j.tcb.2019.08.003

Staeheli, P., & Haller, O. (2018). Human MX2/MxB: a Potent Interferon-Induced Postentry Inhibitor of Herpesviruses and HIV-1. *J Virol, 92*(24). doi:10.1128/jvi.00709-18

Stein, G. H., Drullinger, L. F., Soulard, A., & Dulic, V. (1999). Differential roles for cyclin-dependent kinase inhibitors p21 and p16 in the mechanisms of senescence and differentiation in human fibroblasts. *Mol Cell Biol, 19*(3), 2109-2117. doi:10.1128/mcb.19.3.2109

Steiner, F., & Pavlovic, J. (2020). Subcellular Localization of MxB Determines Its Antiviral Potential against Influenza A Virus. *J Virol, 94*(22). doi:10.1128/jvi.00125-20

Stockl, P., Zankl, C., Hutter, E., Unterluggauer, H., Laun, P., Heeren, G., . . . Jansen-Durr, P. (2007). Partial uncoupling of oxidative phosphorylation induces premature senescence in human fibroblasts and yeast mother cells. *Free Radic Biol Med, 43*(6), 947-958. doi:10.1016/j.freeradbiomed.2007.06.005

Storer, M., Mas, A., Robert-Moreno, A., Pecoraro, M., Ortells, M. C., Di Giacomo, V., . . . Keyes, W. M. (2013). Senescence is a developmental mechanism that contributes to embryonic growth and patterning. *Cell, 155*(5), 1119-1130. doi:10.1016/j.cell.2013.10.041

Studencka, M., & Schaber, J. (2017). Senoptosis: non-lethal DNA cleavage as a route to deep senescence. *Oncotarget, 8*(19), 30656-30671. doi:10.18632/oncotarget.15693

Sudakov, N. P., Apartsin, K. A., Lepekhova, S. A., Nikiforov, S. B., Katyshev, A. I., Lifshits, G. I., . . . Konstantinov, Y. M. (2017). The level of free circulating mitochondrial DNA in blood as predictor of death in case of acute coronary syndrome. *Eur J Med Res, 22*(1), 1. doi:10.1186/s40001-016-0241-x

Sugiura, A., McLelland, G. L., Fon, E. A., & McBride, H. M. (2014). A new pathway for mitochondrial quality control: mitochondrial-derived vesicles. *EMBO J, 33*(19), 2142-2156. doi:10.15252/embj.201488104

Sun, G., Guzman, E., Balasanyan, V., Conner, C. M., Wong, K., Zhou, H. R., . . . Montell, D. J. (2017). A molecular signature for anastasis, recovery from the brink of apoptotic cell death. *J Cell Biol, 216*(10), 3355-3368. doi:10.1083/jcb.201706134

Sun, N., Youle, R. J., & Finkel, T. (2016). The Mitochondrial Basis of Aging. *Mol Cell, 61*(5), 654-666. doi:10.1016/j.molcel.2016.01.028

Sun, P., Yoshizuka, N., New, L., Moser, B. A., Li, Y., Liao, R., . . . Han, J. (2007). PRAK is essential for ras-induced senescence and tumor suppression. *Cell, 128*(2), 295-308. doi:10.1016/j.cell.2006.11.050

Suram, A., Kaplunov, J., Patel, P. L., Ruan, H., Cerutti, A., Boccardi, V., . . . Herbig, U. (2012). Oncogene-induced telomere dysfunction enforces cellular senescence in human cancer precursor lesions. *EMBO J, 31*(13), 2839-2851. doi:10.1038/emboj.2012.132

Tai, H., Wang, Z., Gong, H., Han, X., Zhou, J., Wang, X., . . . Xiao, H. (2017). Autophagy impairment with lysosomal and mitochondrial dysfunction is an important characteristic of oxidative stress-induced senescence. *Autophagy, 13*(1), 99-113. doi:10.1080/15548627.2016.1247143

Tait, S. W., & Green, D. R. (2013). Mitochondrial regulation of cell death. *Cold Spring Harb Perspect Biol, 5*(9). doi:10.1101/cshperspect.a008706

Tait, S. W., Parsons, M. J., Llambi, F., Bouchier-Hayes, L., Connell, S., Muñoz-Pinedo, C., & Green, D. R. (2010). Resistance to caspase-independent cell death requires persistence of intact mitochondria. *Dev Cell, 18*(5), 802-813. doi:10.1016/j.devcel.2010.03.014

Takahashi, A., Loo, T. M., Okada, R., Kamachi, F., Watanabe, Y., Wakita, M., . . . Hara, E. (2018). Downregulation of cytoplasmic DNases is implicated in cytoplasmic DNA accumulation and SASP in senescent cells. *Nat Commun, 9*(1), 1249. doi:10.1038/s41467-018-03555-8

Takauji, Y., En, A., Miki, K., Ayusawa, D., & Fujii, M. (2016). Combinatorial effects of continuous protein synthesis, ERK-signaling, and reactive oxygen species on induction of cellular senescence. *Exp Cell Res, 345*(2), 239-246. doi:10.1016/j.yexcr.2016.06.011

Tanaka, A. (2010). Parkin-mediated selective mitochondrial autophagy, mitophagy: Parkin purges damaged organelles from the vital mitochondrial network. *FEBS Lett, 584*(7), 1386-1392. doi:10.1016/j.febslet.2010.02.060

Tang, H. M., & Tang, H. L. (2018). Anastasis: recovery from the brink of cell death. *R Soc Open Sci, 5*(9), 180442. doi:10.1098/rsos.180442

Tarutani, M., Cai, T., Dajee, M., & Khavari, P. A. (2003). Inducible activation of Ras and Raf in adult epidermis. *Cancer Res, 63*(2), 319-323.

Taylor, R. C., Cullen, S. P., & Martin, S. J. (2008). Apoptosis: controlled demolition at the cellular level. *Nat Rev Mol Cell Biol, 9*(3), 231-241. doi:10.1038/nrm2312

Tchkonia, T., Morbeck, D. E., Von Zglinicki, T., Van Deursen, J., Lustgarten, J., Scrable, H., . . . Kirkland, J. L. (2010). Fat tissue, aging, and cellular senescence. *Aging Cell, 9*(5), 667-684. doi:10.1111/j.1474-9726.2010.00608.x

te Poele, R. H., Okorokov, A. L., Jardine, L., Cummings, J., & Joel, S. P. (2002). DNA damage is able to induce senescence in tumor cells in vitro and in vivo. *Cancer Res, 62*(6), 1876-1883. Retrieved from https://www.ncbi.nlm.nih.gov/pubmed/11912168

Timmis, J. N., Ayliffe, M. A., Huang, C. Y., & Martin, W. (2004). Endosymbiotic gene transfer: organelle genomes forge eukaryotic chromosomes. *Nat Rev Genet, 5*(2), 123-135. doi:10.1038/nrg1271

Todkar, K., Ilamathi, H. S., & Germain, M. (2017). Mitochondria and Lysosomes: Discovering Bonds. *Front Cell Dev Biol, 5*, 106. doi:10.3389/fcell.2017.00106

Tondera, D., Grandemange, S., Jourdain, A., Karbowski, M., Mattenberger, Y., Herzig, S., . . . Martinou, J. C. (2009). SLP-2 is required for stress-induced mitochondrial hyperfusion. *EMBO J, 28*(11), 1589-1600. doi:10.1038/emboj.2009.89

Torralba, D., Baixauli, F., Villarroya-Beltri, C., Fernández-Delgado, I., Latorre-Pellicer, A., Acín-Pérez, R., . . . Sánchez-Madrid, F. (2018). Priming of dendritic cells by DNA-containing extracellular vesicles from activated T cells through antigen-driven contacts. *Nat Commun, 9*(1), 2658. doi:10.1038/s41467-018-05077-9

Torres, C., Lewis, L., & Cristofalo, V. J. (2006). Proteasome inhibitors shorten replicative life span and induce a senescent-like phenotype of human fibroblasts. *J Cell Physiol, 207*(3), 845-853. doi:10.1002/jcp.20630

Toussaint, O., Medrano, E. E., & von Zglinicki, T. (2000). Cellular and molecular mechanisms of stress-induced premature senescence (SIPS) of human diploid fibroblasts and melanocytes. *Exp Gerontol, 35*(8), 927-945. doi:10.1016/s0531-5565(00)00180-7

Toussaint, O., Royer, V., Salmon, M., & Remacle, J. (2002). Stress-induced premature senescence and tissue ageing. *Biochem Pharmacol, 64*(5-6), 1007-1009. doi:10.1016/s0006-2952(02)01170-x

Toyama, E. Q., Herzig, S., Courchet, J., Lewis, T. L., Jr., Loson, O. C., Hellberg, K., . . . Shaw, R. J. (2016). Metabolism. AMP-activated protein kinase mediates mitochondrial fission in response to energy stress. *Science, 351*(6270), 275-281. doi:10.1126/science.aab4138

Tresini, M., Lorenzini, A., Torres, C., & Cristofalo, V. J. (2007). Modulation of replicative senescence of diploid human cells by nuclear ERK signaling. *J Biol Chem, 282*(6), 4136-4151. doi:10.1074/jbc.M604955200

Trumpff, C., Marsland, A. L., Basualto-Alarcón, C., Martin, J. L., Carroll, J. E., Sturm, G., . . . Picard, M. (2019). Acute psychological stress increases serum circulating cell-free mitochondrial DNA. *Psychoneuroendocrinology, 106*, 268-276. doi:10.1016/j.psyneuen.2019.03.026

Uren, R. T., Iyer, S., & Kluck, R. M. (2017). Pore formation by dimeric Bak and Bax: an unusual pore? *Philos Trans R Soc Lond B Biol Sci, 372*(1726). doi:10.1098/rstb.2016.0218

Vafa, O., Wade, M., Kern, S., Beeche, M., Pandita, T. K., Hampton, G. M., & Wahl, G. M. (2002). c-Myc can induce DNA damage, increase reactive oxygen species, and mitigate p53 function: a

mechanism for oncogene-induced genetic instability. *Mol Cell, 9*(5), 1031-1044. doi:10.1016/s1097-2765(02)00520-8

Valente, A. J., Maddalena, L. A., Robb, E. L., Moradi, F., & Stuart, J. A. (2017). A simple ImageJ macro tool for analyzing mitochondrial network morphology in mammalian cell culture. *Acta Histochem, 119*(3), 315-326. doi:10.1016/j.acthis.2017.03.001

van der Veer, E., Ho, C., O'Neil, C., Barbosa, N., Scott, R., Cregan, S. P., & Pickering, J. G. (2007). Extension of human cell lifespan by nicotinamide phosphoribosyltransferase. *J Biol Chem, 282*(15), 10841-10845. doi:10.1074/jbc.C700018200

van Deursen, J. M. (2014). The role of senescent cells in ageing. *Nature, 509*(7501), 439-446. doi:10.1038/nature13193

van Loo, G., Saelens, X., van Gurp, M., MacFarlane, M., Martin, S. J., & Vandenabeele, P. (2002). The role of mitochondrial factors in apoptosis: a Russian roulette with more than one bullet. *Cell Death Differ, 9*(10), 1031-1042. doi:10.1038/sj.cdd.4401088

Vander Heiden, M. G., Cantley, L. C., & Thompson, C. B. (2009). Understanding the Warburg effect: the metabolic requirements of cell proliferation. *Science, 324*(5930), 1029-1033. doi:10.1126/science.1160809

Vasileiou, P. V. S., Evangelou, K., Vlasis, K., Fildisis, G., Panayiotidis, M. I., Chronopoulos, E., . . . Havaki, S. (2019). Mitochondrial Homeostasis and Cellular Senescence. *Cells, 8*(7). doi:10.3390/cells8070686

Venkatesh, D., Fredette, N., Rostama, B., Tang, Y., Vary, C. P., Liaw, L., & Urs, S. (2011). RhoA-mediated signaling in Notch-induced senescence-like growth arrest and endothelial barrier dysfunction. *Arterioscler Thromb Vasc Biol, 31*(4), 876-882. doi:10.1161/ATVBAHA.110.221945

Vizioli, M. G., Liu, T., Miller, K. N., Robertson, N. A., Gilroy, K., Lagnado, A. B., . . . Adams, P. D. (2020). Mitochondria-to-nucleus retrograde signaling drives formation of cytoplasmic chromatin and inflammation in senescence. *Genes Dev, 34*(5-6), 428-445. doi:10.1101/gad.331272.119

von Zglinicki, T. (2002). Oxidative stress shortens telomeres. *Trends Biochem Sci, 27*(7), 339-344. doi:10.1016/s0968-0004(02)02110-2

Vringer, E., & Tait, S. W. G. (2019). Mitochondria and Inflammation: Cell Death Heats Up. *Front Cell Dev Biol, 7*, 100. doi:10.3389/fcell.2019.00100

Wai, T., & Langer, T. (2016). Mitochondrial Dynamics and Metabolic Regulation. *Trends Endocrinol Metab, 27*(2), 105-117. doi:10.1016/j.tem.2015.12.001

Wanders, R. J., Waterham, H. R., & Ferdinandusse, S. (2015). Metabolic Interplay between Peroxisomes and Other Subcellular Organelles Including Mitochondria and the Endoplasmic Reticulum. *Front Cell Dev Biol, 3*, 83. doi:10.3389/fcell.2015.00083

Wang, D., Liu, Y., Zhang, R., Zhang, F., Sui, W., Chen, L., . . . Ji, J. (2016). Apoptotic transition of senescent cells accompanied with mitochondrial hyper-function. *Oncotarget, 7*(19), 28286-28300. doi:10.18632/oncotarget.8536

Wang, E. (1995). Senescent human fibroblasts resist programmed cell death, and failure to suppress bcl2 is involved. *Cancer Res, 55*(11), 2284-2292.

Wang, W., Yang, X., Lopez de Silanes, I., Carling, D., & Gorospe, M. (2003). Increased AMP:ATP ratio and AMP-activated protein kinase activity during cellular senescence linked to reduced HuR function. *J Biol Chem, 278*(29), 27016-27023. doi:10.1074/jbc.M300318200

Wang, X., & Chen, X. J. (2015). A cytosolic network suppressing mitochondria-mediated proteostatic stress and cell death. *Nature, 524*(7566), 481-484. doi:10.1038/nature14859

Wang, X., Weidling, I., Koppel, S., Menta, B., Perez Ortiz, J., Kalani, A., . . . Swerdlow, R. H. (2020). Detection of mitochondria-pertinent components in exosomes. *Mitochondrion, 55*, 100-110. doi:10.1016/j.mito.2020.09.006

Wang, Y. X., Niklasch, M., Liu, T., Wang, Y., Shi, B., Yuan, W., . . . Wen, Y. M. (2020). Interferon-inducible MX2 is a host restriction factor of hepatitis B virus replication. *J Hepatol, 72*(5), 865-876. doi:10.1016/j.jhep.2019.12.009

Wang, Z. B., Zhang, Y., Liu, Y. Q., Guo, Y., Xu, H., Dong, B., & Cui, Y. F. (2006). Bcl-xL overexpression restricts gamma-radiation-induced apoptosis. *Cell Biol Int, 30*(1), 15-20. doi:10.1016/j.cellbi.2005.08.006

Watson, J. D. (1972). Origin of concatemeric T7 DNA. *Nat New Biol, 239*(94), 197-201. doi:10.1038/newbio239197a0

Watt, I. N., Montgomery, M. G., Runswick, M. J., Leslie, A. G., & Walker, J. E. (2010). Bioenergetic cost of making an adenosine triphosphate molecule in animal mitochondria. *Proc Natl Acad Sci U S A, 107*(39), 16823-16827. doi:10.1073/pnas.1011099107

West, A. P., Khoury-Hanold, W., Staron, M., Tal, M. C., Pineda, C. M., Lang, S. M., . . . Shadel, G. S. (2015). Mitochondrial DNA stress primes the antiviral innate immune response. *Nature, 520*(7548), 553-557. doi:10.1038/nature14156

West, A. P., & Shadel, G. S. (2017). Mitochondrial DNA in innate immune responses and inflammatory pathology. *Nat Rev Immunol, 17*(6), 363-375. doi:10.1038/nri.2017.21

West, M. D., Shay, J. W., Wright, W. E., & Linskens, M. H. (1996). Altered expression of plasminogen activator and plasminogen activator inhibitor during cellular senescence. *Exp Gerontol, 31*(1-2), 175-193. doi:10.1016/0531-5565(95)02013-6

Westphal, D., Dewson, G., Czabotar, P. E., & Kluck, R. M. (2011). Molecular biology of Bax and Bak activation and action. *Biochim Biophys Acta, 1813*(4), 521-531. doi:10.1016/j.bbamcr.2010.12.019

White, M. J., McArthur, K., Metcalf, D., Lane, R. M., Cambier, J. C., Herold, M. J., . . . Kile, B. T. (2014). Apoptotic caspases suppress mtDNA-induced STING-mediated type I IFN production. *Cell, 159*(7), 1549-1562. doi:10.1016/j.cell.2014.11.036

Wiley, C. D., & Campisi, J. (2016). From Ancient Pathways to Aging Cells-Connecting Metabolism and Cellular Senescence. *Cell Metab, 23*(6), 1013-1021. doi:10.1016/j.cmet.2016.05.010

Wiley, C. D., Velarde, M. C., Lecot, P., Liu, S., Sarnoski, E. A., Freund, A., . . . Campisi, J. (2016). Mitochondrial Dysfunction Induces Senescence with a Distinct Secretory Phenotype. *Cell Metab, 23*(2), 303-314. doi:10.1016/j.cmet.2015.11.011

Wrobel, L., Topf, U., Bragoszewski, P., Wiese, S., Sztolsztener, M. E., Oeljeklaus, S., . . . Chacinska, A. (2015). Mistargeted mitochondrial proteins activate a proteostatic response in the cytosol. *Nature, 524*(7566), 485-488. doi:10.1038/nature14951

Wu, S., Zhou, F., Zhang, Z., & Xing, D. (2011). Mitochondrial oxidative stress causes mitochondrial fragmentation via differential modulation of mitochondrial fission-fusion proteins. *Febs j, 278*(6), 941-954. doi:10.1111/j.1742-4658.2011.08010.x

Xia, M., Zhang, Y., Jin, K., Lu, Z., Zeng, Z., & Xiong, W. (2019). Communication between mitochondria and other organelles: a brand-new perspective on mitochondria in cancer. *Cell Biosci, 9*, 27. doi:10.1186/s13578-019-0289-8

Xie, L., Ju, Z., Zhong, C., Wu, Y., Zan, Y., Hou, W., & Feng, Y. (2020). GTPase Activity of MxB Contributes to Its Nuclear Location, Interaction with Nucleoporins and Anti-HIV-1 Activity. *Virol Sin*. doi:10.1007/s12250-020-00249-8

Xu, M., Pirtskhalava, T., Farr, J. N., Weigand, B. M., Palmer, A. K., Weivoda, M. M., . . . Kirkland, J. L. (2018). Senolytics improve physical function and increase lifespan in old age. *Nat Med, 24*(8), 1246-1256. doi:10.1038/s41591-018-0092-9

Xu, Y., Li, N., Xiang, R., & Sun, P. (2014). Emerging roles of the p38 MAPK and PI3K/AKT/mTOR pathways in oncogene-induced senescence. *Trends Biochem Sci, 39*(6), 268-276. doi:10.1016/j.tibs.2014.04.004

Xue, Q. L. (2011). The frailty syndrome: definition and natural history. *Clin Geriatr Med, 27*(1), 1-15. doi:10.1016/j.cger.2010.08.009

Yamakoshi, K., Takahashi, A., Hirota, F., Nakayama, R., Ishimaru, N., Kubo, Y., . . . Hara, E. (2009). Real-time in vivo imaging of p16Ink4a reveals cross talk with p53. *J Cell Biol, 186*(3), 393-407. doi:10.1083/jcb.200904105

Yamashita, S. I., Jin, X., Furukawa, K., Hamasaki, M., Nezu, A., Otera, H., . . . Kanki, T. (2016). Mitochondrial division occurs concurrently with autophagosome formation but independently of Drp1 during mitophagy. *J Cell Biol, 215*(5), 649-665. doi:10.1083/jcb.201605093

Yang, H., Wang, H., Ren, J., Chen, Q., & Chen, Z. J. (2017). cGAS is essential for cellular senescence. *Proc Natl Acad Sci U S A, 114*(23), E4612-e4620. doi:10.1073/pnas.1705499114

Yasukawa, T., & Kang, D. (2018). An overview of mammalian mitochondrial DNA replication mechanisms. *J Biochem, 164*(3), 183-193. doi:10.1093/jb/mvy058

Yethon, J. A., Epand, R. F., Leber, B., Epand, R. M., & Andrews, D. W. (2003). Interaction with a membrane surface triggers a reversible conformational change in Bax normally associated with induction of apoptosis. *J Biol Chem, 278*(49), 48935-48941. doi:10.1074/jbc.M306289200

Yi, D. R., An, N., Liu, Z. L., Xu, F. W., Raniga, K., Li, Q. J., . . . Cen, S. (2019). Human MxB Inhibits the Replication of Hepatitis C Virus. *J Virol, 93*(1). doi:10.1128/jvi.01285-18

Yong, C. Q. Y., & Tang, B. L. (2018). A Mitochondrial Encoded Messenger at the Nucleus. *Cells, 7*(8). doi:10.3390/cells7080105

Yoon, Y. S., Yoon, D. S., Lim, I. K., Yoon, S. H., Chung, H. Y., Rojo, M., . . . Yoon, G. (2006). Formation of elongated giant mitochondria in DFO-induced cellular senescence: involvement of enhanced fusion process through modulation of Fis1. *J Cell Physiol, 209*(2), 468-480. doi:10.1002/jcp.20753

Yosef, R., Pilpel, N., Papismadov, N., Gal, H., Ovadya, Y., Vadai, E., . . . Krizhanovsky, V. (2017). p21 maintains senescent cell viability under persistent DNA damage response by restraining JNK and caspase signaling. *EMBO J, 36*(15), 2280-2295. doi:10.15252/embj.201695553

Yosef, R., Pilpel, N., Tokarsky-Amiel, R., Biran, A., Ovadya, Y., Cohen, S., . . . Krizhanovsky, V. (2016). Directed elimination of senescent cells by inhibition of BCL-W and BCL-XL. *Nat Commun, 7*, 11190. doi:10.1038/ncomms11190

Young, A. P., & Kaelin, W. G., Jr. (2008). Senescence triggered by the loss of the VHL tumor suppressor. *Cell Cycle, 7*(12), 1709-1712. doi:10.4161/cc.7.12.6124

Young, A. R., Narita, M., Ferreira, M., Kirschner, K., Sadaie, M., Darot, J. F., . . . Narita, M. (2009). Autophagy mediates the mitotic senescence transition. *Genes Dev, 23*(7), 798-803. doi:10.1101/gad.519709

Young, A. R., Narita, M., Ferreira, M., Kirschner, K., Sadaie, M., Darot, J. F., . . . Narita, M. (2009). Autophagy mediates the mitotic senescence transition. *Genes Dev, 23*(7), 798-803. doi:10.1101/gad.519709

Yu, C. Y., Liang, J. J., Li, J. K., Lee, Y. L., Chang, B. L., Su, C. I., . . . Lin, Y. L. (2015). Dengue Virus Impairs Mitochondrial Fusion by Cleaving Mitofusins. *PLoS Pathog, 11*(12), e1005350. doi:10.1371/journal.ppat.1005350

Yu, T., Jhun, B. S., & Yoon, Y. (2011). High-glucose stimulation increases reactive oxygen species production through the calcium and mitogen-activated protein kinase-mediated activation of mitochondrial fission. *Antioxid Redox Signal, 14*(3), 425-437. doi:10.1089/ars.2010.3284

Zeth, K. (2010). Structure and evolution of mitochondrial outer membrane proteins of beta-barrel topology. *Biochim Biophys Acta, 1797*(6-7), 1292-1299. doi:10.1016/j.bbabio.2010.04.019

Zhang, B., Podolskiy, D. I., Mariotti, M., Seravalli, J., & Gladyshev, V. N. (2020). Systematic age-, organ-, and diet-associated ionome remodeling and the development of ionomic aging clocks. *Aging Cell, 19*(5), e13119. doi:10.1111/acel.13119

Zhang, H., Kim, J. K., Edwards, C. A., Xu, Z., Taichman, R., & Wang, C. Y. (2005). Clusterin inhibits apoptosis by interacting with activated Bax. *Nat Cell Biol, 7*(9), 909-915. doi:10.1038/ncb1291

Zhang, M., Zheng, J., Nussinov, R., & Ma, B. (2017). Release of Cytochrome C from Bax Pores at the Mitochondrial Membrane. *Sci Rep, 7*(1), 2635. doi:10.1038/s41598-017-02825-7

Zhou, H., Hou, Q., Hansen, J. L., & Hsu, Y. T. (2007). Complete activation of Bax by a single site mutation. *Oncogene, 26*(50), 7092-7102. doi:10.1038/sj.onc.1210517

Zhu, Y., Doornebal, E. J., Pirtskhalava, T., Giorgadze, N., Wentworth, M., Fuhrmann-Stroissnigg, H., . . . Kirkland, J. L. (2017). New agents that target senescent cells: the flavone, fisetin, and the BCL-XL inhibitors, A1331852 and A1155463. *Aging (Albany NY), 9*(3), 955-963. doi:10.18632/aging.101202

Zhu, Y., Tchkonia, T., Pirtskhalava, T., Gower, A. C., Ding, H., Giorgadze, N., . . . Kirkland, J. L. (2015). The Achilles' heel of senescent cells: from transcriptome to senolytic drugs. *Aging Cell, 14*(4), 644-658. doi:10.1111/acel.12344

Ziegler, D. V., Wiley, C. D., & Velarde, M. C. (2015). Mitochondrial effectors of cellular senescence: beyond the free radical theory of aging. *Aging Cell, 14*(1), 1-7. doi:10.1111/acel.12287

Zwerschke, W., Mazurek, S., Stockl, P., Hutter, E., Eigenbrodt, E., & Jansen-Durr, P. (2003). Metabolic analysis of senescent human fibroblasts reveals a role for AMP in cellular senescence. *Biochem J, 376*(Pt 2), 403-411. doi:10.1042/BJ20030816